KU LEUVEN

ARENBERG DOCTORAL SCHOOL
FACULTY OF SCIENCE

Mineralogical study of the pozzolanic properties of calcined clays



Sofie Hollanders

Supervisors:
Prof. Dr. J. Elsen
Prof. Dr. Ö. Cizer

Dissertation presented in partial fulfilment of the requirements for the degree of Doctor of Science

April 2017

MINERALOGICAL STUDY OF THE POZZOLANIC PROPERTIES OF CALCINED CLAYS

Sofie HOLLANDERS

Supervisors:
Prof. Dr. J. Elsen
Prof. Dr. Ö. Cizer

Members of the Examination Committee:
Prof. Dr. N. Vandenberghe, *chairman*
Prof. Dr. P. Degryse
Prof. Dr. Ph. Muchez
Prof. Dr. Ir. N. De Belie
Dr. P. Naproux

Dissertation presented in partial fulfilment of the requirements for the degree of Doctor of science

April 2017

ACKNOWLEDGEMENTS

Hier is het dan, het werk van vier jaar onderzoek, samengevat in dit boekje. Vier jaar met de nodige ups en downs. Vier jaar waarbij het antwoord op 1 vraag wel 5 nieuwe vragen met zich meebracht. Vier jaar waarvan ontelbare uren in het labo zijn doorgebracht. Maar vooral ook vier jaar waarin ik kon rekenen op de steun en bijdrage van verschillende mensen om mijn onderzoek tot een goed einde te brengen. Dit woordje van dank is dan ook aan jullie allen gericht.

Mijn promotor Prof. Dr. Jan Elsen zou ik graag als eerste willen bedanken. Bij onze eerste gesprekken betreffende een mogelijk doctoraatsonderwerp stelde je voor om mijn passie voor de kleimineralogie te combineren met de, voor mij toen nog onverkende wereld van de cementwetenschap. Deze uitdaging ben ik met veel enthousiasme aangegaan en heb hier geen spijt van gekregen in de voorbije vier jaar. Bedankt voor het vertrouwen en mij de nodige academische vrijheid te geven om mijn wetenschappelijke creativiteit te ontplooien. Bovendien kon ik altijd bij hem terecht voor het bespreken van bepaalde problemen die zich voordeden en zag hij erop toe dat ik de 'bigger picture' niet uit het oog zou verliezen.

Additionally I would like to thank my co-supervisor Prof. Dr. Özlem Cizer. I would like to thank her for her guidance and her insightful comments. Her knowledge regarding cement research resulted in enlightening discussion, wherefore many thanks.

The members of the examination committee, Prof. Dr. Noël Vandenberghe, Prof. Dr. Nele De Belie, Dr. Pierre Naproux, Prof. Dr. Patrick Degryse and Prof. Dr. Philippe Muchez are kindly acknowledged for their time investment in the review of the manuscript. Their constructive criticism and their „to-the-point"-remarks helped to improve this manuscript significantly. Pierre, you deserve special thanks for the warm welcome and help in the Sibelco's cement lab in Compiègne at the very start of my PhD project.

In the initial phase of my PhD project I got a lot of support from Sibelco. Clays form a crucial element in this research and I would like to express my gratitude to Pim Demecheleer, Gordon Witte and all other persons from Sibelco for all the help gathering sufficient clay samples with variable characteristics. Additionally I had the opportunity to go on field trip in Russia with Gordon and Caroline. Therefore my gratitude to the people from Sibelco Russia for the Hartley welcome, in particularly Andrei Bychkov and Denis Krolovetsky for the accompaniment during our stay and Victor Goryushkin for guiding us in the quarries and helping with sampling.

Ik wil ook mijn dank betuigen aan mijn master studente Caroline voor al haar harde werk zowel op terrein als in het labo en het verduren van mijn veeleisende karakter. Onze trip naar Rusland is voor mij onvergetelijk.

Voor hulp in het labo kon ik altijd rekenen op Nancy, Ria en Wathab! Jullie hebben veel lastige en vooral plakkerige kleistalen voor mij voorbereid en geanalyseerd. Echt merciekes! Er heerste altijd een opgewekte sfeer in het labo en ik heb zeer graag met jullie samengewerkt. Ook Dirk wil ik graag

bedanken, hij is een vaste waarde in het labo en stond altijd paraat om de XRD of TGA weer maar eens opnieuw aan de praat te krijgen. Ook Elvira heeft mij enorm geholpen bij het op punt stellen van de Chapelle test en bij het uitvoeren van chemische analyses, waarvoor dank. Voor problemen met de vriesdroger kon ik altijd terecht bij Gerda, bedankt hiervoor.

Zo nu en dan werd al dat onderzoek me toch allemaal een beetje veel en dan stonden Kim en Bene altijd voor mij klaar. Regelmatig heb ik een klaagpleidooi gehouden over onlogische resultaten, mislukte labo experimenten of over de practica. Algauw werden alle zorgen dan weer vergeten en veranderde het gespreksonderwerp naar iets minder wetenschappelijke onderwerpen zoals de laatste nieuwtjes, kledingstips, reisbestemmingen of de paardjes. Als er iemand van ons op vakantie was, kwam iedereen altijd zeggen dat het zo stil en rustig was. Dus een welgemeende merci! Kim je verdient nog een speciaal bedankje. Je was niet alleen een onvergetelijk bureaugenootje maar ook een geweldige vriendin. Je stond altijd voor mij klaar en was een grote steun bij moeilijke momenten.

Ook alle andere collega's wil ik graag bedanken voor de onvergetelijke koffiepauzes en het creëren van een ontspannen werksfeer. Ook de pingpong lunches zorgden voor de nodige sportieve uitdaging en memorabele momenten. Hierbij ben ik stiekem fier op de bijnaam die ik heb gekregen: 'sneaky balls' bedankt aan Bram, Nick, Niels, Dominique, Jacek, Buruk, Robin, Jeroen en natuurlijk nog vele anderen voor deze leuke momenten.

Ook buiten 'den E' kon ik rekenen op mijn vrienden voor de nodige ontspanning en plezier. Hier wil ik in het bijzonder 'de meisjes' Kim, Nele, Els en Rebecca bedanken voor de leuke girls-avonden en weekendje. Ook Koen, Cindy, Stijn, Nathalie, Benedicta en Jean merci voor de gezellige voetbalavonden en de wandeluitstapjes naar de Ardennen.

Graag wil ook mijn familie bedanken voor de onvoorwaardelijke steun. In het bijzonder wil ik mijn ouders bedanken om mij steeds alle kansen te geven en mijn eigen keuzes te laten maken. Jullie moedigde mij altijd aan en ik kon steeds bij jullie terecht op de momenten dat ik het nodig had. Ook mijn zusjes Elli en Karolien wil ik graag bedanken. Of het nu was om te gaan wandelen in de bossen met de paarden, te gaan shoppen of gewoon eens wat te babbelen, ik kon altijd op jullie rekenen voor de nodige ontspanning.

Dan rest er nog één heel bijzonder iemand. Rieko, zonder jou had dit nooit gelukt. Je wist me altijd weer te motiveren en op te vrolijken als de frustraties hoog zaten. Je hebt altijd super veel geduld met mij en weet al dat mijn slechte humeur wel weer overwaait wanneer ik mijn beklag heb kunnen doen of wanneer je me chocolade geeft. Je bent mijn steun en toeverlaat en ik weet dat je altijd voor mij klaar zult staan. Merciekes voor alles zoet!

ABSTRACT

Portland cement-based materials such as concrete are nowadays the most widely used construction materials. However, the expansion of the cement industry might be a cause of concern due to the high amount of CO_2 emitted during the production process. Blending cement with supplementary cementitious materials (SCMs) is considered to be one of the most effective ways of reducing the environmental impact of the cement industry. Conventional and high-quality SCMs like granulated blast furnace slag and fly ash are being utilized to exhaustion. Hence, there is a shift and interest to search for alternative SCM sources due to supply-and-demand concerns in the future. One of the most promising alternative sources are calcined clays since they have not yet reached their full potential as cement replacement and clay is an abundant and widespread material resource.

Calcined clays other than metakaolin are hardly used as SCMs due to the complexity of clay minerals and ignorance of the underlying reaction mechanisms. To fill this knowledge gap, this study investigates the potential use of calcined clays from a mineralogical point of view by linking the characteristics of the untreated clays to the pozzolanic reactivity of the calcined clays. The key starting point of this study consists of a detailed chemical, mineralogical and physical characterization of both the raw and calcined material. To increase the reactivity of natural clays, the raw clay is calcined in a fixed-bed electrical furnace at temperatures ranging between 500°C and 900°C. The pozzolanic reactivity of the calcined clay is assessed by investigating the reaction between calcined clay and lime ($Ca(OH)_2$) and by identifying the hydration products that are formed.

The combined results of this study indicate the mineralogical composition of the starting material is one of the primary factors controlling the pozzolanic reactivity of the calcined clay. Especially two mineralogical features are critical: 1) the type of the dominant clay mineral, with its characteristic thermal behavior, and 2) the amount of these clay mineral and presence of impurities.

The tested pure reference clay types, consisting of 4 kaolinitic, 3 smectitic and 1 illitic clay, can be considered as the most common naturally occurring clay minerals. Kaolinite rich clays are highly reactive at a broad range of firing temperatures (500–900 °C), which are influenced by the degree of ordering of kaolinite. The smectitic clays possess a clear optimal calcination temperature of 800 °C. Trans vacant smectites are proven to be somewhat more reactive than cis vacant smectites. However, even at 800 °C, its reactivity is significantly lower compared to kaolinite. concersely, while the reactivity of kaolinite rich clays reaches a plateau value at 28 days, the reactivity of the smectitic clays continues to increase steadily up to 90 days. Hectorite and illite calcined at an optimal temperature of 800 and 900 °C respectively, exhibit poor pozzolanic reactivity.

Besides the clay type also the presence of non-clay minerals can have an effect on the pozzolanic reactivity. Even though inert materials like quartz, feldspar and muscovite have no direct influence on the pozzolanic reactivity, feldspar and muscovite enhance the sintering phenomenon upon calcination resulting in a coarser grain size and consequently a decrease of reactivity. Moreover,

several reactivity tests on artificial mixtures with a variable impurity content demonstrated that the quantity of the inert material can be negatively linearly correlated to the pozzolanic reactivity. Additionally the presence of up to 30% of calcite appears to increase the pozzolanic potential of the clay, especially at early stages of the hydration reaction.

The pozzolanic reaction rate is also influenced by physical parameters. The specific surface area of the calcined clay is an important parameter during the first 7 days of the reaction. Higher specific surface area results in a larger reaction surface and as a result the reaction rate increases significantly. Additionally the grain size of the calcined sample is a controlling parameter of the pozzolanic reactivity over longer periods of the reaction. The grain size of the calcined clay is influenced by the chosen calcination temperature and by the type and amount of both clay and non-clay minerals, since these factors determine the extent of the sintering effect upon calcination.

The observed correlations are combined in a mathematical model allowing to predict the pozzolanic reactivity of a natural clay based on the mineralogy of the raw sample and for the early stage also the specific surface area of the calcined material.

The effect of the addition of calcined clay on the reaction product assemblage could also be related to the mineralogical characteristics of the clays. The main hydration products that are formed in calcined clay-lime pastes are hydrated calcium aluminates and calcium silicate hydrate phases. Typically for Al-rich kaolinites strätlingite is formed from 7 days onwards. Calcite rich clays are marked by the formation of additional mono- and hemicarboaluminate at the expense of strätlingite. The quantity and the formation rate of the reaction products are mainly influenced by the amount of clay that is present and by the Si/Al ratio of the amorphous material.

SAMENVATTING

Portland cement gerelateerde materialen, zoals beton, behoren vandaag de dag ontegensprekelijk tot de meest gebruikte bouwmaterialen en zijn bijgevolg alomtegenwoordig. De groei van de Portland cementindustrie brengt echter ook ecologische implicaties met zich mee aangezien er tijdens het productieproces aanzienlijke hoeveelheden CO_2 vrijkomen. Een van de meest succesvolle manieren om de milieu impact in te perken is Portland cement mengen met aanzienlijke hoeveelheden cement vervangende materialen, ook wel puzzolanen of SCMs (Supplementary Cementitious Materials) genoemd. De meest gebruikte SCMs zijn artificiële producten zoals hoogovenslakken en vliegas. Het moet echter opgemerkt worden dat de voorraden van deze hoogwaardige puzzolane materialen eerder gering zijn en lokale reserves zijn vaak al volledig uitgeput. Een van de meest veelbelovende alternatieve SCMs zijn thermisch geactiveerde kleimineralen, ook wel gecalcineerde klei genoemd, aangezien deze beschikken over de vereiste puzzolane eigenschappen en klei bovendien een veel voorkomende natuurlijke grondstof is.

Desalniettemin zorgt de ondermaatse kennis van de onderliggende gecalcineerde klei-Portland cement reacties en de bijhorende reactieproducten ervoor dat ze nauwelijks als SCM gebruikt worden. Vandaar dat deze studie het potentieel van gecalcineerde kleien als puzzolaan onderzoekt vanuit een mineralogisch standpunt waarbij de karakteristieken van de originele klei gecorreleerd worden met de puzzolane reactiviteit van de gecalcineerde kleien. Deze kennis kan dan aangewend worden om het toekomstig gebruik van kleien als SCMs te optimaliseren. Een doorgedreven mineralogische, chemische en fysische karakterisering van zowel de onbehandelde als de gecalcineerde klei vormen dan ook de bakermat van deze studie. Om de puzzolane reactiviteit van natuurlijke kleien te optimaliseren worden deze eerst gecalcineerd door de klei te verhitten tot een temperatuur tussen de 500 en 900°C. Vervolgens wordt de reactie tussen de gecalcineerde klei en gehydrateerde kalk ($Ca(OH)_2$) en de nieuw gevormde reactieproducten gemonitord door middel van thermische analyse om zo de puzzolane reactiviteit van de gecalcineerde klei te evalueren.

Uit de resultaten van deze studie blijkt dat de puzzolane reactiviteit van de gecalcineerde klei grotendeels beïnvloed wordt door de mineralogische samenstelling van de onbehandelde klei. Hierbij kunnen twee parameters onderscheiden worden die cruciaal zijn namelijk: 1) het type van het dominant aanwezige kleimineraal, met zijn bijhorende unieke thermische eigenschappen, en 2) De kwantiteit van de aanwezige kleimineralen en de eventuele aanwezigheid van onzuiverheden.

Een selectie van 8 zuivere referentiestalen werd gemaakt bestaande uit 4 kaolinietrijke, 3 smectiet rijke en 1 illiet rijke klei. Deze kleien werden geselecteerd aangezien ze de meest voorkomende kleimineralen goed vertegenwoordigen. De kaoliniet rijke zijn het meest reactief en bezitten een brede range van optimale activatie temperaturen tussen 500 en 900°C. De kristalliniteit van kaoliniet beïnvloedt zowel de optimale calcinatie temperatuur als de reactiesnelheid in het vroege stadium van de reactie. De smectietrijke kleien worden gekarakteriseerd door een meer uitgesproken optimale activatie temperatuur van 800°C. Trans vacante smectieten blijken bovendien meer reactief

te zijn dan cis vacante smectieten. Toch is ook de reactiviteit voor trans vacante smectieten merkelijk lager dan voor kaoliniet rijke kleien. Hoewel de reactie snelheid voor smectiet rijke kleien lager is dan voor kaolinieten, blijft de reactiviteit van smectieten gestaag toenemen tot 90 dagen terwijl kaolinieten reeds hun plateau waarde na 28 dagen bereiken. Wanneer hectoriet en illiet gecalcineerd worden op hun optimale temperatuur van respectievelijk 800 en 900°C, blijft hun puzzolane reactiviteit beperkt.

Naast het type klei is ook de aanwezigheid van niet-kleimineralen van belang voor de puzzolane reactiviteit. Hoewel inerte materialen zoals kwarts, veldspaat en muscoviet geen directe invloed hebben op de puzzolane reactiviteit, zullen veldspaat en muscoviet wel het sintereffect dat plaats vindt tijdens het calcinatieproces versterken. Hierdoor zal de korrelgrootte van het staal toenemen en bijgevolg daalt de reactiviteit. Daarnaast toonden de resultaten van de reactiviteitstesten van mengsels met een variabel gehalte aan onzuiverheden aan dat de hoeveelheid inert materiaal negatief lineair kan gecorreleerd worden met de puzzolane reactiviteit. De aanwezigheid van calciet (<30%) kan bovendien de puzzolane reactiviteit versterken, met name gedurende de eerste 14 dagen van de reactie.

Naast de mineralogische parameters hebben ook de fysische eigenschappen van het materiaal een duidelijke invloed op de puzzolane reactiviteit. Het specifiek oppervlak van de gecalcineerde klei beïnvloedt eveneens de reactiesnelheid gedurende de eerste 7 dagen van de reactie. Een hoger specifiek oppervlak resulteert namelijk in een groter reactieoppervlak waardoor de reactiesnelheid significant kan verhoogd worden. Daarnaast heeft ook de korrelgrootte distributie van het staal een belangrijke invloed op de reactiviteit over de gehele reactieperiode. De korrelgrootte van het gecalcineerde staal wordt hoofdzakelijk beïnvloed door de gekozen calcinatie temperatuur en door het type en de hoeveelheid van de aanwezige kleimineralen en onzuiverheden, aangezien beide factoren de graad van het sintering fenomeen tijdens het calcinatie proces bepalen.

De opgesomde resultaten en correlaties werden gesynthetiseerd in een mathematisch regressie model dat toelaat om de puzzolane reactiviteit te voorspellen aan de hand van de mineralogische samenstelling van het onbehandelde staal en voor de korte reactietermijn eveneens het specifieke oppervlak van de gecalcineerde klei.

Het effect van de toevoeging van gecalcineerde klei op de assemblage van reactieproducten kan eveneens gerelateerd worden aan de mineralogische eigenschappen van de gebruikte kleien. De voornaamste reactieproducten die gevormd worden in het gecalcineerde klei-kalk systeem zijn gehydrateerde calcium aluminaat en gehydrateerde calcium silicaat fasen. Strätlingiet wordt typisch gevormd in aluminiumrijke kaolinieten vanaf een uithardingstijd van 7 dagen. Calcietrijke kleien worden gekenmerkt door de vorming van extra mono- en hemicarboaluminaat ten koste van strätlingiet. De hoeveelheid en de vormingssnelheid van de reactieproducten worden hoofdzakelijk beïnvloed door de hoeveelheid klei die aanwezig is en door het Si/Al gehalte van de amorfe fase van de gecalcineerde klei.

LIST OF MINERALS AND ABREVIATIONS

MINERALS

Albite	$NaAlSi_3O_8$
Alkali-feldspar	$(Na,K)AlSi_3O_8$
Anatase	TiO_2
Anorthite	$CaAl_2Si_2O_8$
Biotite	$K(Mg, Fe^{2+})_3AlSi_3O_{10}(OH,F)_2$
Calcite	$CaCO_3$
Chlorite (group)	$(Mg,Fe)_3(Si,Al)_4O_{10}(OH)_2.(Mg,Fe)_3(OH)_6$
Dolomite	$CaMg(CO_3)_2$
Gibbsite	$Al(OH)_3$
Glauconite	$(K, Na)(Fe^{3+}, Al, Mg)_2(Si, Al)_4O_{10}(OH)_2$
Goethite	$FeOOH$
Gypsum	$CaSO_4.2H_2O$
Halloysite	$Al_2Si_2O_5(OH)_4$
Hematite	Fe_2O_3
Illite	$K_{0.95}$ $(Al_{1.81}, Fe_{0.01}, Mg_{0.19})$ $(Si_{3.25}, Al_{0.75})O_{10}(OH)_2$
Kaolinite	$Al_2Si_2O_5(OH)_4$
Muscovite	$KAl_2(Si_3AlO_{10})(OH,F)_2$
Microcline	$KAlSi_3O_8$
Plagioclase	$Na_{1-x}Ca_xAl_{1+x}Si_{3-x}O_8$ with $0 < x < 1$
Quartz	SiO_2
Pyrite	FeS_2
Ripidolite	$Mg_{3.75}Fe^{2+}_{1.25}AlSi_3AlO_{10}(OH)_8$
Smectite Group:	
Montmorillonite	$(Na, Ca)_{0.33}(Si_4(Al_{1.67}, Mg_{0.33})O_{10}(OH)_2*nH_2O$
Hectorite	$Na_{0.4}Mg_{2.7}Li_{0.3}Si_4O_{10}(OH)_2$
Spinel	$MgAl_2O_4$
Zincite	ZnO

CEMENT NOTATION

CaO	C	calcium oxide
SiO_2	S	silicon dioxide
Al_2O_3	A	aluminum oxide
Fe_2O_3	F	ferrous iron oxide
K_2O	K	potassium oxide
H_2O	H	water
SO_3	Š	sulphur trioxide
CO_3	Č	carbon dioxide

HYDRATION PHASES

AFm phases:		
Hemicarboaluminate	$Ca_4Al_2O_7(CO_2)_{0.5}.\ 12H_2O$	$C_4A\ Č_{0.5}H_{12}$
Monocarboaluminate hydrate	$Ca_4Al_2O_7(CO_2).\ 11H_2O$	$C_4A\ ČH_{11}$
Strätlingite (hydrated gehlenite)	$Ca_2Al_2SiO_7.\ 8H_2O$	C_2ASH_8
Tetracalcium aluminate hydrate	$Ca_4[Al(OH)_6]_2.\ 7H_2O$	C_4AH_{13}
AFt phases:		
Ettringite	$Ca_6Al(SO_4)_3(OH)_{12}.\ 26H_2O$	$C_6AS_3H_{32}$
Alite (Hatrurite)	Ca_3SiO_5	C_3S
Belite (Larnite)	Ca_2SiO_4	C_2S
Calcite	$CaCO_3$	C Č
Calcium silicate aluminate hydrate	$CaO.\ Al_2O_3.\ SiO_2.\ H_2O$	C-A-S-H
Calcium silicate hydrate phase	$CaO.\ SiO_2.\ H_2O$	C-S-H
Hydrogarnet (katoite)	$Ca_3Al_2(OH)_{12}$	C_3AH_6
Portlandite	$Ca(OH)_2$	CH

ABREVIATIONS

ASTM	American Society for Testing and Materials
BET	Brunauer Emmett Teller
DTG	First derivate of Thermogravimetry
DSC	Differential Scanning Calorimetry
FTIR	Fourier Transform Infrared (spectroscopy)
HI	Hinckley Index
ICP-OES	Inductively Coupled Plasma Optical Emission Spectrometry
LOI	Loss On Ignition
MAS NMR	Magic Angle Spinning Nuclear Magnetic Resonance (spectroscopy)
OPC	Ordinary Portland Cement
PSD	Particle size distribution
SAI	Strength activity index
SCM	Supplementary cementitious material
SSA	Specific Surface Area
TGA	Thermogravimetric Analysis
XRD	X-Ray Diffraction

2θ to d-values according to Bragg's law: λ=2dsinθ, with CuKα (λ=1.5418Å)

2θ	d-value	2θ	d-value	2θ	d-value	2θ	d-value
1	88.34	21	4.23	41	2.20	61	1.52
2	44.17	22	4.04	42	2.15	62	1.50
3	29.45	23	3.87	43	2.10	63	1.48
4	22.09	24	3.71	44	2.06	64	1.45
5	17.67	25	3.56	45	2.01	65	1.43
6	14.73	26	3.43	46	1.97		
7	12.63	27	3.30	47	1.93		
8	11.05	28	3.19	48	1.90		
9	9.83	29	3.08	49	1.86		
10	8.85	30	2.98	50	1.82		
11	8.04	31	2.88	51	1.79		
12	7.38	32	2.80	52	1.76		
13	6.81	33	2.71	53	1.73		
14	6.33	34	2.64	54	1.70		
15	5.91	35	2.56	55	1.67		
16	5.54	36	2.49	56	1.64		
17	5.22	37	2.43	57	1.62		
18	4.93	38	2.37	58	1.59		
19	4.67	39	2.31	59	1.57		
20	4.44	40	2.25	60	1.54		

TABLE OF CONTENTS

CHAPTER 1

CONTEXT AND AIMS

1.1 GENERAL

Portland cement-based materials such as concrete are nowadays the most widely used construction materials. Due to a relative low production cost and versatile application of concrete, its main constituent Portland cement has become a desired material. The annual global production of cement has risen the last 10 years by more than 50% and in 2015 4.2Bt of cement was produced (Cement Industry, 2015). Moreover, the economic growth of developing countries will result in a further increase of the total global cement production. This further expansion of the cement industry is a cause of concern, since the production process is very energy-intensive and has a considerable environmental impact.

During the production process of Portland cement clinker, limestone ($CaCO_3$) is decomposed into calcium oxide and the green house gas carbon dioxide. The amount of CO_2 released upon the decarbonation of calcium carbonate counts for 50 – 60% of the total amount of CO_2 emitted during the production process of cement. The other 40-50% can be attributed to the combustion of fossil fuels that are needed to heat the kiln to the desired temperature of 1450°C and to a minor extent to the grinding and transportation. On average for each ton of cement that is produced approximately 0.85 ton of CO_2 is emitted (Gartner, 2004). As a consequence the cement industry accounts for around 4 % of the total global greenhouse gas emissions and up to 8 % of the total global anthropogenic CO_2 emissions (Barcelo et al., 2013; Damtoft et al., 2008).

In response to the environmental concerns about the high CO_2 emissions, political decisions resulted in the 2050 low-carbon economy proposal of the European union which stated that the industrial CO_2 emission should be reduced by 80% in 2050 compared to the 1990 levels (European Commision, 2011). As a result the cement industry faces a huge challenge to decrease their CO_2 emission without diminishing the quality of the Portland cement produced. Different alternatives to reach this goal have already been suggested whereby both the applied process and the type of fuels have been optimized. However the upper limit of the energy efficiency is nearly reached and the potential to advance becomes rather small.

However, blending cement with supplementary cementitious materials (SCMs) is considered to be one of the most effective ways of reducing the environmental impact of the cement industry (Gartner, 2004; Juenger and Siddique, 2015; Lothenbach et al., 2011). Conventional and high-quality SCMs like granulated blast furnace slag from iron production and fly ash from coal combustion of electricity production face complete utilization (Snellings et al., 2012). There is an interest to search for alternative SCM sources due to supply-and-demand concerns in the future. One of the most promising alternative sources are calcined clays since they have not yet reached their full potential as

cement replacement and clay is an abundant and widespread material which can lower transportation costs (Schneider et al., 2011). The production process of calcined clay is less energy intensive and more environment-friendly due to lower firing temperatures and the absence of a decarbonation reaction. The calcination of clays occurs in the temperature range of 600 and 850 °C, and results in the dehydroxylation of the clay whereby an amorphous phase is formed. The Si and Al in this phase can chemically react at ambient temperatures with $Ca(OH)_2$ (portlandite), which is formed during cement hydration, in the presence of water to form compounds that posses cementitious properties.

Many studies have already demonstrated the effectiveness of calcined clays, particularly for kaolinitic clays to produce metakaolin with increased pozzolanicity, i.e. reactivity with portlandite (Al-Rawas and Hago, 2006; Fernandez et al., 2011; He et al., 1994; Sabir et al., 2001; Tironi et al., 2012) However, calcined clays other than metakaolin are hardly used as SCMs due to the complexity of clay minerals and ignorance of the underlying reaction mechanisms.

Furthermore, only limited studies are conducted to examine pure calcined clays, like the highly reactive metakaolin. Most clays in nature, however, are mixtures of different clay minerals (kaolinite, illite, montmorillonite and mixed layers) and a large proportion of impurities of non-clay materials, such as quartz, calcite, feldspars and mica (Tironi et al., 2012). Consequently the pure clays are not representative for the wide variety of clay deposits. Moreover, pure clays are not economical for cement industry (He et al. 1994; Lara et al. 2011). Pure calcined clays are more costly than other commonly used SCMs due to restricted, regional availability and an energy-intensive manufacturing process. Due to these limitations, there is increasing interest in implementing blended-kaolinite clay minerals that have a widespread availability, as a less expensive alternative to metakaolin (Fernandez et al., 2011). Hence the main aim of this study is to investigate the potential use of calcined clays from a mineralogical point of view by linking the characteristics of the untreated clays to the pozzolanic activity of the calcined clays. To achieve this goal several issues, discussed in the subsequent paragraph, have to be solved and examined in detail.

1.2 OBJECTIVES

The main objectives of this thesis can be summarized as follows:

Obj. 1: Clarify the differences in reactivity based on the structural and physical alterations that occur upon calcination

Determine the pozzolanic reactivity and the optimal calcination temperature of a clay rich material.

Obj. 2: Identify the parameters that control the pozzolanic reactivity and optimal activation temperature of a calcined clay

Obj. 3: Study the impact of the type and composition of the clay on the assemblage of the reaction products

Obj. 4: Predict the reactivity of a natural clay based on its characteristics

1.3 SCOPE OF THE RESEARCH

An overview of the research strategy is given in Figure 1.1. First of all in several studies the clays are often poorly characterized and only a rough estimation of the mineralogical composition is made. A detailed physical, chemical and mineralogical characterization and comparison of the raw and calcined clays will provide a better understanding of the changes that occur upon calcination to clarify the changes in reactivity between different clays and clay minerals. Furthermore this characterization is crucial to determine which of these characteristics, that are controlled by the type of the raw material and the thermal treatment, will also have a significant influence on the reactivity. Regarding mineralogy it is also important to know the effect of the presence of mineral impurities on the pozzolanic reactivity. Furthermore not only the pozzolanic reactivity but also the optimal activation temperature can be influenced by the characteristics of the clay. Therefore the optimal activation temperature for different clay types and clay mixtures will be determined.

The eventual performance of the calcined clay as lime-based binder will be influenced by the type and proportion of the reaction products that are formed. The type of clay mineral and presence of impurities can significantly influence both the type of reaction products and the time at which they are formed. Therefore it is important to monitor the reaction product assemblage of the calcined clay lime pastes over time.

Finally a more general acceptance and use of calcined in blended cements can be stimulated when their reaction with lime is better understood and reactivity could be predicted. Therefore providing a tool that allows estimating the pozzolanic reactivity of natural occurring clay based on its characteristics would be a great help.

1.4 OUTLINE OF THE THESIS

The thesis can be subdivided into four major parts. The first part comprises an overview of the background regarding calcined clays and the applied methodology. The second part focuses on gathering the input of the mineralogical predictive model and is based on the analyses of pure reference clays and artificial mixtures in order to understand the reaction processes and the controlling parameters. In the third part natural clays with various mineralogical compositions are taken into consideration and their pozzolanic potential is assessed. The last part includes the discussion regarding the established model and general conclusions and perspectives.

Part I
Chapter 2 presents the general background of calcined clays and their use as supplementary cementitious materials. Furthermore a detailed literature review was performed in order to gain insight in the present day state-of-the-art regarding calcined clays and their optimal activation temperatures and reaction products. Additionally the potential of calcined clays and the contribution to the decrease of the environmental impact of the CO_2 emission is discussed. In chapter 3 the applied methodologies are discussed and a comparison and validation of two different reactivity tests is given.

Part II
In Chapter 4 the thermal behavior and reactivity of pure reference clays is studied in order to understand the ongoing reaction processes in more detail and determine the main parameters that influence the reactivity without interference of other mineral impurities. However in nature clays are rarely completely pure, and therefore the influence of mineral impurities was evaluated in chapter 5 by using artificial mixtures.

Part III
Chapter 6 focuses on the reactivity of naturally occurring kaolinitic rich clays while chapter 7 includes smectitic clays. Chapter 8 is a case study of the Latneskoye clay deposits that mainly consist of kaolinite rich clays with some minor smectite overburden samples.

Part III
Chapter 9 combines the experimental results derived from Chapters 4 and 5 and combines it into a mathematical mineralogical model that allows predicting the pozzolanic reactivity of given clay. This model is evaluated with the natural clay samples that were investigated in Chapter 6, 7 and 8. In Chapter 9 the main research results regarding the pozzolanic reactivity of calcined clays are summarized and future perspectives are given to indicate the overall implications and conclusions of the work.

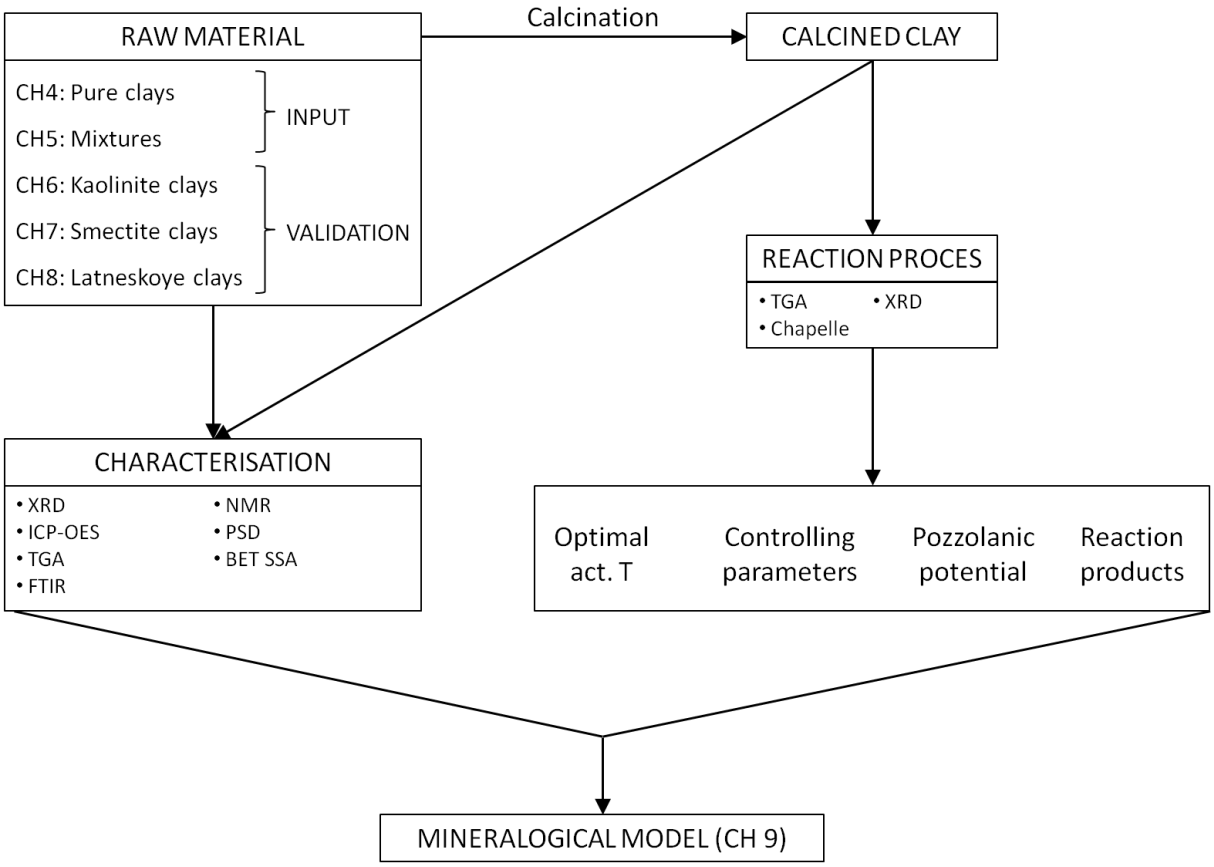

Figure 1.1: *Overview of the research strategy*

CHAPTER 2

BACKGROUND

2.1 CLAYS AND CLAY MINERALS

2.1.1 INTRODUCTION

Clay minerals belong to the phyllosilicate group and usually occur in a particle size of 2 µm or less (Moore and Reynolds, 1997). Clay minerals are the result of the chemical weathering of other silicates that are present in rocks, mainly feldspar, micas, pyroxenes and amphiboles. After weathering they are often the most abundant component in sedimentary deposits and soils (Garrels and Mackenzie, 1971). There is no uniform definition for clay or clay minerals, however the Clay Minerals Society recommends the use of the following definition: "*Clay is a naturally occurring material composed primarily of fine grained minerals, which is generally plastic at appropriate water contents and will harden when dried or fired*" (Guggenheim et al., 1995). The referring to fine grained materials can be misleading as not all disciplines maintain the same boundaries regarding grain size. Moreover, when referring to clay, the clay sized fraction <2 µm is taken into account and not the actual composition (Klein et al., 2002). However, clay minerals can vary in grain size and can also be larger than 2 µm. Furthermore non-clay minerals can also occur as particles with a diameter smaller than 2 µm. The typical physical characteristics of clay, like their platy morphology, layered structure and their plasticity can mainly be correlated to the structure and chemical composition of the clay mineral.

2.1.2 STRUCTURE OF CLAY MINERALS

Clay particles are composed of tens to hundreds of alternating tetrahedral and octahedral sheets. The tetrahedral sheet (T) contains Si^{4+} cations that are surrounded by four oxygen ions. In each tetrahedron three of four oxygen ions are shared with the neighboring units to form a (pseudo-) hexagonal network (Figure 2.1). The octahedral sheets are composed of Al^{3+} in 6-fold coordination with oxygen or hydroxyl (OH^-) groups. The octahedra are joined by sharing all of their hydroxyl groups with each other. The tetrahedral sheet can then be linked to the octahedral sheet by sharing the apical oxygen atoms of the tetrahedra. The hydroxyl groups of the octahedral sheets are positioned in the pseudo-hexagonal cavity of tetrahedral sheet.

The stacking arrangement of the tetrahedral and octahedral sheets determines the clay mineral group. Two main groups can be distinguished. The first comprises TO or 1:1 clays whereby 1 tetrahedral sheet is combined with one octahedral sheet. Clays that belong to this group are kaolinite, halloysite and serpentine. For the second group the clay layer is formed by sandwiching one octahedral sheet between two tetrahedral sheets resulting in TOT or 2:1 clays. This group is by

far the largest group and contains illite, smectite, vermiculite and micas. A third possibility is seen for the clay mineral chlorite whereby the interlayer space of a 2:1 clay is filled with an additional octahedral layer resulting in a TOTO or 2:1:1 clay. Isomorphic substitution often occurs in clay minerals. In the tetrahedral layer a common substitution is the replacement of Si^{4+} by Al^{3+}. In the octahedral layers divalent cation (Mg^{2+}, Fe^{2+} and Mn^{2+}) can substitute for Al^{3+} whereby a negative layer charge is created. This layer charge is compensated by incorporating cations in the interlayer space.

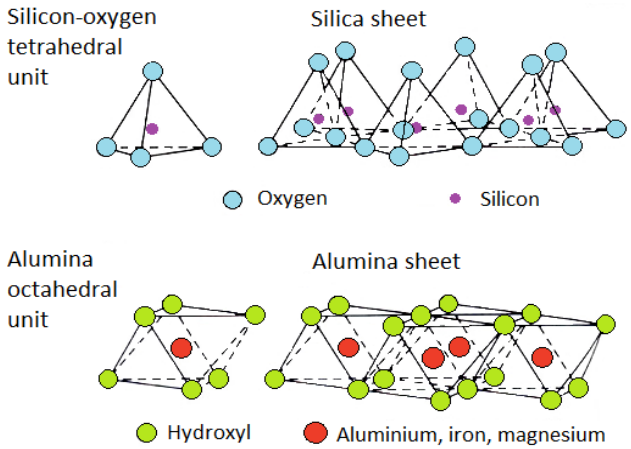

Figure 2.1: *The silicon-rich tetrahedral sheet and alumina-rich octahedral sheet that form the building stones of clay layers (modified after Grim, 1968).*

Within the two main groups (TO and TOT), clay minerals can be further subdivided depending on the cation present in the octahedral sheet. When the octahedral sheet contains trivalent cations like Al^{3+} or Fe^{3+} only two out of three octahedra are filled and these clay minerals are classified as dioctahedral. Less commonly, divalent cations, like Mg^{2+} and Fe^{2+} fill all octahedral sites and a tri-octahedral clay is formed. The dioctahedral clay can be further differentiated depending on the specific occupancy of the octahedral site. In dioctahedral clay only two of the three octahedra are occupied and as a result vacancies are present in the octahedral sheet. Depending on the position of the hydroxyls the octahedra of the octahedral sheet can either be cis- or trans-vacant, as shown in figure 2.3. For a cis-vacant clay (cv) one of the cis positions is left empty. A final differentiation is based on the displacement of the layers in respect to each other. The displacement of the layer can be done according to a systematic pattern whereby poly-types are created. Random rotation or translation of the layers causes more structural disorder of the clay mineral (such as seen in the disordering of kaolinite).

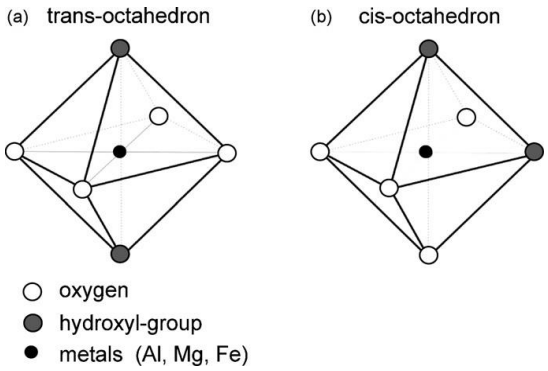

Figure 2.2: *(a)Trans- and (b) cis-octahedra with various positioning of the hydroxyl groups (modified after Wolters and Emmerich, 2007).*

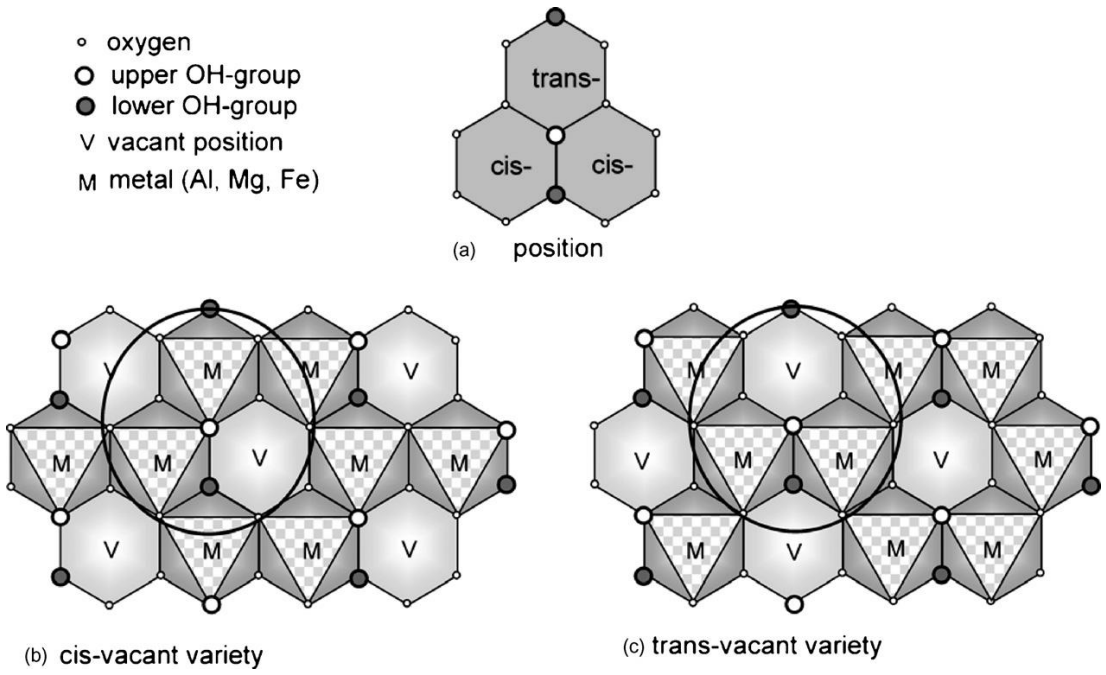

Figure 2.3: *Projection perpendicular to the c-axis of the octahedral sheet of a dioctahedral 2:1 clay mineral. (a) Trans (M1)- and cis (M2)-positions with respect to the location of the hydroxyl groups, (b) the cis-vacant (cv) variety, and (c) the trans-vacant (tv) variety (modified after Wolters and Emmerich, 2007).*

The structures of the three main clay minerals that are encountered in this research are described in more detail. The main characteristics of the different clays are summarized in Table 2.1. Kaolinite minerals belong to the 1:1 clay group and its structural unit is therefore composed of one octahedral and one tetrahedral sheet (Figure 2.4). The basal spacing in the c direction is about 7.16 Å. In the plane of the shared atoms, only one third are hydroxyls while two-third are oxygen atoms. The linkage of the octahedral and tetrahedral sheets can only take place as the angles and distances between the oxygen atoms are slightly deformed (Meunier, 2005). This distortion of the tetrahedral network explains why kaolinite is triclinic instead of monoclinic with pseudo hexagonal habitus. High ordered kaolinite particles occur in booklets containing nicely shaped hexagonal plates while less ordered particles will be smaller with an irregular shape. The dimensions of kaolinite particles can therefore vary significantly, with a range of the lateral dimension between 0.1 and 4 μm. The bounding between two successive layers is a combination of hydrogen bounds and Van der Waals forces. The structural formula of kaolinite is $Al_2Si_2O_5(OH)_4$ and is di-octahedral. The negative charge of the oxygen framework is balanced by the positive charge of the Al^{3+} cations present in the octahedral layer. Substitution in the tetrahedral and octahedral sheet is uncommon. As a result the main TO unit is electric neutral. Kaolinite has two poly-type variations, dickite and nacrite (Bailey, 1963), and a hydrated variety, halloysite.

Table 2.1: *Characteristics of the most abundant clay minerals kaolinite, illite and montmorillonite.*

Clay mineral	Group	Crystal system	(001) d-spacing	Ideal structural formula	Octahedral occupancy	Interlayer bond
Kaolinite	1:1 (TO)	Triclinic	7.2	$Al_2Si_2O_5(OH)_4$	Dioctahedral	O-OH (Strong)
Illite	2:1 (TOT)	Monoclinic	10	$K_{0.95}$ ($Al_{1.81}$, $Fe_{0.01}$,$Mg_{0.19}$) ($Si_{3.25}$, $Al_{0.75}$)$O_{10}(OH)_2$	Dioctahedral	K ions (Strong)
Montmorillonite	2:1 (TOT)	Monoclinic	>9.5	$(Na, Ca)_{0.33}(Si_4(Al_{1.67}, Mg_{0.33})O_{10}(OH)_2*nH_2O$	Di- and triochtahedral	O-O (Weak) Swelling clay

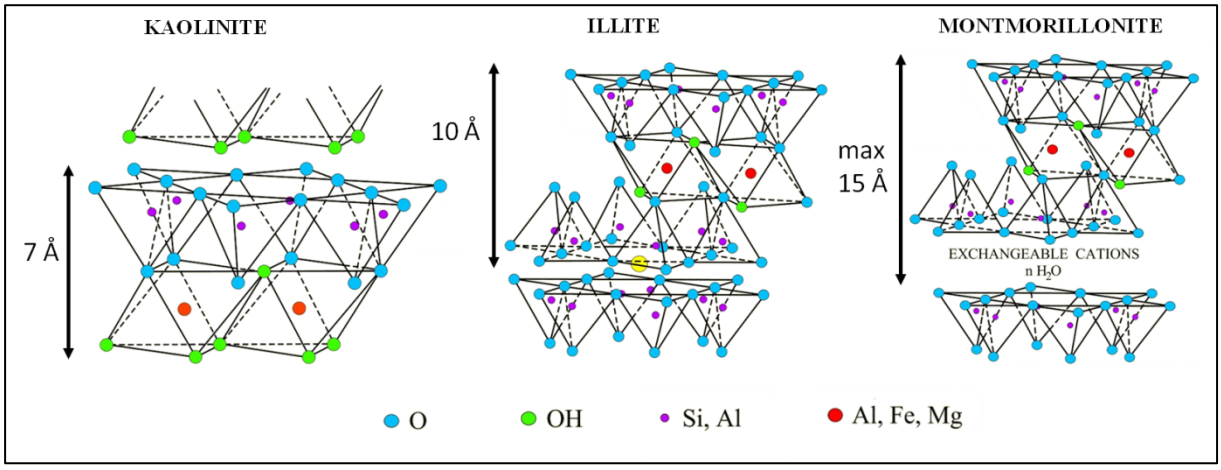

Figure 2.4: *Structure of the 3 main clay minerals kaolinite (TO), illite (TOT) and montmorillonite (TOT) (modified after Grim, 1968).*

Illite is a 2:1 dioctahedral clay mineral comprised of a gibbsite-like octahedral sheet sandwiched between two tetrahedral layers (Figure 2.4). Due to its similarity with the muscovite (mica) structure Illite is often called hydro mica. The building unit of illite has cell dimensions according the c direction of 10 Å. Illitic particles are generally fine grained with lateral dimension that are comparable to those of kaolinite. The thickness of the plates can however be much smaller and values as low as 30 Å have been recorded. High-purity deposits of illite are uncommon and therefore illite is defined as a dioctahedral 10 Å mineral containing less than 5% of expandable layers (Meunier, 2005). The boundary of 5% is set because the presence of only 5% or less expandable layers is hardly detectable by glycolation, especially when the sample contains multiple clay minerals (Adriaens, 2015). Illite is marked by two types of isomorphic substitution. One fourth of the Si^{4+} atoms are replaced by Al^{3+}. To assure the electric neutrality of the structure the cation K^{+} is incorporated in the interlayer space. The strong interlayer bonding of potassium results in the fact that illite does not swell in the presence of polar liquids and its basal spacing remains fixed at 10 Å. A second substitution that can occur is the partial replacement of aluminum in the octahedral sheets by magnesium or iron (Moore and Reynolds, 1997). The general chemical formula of illite can be written as follows according to Środoń et al. (2009): $K_{0.95}(Al_{1.81}, Fe_{0.01}, Mg_{0.19})\ (Si_{3.25}, Al_{0.75})(O_{10}(OH)_2$.

Smectite clay minerals also belong to the 2:1 clay minerals and contain both di- and trioctahedral clays. The dioctahedral subgroup is the most common and contains the clay mineral species montmorillonite. The dioctahedral clays are marked by the presence of trivalent cations such as Al^{3+}, while trioctahedral clays contain divalent cations like Mg^{2+}. Hectorite is a typical trioctahedral magnesium rich smectite variety. For montmorillonite, the resemblance with the structure of illite is striking. The main difference is the occupation of the interlayer space (Figure 2.4). For montmorillonite different cations like Na^{+} and Ca^{2+} form the bonding between the successive TOT clay layers and act as a counterbalance of the charge deficiencies. Since these bonds are rather weak the cations can easily be exchanged and water or other polar liquids can be adsorbed. The d-spacing will increase when the amount of adsorbed liquid is increased and as a result the basal spacing in the c direction can vary from 9 to 15 Å. This phenomenon can be linked to the swelling behavior typical for montmorillonite. The chemical composition of montmorillonite is very variable and the ideal structural formula according to Moore and Reynolds (1997) is: $(Na, Ca)_{0.33}(Si_4(Al_{1.67}, Mg_{0.33})O_{10}(OH)_2*nH_2O$.The dimensions of montmorillonite crystallytes are usually much smaller than for kaolinite and illite. The lateral dimension is often smaller than 1 µm, while the thickness lies between 1 and 20 nm. This indicates montmorillonite is a very fine grained mineral and can mostly be found in the clay fraction <2 µm.

2.2 SUPPLEMENTARY CEMENTITIOUS MATERIALS

Supplementary cementitious materials (SCMs) are used to partially replace Portland clinker in the production of cement to lower the CO_2 emission and the energy costs of the cement industry (Lothenbach et al., 2011; Snellings et al., 2012). Furthermore the addition of these materials can even improve durability and sustainability of the cement. The use of SCMs can be traced back to ancient Roman times, were volcanic ashes were used. Silica and alumina rich materials were finely ground and mixed with slaked lime and water to improve the formation of cementitious binder and thereby to improve the mortar's properties. Due to the recent environmental concerns the blending of cement with supplementary cementitious materials has received renewed attention. Often 20% of the Portland cement is substituted by mineral admixtures (Habert et al., 2010), however, appropriate replacement levels depend mainly on the type of SCM and can vary between 3 and 95% (European committee for standardization, 2004).

The supplementary cementitious materials can be subdivided into two groups based on their reaction behavior and can be seen as either latent hydraulic or pozzolanic binders. Latent hydraulic binders react and harden directly when submerged in water, which is the case for iron blast furnace slag and calcareous fly ash (Lang, 2002; Metha, 1989). Pozzolanic materials can only react in the presence of both water and lime. Initially the name pozzolan was derived from a town in the bay of Naples called Pozzuoli that provided the highly reactive weathered ash from the Vesuvius. Nowadays the term pozzolan is used for all reactive aluminosilicate materials that are either of natural or industrial origin and react with calcium hydroxide when blended with water to form new cementitious phases.

According to the ASTM C618 a pozzolanic material can be defined as: "*a siliceous or siliceous and aluminous material which, in itself, possesses little or no cementitious value but which will, in finely divided form and in the presence of moisture, react chemically with calcium hydroxide (lime) at ordinary temperature to form compounds possessing cementitious properties*" (Metha, 1987).

Supplementary cementitious materials can be classified according to their generic characteristics and can be either natural or artificial (Figure 2.5). The first group needs little processing and only the particle size is controlled by grinding and sieving steps. Typical examples of this group are pyroclastic rocks and siliceous sedimentary rocks (Snellings et al., 2012). The second group comprises materials that underwent structural modifications as a result of an industrial process. These materials can be made deliberately, for instance by thermal activation or it can be industrial by-products like blast furnace slag, fly ash, silica fume or rice husk ash.

The origin of the material can however not directly be related to the pozzolanic potential of the material since natural materials with similar origin can have various physical and chemical characteristics. These physico-chemical properties have a much greater influence on the hydraulic or pozzolanic reactivity of the materials than their origin. Therefore, the chemical characteristics of the most common SCMs are relatively compared to each other by plotting their CaO-SiO_2-Al_2O_3 ratios in a ternary diagram (Figure 2.6). All SCM groups consist of a large variety in composition and two generically different SCMs can show a significant overlap, as can be seen for fly ash and natural pozzolans. The two most important SCM groups of today's cement industry are latent hydraulic blast furnace slag and fly ash. Calcined clays like metakaolin show an overlap with the composition of natural pozzolans. Both SCMs are generally depleted in CaO and the SiO_2 content is slightly higher than the Al_2O_3 content.

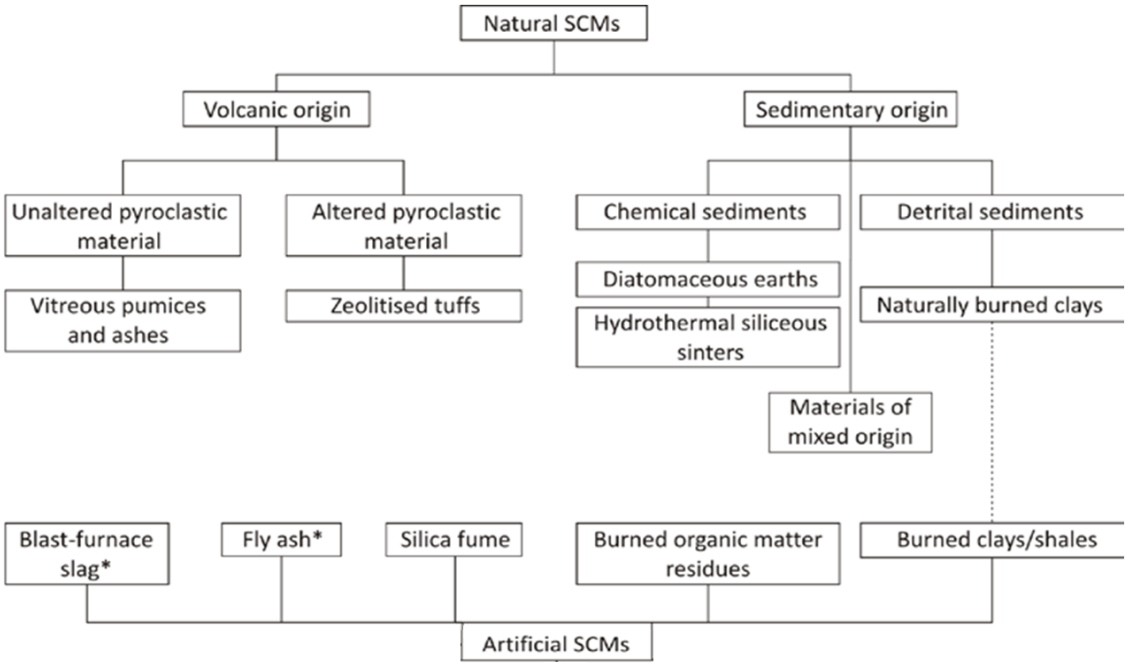

Figure 2.5: *General generic classification of SCMs. * marks the materials that can act as (latent) hydraulic binder, while the other materials are characterized by pozzolanic reactivity (modified after* Massaza, 2009*).*

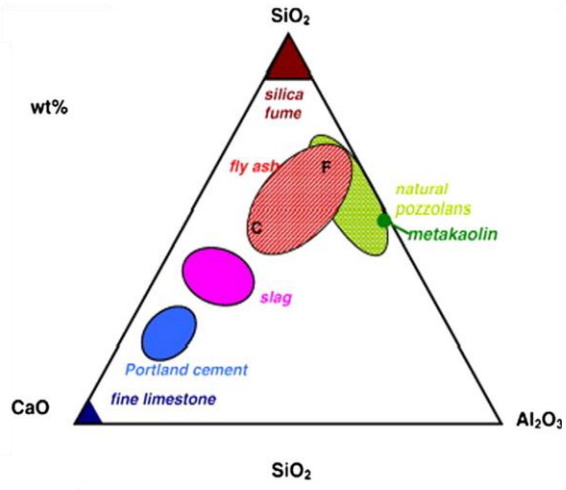

Figure 2.6: *CaO–Al_2O_3–SiO_2 ternary diagram (wt% based) of the most common SCM groups and Portland cement (Lothenbach et al., 2011).*

2.3 CALCINED CLAYS AS SUPPLEMENTARY CEMENTITIOUS MATERIAL

The pozzolanic activity of untreated clays has been studied in the past and even though they are promising in long-term projects like nuclear waste barriers (Müller, 2005), they gave unsatisfactory results for cement applications (He et al., 2000). The stable crystal structure of clay minerals and their platy morphology in combination with a high specific surface area, which results in a high water to binder ratio, are the cause of the low pozzolanic potential of untreated clays (He et al., 2000). A common process to increase the pozzolanic activity of these clays is by thermal treatment, also called calcination. In ancient times crushed potsherds and ceramic waste material was often used to be blended with lime to enhance a mortars properties (Snellings et al., 2012; Spence and Cook, 1983). The first research reports regarding the use of calcined clays date back to the 1950's, when Mielenz

et al. (1950, 1951) studied the effect of calcination on natural pozzolans. In the 1960's calcined kaolinite, or metakaolin, was used in large construction units as reported by Ramachandran (1996) and Saad et al. (1982). From the mid 1990's the amount of studies regarding calcined clays increased significantly, but nevertheless the use of calcined clays in cement industry remains limited compared to other SCMs, mainly due to the complexity of clay minerals. The worldwide availability and the high number of clay resources make that calcined clays are rather unique in comparison to the other SCMs.

2.3.1 CLAY ACTIVITION

To achieve good pozzolanic properties the clay needs to be activated by modifying its original crystalline structure. Mechanical activation processes include attrition milling whereby the clay, present as a slurry, is directly agitated and both impact and liquid shearing forces are present (Szegvari and Yang, 1999). As a result not only the grain size is reduced but the clay is also delaminated and as a result its structure becomes more open (Baudet et al., 1999; Mitrović and Zdujić, 2014). Other milling techniques are high-energy ball milling during which the clay particles are disintegrated while prolongation of the milling time results in amorphisation (Vdovic et al., 2010). Chemical activation can be achieved by adding alkali rich solutions whereby the solubility of silica and alumina in the system is improved (Alonso and Palomo, 2001; Elert et al., 2008; Jiang et al., 2008). The most effective technique to activate clay minerals is by thermal activation, also called calcination.

During calcination the clay is heated to a certain temperature to remove the structurally bound water whereby the clay structure is modified and a less ordered phase is created. This phenomenon is referred to as the dehydroxylation of clay minerals. During the heating process several stages can be distinguished. Water removal at low temperature (30-60°C) is generally reversible and has no permanent influence on the mineral structure (Karathanasis, 2008). During the following step, dehydration takes place and the adsorbed water is released at temperatures below 300°C. This step is especially noticeable for swelling 2:1 clays like montmorillonite, since they release their water situated in the interlayer space between two TOT layers.

Between 500 and 800°C, the structurally bound water, present as hydroxyl groups in the octahedral sheet, is removed. Because the OH groups formed the bound between the octahedral and tetrahedral sheets, their removal leads to a full or partial collapse of the clay structure forming a more disordered metastable clayey phase. This newly formed phase is no longer purely crystalline and can be classified as semi-crystalline, in case of partial dehydroxylation, and amorphous when the entire clay structure has collapsed. The metastable phase of kaolinite is called metakaolinite and becomes completely amorphous after calcination at a sufficiently high temperature. As such, Si and Al become more available to react with Ca in lime or cement to form new cementitious phases. Furthermore the calcination process has a positive effect on the workability of the paste since the water demand of the calcined clay is decreased compared to untreated clay.

The dehydroxylation temperature is, however, unique for each clay mineral and is not only determined by the bonding of the hydroxyl groups, but also by the crystallinity and the grain size distribution (Fernandez et al., 2011; He et al., 1994). In addition a higher firing temperature results in an increase of particle agglomeration and crystallization of inactive high-temperature phases (Snellings et al., 2012). Therefore it is important that the calcination temperature is well chosen in order to be sufficiently high to assure complete dehydroxylation of the clay mineral, but low enough so that the recrystallisation temperature is not yet reached. Furthermore the recrystallisation temperature is characteristic for the type of clay mineral. For kaolinite, for example, the crystalline phase mullite can form at 950°C, while for illite and smectite recrystallisation can already occur at 850°C (He et al., 1994; Liebig and Althaus, 1997).

Additionally also the influence of the thermal treatment on the grain size is controlled by the type of clay mineral. Kaolinitic clays are less affected than 2:1 Al-clays like illite and smectite. Nevertheless all three clays are characterized by a coarsening of the particles as the result of the combined effect of agglomeration and sintering. Agglomeration of the clays can already start at low temperatures and can be defined as the sticking of particles to one another without modification of the particle itself. From 800°C onwards, however, the sintering phenomenon will dominate (Danner, 2013). This sintering is the result of the amorphisation of the clay, whereby the clay structure is altered and densified. As a result the specific surface area of the clay decreases (Fernadez, 2009), which is typical for the initial stage of the sintering process (De Jonghe and Rahaman, 2003).

2.3.2 OPTIMAL ACTIVATION TEMPERATURE

The optimal activation temperature depends mainly on the type and structure of the clay mineral. Several previous studies have therefore focused on determining the pozzolanic activity and the optimal calcination temperature for pure clays. An overview of these studies and the most important conclusions drawn are given in Table 2.2.

Table 2.2: *Overview of the calcination temperatures for different clay types reported in literature* (Ambroise, 1984; Chakchouk et al., 2006; Fernandez, 2009; He et al., 1995; Taylor-Lange et al., 2015).

Author	Year	Clay type	Calcination T (°C)	Optimum act. T (°C)	Pozzolanic activity
Ambroise	1984	Kaolinite	750	750, 5h	High
		Montmorillonite			Low
		Illite			Low
		Lateritic soils			Medium
Martin-calle	1989	Kaolinite	600, 650, 700, 750, 800, 850	700, 24h	High
		Brick clay (illite/kaolinite)			Medium
He	1995	Kaolinite	550, 650, 800, 950	650	High
		Na-montmorillonite	740, 830, 920	830	Low
		Ca-montmorillonite	730, 830, 920	830	Medium
		Illite	650, 790, 930	930	Low
		Sepiolite	370, 570, 830	830	Low
		Mixed layer Mica-smectite	560, 760, 960	960	Low
Chakchouk	2006	Kaolinite	500, 600, 700	700-800	High
		Illite/ Montmorillonite clay	500, 700, 800	-	Low
Fernandez	2013	Kaolinite	600, 800	600	High
		Illite		800	Low/Inert
		Montmorillonite		800	Medium
Taylor-Lange	2015	Kaolinite	650, 830, 930	650	High
		Kaolinite – Ca-montmorillonite		930	Medium
		Kaolinite – Na-montmorillonite		830	Medium to high

Ambroise et al. (1985) mainly focused on the differences in pozzolanic reactivity of different clay minerals and calcined the samples at 750°C according the results of Murat (1983). He concluded that only kaolinite was highly reactive while montmorillonite and illite did not yield adequate strength results. His test results of mixed clays from a lateritic deposits with a kaolinite content varying between 33 – 55% did however show that lateritic soils can have a reasonable pozzolanic reactivity when calcined at 750°C and blended with calcium hydroxide. Furthermore a direct correlation between the kaolinite content and the achieved strength at 28 days could be found.

A more extensive study was conducted by He et al. (1994, 1995, 1996, 2000), whereby they determined the optimal activation temperature and evaluated the pozzolanic potential of six reference clays when blended with lime or cement. The calcination temperatures that were found varied depending on the nature of the clay mineral. Kaolinite had the lowest optimal temperature of 650 °C, while for Ca-montmorillonite, Na-montmorillonite and sepiolite, 830°C was found. For illite the optimum temperature was 930°C and the mixed layer mica-smectite clay had the highest temperature of 960°C. They concluded that while kaolinite seemed to be highly reactive, Na- and Ca-montmorillonite showed only mediocre reactivity and the rest of the clays did not show satisfying results. However the different binder to solid ratios that were applied had to be corrected and therefore the comparison between the different samples is not ideal.

Fernandez (2009) also indicated that kaolinite showed the highest potential as clay mineral and that the optimal firing temperature is a broad range starting from 600°C up to 800°C. Illitic clays behaved like an inert filler without significant signs of improving the reactivity even after calcining at its optimal temperature of 800°C. Calcined montmorillonite did show some reactivity, though rather limited and mainly at later curing ages. The optimal activation temperature of illite and montmorillonite was set at 800°. Nevertheless, only two different activation temperatures of 600 and 800°C were tested and it is possible that after increasing the calcination temperature of illite to 930°C, similar as the temperature used by He et al. (1995), illite will not be completely inert anymore.

Based on the literature it can be concluded that kaolinite possesses the highest pozzolanic potential in comparison to the other clay minerals. The optimal calcination temperature for kaolinite can be chosen between 550°C (He et al., 1994) and 850°C (Ayub et al., 1988) depending on the nature and amount of impurities in the material. This temperature range is rather broad because kaolinite has the advantage that there exists a broad gap between its dehydroxylation and recrystallisation temperature, resulting in a less critical calcination temperature (Andrejkovičová et al., 2014; De Silva and Glasser, 1992; Snellings et al., 2012). Furthermore, the direct exposure of the octahedral Al-OH groups upon the interlayer space, makes it more easy to remove them during the dehydroxylation process and achieve more easily structural disorder than for 2:1 clays whereby the octahedral sheet is shielded by the two tetrahedral sheets (Fernandez et al., 2011). The disordering of kaolinite upon calcination (up to 800°C) is confirmed by ^{27}Al MAS NMR results that indicate 6-coordinated Al in the octahedral sheet is transformed into 4- and 5- coordinated Al, due to the removal of hydroxyl groups from the structure (Fernandez et al., 2011; Gilson, 1987). The presence of the 4 and 5 coordinated Al is typical for a disordered metastable phase. When the calcination temperature was further increased (>800°C), the amount of 6-coordinated Al increased again, which can be correlated to the recrystallisation of mullite (Rocha and Klinowski, 1990). Also Martin-Calle (1989) found that a calcination temperature of 800°C yields the highest amount of amorphous material for an ordered kaolinitic clay. However, it is not always the calcination temperature that results in the highest amount of amorphous material that also gives the best pozzolanic activity. Often the optimal calcination temperature is finding a compromise between the amount of amorphous material, particle size distribution and the surface properties. Most reported optimal activation temperatures for kaolinite cluster between 650 and 750°C (Ambroise et al., 1994; Chakchouk et al., 2009; De Silva and Glasser, 1992; Kakali et al., 2001; Murat, 1983).

The optimal activation range for montmorillonite rich clays is narrower than that for kaolinite and varies between 800 and 830°C (He et al., 1996; Liebig and Althaus, 1997; Mielenz et al., 1950). This can be explained as recrystallisation is easily obtained due to overheating and can already occur at temperatures as low as 850°C depending on the chemical composition of the clay. The dehydroxylation temperature of montmorillonite is mainly influenced by the octahedral occupancy (Drits et al., 1995). The dehydroxylation of trans-vacant clays starts already at about 500 – 550°C, while for cis-vacant clays this is at 650 – 700°C (Wolters and Emmerich, 2007). Nevertheless also other parameters like the nature of the interlayer cation can change dehydroxylation with 60°C (Emmerich et al., 1999; Mackenzie and Bishui, 1958). Overall montmorillonite can yield a good pozzolanic activity and can contribute to the strength when blended with Portland cement (He et al., 1996). Other 2:1 clays like illite have only a low pozzolanic potential. Even though the dehydroxylation of illite takes place at a relatively low temperature of 580°C, this process does not result in a collapse of the structure and illite remains mainly crystalline. Without the formation of a substential amorphous phase, illite shows much lower pozzolanic activity than the metastable phases of kaolinite and montmorillonite.

The optimal calcination temperatures that are listed here for kaolinite, illite and montmorillonite are correct for pure, single clay minerals. Natural clays are often composed of several different clay minerals and non-clay minerals. All these components can also have an influence on the calcination temperature and therefore it is hard to define the optimal temperature for mixtures and natural clays. Furthermore the decomposition temperature determined by means of thermal analyses cannot always be directly correlated to the optimal temperature since also the calcination process, firing time and properties of the clay such as initial disordering of the clay and chemical composition influence the eventual pozzolanic activity (Forrester, 1974).

2.4 CEMENT AND POZZOLANIC REACTION

2.4.1 PORTLAND CEMENT

Portland cement is the most used binder for concrete and mortars and possesses hydraulic characteristics. Portland cement is produced by calcining limestone and small proportions of marl, clay or shale to 1450°C to create clinker material. During this process limestone is converted to calcium oxide and carbon dioxide according to the following equation:

$$CaCO_3 \rightarrow CaO + CO_2 \qquad \textit{(equation 2.1)}$$

The combination of the high firing temperatures and the emission of CO_2 results in a high energy cost and a considerable environmental impact. After rapid cooling, the clinker material is ground and blended with approximately 5% gypsum. According to the ASTM C 150 Portland cement can be described as followed:

> *"Portland cement clinker is a hydraulic material which shall consist of at least two-thirds by mass of calcium silicates (3 $CaO{\cdot}SiO_2$ and 2 $CaO{\cdot}SiO_2$), the remainder consisting of aluminum- and iron-containing clinker phases and other compounds. The ratio of CaO to SiO_2 shall not be less than 2.0. The magnesium oxide content (MgO) shall not exceed 5.0% by mass."*

True Portland cement consist of 95 – 100% pure clinker material and is classified as CEM I according to the EN-197-1 listed by the European Committee for Standardization (European Committe for Standardization, 2000). The average main constituents that are present in the Portland clinker are Tricalcium silicate (C_3S, also known as alite), dicalcium silicate (C_2S, called belite), tricalcium

aluminate (C_3A), tetracalcium aluminoferrite (C_4AF). When part of the Portland cement is replaced by calcined clays, the cement is referred to as a pozzolanic cement of type CEM IV that contains between 45 to 89% clinker and 11-55% pozzolanic material.

2.4.2 CEMENT HYDRATION

Since Portland cement is characterized by a hydraulic reaction, the chemical reactions that contribute to the setting and hardening of the cement paste are triggered by adding water to the cement. This reaction between the constituent compounds of the cement and water are referred to as hydration while the newly formed phases are designated as hydration products. The reaction of alite (C_3S) with water (equation 2.2) results in the formation of calcium silicate hydrate (C-S-H) with various compositions and calcium hydroxide (CH), often referred to as lime[1] or portlandite. Also belite hydrates in a comparable way and again C-S-H and CH are formed as reaction products (equation 2.3).

$$2\ C_3S + 7\ H \rightarrow C_3S_2H_4 + 3\ CH \qquad \textit{(equation 2.2)}$$
$$2\ C_2S + 5\ H \rightarrow C_3S_2H_4 + 3\ CH \qquad \textit{(equation 2.3)}$$

Tricalcium aluminate (C_3A) reacts in the presence of gypsum with water to produce ettringite (equation 2.4). Ettringite is a prominent AFt phase in the cement hydration. Once all the sulphate, provided by gypsum is used, ettringite becomes unstable and reacts with the remaining tricalcium aluminate in the presence of water to form monosulfate aluminate hydrate (AFm) (equation 2.5).

$$C_3A + 3\ C\underline{S}H_2 + 26\ H \rightarrow C_6AS_3H_{32} \qquad \textit{(equation 2.4)}$$
$$2\ C_3A + 3\ C_6A\underline{S}_3H_{32} + 22\ H \rightarrow 3\ C_4ASH_{18}, \qquad \textit{(equation 2.5)}$$

In general the hardened cement paste consists of an assemblage of these reaction products. The main hydration product is C-S-H with an amount of 50 to 60%, lime will comprise 20 -25%, ettringite 15 -20% and 5-6% will be occupied by capillary voids and entrapped air. The presence of the unreacted lime acts as a trigger for the pozzolanic reaction.

2.4.3 POZZOLANIC REACTION

The pozzolanic reaction is based on the interaction between the aluminosilicate material, or pozzolan, and CH in the presence of water. As a consequence new hydration products that contribute the cementitious properties of the paste are formed and the reaction can be formulated according to equation 2.6.

$$AS + CH + H \rightarrow C\text{-}S\text{-}H + C\text{-}A\text{-}H \qquad \textit{(equation 2.6)}$$

When pozzolanic materials are blended with cements the reactive alumina and silica phases will react with the calcium hydroxide that is formed during the cement hydration (see equation 2.2 and 2.3) and produce additional C-S-H phases, C-A-H and C-A-S-H phases. As a consequence the porosity of the cement paste decreases which can enhance strength and durability of the final product. The reaction is driven by the difference in Gibbs free energy between the starting material and the eventual reaction products. The reaction rate is therefore controlled by the process that requires the highest activation energy, which is the release and dissolution of silica and alumina from the pozzolan (Snellings et al., 2012). The high alkali content of the clinker material and the formation of

[1] Normally the term lime is used for calcium oxide (CaO), in cement research and industry however lime refers to calcium hydroxide ($Ca(OH)_2$). As this study focuses on cement research, lime will also refer to $Ca(OH)_2$.

CH results in an alkaline environment. Due to high pH of the pore solution the hydroxyl ions, provided by the dissolution of calcium hydroxide, attach themselves to the pozzolan and break down the Al_2O_3-SiO_2 framework (Fernandez, 2009). For metakaolin the reaction can be written as follows:

$$Al_2O_3(SiO_2)_2 + 6\ OH^- + 3\ H_2O \rightarrow 2\ Al(OH)_4^- + 2\ H_2SiO_4^{2-} \qquad \textit{(equation 2.7)}$$

After the dissolution process the end products can react with the available Ca^{2+} and OH^- ions to produce C-S-H and AFm phases. In general first the C-S-H phases precipitate as a result of the reaction between the silica and the Ca^{2+} ions and the amount mainly depends on the Si/Al ratio of the starting material (Richardson, 2008). High alumina concentrations will enhance the uptake of alumina in the C-S-H structure and C-A-S-H will additionally precipitate (Richardson and Groves, 1993). The most common C-A-S-H for metakaolin is strätlingite (C_2ASH_8), which is classified as an AFm phase (Matschei et al., 2007). However also other aluminate phases like hydrogarnet (C_3AH_6) or C_4AH_{13} can theoretically form. The reaction is commonly generalized in literature as follow:

$$AS_2 + 3\ CH + 6\ H \rightarrow C_2ASH_8 + C\text{-}S\text{-}H \qquad \textit{(equation 2.8)}$$

Instead of blending the pozzolan directly with cement, $Ca(OH)_2$ saturated solutions are often used to simulate the reaction to study the pozzolanic hydration products in more detail and to measure the actual reactivity of the pozzolan. The influence of the chemical composition on the formation of the reaction products was visualized by Lothenbach et al. (2011) in a ternary diagram of the main constituents CaO-SiO_2-Al_2O_3 (Figure 2.7). Most natural pozzolans have a similar composition, the Si/Al ratio will however have a significant influence on the amount and type of the AFm phases that will form. Also for calcined clay this can give an indication of the reaction products that will form. More alumina will provoke the precipitation of strätlingite, while more silica will preferably form C-A-S-H phases.

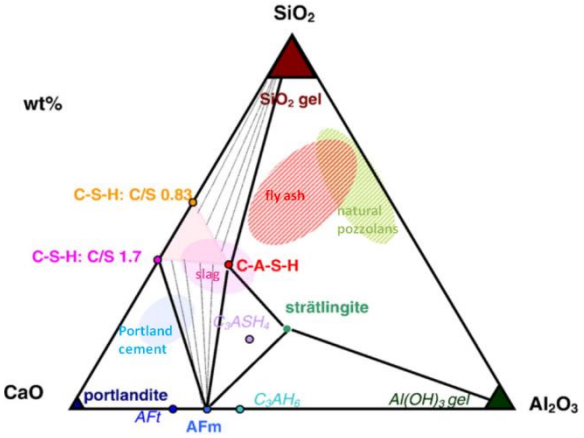

Figure 2.7: *Ternary diagram of the CaO-SiO_2-Al_2O_3 system with indication of the hydration products (modified after Lothenbach et al., 2011).*

2.4.4 BLENDED CEMENTS WITH CALCINED CLAY

The hydration reaction of calcined clay, mainly metakaolin, has been studied in the past both for clay-lime as well as for clay-cement systems. In general most authors report similar main reaction products consisting of: strätlingite, calcium silicate hydrate, tetra calcium hydrate, monocarboaluminate and portlandite (Fernandez et al., 2011; Gameiro et al., 2012; Silva et al., 2014; Tironi et al., 2014a). Higher curing temperatures or an excess of kaolinite can lead to the formation of hydrogarnet at longer curing times (Serry et al., 1984; Silva et al., 2014). It is interesting that the hydration phases formed are comparable for both lime- and cement-based systems. Even though the

pozzolanic reaction itself is not affected as long as calcium hydroxide is present in the system, the reaction kinetics can somewhat vary since the alkalis present in cement-based systems will facilitate the dissolution of the calcined clay and the cement hydration takes place simultaneously. An overview of the different studies on calcined clay – lime pastes with their identified reaction products is given in Table 2.3.

Table 2.3: *Overview including the most important research regarding the calcined clay – lime system and the formed reaction products.*

Author	Year	Clay type	Substitution rate	Curing	Reaction phases
Murat	1983	Metakaolin	20 – 66%	20°C, air-thight boxes	C-S-H, C_2ASH_8, C_4AH_{13}
Ambroise	1985	Metakaolin	0.66 – 90%	20°C, in water	C-S-H, C_2ASH_8
De Silva	1993	Metakaolin	20 – 83 %	20, 55 and 85°C	C-S-H, CH, C_2ASH_8, C_4AH_{13} **At 55 and 85°C:** C-A-S-H, C_3AH_6, CAS_2H_4
Frias & Cabreara	2001	Metakaolin	50%	20 and 60°C	C-S-H, CH, C_2ASH_8, C_4AH_{13}, C_3AH_6 (60°C)
Cara	2006	Calcined clay	50%	Sealed container	C-S-H, C_2ASH_8, C_4AH_{13}
Gameiro	2012	Metakaolin	50%	23°C	C_2ASH_8, C_4AH_{13}, $C_4A\underline{C}H_{11}$
Silva	2014	Metakaolin	5 – 50%	23°C	C_2ASH_8, C_4AH_{13}, $C_4A\underline{C}H_{11}$, CH, C-S-H, calcite, calcium aluminate hydrate type ($Ca_2Al(OH)_7{\cdot}6.5H_2O$) **After 1 year for a substitution rate of 33 and 38% MK:** katoite ($Ca_3Al_2(SiO_4)(OH)_8$)

Besides the formation of additional binding phases, the blending of calcined clay with cements also provides supplementary benefits. The fine particle size of the clay and the formation of new phases result in a general decrease in pore size. In addition, these blended cements show a lower permeability which is beneficial to suppress the alkali silica reaction or block the intrusion of corrosive sea water. The only drawback of the addition of calcined clay is the decrease of the workability of the mortar. The water demand often increases significantly and this can only be countered by the use of superplasticizers to obtain similar water to binder ratios to regular Portland cement mortars (Danner, 2013).

To enhance the characteristics of Portland cement mortar it is important to select an appropriate substitution ratio that is without a significant loss of cement properties. Singh and Garg (2006) and Zhang and Malhotra (1995) both replaced 10% of Portland cement by calcined kaolinitic clays and reported that the mechanical properties of the cement increased compared to the reference sample, the porosity decreased considerable and the durability tests showed good results indicating metakaolin could be applied to provide high-performance concrete. They already stressed that it could be interesting to investigate higher replacement ratios.

Ambroise et al. (1994) found that even with substitution levels of 30% metakaolinite the compressive strength is not affected and the mechanical properties and durability of the mortars remain similar. This can be attributed to a decrease in the pore size and decrease in the amount of portlandite that has not reacted in the metakaolin blended cement. Also other authors indicate that for replacement levels between 20 – 30% the strength results are comparable with those of ordinary Portland cement (Amin et al., 2015; Andrejkovičová et al., 2014; Badogiannis et al., 2005; Fernandez, 2009). Antoni et al. (2012) demonstrated that the substitution ratio can even be further increased up to 60% when a mixture of calcined clay and lime is added to the cement. The results of the durability test are promising and the early strength (7 days) is significantly improved compared to the other blends.

Besides the extended research on pure calcined kaolinitic clays, during the last years the interest of scientist has shifted towards more natural and less pure clays. However, the focus is still mainly on kaolinitic clays and only in a limited number of studies other clays are considered. Badogiannis et al. (2005) looked at the influence of the kaolinite content on the cement properties by using Greek clays with a kaolinite content ranging between 38 and 65%. Even though some clays showed a good potential after calcining at 650°C, the lack of proper and accurate mineralogical composition and neglecting the influence of the particle size made it impossible to link the kaolinite content directly to the mechanical properties. Tironi et al. (2014) was able to correlate the kaolinite content with the clays reactivity and determined that the minimum amount of kaolinite that was necessary to have pozzolanic reactive clay is 45%. To come to these conclusions, the authors studied five natural clays from Argentine with variable kaolinite content and used 700°C as calcination temperature.

Fernandez (2009) studied low grade Cuban clays and managed to improve this minimum percentage and stated that only 40% of kaolinite can be sufficient to provide a good pozzolan. The optimal calcination temperature was 800°C and he applied a cement replacement level of 30%. He also indicated that there was a good correlation between the pozzolanic activity observed in pastes and the strength measurement on mortars. Also Alujas et al. (2015) investigated Cuban low grade kaolinitic clays and concluded that the contribution of the calcined clays to the strength development is a combination of a filler effect, enhancement of the Portland cement hydration in the early stage as a result of additional nucleation sites and eventually the pozzolanic reaction itself. Furthermore they stated that the contribution of 2:1 clay minerals to the total pozzolanic reactivity should not be neglected.

Danner (2013) studied natural clays from different locations including Portugal, Denmark and Poland. He concluded that 30% of kaolinite gave already good pozzolanic reactivity after calcination. Furthermore the pozzolanic potential of illitic and smectitic clays can be significantly increased when calcite is present in the original sample, which is the case for marls. However the term marl is often used incorrectly in cement research since the calcite content is generally not sufficient to classify the sediment as marl. The actual promising calcite-rich clays can be classified as either argillaceous marl (25-30% $CaCO_3$) or calcareous mudstone (5-25% $CaCO_3$).

Multiple studies already indicated that the high potential of calcined clays and the use of calcined clay as a SCM is not a complete new idea. However the shift of the research focus to lower grade clay in the last years indicates these clays can be a valid option in the future for cement and concrete applications. Therefore it is crucial to properly characterize the starting material, regarding mineralogy, chemistry, physical properties and thermal behavior in order to gain insight in the parameters that influence the pozzolanic reactivity. Both the effect of the clay minerals as well as the accompanying non-clay mineral impurities should be studied in more detail to fully understand the achieved pozzolanic reactivity of the starting material and to be able to explain the differences in reactivity between different natural clays.

2.5 ENVIRONMENTAL AND ECONOMIC POTENTIAL

Besides the pozzolanic reactivity and the cement properties also some other parameters have an influence on the decision whether a certain clay can and will be used as SCM. One of these parameters is the cost of implementing calcined clay in cement. Furthermore, it is also important to know whether the initial goal of lowering the CO_2 emission of the cement industry is indeed positively influenced by adding calcined clay, since these also require a calcination process. These two parameters will be discussed in more detail below.

2.5.1 ECONOMIC POTENTIAL

To calculate the economic potential of making blended cement with the addition of calcined clay the extra cost of the clay and its production process have to be taken into account and compared to the decrease in cost of the preparation of ordinary Portland cement. However, this cost is controlled by various factors and here only the difference in production cost will be taken into account and not the innovation costs since in general the existing manufacturing equipment can be used and only marginal investment are needed for the calcination equipment. Furthermore the assumption is made that the blended end product has a comparable price to that of regular Portland cement. In general the production steps between Portland cement and calcined clays are comparable. In the first step the limestone is mined, crushed, grounded and blended with additional products. Afterwards the material is heated to 1450°C and ground again to produce clinker material. The main difference between the production of calcined clays is that the calcination temperature is much lower: generally around 700 to 800°C. Therefore the variation in the amount of energy needed to calcine the materials and as a result the difference in fuel that is needed is a controlling cost parameter. The energy needed to heat a certain material can be theoretically described by the following equation (Kittel and McEuen, 1976):

$$dQ = m*c*dt \qquad \textit{(equation 2.8)}$$

With:

dQ= heat change (J)
m= mass (kg)
c= specific heat (J/°C)
dT= temperature change (°C)

The calcination process of limestone is very energy consuming and even though optimization of the production process resulted in a decrease of the energy demand, still between 3000 and 4000 MJ per ton of cement is needed depending on the exact process (Ohunakin et al., 2013; Schneider et al., 2011). The amount of energy that is needed per kg of material to increase the temperature by 1°C is called the specific heat and is characteristic for each material. The specific heat value of limestone and clay are comparable and are 0.815 and 0.86 KJ/°C kg respectively (Waples and Waples, 2004). This results in almost a duplication of the amount of energy that is needed when one ton of calcined clay (800°C) is compared to one ton of limestone (1450°C) (Table 2.4). A recalculation of the amount of energy that is needed to kWh allow to estimate the accompanying electricity cost based on the average electricity prices for industrial consumers in 2015 of EUR 0.119 per kWh (EU, 2015). This gives a cost difference of EUR 16.32 (Table 2.4), indicating the production of calcined clay is 42% cheaper. However it should be mentioned that this is a simplification of the production process. Additional parameters like the difference in the loss of ignition of the starting materials will influence the end-mass of the material. Nevertheless in general the loss of ignition will be higher for limestone than for clayey materials so the difference in cost price will be positively influenced. Furthermore

clays can contain organic material which can lower the amount of fuel/electricity that is needed to reach the preferred temperature.

Table 2.4: *Comparison between the energy and cost needed to calcine limestone at 1450°C and clay at 800°C.*

Raw material	Calcination T (°C)	Specific heat (kJ/°C kg)	Energy to calcine 1 ton (kJ)	Work to calcine 1 ton (kWh)	Cost to calcine 1 ton (EUR)
Limestone	1450	0.815	1 181 750	328.23	39.06
Clay	800	0.860	688 000	191.11	22.74

A second parameter is the price difference of the raw materials. Limestone prices vary around 20 EUR/ton while kaolinitic rich clays can vary significantly with prices between 15 and 45 EUR/ton depending on the kaolinite content or the quality of the clay (prices are based on the clays of the Latneskoye case study Russia) (or. com. Sibelco). For a substitution rate of 30% of calcined clay, the initial raw material will cost between 18.5 and 27.5 EUR/ton. When the calcination costs are taken into account, prices will vary between 52 and 61.5 EUR for the blended cement. These prices are equivalent and even slightly cheaper than the 59 EUR for a ordinary Portland cement. Moreover, also in this calculation the higher LOI of limestone is not taken into account. When 1 kg of limestone is fired, only 0.56 kg CaO will remain. Clays are, however, marked by a smaller weight loss upon calcination up to 800°C and on average 0.85kg of material will remain. This indicates that for a calcined clay blended cement less starting material is necessary to produce the same amount of cement.

2.5.2 ENVIRONMENTAL POTENTIAL

Besides requiring a high energy intensive process, cement manufacturing also has a large impact on the environment. For the production of 1 ton of Portland cement approximately 0.85 ton of CO_2 is emitted. As a consequence the cement industry is responsible for 5-8% of the global anthropogenic CO_2 emission (Damtoft et al., 2008; Zhang et al., 2014). During the calcination process of the clinker material, CO_2 is emitted as a result of the decarbonization of limestone and the combustion of fossil fuels that are needed to heat the kiln to the desired temperature of 1450°C. The environmental concerns about the high CO_2 emissions resulted in a low-carbon economy proposal of the European union which stated that the industrial CO_2 emission should be reduced by 80% in 2050 compared to the 1990 levels (European Commision, 2011). The question rises whether calcined clay blended cement can lower the CO_2 emission of the cement industry significantly.

The calcination process accounts for 50-60% of the total CO_2 that is emitted during cement production. The decarbonization of limestone, expressed according to equation 2.1, shows that for the production of 1kg CaO 0.79kg of CO_2 is emitted. Because the actual clinker material comprises generally of 65% of CaO, only 0.51kg CO_2 is emitted per kg of clinker material (Taylor, 1997).

$$CaCO_3 \rightarrow CaO + CO_2 \qquad \text{(equation 2.1)}$$
$$1\ kg \quad 0.56kg + 0.44kg$$

In most natural clay deposits the amount of carbonates that are present are negligible. However it should be mentioned that also more carbonate-rich clays like marls and calcareous mudstone that do contain considerable amounts of carbonates can be used. When these clays are calcined they will also be marked by a release of CO_2 due to the decarbonization of calcite. Furthermore also the presence of organic material will contribute to the CO_2 emission as organic material will be

decomposed at a temperature around 300°C. Therefore the chosen clay type will have a considerable impact on the amount of CO_2 that is emitted during the calcination process.

The energy and fossil fuels that are required during the production process are responsible for the remaining 40% of the total CO_2 emission during the production of cement. The production process of both cement and calcined clay is rather similar and accounts for 0.23 kg of CO_2 per kg of binder. The difference in the amount of fuel that is necessary to calcine either cement or clay is, however, significant since the calcination temperature that is necessary to activate clay is 550°C lower than for cement. To calculate the amount of CO_2 per ton of clinker that is released due to the combustion of fossil fuels the average values are used. For the heating of 1kg of clinker material, 0.11 kg CO_2 is released on average (Worrell et al., 2001). This amount is however affected by the equipment and the type of the process that is applied. The lower calcination temperature of clays (800°C) makes that only 55% of the energy is needed to fully heat the clay to the appropriate temperature. Thereby also the CO_2, which is emitted, can be reduced by 45% compared to ordinary Portland cement.

Table 2.5: *Overview of the CO_2 emission rates (expressed in kg per kg binder) of the different parameters in the cement production process. Portland cement is compared with blended cement with different substitution rates.*

Cement type	CO_2 emission calcination	CO_2 emission fuel combustion	CO_2 emission energy	Total CO_2 emission	CO_2 emission reduction
Ordinary Portland cement	0.510	0.110	0.23	0.850	-
Calcined clay	0	0.061	0.23	0.291	-
Portland cement + 10% calcined clay	0.459	0.105	0.23	0.794	7%
Portland cement + 30% calcined clay	0.357	0.095	0.23	0.682	20%
Portland cement + 60% calcined clay	0.204	0.08	0.23	0.514	40%

The CO_2 emission rates of all parameters are summarized in Table 2.5. A comparison is made between Ordinary Portland cement and blended cements with different substitution rates. The decarbonization process of limestone has the largest influence on the total CO_2 emission when Ordinary Portland cement is compared with blended cements. A replacement of 20 – 30% of cement by calcined clay is commonly reported in literature without significant loss of strength and other cement properties. These replacement levels yield a reduction of up to 20% of the total CO_2 emission per kg binder. Higher replacement levels can even have a more drastic effect up to 40% under ideal circumstances. However when a 60% replacement level is maintained often calcined clay is blended with ground limestone in order to maintain the strength of the cement (Antoni, 2013).

CHAPTER 3

METHODOLOGY

In the past much attention has been given to the mechanical properties and behavior of a calcined clay- Portland cement or lime blend. However, often the characterization of the starting material was neglected and considered to be less important. Nevertheless, differences in the chemistry, mineralogy and physical properties of the calcined clay can influence its pozzolanic reactivity drastically (Fernandez et al., 2011; He et al., 1994; Kakali et al., 2001). Therefore, an extensive characterization of both the raw clay and its calcined product is necessary to gain insight in the decomposition mechanism and pozzolanic behavior of the sample. Several analytical methods were applied such as ICP-OES, XRD, TGA, BET, PSD, FTIR and NMR to characterize the clays. Two reactivity tests, the chapelle test and the quantification of portlandite by means of TGA, were used to estimate the pozzolanic potential of the calcined clay. The combination of all these different analyses provides insight in the relation of the characteristics of the starting material (raw and calcined) and its pozzolanic reactivity.

3.1 CALCINATION

The optimal calcination temperature is influenced by the mineralogy and chemical composition of the clay. When the temperature is not sufficiently high, the dehydroxylation of the clay minerals is not completed and the structure remains partially intact. However, high calcination temperature > 900°C can lead to recrystallisation of high temperature phases and additional sintering resulting in a decrease in rthe pozzolanic reactivity of the material. Therefore the optimal activation temperature was determined for different clay types. To estimate the influence of the differences in decomposition on the pozzolanic reactivity, a temperature range between 500 and 900°C was used for the pure clays and the mixtures in order to obtain different stages of the degree of dehydroxylation for all studied clay types. For the natural clays only one optimal calcination temperature was chosen within this range depending on the clay type. Clays that predominantly consist of kaolinite were calcined at 750°C, while for more smectitic clays 800°C was applied.

Raw clays were thermally treated in a laboratory programmable fixed-bed furnace. The clay was spread out as a thin layer (<1.5 cm) in porcelain crucibles to insure homogenous firing of the samples. In this process, the heating rate was divided in three major steps, 20°C/min for the first step, 10°C/min for the second step and 5°C/min for the last 100°C (Table 3.1). The different steps were introduced to limit the overheating of the clay. The residence time at the desired temperature was set at 2 h.

Table 3.1: *Overview of the heating rate steps for each calcination temperature*

Calcination T	Heating rate		
(°C)	20°C/min	10°C/min	5°C/min
500	20-300°C	300-400°C	400-500°C
700	20-500°C	500-600°C	600-700°C
800	20-600°C	600-700°C	700-800°C
900	20-700°C	700-800°C	800-900°C

After gradually cooling, the calcined clays were ground to achieve a more similar fine grain size distribution. This milling step is done to minimize the sintering effect of the calcination process and has a positive effect on the surface interaction when blended with lime or cement (Gamelas et al., 2014). Furthermore the grain size might overshadow the effect of mineralogical parameters on the pozzolanic properties especially for smectitic clays which easily sinter. Some authors suggested that the pozzolanic reactivity can be influenced by the milling step as it can induce the formation of a thin amorphous layer that covers the surface of the mineral grains (Benezet and Benhassaine, 1999; Vdovic et al., 2010). This effect was however reduced by applying wet milling with a McCrone Micronizing mill® for 5 min using ethanol as grinding agent instead of other more common grinding techniques (Środoń et al., 2001).

3.2 CALCINED CLAY – LIME PASTES

To assess the pozzolanic reactivity and identify the formed hydration phases calcined clay – lime pastes were prepared. In previous studies the calcined clay-slaked lime ratio of the prepared pastes varies between 20:80 and 50:50 (Danner, 2013; Gameiro et al., 2012; Silva et al., 2014). To optimize the reaction rate in order to study the evolution of the calcined clay-lime system a ratio of 30:70 was chosen. The mixtures of calcined clay and hydrated lime were dry-blended using a Turbula mixer for 4 h. Distilled water was added to obtain a water/solid ratio of 1:1. The pastes are blended by hand for 5 min and divided over eight sealed recipients of 3ml each. During this process it is important to work quickly and efficient to prevent carbonation. Moreover, inclusions of air bubbles, which contain CO_2, should be avoided by tapping the sample tubes during filling. Afterwards, the pastes are stored in an acclimatized room with a temperature of 20°C and a relative humidity of 95% ± 5% to favor the hydration reaction over the carbonation reaction (Cizer, 2009).

In cement research the pozzolanic reactivity of the samples is determined after 3, 7, 14, 28, 56 and 90 days. After each period the hydration reaction needs to be stopped in order to be able to compare the pozzolanic reactivity of the different samples and identify the formed reaction products by XRD. Investigation of different techniques pointed out that vacuum freeze drying of the samples is a good and reliable method (Gallé, 2001). During vacuum freeze drying the excess of water that is not bound by the formed hydration phases is removed to obtain a stable powder (Mertens, 2009). The pastes were vacuum dried using a Christ Alpha 1-2 LD at 0.03 mbar for 2 h to stop the hydration reactions according to the procedures described in Knapen et al. (2009). The dried samples were then stored in a desiccator until measurement to prevent hydration.

3.3 CHEMICAL ANALYSIS

For the cement industry the chemical composition of the product used to be of key importance in selecting natural pozzolans. Moreover, the norm for SCMs in ASTM C618-98 states that the sum of the three components aluminum, silicon and iron oxide must exceed 70%. Nowadays it is known that the pozzolanic activity cannot be directly related to the chemical composition. However, chemical analyses are carried out to make a first clear distinction between the different clay samples and determine the SCM group so reaction products, which are expressed in their chemical formula in the cement industry, can be estimated. Furthermore, the French norm for metakaolin, NFP 18-513, still incorporates several chemical parameters that should be taken into account when looking at the pozzolanic potential of any clayey material. First of all the loss on ignition value (LOI) should be smaller than 4% in order to qualify the clay as metakaolin. Other parameters are MgO (<4.0%), SO_3 (<1.0%) and the sum of the alkalis expressed in Na_2O equivalent (<4%) (NFP 18-513).

The bulk chemical composition of the starting material was analyzed using a Varian 720ES inductively coupled plasma optical emission spectrometer (ICP-OES). Powdered samples (<250 µm) are fused with lithium metaborate ($LiBO_2$), which is an effective flux for silicates, at 1000°C (Suhr and Ingamells, 1966). The concentrations of 10 different elements (Al, Si, Ca, Mg, K, Na, Fe, Ti, Mn and P) were determined. Three standard reference materials, BCS 269, BCS 267 and GBW-7411, were analyzed together with each batch of samples to calibrate the measurements.

To estimate the weight loss of the raw clay upon heating, standard LOI measurements were performed by heating the sample up to 1000°C. During heating several components like carbonaceous materials and carbonates decompose while structural water will vaporize resulting in weight loss. In general analyses were performed on the raw clays; however, for seven kaolinitic clays (Chapter 7) also the LOI of their calcined product was analyzed to see if they met the requirements to qualify it as metakaolin with a LOI below 4%. Furthermore, the sulfur content was determined for those seven calcined kaolinitic clays with a Torontech Carbon & Sulfur Analyzer.

3.4 X-RAY DIFFRACTION

The chemical data is complemented with information on the mineralogical composition obtained by X-ray diffraction (XRD). The mineralogy is one of the most important parameters that affect the pozzolanic reactivity, especially on the long term (Fernandez, 2009; Tironi et al., 2012). Therefore the bulk mineralogy of the raw clay samples was accurately qualified and quantified to investigate the influence of clay and non-clay minerals on the reactivity. Previous studies indicate that in general the pozzolanic reactivity can be correlated to the type of clay mineral. The reactivity can be summarized accordingly kaolinite > montmorillonite > illite (Danner, 2013; Fernandez et al., 2011; He et al., 1995). Since the hkl reflections of clay minerals are not very diagnostic in randomly oriented slides and bulk mineralogy only allows to quantify clay minerals in groups (kaolinites, 2:1 Al clays), it is crucial to specify and quantify the clay minerals within the clay fraction to distinguish montmorillonite from illite and mixed layer illite/smectite (Moore and Reynolds, 1997). Furthermore, the mineralogical phase transformations during the calcination process were characterized to gain a better knowledge about the evolution of a crystalline phase to a semi-crystalline and amorphous phase upon thermal treatment.

Secondly the long term (3 - 90 days) hydration reactions occurring in the calcined clay – slaked lime system were analyzed by XRD. The reaction products of calcined clay lime mixtures were identified to deduce a relation between the mineralogy of the raw sample and the hydration products formed.

Moreover, the calcined clay – slaked lime pastes were monitored trough time to study the reaction rate of the formed hydration phases.

3.4.1 BULK MINERALOGY

To obtain a good repeatability and accuracy of the quantification, the raw and calcined clay samples are prepared for bulk XRD measurements according to the standardized procedure described in Środoń et al. (2001). The samples are mixed with 10% ZnO as internal standard and wet ground in a McCrone Micronizing mill®. To minimize preferred orientation, samples are side-loaded in aluminum sample holders. All bulk XRD diffraction spectra are recorded on a Philips PW 1830 diffractometer equipped with CuKα radiation in the range of 5 to 65° 2θ at 40 kV and 20 mA. The step size was 0.02° 2θ with a counting time of 2 s.

Mineral identification and quantification were performed with X-ray Viewer and QUANTA respectively (© Chevron ETC). The Quanta software combines whole-pattern fitting for pure mineral standards and single peak quantification. For each mineral one diagnostic peak is selected to assure that the measured intensity can be directly correlated with the amount of the mineral. For clay mineral the (060) reflections are ideal because they have a low sensitivity for chemical and structural variability and have no tendency for preferred orientation (Środoń et al., 2001). The advantage of this technique is that both non-clay minerals and clay groups can be quantified as weight percentage in the bulk rock and quantification is less time consuming than conventional Rietveld refinement techniques. The major disadvantage, however, is that the technique depends on the availability of pure standards. Nevertheless a comprehensive collection of standards of both non-clay and clay minerals has been collected during previous PhD projects (Adriaens, 2015; Zeelmaekers, 2011). The accuracy and reliability of this quantification method have been proven by previous studies and the Reynolds cup (Adriaens, 2015; Hubert et al., 2009; Kleeberg, 2005; Omotoso et al., 2006).

The degree of ordering of the kaolinite can be deduced from the bulk X-ray diffraction data. However caution is advised since the degree of ordering can only be measured meaningful in samples containing at least 20% of kaolinite and the precision increases with higher kaolinite content. Furthermore, the reliability is dependent on the other minerals present in the sample (Galan et al., 1998). In this study, two different indices were empirically calculated, the Hinckley index and the Lietard index. The calculation methods are illustrated in Figure 3.1.

The Hinckley index (HI) does not take the crystal defects of kaolinite into account but is determined by the proportion of the two kinds of kaolinite (ordered or disordered) that are present in the sample (Plançon, 1988). The method is, however, influenced by the presence of other clay minerals and non-clay minerals like quartz, feldspar and iron oxides (Benea and Gorea, 2004; Galan et al., 1998). The HI is the ratio of the sum of the intensity of the (110) and (111) reflection peak of kaolinite measured from the inter-peak background and the intensity of the (110) reflection measured from the general background (Hinckley, 1962). The lower the HI is the more disordered the kaolinite is hereby the lower the crystallinity is.

Another less known index, is the index of Liétard (R2) established by Liétard (1977) is less sensitive to the presence of other mineral impurities (Cases et al., 1982). R2 is calculated by the intensities of the (1-31) and (131) peak reflections of kaolinite as illustrated in Figure 3.1. The main advantage of this technique is the fact that it can also be used in the presence of halloysite and it is hardly influenced by other minerals present in the sample (Galan et al., 1998). As reported in literature, R2 values range from <0.7 (disordered) to 1.2 (ordered) (Cases et al., 1982; Galan et al., 1998).

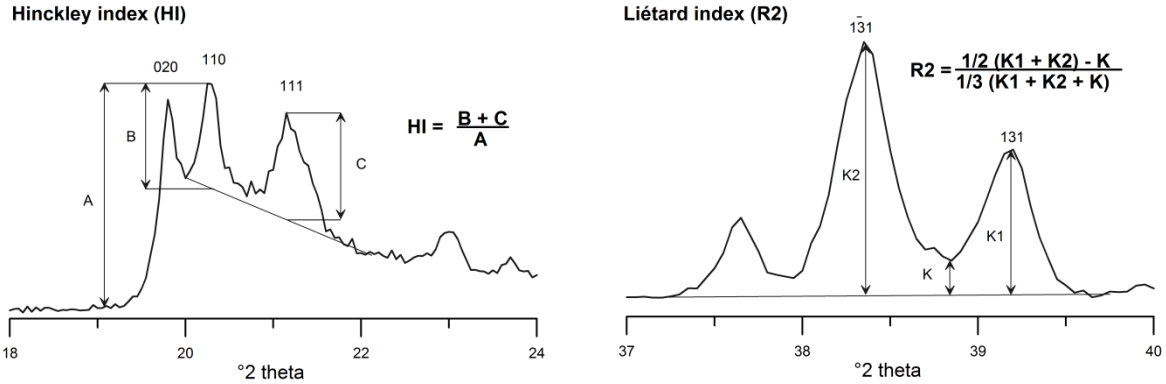

Figure 3.1: *The calculation method of the Hinckley index and Liétard index to determine the degree of ordering of kaolinite. The XRD pattern of a pure kaolinite, K1, was used.*

3.4.2 HYDRATION PHASES

In a second phase the pozzolanic reaction products were studied. Cements are complex mixtures and often the peak reflection of the hydrous cement phases are marked by considerable overlap. This makes the identification of the pozzolanic reaction products more difficult. To avoid interference with the hydrous cement phases, lime pastes with a calcined clay lime ratio of 30:70 were prepared instead of cement pastes. The newly formed hydration products of the calcined clay – lime mixtures are identified and monitored over time (3 - 90 days). Due to the limited sample amount (± 1.5 g) the samples were thoroughly mixed with zincite in an agate mortar by hand. The samples were side loaded and measured with the same settings as the other bulk samples. For analyzing the samples X-ray viewer was not applicable since the newly formed hydration products are not implemented in the database. Since these hydration phases are not often found in their pure form, it is not possible to add them to the database. Therefore the software DiffracPlus EVA (© Bruker) was used to identify all pozzolanic and hydraulic phases since it contains a specialized cement minerals database. In this database the pattern is calculated based on the crystal structure of the mineral and no pure reference phases are needed. This program is ideal for identifying the major phases that are present. However, some of the newly formed hydration phases are only present in small quantities and difficulties arises in identifying such minor phases. Additionally some peak overlap with the major phases might occur. Therefore Snellings (2016) provided a search list that is designed to find suitable candidates for minor unidentified peaks in the XRD patterns. An overview of the highest reflection peaks of the most important pozzolanic reaction phases in the calcined clay – lime system are given in Table 3.2. A combination of this list and results reported in literature allow a proper identification of both major and minor phases that are presented in the paste.

The combination of reflection peaks of non-reacted semi amorphous calcined clay and both crystalline and amorphous newly formed hydration products with an imprecise crystal structure makes it hard to perform a proper quantification by the Rietveld analyses. Furthermore the portlandite peaks are subjected to severe preferential orientation, making quantification of the remaining portlandite untrustworthy (Fernandez, 2009). As a result only semi-quantification, based on the peaks increasing or decreasing intensity was applied. The peak intensities of portlandite were clearly marked by a decreasing trend over time, indicating the portlandite was consumed to form hydration phases, for which the peak intensities increased. Therefore the semi-quantitative approach can be used to reconstruct the evolution of the pozzolanic reaction and enables us to link the original mineralogy and chemistry to the formed hydration products.

Table 3.2: *Overview of the peak positions of the most important phases in the calcined clay – lime system based on the search table of Snellings (2016). The most distinct reflection of each phase is listed in the first column of the peak reflections.*

Phase		**Peak reflection**			
Strätlingite	d-value (Å)	12.57	6.26	4.18	2.87
	2θ (°)	7.00	14.15	21.25	31.15
Hemicarboaluminate	d-value (Å)	8.2	4.1	2.88	
	2θ (°)	10.79	21.65	31.05	
C_4AH_{13}	d-value (Å)	7.92	3.88	2.87	1.66
	2θ (°)	11.17	22.92	31.16	55.34
Monocarboaluminate	d-value (Å)	7.57	3.78		
	2θ (°)	11.69	23.54		
Portlandite	d-value (Å)	4.89	2.62	1.79	
	2θ (°)	18.14	34.23	51.02	
CSH	d-value (Å)	3.06	2.8	1.83	1.66
	2θ (°)	29.19	31.96	49.83	55.34

3.4.2 CLAY MINERALOGY

Bulk measurement gives a first idea of the clay minerals that are present in a sample. Since it is of key importance to be able to distinguish the 2:1 Al-clays separately in relation to their different pozzolanic behavior, oriented aggregates of the fraction < 2 µm of all raw clay samples, with exception of the artificial mixtures, are qualified and quantified. In oriented aggregates the *00l* reflections, which are diagnostic for each clay mineral, are enhanced. When the oriented slides are measured in different standard conditions, air-dry and ethylene glycolated, the identification becomes more straightforward since the ethylene glycol treatment causes a shift of the peak positions of swelling clay minerals like montmorillonite while the illite reflections remain stationary (Brindley and Brown, 1980; Moore and Reynolds, 1997). To obtain optimal orientation and maximize the yield of the clay fraction, it is necessary to remove all the cementing agents. The maintained standard procedure, used at the clay mineralogy laboratory of the Department of Earth and Environmental Science at the KU Leuven, was established by Jackson (Jackson, 1975) and refined by Zeelmaekers and Adriaens (Adriaens, 2015; Zeelmaekers, 2011). In the first step cementing agents like organic material, carbonates and Fe-oxides coatings are removed. Afterwards the fraction <2 µm was separated by centrifugation. In the following step the clays are Ca-saturated to provoke homogenous swelling and placed in dialysis to remove the excess of electrolytes. Oriented slides of the purified samples <2 µm were prepared by dissolving 160 mg of the extracted clay fraction with 4 ml deionised water, followed by an ultrasonic treatment. The sedimentation slides were recorded under both air-dry and ethylene glycol saturated conditions on a Philips PW 1830 diffractometer equipped with CuKα radiation with step size of 0.02° 2θ, counting time of 1 s and a range of 2 to 47° 2θ.

The identification and quantification were achieved with X-ray-viewer and SYBILLA respectively (© Chevron ETC). To fit the experimental diffraction pattern in SYBILLA, the clay minerals are modeled individually based on the structural and compositional parameters (i.e. crystallite size, Fe-content, water content and Interlayer cation) and sigma star values that are introduced as input by the user (Hubert et al., 2009; Zeelmaekers, 2011). The summation of these patterns results in a whole pattern fit. An important parameter is the sigma star value, which is a measure for the preferred orientation:

the lower the value the better the orientation (Moore and Reynolds, 1997). The function that describes how well each clay mineral is oriented according to the flat surface of the clay slide. The starting sigma star values applied in this research are 6.68° for kaolinite and illite and 11.36° for smectite, as proposed by Zeelmaekers (2011).

The drawback of this method is the fact that it is user dependent as the fit is based on the judgment of the user. Small variation of the parameters results in drastic change in the output and therefore in quantification. However, similar to the accuracy and repeatability for the QUANTA software, the results from the Reynolds cup indicate this is a reliable method. Nevertheless, it is important to analyze each sample in a systematic manner.

Furthermore care should be taken into account when total bulk mineralogy is calculated because the results from SYBILLA cannot unambiguously be linked to the bulk QUANTA results. Since only the fraction <2 µm is analyzed, it is possible that larger clay minerals are left out of the quantification. This is especially important for the 2:1 Al clays. Therefore a bulk measurement of the fraction >2 µm was additionally performed. Since there were no 2:1 Al clays detected in the fraction >2 µm other than muscovite, which is quantified separately, calculations of the total bulk sample could easily be made for all samples.

3.5 THERMAL ANALYSIS

The dehydration, dehydroxylation and recrystallisation process of the clay minerals upon heating can be studied by Thermo Gravimetric Analyses (TGA). TGA measures the weight loss of the sample upon heating as a function of time and temperature. Since calcined clays are generally the most reactive when dehydroxylation is completed and no recrystallisation has taken place, TGA can give a first idea of optimal activation temperature. The dehydroxylation temperature of clay minerals depends on the crystal structure of the clay mineral and the bond strength. However, parameters like the presence of impurities and crystal defects can alter the dehydroxylation temperature (Snellings et al., 2012). Therefore also the effect of the impurities on the dehydroxylation temperature can be studied by TGA. The ongoing thermal reactions are simultaneously studied with differential scanning calorimetry (DSC). In this technique the temperature change between the sample and the reference is recorded whereby all exothermic reactions, like recrystallisation and phase transition, and endothermic reactions, like dehydration, can be detected. Since the stability of crystal structures is temperature dependent, specific phases can be linked to certain temperature changes (Stucki et al., 1990). Both TGA and DSC are valuable tools to characterize raw materials, especially fine grained minerals of low crystallinity like clays (Emmerich, 2011).

Furthermore, previous studies indicate the amount of amorphous material within the calcined clay is linearly related to the weight loss determined by TGA (Shvarzman et al., 2003). They stated that when the weight loss becomes negligible the highest degree of dehydroxylation of the clay is reached. Higher calcination temperatures give rise to additional dehydroxylation and amorphisation of the clay and corresponding the additional weight loss of the calcined sample will decrease. Therefore, TGA analysis can be very useful to estimate the optimal activation temperature. The degree of dehydroxylation can be calculated by dividing the weight loss caused by the remaining kaolinite by the weight loss of the initial kaolinite fraction. Optimal reactivity for kaolinite can be obtained when the degree of dehydroxylation is higher than 95% (Bich et al., 2009).

The degree of dehydroxylation is a good indicator to determine the optimal activation temperature. This parameter is defined as the remaining kaolinite fraction divided by the total, kaolinite fraction, measured by TGA (Antoni, 2013; Bich et al., 2009). In general good reactivity values are obtained

when the degree of dehydroxylation reaches values above 95%. Nevertheless, results can be influenced by crystallinity of the clay and the dispersion can be rather high. To obtain a comparable humidity levels for the measured raw samples, the clay were dried overnight in an oven at 60°C and stored in a desiccator prior to analyzing to assure a similar humidity for all samples.

For these measurements a Netzsch STA 409PC instrument with simultaneous TGA and DSC recordings was used. The sample was heated in Al_2O_3 crucibles from 25°C to 1000°C with a heating rate of 10°C/min in a N_2 atmosphere with a 60 mL/min flux. The derivate of the TGA patterns, the DTG, were calculated to clearly see the temperature range of the weight loss. To assure reliable quantitative results the device was calibrated by measuring pure calibration standards for which the transformation temperatures are known with sufficient accuracy to establish a calibration curve for both the temperature as the sensitivity. The five standards that were selected are Al, Au, Bi, In and Zn. The calibration was carried out under exactly the same conditions regarding crucibles, heating rates, atmosphere and comparable sample weight, as the corresponding sample measurements. Additionally a correction for the baseline is made by measuring an empty clean crucible.

3.6 BET SPECIFIC SURFACE AREA

The specific surface area of the calcined clay influences the pozzolanic reaction and is therefore an important parameter at early stage of the calcined – clay cement/lime reaction (Fernandez et al., 2011; Kakali et al., 2001; Tironi et al., 2013, 2012). This can be explained because the initial phase of the reaction is located at the liquid-solid interface and high specific surface area yields an increase of the early stage reaction surface (Mertens et al., 2009). The determination of the specific surface area of solids by gas adsorption—BET method, is a standardized method for powder samples and often used for both clays as SCMs. The specific surface area that is measured by the BET method includes the pore size distribution and can be used to estimate dissolution rate (Gautier et al., 2001). Also in the pozzolanic reaction the dissolution rate of the calcined clay is a crucial parameter that influence the reaction. Therefore the BET technique is for this study the most appropriate specific surface are measurement.

In function of the pozzolanic reactivity, it is important to determine the BET specific surface area of the calcined clays (Brunauer et al., 1938). Nevertheless, the specific surface area of the raw clays can give insight in the evolution of the surface area upon thermal treatment. Therefore, the specific surface area of both raw and calcined clays was analyzed.

The specific surface area was obtained by the Brunauer-Emmer-Teller (BET) method, which is based on the theory of physical adsorption of gas molecules to the surface of a material. The measurement was performed on a Micrometrics Tristar 3000 using N_2 as an adsorbate. Since the pre-treatment of the clay samples strongly influences the measured BET values, it is critical to retain the same conditions for all samples to be comparable. Furthermore, the temperature window where only adsorbed water is vaporized and no structural water is removed, is sometimes rather narrow (Michot and Villiéras, 2006). Initially the pretreatment temperature of 60°C was chosen to assure the clay structure was not affected. However this temperature proved to be insufficient for smectite rich clays. For the Ca-montmorillonite the correct BET SSA of the raw sample is known and should be around 97 m^2/g according to the data report of the source clay (Van Olphen and Fripiat, 1979). However the BET SSA after pretreatment of the sample for 12h at 60°C was only 15.20 m^2/g, which is fairly when compared to the expected value. Next, the sample was pretreated by heating it to 110°C for 24 h to make certain all the adsorbed water is removed and cannot interfere with the measurement while the structural bound water is still not affected. This resulted in an average BET value of 85.93 m^2/g. This indicates the preparation method of clay samples, especially smectite rich

clays, is crucial to obtain a reliable result. To compare the BET SSA results to each other the preparation needs to be the same for all samples. Therefore, all samples were measured after a pretreatment with a heating temperature of 110°C, a duration of 24 h and in a continuous N_2 gas flow.

The repeatability of this method was tested by analyzing in duplicate three samples with different mineralogy and thermal treatment, so they are representative for the whole sample set. The relative repeatability errors (%RSD = 100*(standard deviation / mean)) are below 2.7%, which indicates the error margin is still acceptable (Table 3.3) and the applied pre-treatment delivers repeatable results.

Table 3.3: *Relative repeatability error (%RSD) for BET specific surface area.*pretreatment at 60°C for 12h.*

Sample	Mineralogy	State	BET 1 (m^2/g)	BET 2 (m^2/g)	Mean (m^2/g)	% RSD
KGA-2	98.5 % kaol.	Raw	19.27	19.30	19.29	0.12
		C: 700°C	19.41	19.44	19.43	0.10
SAz-1	98 % montm.	Raw*	15.20	-	-	-
		Raw	87.26	84.60	85.93	2.19
		C: 800°C	4.30	4.47	4.38	2.62
WS 35/38	46% kaol.	Raw	39.95	38.59	39.27	2.45
	30% 2:1 Al clays	C: 800°C	44.94	45.26	45.10	0.49

3.7 GRAIN SIZE ANALYSIS

Besides the specific surface area also the particle size distribution (PSD) influences the pozzolanic reactivity considerably. In general finer ground calcined clays will provide higher pozzolanic reactivity since a lower particle size means higher potential reactive surface area (Danner, 2013). Furthermore the particle size is influenced by the calcination process, whereby a higher calcination temperature gives rise to additional sintering of the clay particles and an increase of the particle size.

The particle size distribution of the raw and calcined clays was determined by laser diffraction. This technique relies on the fact that particles scatter light at a range of angles, which are characteristic of their size. The volumetric particle size distribution is than calculated by using a mathematical deconvolution procedure based on the Mie theory, which transforms each particle to a perfect sphere. In practice and in theory it has been shown that for clay minerals, which are not perfect spheres, the clay size fraction is often underestimated (Eshel et al., 2004; Konert and Vandenberghe, 1997).

The clays, both raw as calcined, were pretreated by boiling the samples after adding peptiser (Na-polyphosphate). No removal of organic material, carbonates or iron coating was done, since this would not resemble how the particles are available in the sample during either the calcination process or during the pozzolanic reaction. Afterwards the samples were subjected to an ultrasonic treatment of 2 min and measured with a Malvern Mastersizer S in aqueous environment. In general samples were measured in duplicates and the average values are taken into consideration.

3.8 FTIR ANALYSIS

Fourier transform infrared spectrometric analyses (FTIR) are used in mineral research to study the structure and bonding of the molecules within the clay minerals. The vibration and rotation energies of the bonds present in the molecule absorb specific resonant frequencies that reflect the characteristics of the molecules structure (Madejova, 2003). The transformation of the OH-bonds upon calcination of the clay can easily be monitored.

Furthermore, the stretching of the hydroxyl groups can be used to give qualitative and quantitative information on the degree of ordering of the kaolinite structure. The ratio between the intensities of the bands observed at 3620 and 3695 cm^{-1}, known as the P_0 index, allows to quantify the degree of ordering (Bich et al., 2009). Kaolinite can be seen as high ordered when $P_0 > 1$. The main advantage is that the P_0 index is not influenced by additional mineral components like quartz or feldspar and can therefore also be used in natural clay mixtures (Galos, 2011). FTIR analysis was carried out on KBr-pellets using a Nicolet^{TM} 760 spectrophotometer and a mid-IR spectral range from 400 to 4000 cm^{-1}. A DTGS-KBr detector was used and the resolution was 4 cm^{-1} with a co-addition of 100 scans.

3.9 NMR ANALYSIS

Nuclear Magnetic Resonance (NMR) spectroscopy gives insight into the local bonding environment of atoms and their interactions with neighboring atoms. Furthermore, this technique allows gaining insight in the structural features of the semi-crystalline and amorphous materials. The method relies on the interaction of the atomic nuclei with an imposed electromagnetic field. The atomic nuclei will resonate with a specific frequency that is a function of the magnetic field that surrounds the nucleus and the presence of neighboring electrons. This effect is called 'shielding' and results in a shift in the resonance frequency which is characteristic and gives information about the type and number of neighboring atoms (Sanz, 2006). To determine the coordination number, estimate the number of oxygen atoms shared with neighboring Si atoms and the type of neighboring atoms ^{29}Si MAS NMR was used. ^{27}Al MAS NMR is used to make a distinction between the coordination of Al (octahedral, tetrahedral or 5-fold) (Lippmaa et al., 1982). The iron (Fe_2O_3) content of the clay sample should be preferably below 4%, since higher iron contents provoke significant signal weakening and broadening of the spectra, which makes interpretation and accuracy more difficult (Zhang et al., 2010).

In this study NMR was applied to study the evolution of the Si and Al environments caused by structural changes during calcination of Na- and Ca-montmorillonite. The ^{29}Si MAS NMR spectra were recorded on a Varian INOVA-400 spectrometer (9.39 T) equipped with a homebuilt CP/MAS NMR probe for 7 mm o.d. zirconia (PSZ) rotors. The sample spinning frequency was 6.0 kHz, the pulse width 3.0 µs (~45°), the relaxation delay 15 s, and typically 5600 scans were acquired. The ^{27}Al MAS NMR spectra were obtained on a Varian DirectDrive VNMR-600 (14.09 T) spectrometer using a homebuilt CP/MAS probe for 4 mm o.d. zirconia (PSZ) rotors. A spinning speed of 13.0 kHz, single-pulse excitation with a pulse width of 0.5 µs a relaxation delay of 2.0 s, and typically 4096 scans were used.

3.10 POZZOLANIC REACTIVITY TESTS

3.10.1 INTRODUCTION

The pozzolanic reactivity is a measure of the potential of the material to be used as Supplementary Cementitious Material (SCM) and the reaction rate. In industry and research several test methods exist based on chemical, physical and mechanical methods. In this study two different test methods were applied. The first method determines the remaining portlandite of pozzolan – lime pastes by means of TGA. Since representative results can only be obtained after 28 days, this method is rather time consuming. Therefore a second normalized (NF P 18-513) test was introduced, the Chapelle test, whereby an aqueous solution containing lime and the pozzolanic material is prepared and heated to speed up reaction. The amount of unreacted free lime can be obtained within 24 h. Both methods provide quantitative information on the pozzolanic reaction and can therefore be seen as direct testing methods.

3.10.2. CALCIUM HYDROXIDE QUANTIFICATION BY THERMOGRAVIMETRIC ANALYSIS

The pozzolanic potential and the reaction rate of calcined clays have been studied in detail by preparing calcined clay - lime mixtures. Thermogravimetric analysis allows to determine to which extent the calcined clay reacts with the lime by calculating the weight loss of the unreacted lime. Research has shown that this method gives an accurate determination of the pozzolanic reactivity (Mertens et al., 2009; Rojas and Cabrera, 2002; Roszczynialski, 2002; Serry et al., 1984; Silva et al., 2014; Snellings et al., 2012; Tironi et al., 2014). In addition, it has been proven that also the evolution of the activity in time and the formed hydration phases, specific for the calcined clay –lime system, can be monitored efficiently (Gameiro et al., 2012; Silva et al., 2014; Tironi et al., 2014).

In previous studies the calcined clay-slaked lime ratio of the prepared pastes varies between 20:80 and 50:50 (Danner, 2013; Gameiro et al., 2012; Silva et al., 2014). To optimize the reaction rate in order to study the evolution of the calcined clay-lime system a ratio of 30:70 was chosen. The mixtures of calcined clay and hydrated lime were dry-blended using a Turbula mixer for 4 h. Distilled water was added to obtain a water/solid ratio of 1:1. The pastes are blended by hand for 5 min and divided over eight sealed recipients of 3ml each. During this process it is important to work quickly and efficient to prevent carbonation. Moreover, inclusions of air bubbles, which contain CO_2, should be avoided by tapping the sample tubes during filling. Afterwards, the pastes are stored in an acclimatized room with a temperature of 20°C and a relative humidity of 95% ± 5% to favor the hydration reaction over the carbonation reaction (Cizer, 2009).

In cement research the pozzolanic reactivity of the samples is determined after 3, 7, 14, 28, 56 and 90 days. After each period the hydration reaction needs to be stopped in order to be able to compare the pozzolanic reactivity of the different samples. Investigation of different techniques pointed out that vacuum freeze drying of the samples is a good and reliable method (Gallé, 2001). During vacuum freeze drying the excess of water that is not bound by the formed hydration phases is removed to obtain a stable powder (Mertens, 2009). The pastes were vacuum dried using a Christ Alpha 1-2 LD at 0.03 mbar for 2 h to stop the hydration reactions according to the procedures described in Knapen et al. (2009). The dried samples were then stored in a desiccator until measurement to prevent hydration.

The portlandite ($Ca(OH)_2$) consumption over time was monitored by thermo gravimetric analysis (TGA). For the measurements a Netsch STA 409PC instrument with simultaneous TGA and DSC

recordings was used. The sample was heated in Al_2O_3 crucibles from 25°C to 1000°C with a heating rate of 10°C/min in a N_2 atmosphere with a 60 mL/min flux.

Portlandite decomposes between 420 and 450°C to CaO, resulting in a weight loss due to the water that is released. The pozzolanic reactivity can then be estimated by calculating the weight loss of the remaining calcium hydroxide in the 350-600°C range by linear extrapolation, shown in Figure 3.2. This method, proposed by Taylor (1997), is expressed relative to the dry weight and is corrected for the background mass loss.

The portlandite that is fixed on the calcined clay can be calculated with the following formula:

$$\%\ \text{Portlandite consumed} \ = \ 100 \ \times \left(1 - \frac{Mr(Ca(OH)_2) \ \times \ \%\, H2O}{Mr(H_2O) \ \times \ \%Ca(OH)_2}\right)$$

With:

Mr ($Ca(OH)_2$) = 74.08 g/mol
Mr (H_2O) = 18 g/mol
% H_2O = mass loss from decomposition of portlandite
% $Ca(OH)_2$ = amount of portlandite in the mix when blended. For all samples this is 70%.

The rate of the consumption of calcium hydroxide provides an estimation on the pozzolanic reaction rate. Furthermore, the first derivate (DTG) allows to identify the different hydration products that were formed as a result of the pozzolanic reaction. The temperatures of dehydration, dehydroxylation, release of CO_2 and other volatiles are characteristic for each mineral and hydration phase. To study these phases in detail it was opted to work on calcined clay lime mixtures to avoid the interference of cement phases. Additional XRD measurements were performed on the paste to supplement the results from TGA (see paragraph 3.4.1.).

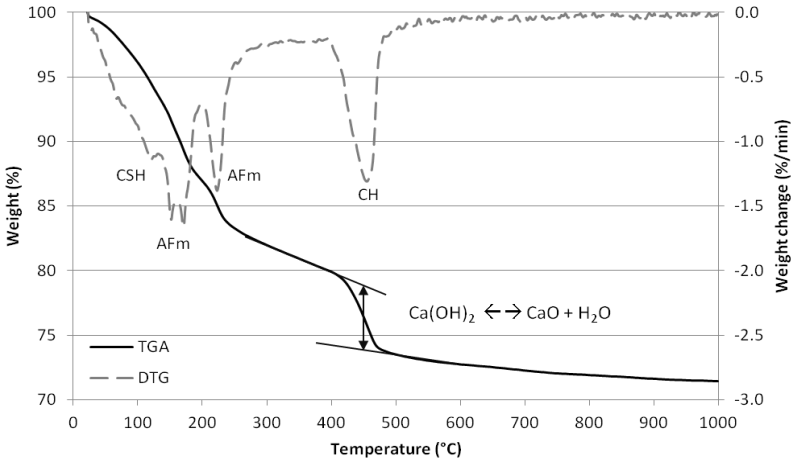

Figure 3.2.: *Calculation of the weight loss of the decomposition of calcium hydroxide (CH) between 350°C and 550°C by the tangent method. The DTG allows to identify the hydration phases that are formed (C-S-H: calcium silicate hydrate, AFm: monosulfoaluminates, CH: portlandite).*

3.10.3 CHAPELLE TEST

Since TGA-reactivity tests are rather time consuming, a more rapid test method, the Chapelle test, was also used. The chapelle test is a direct and rapid method to evaluate the pozzolanic reactivity of SCMs in terms of the decrease of the free lime in the system. For calcined clays, and metakaolin in

particular, a modified chapelle test was established and included into the French norm to qualify as metakaolin (NF P 18-513 2013).

According to this test, the measure of the quantity of fixed calcium hydroxide by the calcined clays gives an estimation of the pozzolanic reactivity of that calcined clay. In this test 1.0 g ground calcined clay is blended with 2.0 g CaO and 250 mL distilled water and heated to 85°C for 16 h. With each batch of samples also a blank sample was made which only contained CaO and water. The non-reacted lime was leached with sucrose solution and the amount was determined by means of titration with 0.1N HCl(aq.) and phenolphthalein as coloring agent. The amount of $Ca(OH)_2$ that was fixed by the calcined clay is calculated with the following formula:

$$\textit{mg of } Ca(OH)_2 \textit{ per g of calcined clay} = 2 \times \frac{V\ (0.1N\ HCl)_{blank} - V\ (0.1N\ HCl)_{sample}}{V\ (0.1N\ HCl)_{blank}} \times \frac{Mr(Ca(OH)_2)}{Mr(CaO)} \times 1000$$

With:

$V(0.1N\ HCL)_{blank}$: The volume of 0.1N HCl in ml consumed by the 25 ml blank solution
$V(0.1N\ HCL)_{sample}$: The volume of 0.1N HCl in ml consumed by the 25 ml sample solution
$M_r(Ca(OH)_2)$: molecular mass of calcium hydroxide: 74.09 g/mol
$M_r(CaO)$: molecular mass of calcium oxide: 56.08 g/mol

The result is then expressed in mg $Ca(OH)_2$ fixed by the calcined clay. The precision of this method is stated to be 10% (NF P 18-513, 2013).

3.10.4 CHAPELLE VERSUS THERMOGRAVIMETRIC ANALYSIS

INTRODUCTION

The chapelle test has been applied to metakaolin in several studies (Badogiannis et al., 2005; Ferraz et al., 2015; Ilic et al., 2010; Kakali et al., 2001; Silva et al., 2014), delivering comparable results. However, it has not often been applied on other calcined clays and impure clays. Therefore the results of the chapelle test are compared with those determined by TGA in calcined clay – slaked lime pastes. Two different sample sets were analyzed, 8 pure reference clays (Chapter 4) and 7 natural clays with variable kaolinite and 2:1 Al clay content (Chapter 7). The following three research questions were investigated regarding the Chapelle test:

- Is it possible to estimate the optimal activation temperature?
- Can this method be applied on smectitic and illitic clays?
- Can this method be applied on natural clay mixtures?

RESULTS AND DISCUSSION

The amount of $Ca(OH)_2$ that was fixed by the clay is visualized in Figure 3.4. For the kaolinitic clays the qualitative test results are rather similar to those defined by means of TGA (Figure 3.3), especially when the plausible error of 10% for the chapelle test is taken into account. A broad range of calcination temperatures seems to be suitable and the high ordered kaolinites K1 and K2 have lower activity when fired at 500°C. Therefore, a good estimation of the reactivity of kaolinites can be made based on the chapelle test.

However, for the smectites S1 and S2 calcined at 800°C the reactivity seems to be similar to the reactivity of the kaolinites. This indicates that there is an overestimation of the reactivity of S1 and S2 by the chapelle test compared to the portlandite consumption determined by TGA at 28 days.

Nevertheless, the results show that S2 is more reactive than S1, which is more reactive than I1 and S3. Furthermore, the optimal calcination temperature at 800°C for smectites and at 900°C for illite can be determined correctly. The overestimation is probably associated with the enhanced thermal energy of the chapelle test (85°C) compared to TGA (20°C). This results in an acceleration of the pozzolanic reaction kinetics and thereby of the portlandite consumption. Due to this significant difference in the reaction kinetics the chapelle test is measuring the maximum amount of portlandite that can be fixed by the clay. Regarding the TGA results, the optimal activation temperature is determined at 28 days and while most kaolinite is already consumed, smectitic clay reacts much slower. Moreover, the difference between the portlandite consumption of smectite versus kaolinite becomes smaller at a later stage of the reaction (≥ 90 days). As a result the result of the Chapelle test of the smectitic clays are qualitatively more comparable with the TGA results at a later stage of the reaction (≥ 90 days).

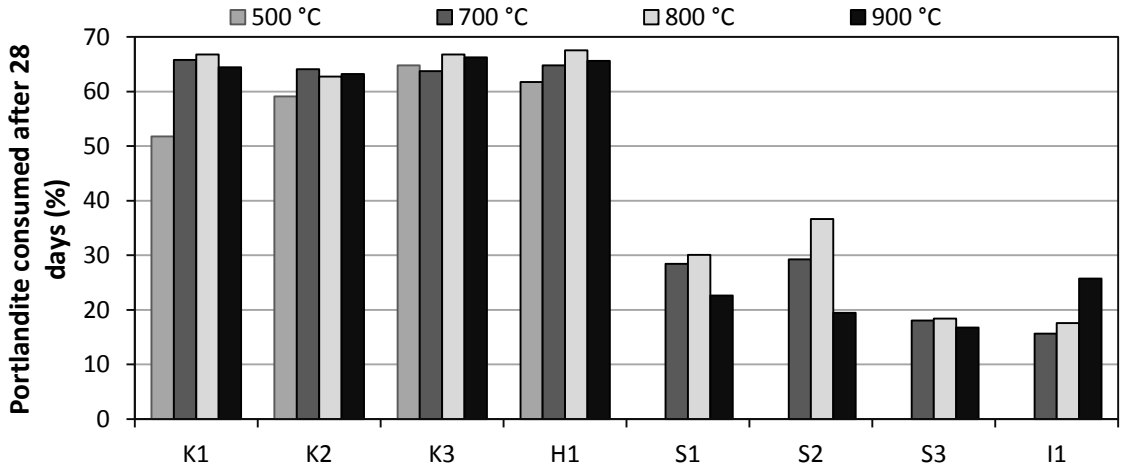

Figure 3.3: *Portlandite consumption of the pure reference clays determined on calcined clay – lime pasts after 28 days by TGA. The clays were calcined at different temperatures. Kaolinitic clays K1, K2, K3 and H1; Smectitic clays: S1, S2 and S3; and illitic clays I1. A more detailed description of the samples can be found in Chapter 4.*

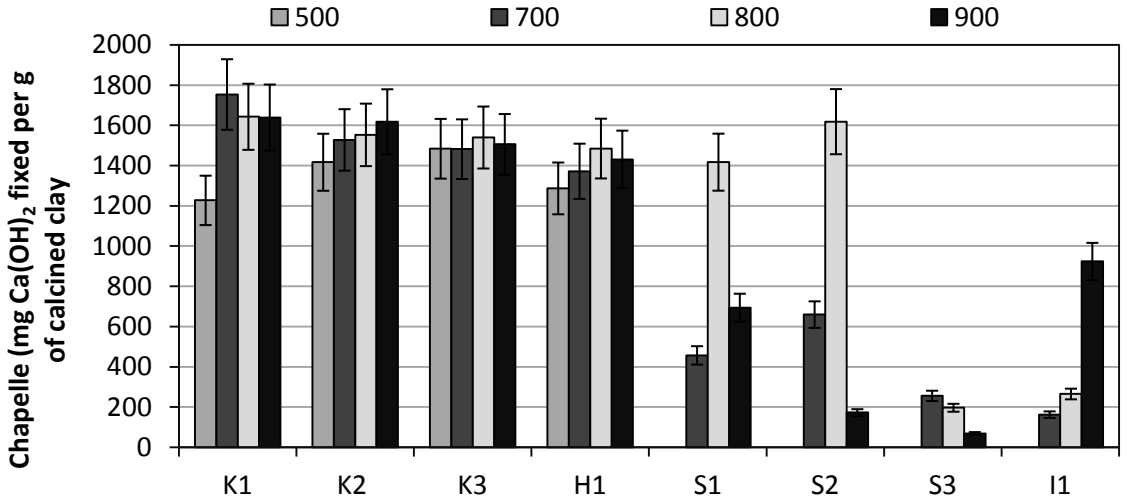

Figure 3.4: *Chapelle test of the pure reference clays giving the amount of $Ca(OH)_2$ fixed by the different clays calcined at 500, 700, 800 and 900°C.The error bars represent the general accepted error of 10%. Kaolinitic clays K1, K2, K3 and H1; Smectitic clays: S1, S2 and S3; and illitic clays I1. A more detailed description of the samples can be found in Chapter 4.*

The pozzolanic reactivity results of the natural clay deposits, rich in kaolinite, are given in Figure 3.5. In general the findings of the chapelle test do not correspond to those determined by TGA. The R-ALK-R clay is seen as the most reactive clay based on the chapelle test, while this clay only comes at the 5th position when TGA is used. Furthermore the pozzolanic reactivity of the clays archi, CS S and WS 35/38 is fairly low in the chapelle test. The mineralogical composition of these clays shows that, besides kaolinite, they all possess more than 15% of 2:1 Al-clays. This indicates that there is a relation between the reliability and usability of the chapelle test and the presence of 2:1 Al-clays. The Fos Bianca, containing only 8% of 2:1 Al-clays, is more reactive and is placed before Archi and CS S according to the chapelle test.

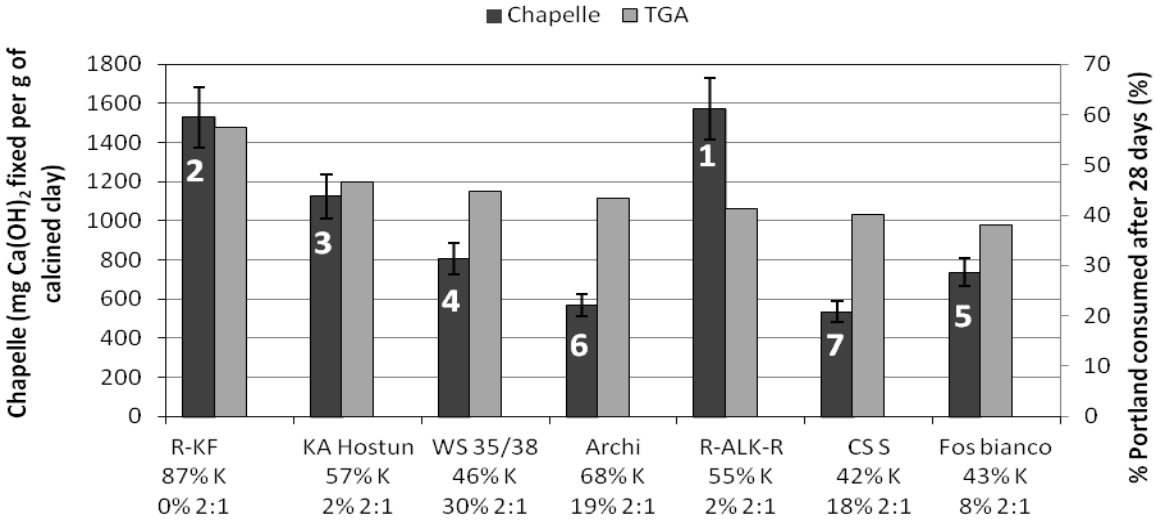

Figure 3.5: *Comparison between the $Ca(OH)_2$ consumption of the natural kaolinitic clays between the chapelle test and TGA. The following calcination temperatures were applied: 750°C R-KF, KA Hostun, R-ALK-R and 800°C archi, WS35/38, Fos bianco and CS S. The clays are arranged from highest (left) pozzolanic reactivity determined by TGA to lowest (right).The content Kaolinite (K) and 2:1 Al-clays (2:1) is indicated. A more detailed description of the samples can be found in Chapter 6.*

To test the reliability of both methods a repeatability test was performed. For the Chapelle test five clays with a variable mineralogical composition were selected, three samples were analyzed in duplicate and two in triplicate (Table 3.4). The clays which only contain kaolinite as clay mineral, H1 and R-KF, have an excellent repeatability with the relative repeatability errors (RSD) below 3%. The non-clay mineral impurities present in sample R-KF apparently do not negatively influence the repeatability of the measurements. The RSD values of the smectitic rich clays S2 are already elevated, especially for the clay fired at 800°C with a RSD of 17.58%. When also impure clays containing 2:1 Al-clays are taken into account, the repeatability is even worse, above 30%, indicating a poor repeatability of natural occurring clays, certainly when they contain 2:1 Al clays.

Table 3.4: *Relative repeatability error (%RSD) for the chapelle test.*

Sample	Mineralogy	Calc T	Chap 1	Chap 2	Chap 3	Mean	% RSD
			Expressed in mg $Ca(OH)_2$ fixed on the calcined clay				
H1 (hal.)	99% halloy.	800°C	1485	1431	-	1458	2.62
S2: SAz-1	98% montm.	700°C	618	660	-	639	4.65
S2: SAz-1	98% montm.	800°C	1261	1619	-	1440	17.58
Fos bianco	43% kaol. 8% 2:1 Al clays	800°C	751	505	956	737	30.63
R-KF	87% kaol.	750°C	1529	1539	1516	1528	0.75

The relative repeatability error was also calculated for the TGA method (Table 3.5). For four samples two sets of pastes were prepared and after curing measured by TGA. The portlandite consumption after 28 days was tested in triplicate, since this day is the most important to assess the reactivity and optimal activation temperature in the cement industry. All samples, both pure and natural clays, show good RSD values below 4.1% for all days. The measurements on day 3 and 7 of the reaction exhibit the highest RSD percentages. At the early stage of the reaction, the reaction rate is often the highest, resulting in larger errors on the measurement repeatability. For 28 days the RSD varies between 0.70 and 1.30%, which indicates this method has a much better repeatability than the chapelle test and is therefore prefered. Especially for the clay Fos bianco this is well illustrated since the RSD value by means of chapelle is 30.63% while for TGA this is only 1.27%. Furthermore the RSD for kaolinites, smectite and natural mixtures is equivalent for TGA. On the longer term (56 – 90 days) the reaction slows down and errors are leveled out resulting in low RSD < 1%. The calculated RSD values correspond well to the error ranges that are reported in literature for determining the portlandite consumption with TGA. For calcined clays errors of 2% (Fernandez, 2009) are listed while for other materials the error can increase to 5% (Aubert et al., 2012).

Table 3.5: *Relative repeatability error (%RSD) for the TGA test*

Sample	Mineralogy	Day	TGA 1	TGA 2	TGA 3	Mean	% RSD
			Expressed in % $Ca(OH)_2$ consumed by the calcined clay				
H1 (hal.)	99% halloy.	3	34.75	34.92		34.84	0.33
		7	50.46	52.92		51.69	3.37
		14	62.90	63.82		63.36	1.02
		28	66.60	67.55	66.98	67.05	0.71
		56	66.90	67.52		67.21	0.66
		90	67.42	67.68		67.55	0.28
S2: SAz-1	98% montm.	3	16.30	17.11		16.70	3.45
		7	22.49	23.82		23.15	4.06
		14	29.82	28.78		29.30	2.49
		28	36.66	37.63	37.03	37.11	1.31
		56	47.71	47.73		47.72	0.04
		90	52.09	52.53		52.31	0.60
Fos bianco	43% kaol.	3	21.82	20.69		21.25	3.77
	8% 2:1 Al clays	7	29.52	30.85		30.19	3.12
		14	35.61	35.00		23.54	1.85
		28	38.15	39.03	38.98	38.72	1.27
		56	40.76	41.09		40.92	0.57
		90	42.19	41.99		42.09	0.34
CS S	42% kaol.	3	23.84	23.13		23.48	2.11
	18% 2:1 Al clays	7	30.58	29.64		30.11	2.21
		14	38.75	37.97		38.36	1.44
		28	40.08	40.74	37.03	40.46	0.85
		56	41.51	41.03		41.27	0.82
		90	42.58	43.16		42.87	0.95

CONCLUSION

The chapelle can still be used as a qualitative technique for pure clays (kaolinite, montmorillonite and illite) to determine the optimal activation temperature. However, the test results should not be compared quantitatively to each other when other clay minerals besides kaolinite are involved since the pozzolanic reactivity of pure smectites is overestimated. The only advantage is the limited amount of time (<24 h) that is needed to gain information of the optimal calcination temperature

compared to the 28 days of the TGA test. When natural clays are taken into account, the pozzolanic reactivity is not determined correctly, especially not when 2:1 Al clays (illite and smectite) are involved. Furthermore the repeatability decreases drastically for smectite (up to RSD 17%) rich clays and for natural clay mixtures (up to RSD 30%), which negatively affect the reliability of the chapelle test.

CHAPTER 4

PURE CLAYS

Several studies have already demonstrated the effectiveness of calcined clays, particularly for kaolinitic clays to produce metakaolin with increased pozzolanicity, i.e. reactivity with portlandite (Al-Rawas and Hago, 2006; Fernandez et al., 2011; He et al., 1994; Sabir et al., 2001; Tironi et al., 2012). However, calcined clays other than metakaolin are hardly used as SCMs due to the complexity of clay minerals and ignorance of the underlying reaction mechanisms. Furthermore the characteristics of the clay like degree of ordering, the exchangeable cations and the variation in clay structure are often neglected. Hence this study investigates the potential use of calcined clays from a mineralogical point of view by linking the characteristics of the untreated clays to the pozzolanic reactivity of the calcined clays. Since it is of key importance to understand the origin of the pozzolanic reactivity and determine the main parameters that influence the reactivity, pure reference clays (kaolinitic, smectitic, illitic) are used to avoid interference of impurities. Eight clays were selected to have an optimal range of clay minerals, variable degree of ordering, di- and tri-octahedral smectites and differences in the predominant cations.

4.1 MATERIALS

Eight rather pure clays, four kaolinitic clays, with differences in degree of ordering, three smectitic clays and one illitic clay were selected for this study (Table 4.1). Kaolinite (KGA-1 and KGA-2), Ca-montmorillonite (SAz-1), Na-montmorilonite (SWy-1), hectorite (SHCa-1) and illite (IMt-1) were obtained from the Clay Minerals Society repository. The kaolinite Capim and halloysite were supplied by an industrial mineral producer.

However, these reference clays are natural materials and as such, they are not entirely pure as proven by previous studies (Chipera and Bish, 2001). Impurities of titanium-oxides, quartz, feldspar and calcite can influence the activity of the clay. The smectitic and illitic clays with a high content of impurities (5-50%) according to the bulk mineralogical analyses of the raw clays, were therefore first purified according to the Jackson procedure (Adriaens, 2015; Jackson, 1975; Zeelmaekers, 2011). Afterwards the fraction <2 µm of the smectitic clays was separated by centrifugation to obtain a clay containing less than 2% impurities. Since the illitic clay mainly contained coarse illite (>2 µm) the fraction <63 µm was used in order to limit the amount of impurities to 8%.

The difference of the diffraction pattern before and after purification is shown in Figure 4.1 for the least pure clay, S3. The predominant impurity of S3 was calcite and also some traces of dolomite and quartz were present. Since some quartz was present in the clay fraction <2 µm, this impurity could

not be removed entirely. The other smectites and illite mainly contained quartz, muscovite and calcite as impurities which could mainly be removed. The kaolinitic clays contain anatase as impurity. Even with magnetic separation techniques it was not possible to remove this anatase. Furthermore since the quantities were low (<2%) it was decided to use the kaolinites as received.

Table 4.1: *Overview of the selected clay minerals with the Characteristics of the raw and calcined clays, Hinckley index (HI), ordering (P_0) and BET specific surface area (SSA).*

	Clay	Ordering HI	Ordering P_0	Ordering	SSA (m^2/g) raw	SSA (m^2/g) Fired at 800°C
K1	Capim	0.85	1.580	High	8.86	9.54
K2	KGA-1	0.74	1.360	High	7.02	7.51
K3	KGA-2	-	0.380	Medium	19.27	19.71
H1	Hal.	-	-	Low	34.38	32.62
S1	SWy-1	-	-	-	23.36	4.19
S2	SAz-1	-	-	-	87.26	4.32
S3	SHCa-1	-	-	-	123.46	1.47
I1	Imt-1	-	-	-	19.91	0.79 (900°C)

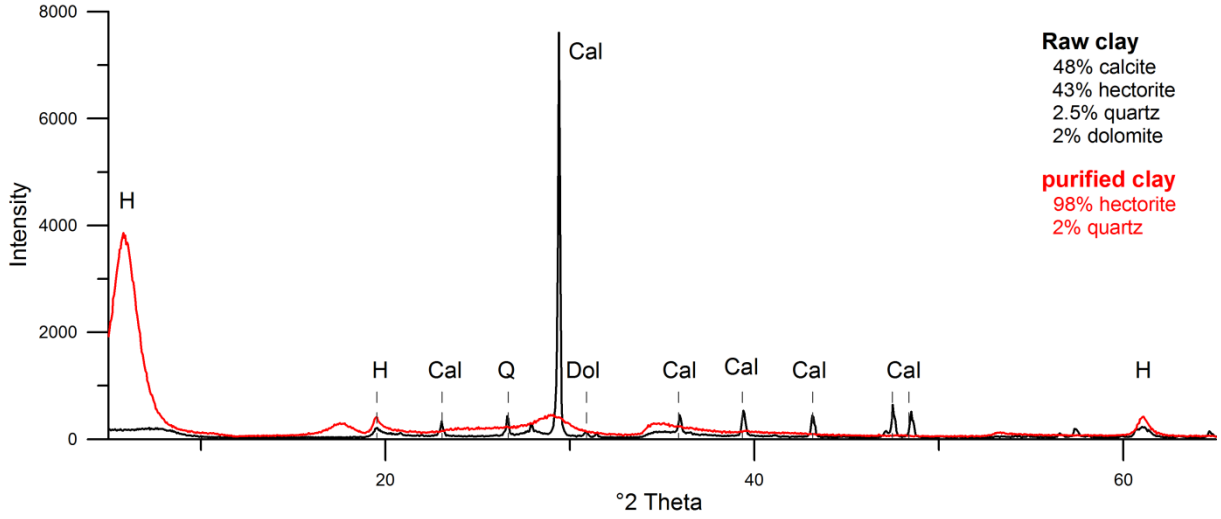

Figure 4.1: *XRD pattern of hectorite, S3, before and after purification. H: hectorite, Cal: calcite, Q: quartz and Dol: dolomite.*

4.2 CHARACTERIZATION

4.2.1 CHEMISTRY

The bulk chemical composition of the unfired clays (kaolinites, purified illite <63 µm and purified smectites <2 µm) is reported in Table 4.2. Kaolinitic clays contain a high alumina content up to 40 wt.%, with Si/Al ratio of 1.16, calculated based on SiO_2/Al_2O_3. The 2:1 clays S1, S2 and I1 show a higher Si/Al ratio of on average 3 due to the lower amount of alumina present in these clays.

Smectitic clay S3 contains only some traces of alumina, since the dominant cation occupying the octahedral position is magnesium, resulting in a clay that contains >20 wt.% Mg.

Table 4.2: *Bulk chemical composition and Si/Al ratio (in wt%) of the kaolinites, purified illite (<63 µm) and purified smectitic clay fraction, calculated based on SiO_2/Al_2O_3, of the unfired clays.*

% Weight	SiO_2	Al_2O_3	Fe_2O_3	CaO	MgO	K_2O	Na_2O	TiO_2	LOI	Si/Al
K1	45.82	38.79	0.56	0.01	0.05	0.03	0.20	0.42	14.12	1.18
K2	46.24	40.03	0.27	0.03	0.04	0.03	0.02	1.59	11.76	1.16
K3	44.77	38.45	1.12	0.02	0.06	0.05	0.01	2.23	13.29	1.16
H1	44.85	38.62	0.17	0.04	0.04	n.d.	n.d.	0.01	16.27	1.16
S1	58.03	19.60	4.08	0.02	2.36	0.04	3.04	0.09	12.74	2.96
S2	57.72	16.92	1.49	3.31	5.82	0.03	0.06	0.22	14.41	3.41
S3	52.62	0.46	0.34	2.28	23.67	0.09	0.15	0.02	20.48	/
I1	52.62	22.63	6.64	0.12	2.32	7.72	0.48	0.78	6.68	2.32

4.2.2 THERMAL ANALYSIS

To study the thermal behavior of the different clays thermogravimetric analysis (TGA) was used. Calcination of the clay results in thermal events like dehydration, dehydroxylation and possible recrystallization. Especially the temperature at which full dehydroxylation is achieved is important since clays that are fully dehydroxylated tend to posses better pozzolanic properties (Danner, 2013). Furthermore the dehydroxylation temperature range can give more information on the type of the clay mineral and the structure of the clay. The differential of the TGA (DTG) patterns are given in Figure 4.2. The kaolinitic clays show already a clear distinction in their thermal behavior. The dehydration of kaolinite takes place in the temperature range between 50 and 150 °C. The intensity of the dehydration peak can be correlated to the degree of ordering of kaolinite. Low ordered clays tend to contain more water molecules absorbed to the outer surface which are released at low temperatures (Emmerich, 2011). The halloysite can therefore be seen as the least ordered clay since it has a large dehydration peak with a corresponding weight loss around 2%. While K1 and K2 have no significant weight loss in this region K3 is marked by 0.6 % weight loss due to dehydration. This indicates K3 is less ordered than K1 and K2 but more ordered than H1.

In the temperature range of 530 to 700°C dehydroxylation of kaolinite takes place. Both peak intensity and position vary for the 4 kaolinite samples. Peak intensity can be correlated to the amount of hydroxyl groups incorporated in its structure. K1 and K2 have lower peak intensities than K3 and H1. The peak position refers to the ease, or the amount of energy that is needed to remove the hydroxyl groups from the structure. A high ordered kaolinite is therefore marked by a higher dehydroxylation temperature. The highest dehydroxylation temperature is that of K1 with a value of 535°C. K2 dehydroxylates at 522°C while K3 has a lower temperature of 501°C. The halloysite clay has a similar behavior as that of kaolinite and its dehydroxylation temperature of 519°C is rather high. However the determination of the degree of ordering based on thermal analyses for halloysite cannot be directly compared to that of kaolinite, only to other halloysite clays.

The DSC signal (Figure 4.3) revealed a third important thermal reaction, namely recrystallization. At 1000 °C a sharp exothermic peak could be observed for all four clays. At this temperature silica is segregated and a new crystalline phase mullite is formed. Recrystallisation should be avoided as Si and Al will no longer be freely available to react with lime.

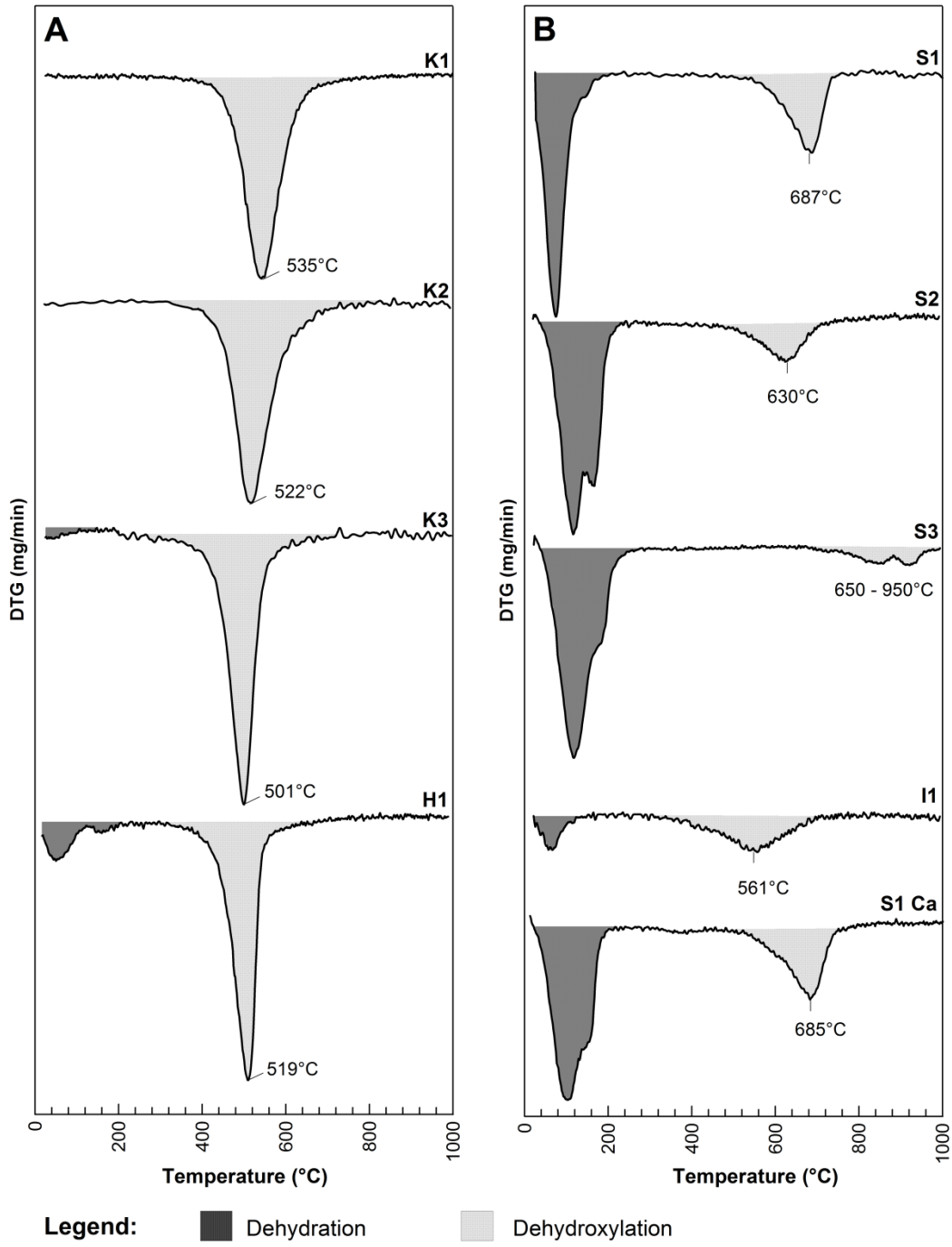

Figure 4.2: *DTG analyses of the raw clays kaolinitic clays (A) and purified smectitic and illitic clays (B).*

For the 2:1 Al clays the thermal behavior depends on their swelling behavior and the cation that is present. The dehydration reaction takes place up to 300°C. Non-swelling clays are marked by a weak dehydration reaction while for swelling clays like montmorillonite the dehydration is more intense. The weight loss of I1, a non-swelling clay, is therefore limited to 1.3% and can be compared to the weight loss of kaolinite. The smectitic clays are marked by weight losses between 7 and 9%. The position and number of the dehydroxylation peaks can be correlated to the cation that is present. Monovalent interlayer cations give rise to an intense single peak while divalent cations are marked by a double peak or shoulder is visible at the high temperature side of the peak (Emmerich, 2011). This indicates S1, with its single peak, contains monovalent (Na^{+}) cations while S2 and S3 contain divalent cations (Ca^{2+}). These results are in agreement with the chemical composition of the smectitic

clays. The influence of the cation on the dehydration is further demonstrated when sample S1, which contains Na^+ as dominant exchangeable cation, is compared to S1-Ca whereby Na^+ has been exchanged for Ca^{2+}. The single peak of S1 is converted to a double peak and shifted to a higher temperature range (figure 4.2).

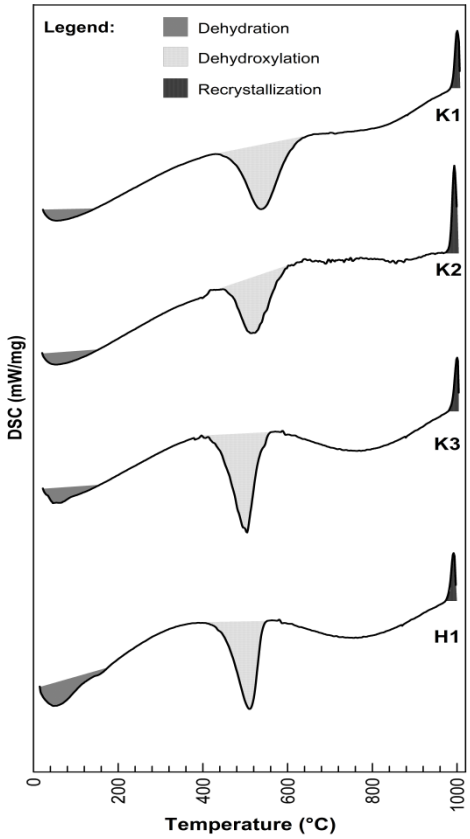

Figure 4.3: *DSC curve of the kaolinitic clays with indication of the three main thermodynamic reactions: dehydration, dehydroxylation and recrystallization.*

The dehydroxylation of 2:1 clays can take place over a broad range of temperatures generally between 450 and 850°C, nevertheless even temperatures as high as 1050 °C have been recorded in the past (Emmerich, 2011). The clay I1 has a rather weak and low dehydroxylation temperature at 560 °C which is typical for illitic clays. For smectitic clays the difference in dehydroxylation peak temperature can be attributed to the vacancies in the octahedral sheet (Drits et al., 1995; Emmerich, 2011; Środoń et al., 2001). For dioctahedral smectites like S1 and S2 the peak position gives more structural insight in whether the octahedral cation occupies the M1 (trans) or M2 (cis) site (Güven, 1988). Trans vacant clays are characterized by a lower dehydroxylation temperature between 500 and 550°C while cis vacant clays dehydroxylate between 650 and 700°C (Wolters and Emmerich, 2007). The dehydroxylation peak of S1 at 687°C demonstrates that it is predominantly a cis vacant montmorillonite as was proven in previous studies (Drits et al., 1995). S2 shows a lower dehydroxylation temperature at 630°C, which indicates the presence of a mixture of cis and trans vacant (Wolters and Emmerich, 2007). The similarity between the dehydroxylation peak of S1 and S1-Ca indicates that the influence of the interlayer cation on the position and intensity of the dehydroxylation is negligible. The dehydroxylation of the trioctahedral hectorite S3 is situated in the temperature range between 650 and 950°C and is characterized by a double peak.

To study the difference in dehydroxylation behavior in more detail and to estimate the calcination temperature the degree of dehydroxylation was calculated for each sample and plotted in Figure 4.4. For the kaolinitic clays it can be observed that the dehydroxylation of K3 and H1 starts earlier than for K1 and K2. Nevertheless the curve is for all four samples steep and fairly similar. K1 and K2 reach 90% of dehydroxylation just above 600°C while for K3 and H1 this is at 600°C and 550°C respectively. This confirms the DTG results and indicates that K3 and H1 dehydroxylates faster than K1 and K2 and most likely a lower calcination temperature will already be sufficient. The dehydroxylation behavior of the smectitic clays is more diverse. I1 and S2 dehydroxylate first and reach 90% of dehydroxylation at a temperature below 600°C. For S1 this is approximately 650°C and for S3 850°C. Furthermore S3 is marked by a gradual dehydroxylation curve while for the other smectites it is steeper. Based on these results S2 and I1 would need lower calcination temperature than S1 and certainly than S3. Based on these results 4 different calcination temperatures were chosen for the kaolinitic clays, namely 500, 700, 800 and 900°C. For the smectitic and illitic clays only three temperatures of 700, 800 and 900°C were selected.

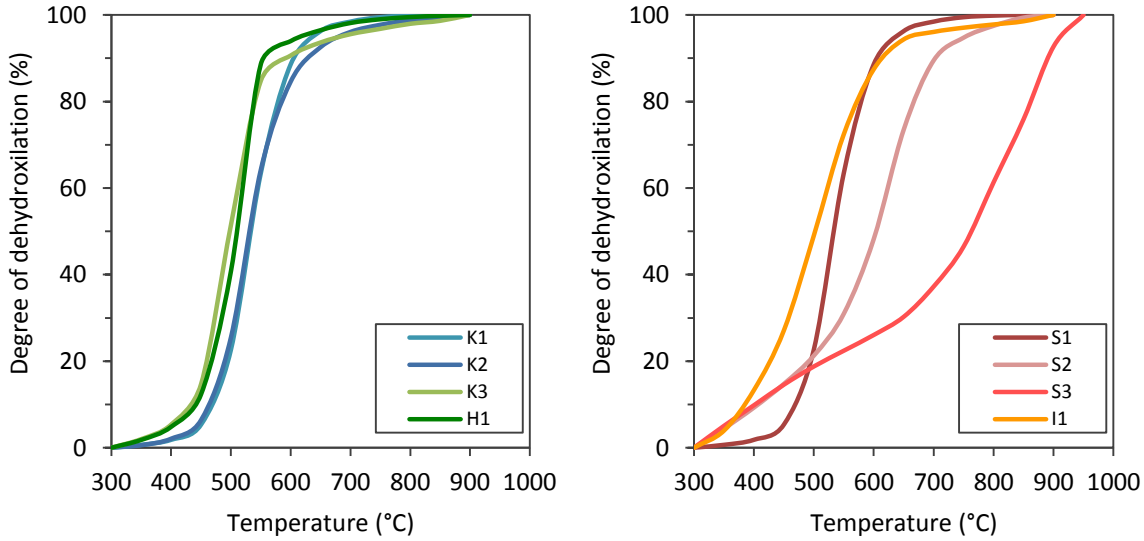

Figure 4.4: *Degree of dehydroxylation in the interval range of 300 to 1000°C.*

4.2.3 MINERALOGY

XRD patterns of the unfired kaolinites, the purified illite, the smectite clay fraction and of the calcined clays are presented in Figure 4.5. The kaolinitic clays, K1 and K2, indicate strong reflections of kaolinite and a poor intensity diffraction peak of anatase (0.5 and 1.5% respectively). In the range of 19° and 22° 2θ, three distinctive, sharp kaolinite diffraction peaks can be observed, indicating that these are well-ordered kaolinites with high crystallinity (H), as determined by the Hinckley index (Hinckley, 1962). For K3 the XRD pattern shows clearly the presence of kaolinite and also weak reflections of anatase (2%). The kaolinite reflections in the range of 19–22° 2θ of K2 consist of one main diffraction peak and a broad shoulder to the right, representing lower ordering (M) than K1 and K2. The H1 clay presents broad reflections of halloysite and no distinctive impurities. Based on the broadness of the reflection peak at 12.3° 2θ, this clay can be classified as low ordered (L). The smectitic clays have clear reflections with wide bases. S2 and S3 have a rather sharp (001) reflection at 5.8°2θ, while S1 has a more broad reflection in the range of 7.5–9° 2θ. The shift of the position of the reflection can be explained by the exchangeable cation present in the clay. For S2 and S3 this is Ca, while for S1 it is Na. The position of the (060) reflection of smectitic clays allows distinction of trioctahedral-hectorite (S3) at 61.1° 2θ, from dioctahedral montmorillonite (S1 and S2) at 61.9° 2θ (Moore and Reynolds, 1997). Only fine-grained quartz is present as impurity in S1 (2%), S2 (<0.5%)

and S3 (2%). The illitic clay, I1, consists predominantly of illite with clear reflections of quartz and some minor traces of anatase, rutile and kaolinite.

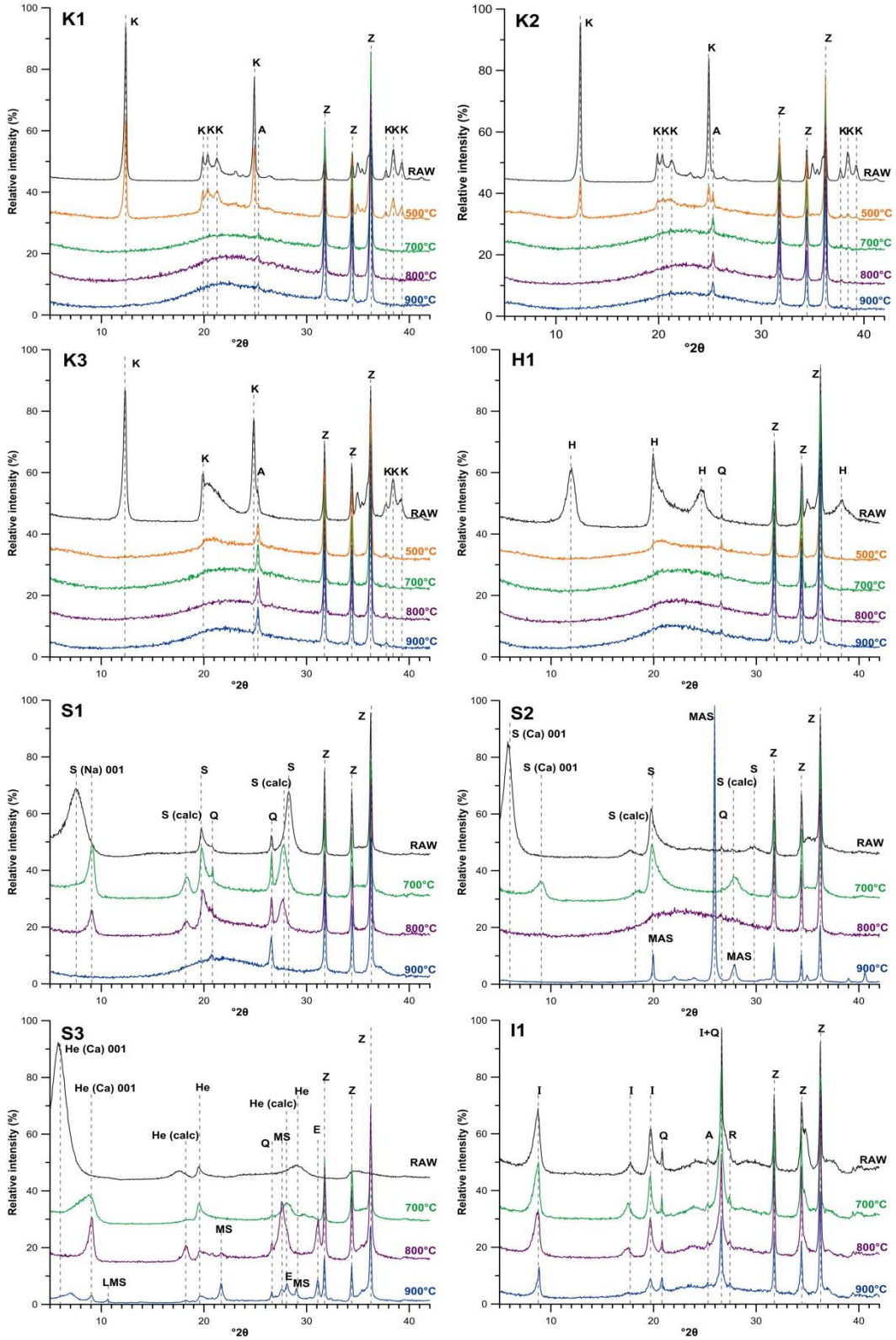

Figure 4.5: *XRD pattern of untreated and calcined clays. The identified minerals are: K: kaolinite, H: halloysite, S: smectite (with Ca or Na), He: hectorite, Q: quartz, A: anatase R: rutile and Z: zincite (internal standard), MAS: magnesium aluminum silicate, E: enstatite, MS: triclinic magnesium silicate and LMS: lithium magnesium silicate.*

In order to gain more detailed qualitative and quantitative information about the individual clay minerals oriented clay slides were analyzed and the results are presented in Figure 4.6. Especially for the smectitic and illitic clays these slides give additional information. For I1 no shift in the pattern of the ethylene glycolated (EG) versus the air dried (AD) sample can be observed. However, since illite is rarely found 100% pure, the change in peak intensity implies that I1 consists of illitic clay dominated by illite with 5% of expandable layers (Meunier and Velde, 2004; Środoń, 1984). Furthermore some minor traces of kaolinite (2%) are present, visible by the weak reflection at 12.3°2θ. The smectitic clays do show a clear shift in the EG pattern which confirms its swelling nature. The AD pattern confirms that Ca is the predominant exchangeable cation for S2 and S3, indicated by the 001 reflection at 6° 2θ, while for S1, which contains Na in the interlayer, this is indicated at 7° 2θ.

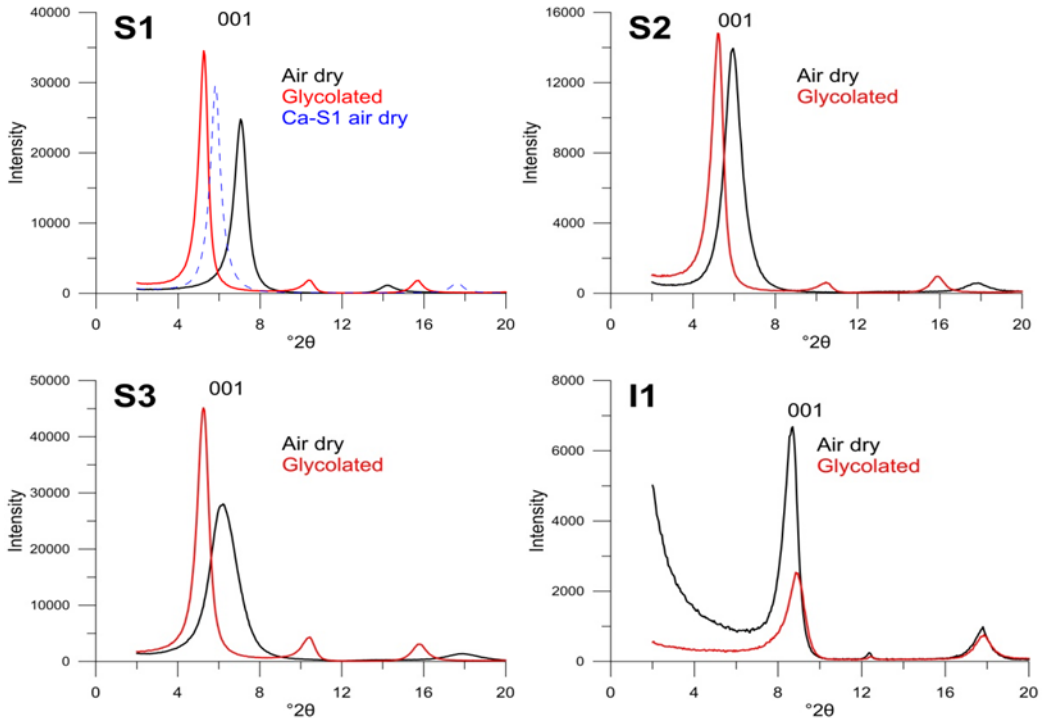

Figure 4.6: *XRD patterns of air dried and glycolated sedimentation slides for smectitic and illitic clays. The shift of the (001) reflection when glycolated represents the swelling behavior of the smectite. For S1 also the Ca-saturated pattern is shown.*

XRD patterns of the calcined clays show that calcination of kaolinitic clays for 2 h at 700 °C is sufficient to make the structure amorphous, since all reflections corresponding to kaolinite/halloysite have disappeared. This amorphous phase can be identified by the dome structure in the XRD patterns between 15 and 35° 2θ. The heat treatment does not affect anatase and its reflection remains unaltered. A higher firing temperature of 800 or 900 °C gives no significant differences in the diffraction pattern and the amorphous phase remains similar.

For lower firing temperatures at 500 °C, a relation between the degree of ordering and the amount of amorphous material can be observed. High ordered kaolinites still have traces of crystalline kaolinite when fired at 500 °C. K1 still shows three clear reflections of kaolinite in the range of 19.8 to 21.3° 2θ. For K2 these reflections are less well developed, but a reflection at 12.2° 2θ is still evidently visible. Regarding the M and L ordered kaolinites, the dehydroxylation seems to be almost completed and no reflection at 12.2° 2θ can be observed. However, still some traces of more crystalline kaolinite remain visible at around 21° 2θ, hereby indicating that only a limited proportion of the sample is still crystalline.

In contrast to the kaolinitic clays, the structure of the smectitic clays does not collapse entirely after heat treatment at 700 °C, but a shift of the basal planes (001) can be observed. This can be explained by the removal of interlayer water during the heating process which does not contribute to the pozzolanic reactivity of the sample (Fernandez et al., 2011). For Na-montmorillonite, S1, the basal planes collapse from 7.5° to 9.1° 2θ. Further heating of the sample substantially weakens the smectite reflections. This is in agreement with the elevated background observed for the calcined sample in the range of 20–25° 2θ. This indicates that part of the sample has become amorphous, but crystalline phases remain present, at 800 °C. Only at a calcination temperature of 900 °C the sample becomes entirely amorphous, which is similar to the findings of (He et al., 1996).

The Ca-montmorillonite, S2, shows a shift of the basal planes from 5.7° to 9.7° 2θ. When fired at 800 °C, S2 distinguishes itself from the other smectites by already becoming amorphous. Thermal analysis already indicated that the difference in dehydroxylation behavior between S1 and S2 can be assigned to the structural arrangement of the octahedral cation over the trans (M1) and cis (M2) positions. Since S2 consists of a mixture of cis and trans vacant octahedral positions, dehydroxylation and therefore also amorphisation of the clay takes place at lower temperature compared to the mainly cis vacant S1. At 900 °C, S2 shows strong reflections indicating the formation of a high temperature phase, identified as magnesium aluminum silicate ($MgAl_2Si_4O_{12}$), in line with the findings of (He et al., 1995b).

Hectorite, S3, also shows a collapse of the basal spacing from 5.8 to 9° 2θ. Moreover, the heating process provokes formation of new crystalline phases. For S3 the magnesium silicate enstatite ($MgSiO_3$, orthorhombic) has already formed at 800 °C as seen by the strong reflection at 31.1° 2θ. Further calcination up to 900 °C results in an increase in the amount of the enstatite phase and the formation of another magnesium silicate phase ($MgSiO_3$, triclinic) with its main reflections at 21.7°, 26.6°, 27.7°, 29.1° 2θ. The reflection at 10.7° 2θ was identified as lithium magnesium silicate. The presence of Li can be explained by the fact that one in nine of the octahedral Mg cations in hectorite is substituted by Li. Regarding I1, the intensity of the basal illite reflection gradually weakens with increasing calcination temperature. However the decomposition of illite has not completed as its reflection peaks at 8.8 and 19.8°2θ still remain even after thermal treatment at 900 °C. Nevertheless the presence of amorphous material is clearly observed at 900 °C by the broad and diffuse band elevating the background between 15° and 30° 2θ.

4.2.4 FTIR ANALYSIS

Qualitative and quantitative information on the degree of ordering of kaolinites structure has been obtained by FTIR analysis (Bich et al., 2009). In general kaolinite exhibits four distinctive bands in the OH stretching region, 3700–3600 cm^{-1}, shown in Figure 4.7. The band near 3620 cm^{-1} represents the inner OH groups, while the other bands near 3695, 3669 and 3653 cm^{-1} originate from internal octahedral surface OH groups (Frost and Vassallo, 1996; Madejov et al., 2001; Madejova, 2003). When the degree of ordering decreases, the intensities of the bands at 3669 and 3653 cm^{-1} tend to weaken and eventually disappear. Both K1 and K2 have four well defined bands indicating these are high ordered kaolinites. The bands at 3669 and 3653 cm^{-1} for K3 are less developed, which is characteristic for lower degree of ordering. Infrared spectra of the OH stretching region of the halloysite clay, H1, shows only two main bands at 3694 and 3620 cm^{-1}, indicating that some OH groups are not present and the clay is more disordered (Kloprogge and Frost, 1999).

For the three kaolinites a more quantitative approach uses the P_0 index, which is given by the ratio between the intensities of the bands observed at 3620 and 3695 cm^{-1}. The results are listed in table 4.1. Kaolinite can be seen as high ordered when $P_0 > 1$ (Bich et al., 2009). For the tested kaolinites this indicates that K1 and K2 are high ordered ($P_0 > 1$) and K3 is disordered ($P_0 < 1$). These results correspond well with the findings obtained from the XRD patterns.

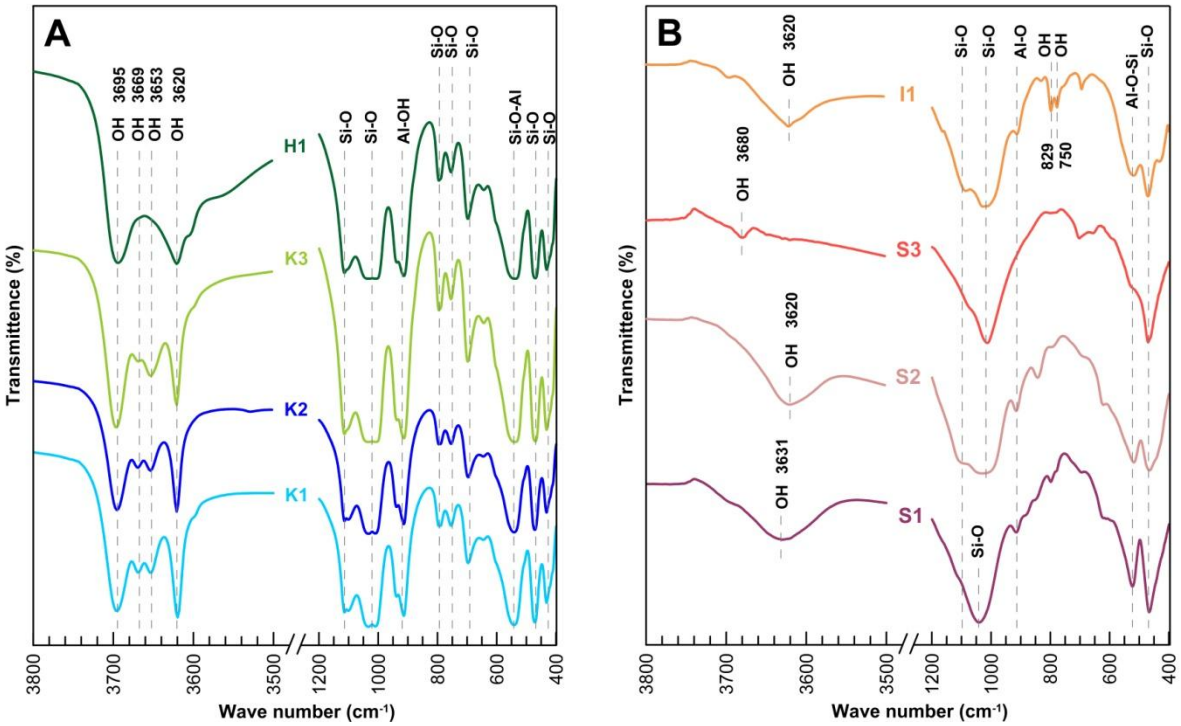

Figure 4.7: *FTIR spectra of the raw kaolinitic (A) and smectitic and illitic (B) clays.*

In contrast to the kaolinitic samples, the smectitic clays have more broad absorption bands with only a single band in the OH-stretching region. The position of the OH stretching bands between 3610 and 3650 cm^{-1} is mainly dominated by the octahedral cation coordinating with the hydroxyl groups (Madejova, 2003). Regarding S2, the absorption at 3620 cm^{-1} is typical for smectites with low Fe content and high Al substitution in the octahedral sites (Madejov et al., 2001; Wilson, 1994). The band of the more iron rich S1 is shifted towards 3631 cm^{-1}. The OH-stretching region of S3, with mainly Mg_3OH groups in the octahedral sheets, reflects its trioctahedral character absorbing near 3680 cm^{-1}. The illitic clay, I1, is characterized by a broad OH-stretching band near 3620 cm^{-1} and a doublet at 829 and 750 cm^{-1} (Farmer, 1973; Wilson, 1994).

4.2.5 NMR ANALYSIS

The difference in the effect of the calcination process on the local Si and Al environments of S1 and S2 has been studied by solid-state NMR. The ^{29}Si MAS NMR spectrum (Figure 4.8) of S2 contains a rather narrow resonance at -93.6 ppm and shows no indication of the presence of a quartz impurity (peak at -107.6 ppm), indicating an almost pure phase. The corresponding ^{27}Al NMR spectrum (Figure 4.8) is dominated by the octahedral resonance at 3 ppm and contains very low-intensity peaks at 59 ppm and 69 ppm, arising either from an impurity phase or tetrahedral Al^{3+} ions in the silicate sheets of the montmorillonite structure, following a recent ^{27}Al and ^{29}Si MAS NMR investigation of a similar sample of montmorillonite (Garg and Skibsted, 2014). After calcination at 800°C, the ^{29}Si MAS NMR spectrum contains a broad resonance, ranging from ca. -75 ppm to – 125 ppm with a center of gravity at -103.3 ppm. This peak originates from a range of different SiO_4 environments (Q^1 – Q^4 sites with different degrees of Al substitution), indicating that a highly disordered material is obtained. The ^{27}Al MAS NMR spectrum shows a single ^{27}Al centerband resonance at roughly 50 ppm with a tail towards lower frequency which is a characteristic feature for a distribution of Al environments. The spectrum reveals that Al is predominantly present at tetrahedral sites, where the small chemical shift

indicates a high number of Si atoms in the second coordination sphere, i.e., $Al(OSi)_4$ and $OAl(OSi)_3$ sites.

The corresponding spectra of the S1 clay differ from those of the Ca-form by the fact that the S1 contains a higher amount of Fe_2O_3, as evidenced from the higher intensities of the spinning sidebands, and an impurity of quartz (SiO_2). The main resonance in the ^{29}Si NMR spectrum of S1 is observed at -93.0 ppm (FWHM = 8.7 ppm), in accordance with Q^3 sites from silicate sheets. The second resonance at -108.7 ppm is assigned to the presence of a polymorphic form of a SiO_2 impurity. After calcination, the resonance at -108 ppm is still present, whereas the dominating resonance has become significantly broader with a low-frequency shift of the center of gravity to -102.4 ppm. The corresponding ^{27}Al MAS NMR spectrum (Figure 4.9) is dominated by the resonance from Al in octahedral coordination at 3.5 ppm with minor peaks at 59 ppm and 69 ppm that may originate from Al^{3+} sites in the silicate sheets or an impurity phase. After calcination, the material primarily contains Al in tetrahedral coordination (53.5 ppm peak), however, a significant amount of intensity is also observed in the region from approx. 30 ppm to -15 ppm, demonstrating the presence of five-fold and octahedrally coordinated Al sites as well. This is in agreement with the XRD results, where S1 still shows reflection peaks, though shifted, after calcination at 800°C. Overall, the ^{27}Al and ^{29}Si NMR spectra of the S1 sample reveal that the clay component has dehydroxylated and that a new and less-ordered phase has formed. This is evidenced by the low-frequency shift and broadening of the ^{29}Si resonance and the change in coordination environment from octahedral Al to mainly tetrahedral Al in the calcined sample. The formation of a less ordered phase is related to the broadening of the resonances in the ^{27}Al and ^{29}Si NMR spectra and the absence of diffraction peaks from the starting material in the XRD pattern.

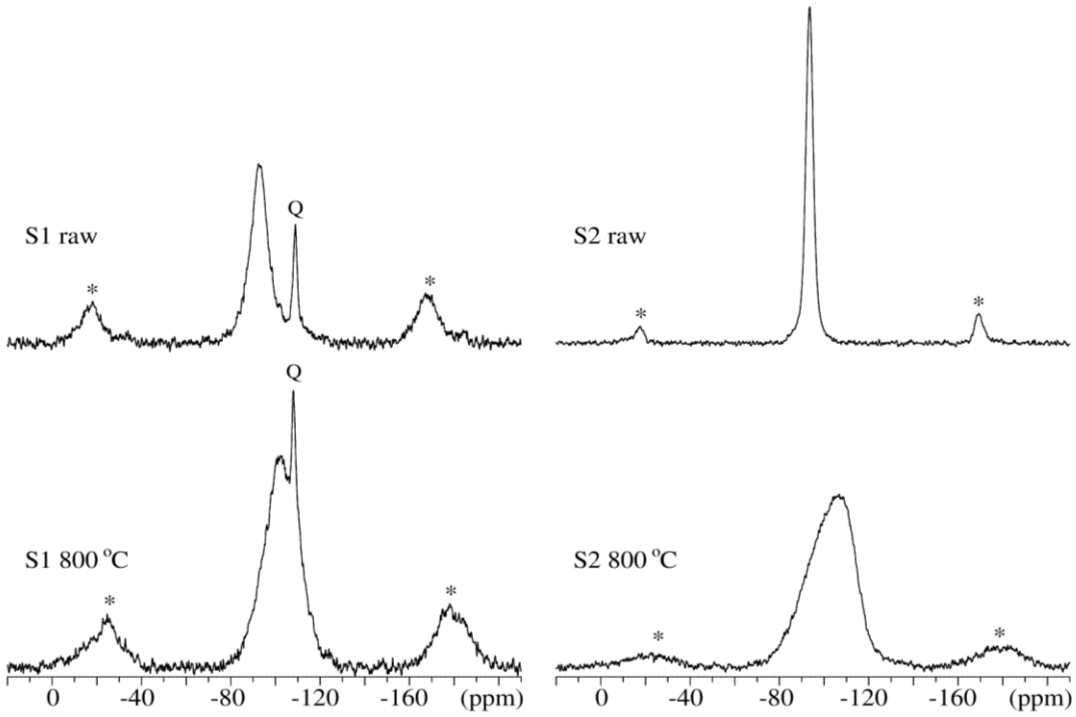

Figure 4.8: *^{29}Si MAS NMR spectra (9.39T, 6.0kHz) of the raw and calcined (800°C) samples of the S1 and S2 clays. The asterisks indicate spinning sidebands and Q the resonance from an impurity of quartz.*

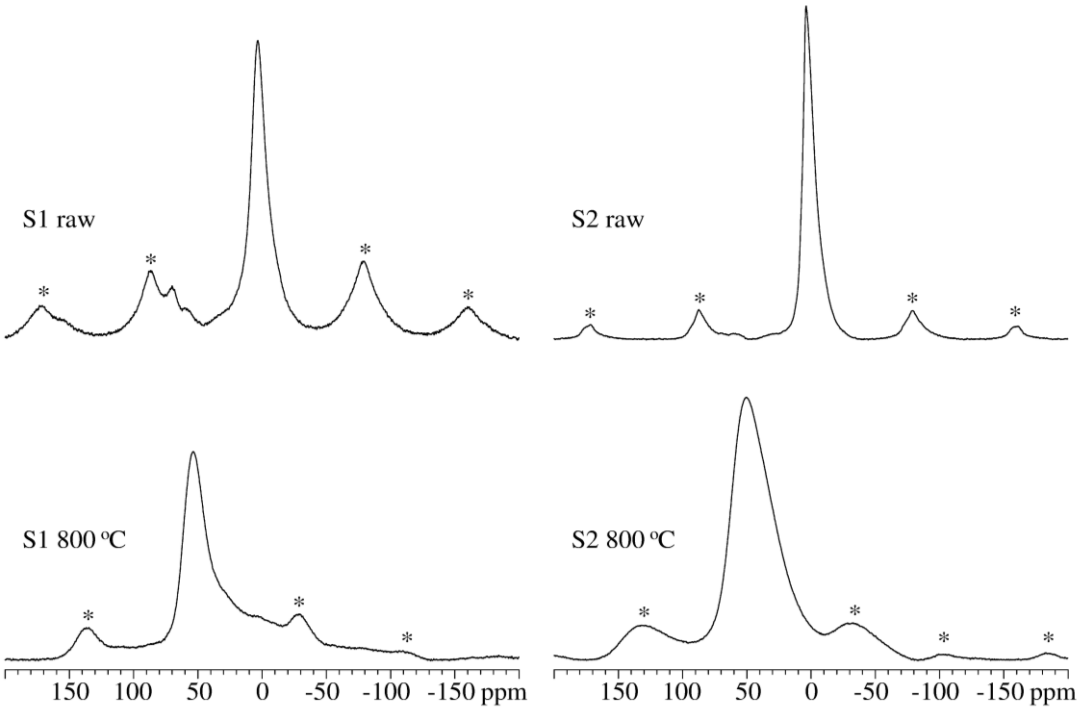

Figure 4.9: *^{27}Al MAS NMR spectra (14.09 T, 13.0 kHz) of the raw and calcined (800°C) samples of the S1 and S2 clays. The asterisks indicate spinning sidebands.*

4.2.6 BET SPECIFIC SURFACE AREA

BET specific surface area (SSA) of clays was measured before and after calcination to gain knowledge about the differences of the SSA of the natural clay and of the physical changes during the calcination phase (Table 4.1). According to Galan et al. (1998), the specific surface area of the raw kaolinites can be related to the degree of ordering. This is also observed for this sample set, since high ordered kaolinite (K1 and K2) consists of larger hexagonal plates and this is reflected in a rather low SSA of 8 m^2/g. The medium ordered clay, which consists of smaller clay plates, has a larger SSA of 20 m^2/g. H1, the most disordered clay, has the highest SSA of 34 m^2/g. The evolution of the SSA with increasing calcination temperature is given in Figure 4.10. The SSA of the kaolinites shows a slight increase between 500 and 700°C, which can be explained by the dehydroxylation of kaolinite whereby the interlayer region gets partially disordered resulting in higher SSA values (Alujas et al., 2015; He et al., 1994). Calcination temperatures above 700°C provoke a sudden decrease in the SSA, likely due to enhanced sintering phenomena typical for higher firing temperatures (Lee and Yeh, 2008). Regarding smectitic clays and illite, the differences in SSA are more pronounced. SSA of the raw clays varies from 20 to 123 m^2/g and can be summarized as I1 < S1 << S2 < S3. When smectitic and illitic clays are calcined, the particles tend to agglomerate much more than the kaolinitic clays resulting in a decrease of the specific surface. The agglomeration is more pronounced for the smectitic clays than for the kaolinites resulting in a significant drop in SSA to 0.5 – 4 m^2/g when calcined at 800°C. Increasing calcination temperature results in a small, further decrease in the SSA due to additional sintering.

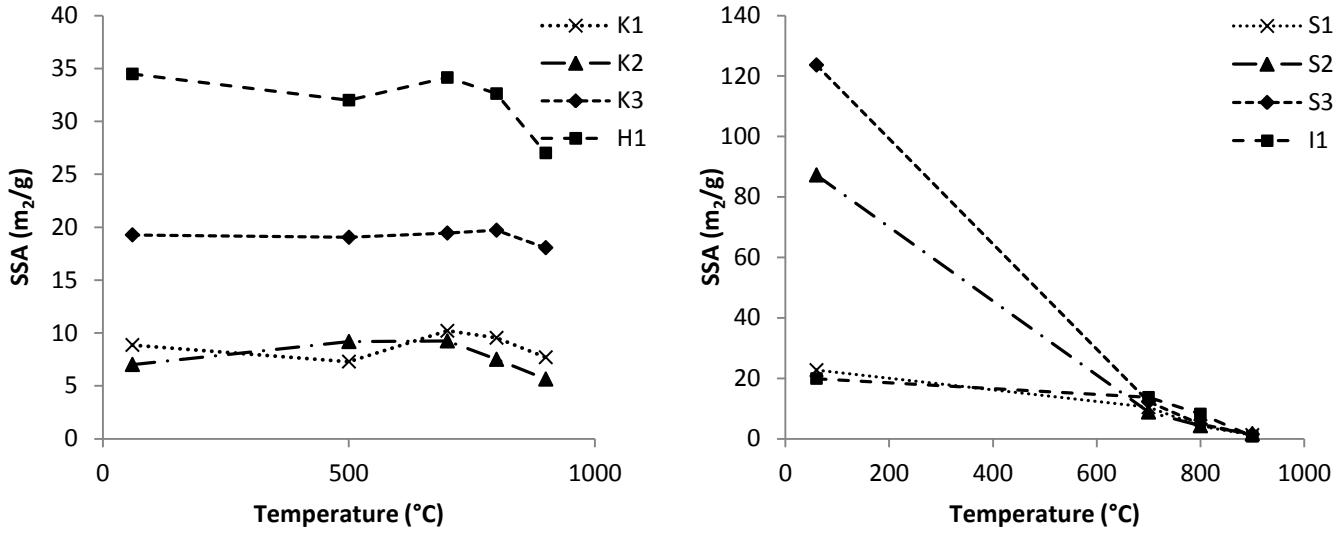

Figure 4.10: *Evolution of the BET specific surface area with increasing calcination temperature of the clays with a relative repeatability error (%RSD) of 0.2% for kaolinitic clays and 2.5% for smectitic/illitic clays.*

4.3 POZZOLANIC REACTIVITY

Figure 4.11 presents the amount of portlandite that was consumed by the calcined clays after 28 days of pozzolanic reaction. To determine the optimal activation temperature, clays were calcined at different temperatures (500, 700, 800 and 900°C). The kaolinitic clays show a high amount of portlandite consumption corresponding to 63 - 67% for calcination temperatures from 700°C onwards. The pozzolanic reactivity at different calcining temperatures is for most kaolinites fairly similar. However, there appears to be a relation between the optimal firing temperature and the ordering of kaolinite. High ordered kaolinites, K1 and K2, tend to be less reactive when calcined at only 500°C compared to medium and low ordered kaolinites, K3 and H1. Especially for K1, with the highest degree of ordering, the reactivity is 20% lower than when it is fired at 700°C or higher. This was confirmed by the XRD patterns of the kaolinitic clays fired at 500°C, which show that high ordered kaolinites still contain crystalline kaolinite. Regarding the M and L ordered kaolinites, however, it can be economically interesting to know that firing at 500°C, instead of 700°C, gives only a small difference in pozzolanic activity, especially for low and medium ordered kaolinites.

The optimum calcination temperature for the smectitic clay, S3, is also less-defined and all three calcination temperatures give rise to similar pozzolanic activities. This is in agreement with the XRD patterns which clearly demonstrate that increasing the calcination temperature results in a gradual weakening of the smectite reflections and an increase in the amorphous content, improving reactivity. Nevertheless, also new crystalline phases are formed which will reduce the reactivity again, as shown in a recent study (Garg and Skibsted, 2014). This results in a rather steady state reactivity.

S1 and S2, have a more distinctive optimum activation temperature of 800°C. Nevertheless compared to the kaolinitic clays their reactivity is still lower with only 30 - 38% portlandite consumption after 28 days. For both clays, especially a higher calcination temperature at 900°C, gives rise to a sudden drop in reactivity. S2 is clearly the most reactive smectite, which can be explained by its amorphization at 800°C (Figure 4.5). A major part of the smectite structure of S1 remained unaltered when fired at 800°C. Calcination at 900°C, however, resulted in a complete amorphization of S1. This additional loss of crystallinity is not reflected by an increase of reactivity; on the contrary,

it resulted in a significant drop in reactivity, possibly due to a decrease in soluble Si and Al (He et al., 1996). Nevertheless, calcination at 900°C results in higher portlandite consumption for the amorphous S1 compared to S2, which is becoming more crystalline again. In the studies of He et al. (1995b, 1996) a similar optimal activation temperature of 830°C was found for both Ca and Na montmorillonite. Increasing the calcination temperature past the dehydroxylation temperature tends to be beneficial for smectitic clays.

I1 has a clear optimal firing temperature at 900°C. Nevertheless even at 900°C the structure of illite is still partially crystalline as shown by the XRD measurements (Figure 4.5). Therefore pozzolanic reactivity of illite is rather weak compared to kaolinite and even di-octahedral smectites (S1 and S2).

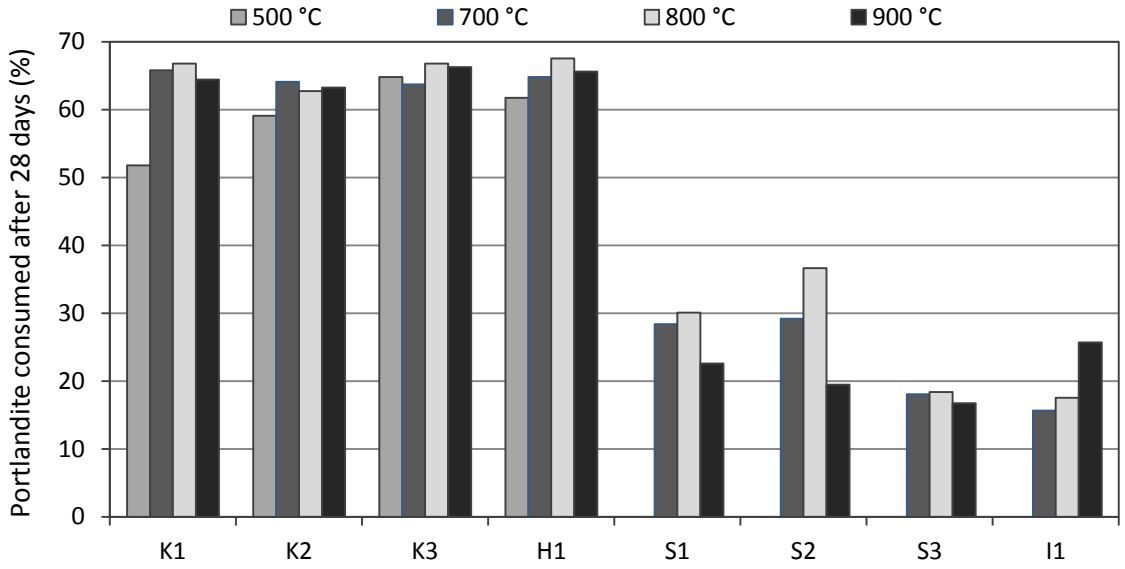

Figure 4.11: *Comparison between activation temperature and portlandite consumption of calcined clays after 28 days of pozzolanic reaction with a relative repeatability error of 1.57%.*

Figure 4.12 shows the evolution of the portlandite consumption over time for different calcined clay-lime mixtures, as determined by TGA. After 28 days, all three kaolinitic clays indicate a similar portlandite consumption corresponding to 64-67%. Up to 90 days, the reactions continue barely and values reach to 69%. This implies that the pozzolanic reaction of calcined kaolinites occurs mainly within 28 days and the reaction slows down thereafter. However, the reaction before 28 days progresses differently for the H ordered clays (K1 and K2) compared to the M (K3) and L ordered (H1) clays. The L and M ordered clays tend to consume portlandite more rapidly than high ordered clays, which is reflected in a higher pozzolanic activity during the first 28 days. This behaviour can be related to the specific surface area of the clays. The H ordered clays have a specific surface area around 8 m^2/g, while for the M and L ordered clays this is between 19 and 35 m^2/g. This means that the reaction surface of the M and L ordered clays is 2 to 4 times higher than that of the H order kaolinites, so that more portlandite can react in the early stage of the reaction. The evolution of the portlandite consumption for smectitic clays shows that S2 exhibits a faster reaction rate than S1. For both clays the reaction continues steadily after 28 days and even after 56 days, indicating that there is still smectite available for the reaction. In the studies of He et al. (1996, 1995b), it was also observed that Ca-montmorillonite was more reactive and yielded higher strength values than Na-montmorillonite. However in this study amorphous silica was present in the Ca-montmorillonite, which enhances the reactivity. Therefore it is not clear if part of the higher strength values of Ca-montmorillonite are caused by the exchangeable cation (He et al., 1996, 1995b).

Whether the difference between S1 (Na-smectite) and S2 (Ca-smectite) could be explained by the dominant exchangeable cation, has been taken into account. S1 was Ca-saturated during the Jackson

procedure and new XRD measurements and activity tests were carried out. The smectite (001) reflection at 5.8° 2θ shown in XRD pattern in Figure 4.6 demonstrates that the conversion was successful. The portlandite consumption over time (Figure 4.12) indicates that the Ca-S1 is more reactive than the Na-S1, but still less reactive than Ca-S2. This indicates that the exchangeable cation can influence the reactivity of the sample but does not explain the difference in activity between Na-S1 and Ca-S2 entirely.

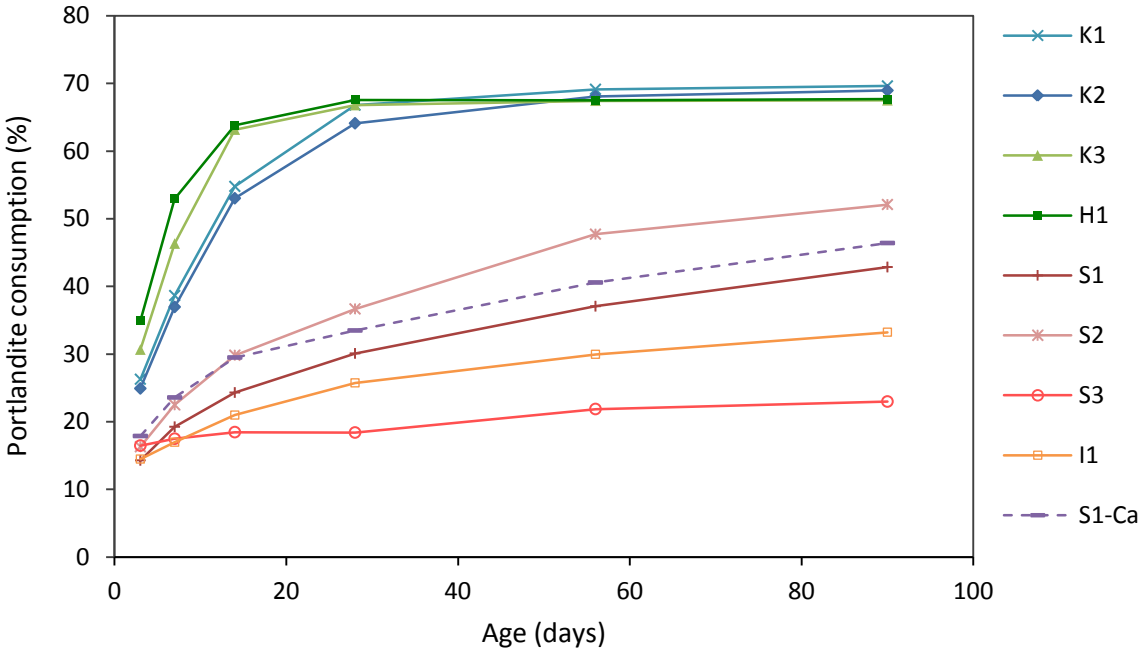

Figure 4.12: *Portlandite consumption after 3, 7, 14, 28, 56 and 90 days measured with TGA for kaolinites and smectites calcined at 800°, and illite calcined at 900°C. The dotted line represents S1 Ca-saturated instead of Na-saturated. The mean RSD is 1.57%.*

S3 only consumes limited amounts of portlandite (around 20%) and the reaction rate is lower. This low reactivity can be explained by the chemical composition of this clay. The alumina content in this clay is fairly low 0.42% while for S1 and S2 this is around 17 - 20%. Therefore, the reactivity for S3 is mostly based on the available Si, which is also lower than for S1 and S2, resulting in an overall lower portlandite consumption. For the illitic clay, I1, the consumption curve is rather flat, implying its low pozzolanic reactivity in time.

Even though the Si and Al content of the illitic clay I1 is higher than for the di-octahedral smectites (S1 and S2), its portlandite consumption is less and also the reaction rate is lower. This can be explained by the higher thermal resistance of the illite structure, which causes only a partial amorphisation of illite at 900°C. These results are consistent with previous research (Fernandez et al., 2011; He et al., 1995a, 1995b).

Since TGA-reactivity tests are rather time consuming a more rapid test method, the Chapelle test, was additionally used. The optimal activation temperatures determined by TGA were confirmed by means of the chapelle test (Figure 4.13). Kaolinitic clays have a broad range of optimal calcination temperatures while a more specific temperature of 800°C was found for the smectitic clays and 900°C for the illitic clays. more detailed comparison between the pozzolanic reactivity determined by means of TGA and amount of $Ca(OH)_2$ that was fixed by the clay according to the Chapelle test described in Chapter 3.

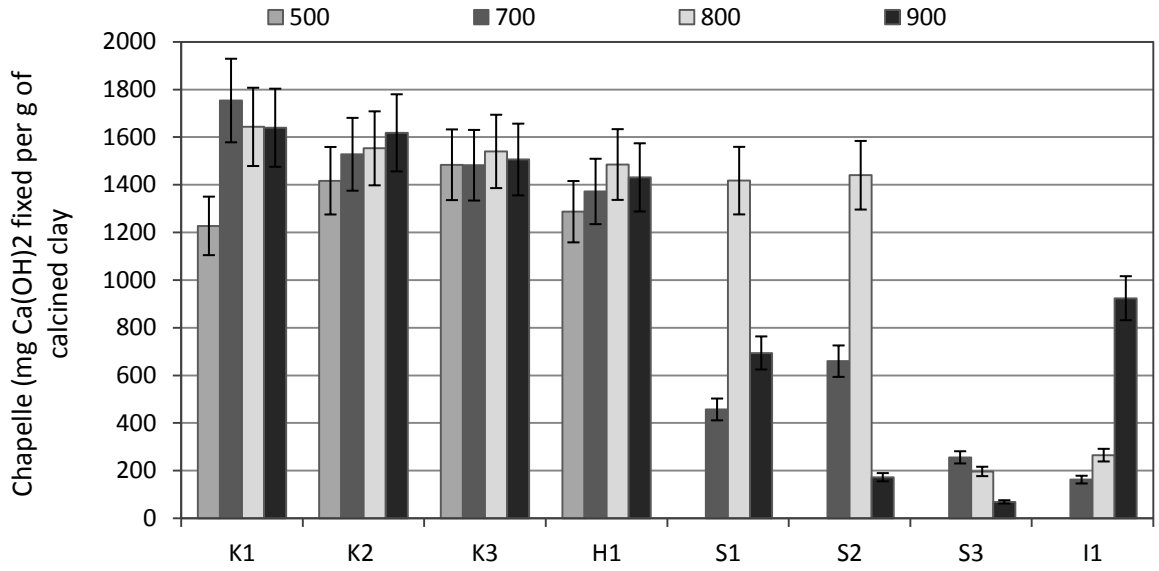

Figure 4.13: *Chapelle test giving the amount of $Ca(OH)_2$ fixed by the different clays calcined at 500, 700, 800 and 900°C.*

4.4 POZZOLANIC REACTION PRODUCTS

4.4.1 X-RAY DIFFRACTION

The evolution over time of newly formed hydration products of the calcined clay lime pozzolanic reaction was monitored by XRD. The diffractograms of the pastes that were cured for 28 days are given in Figure 4.14. According to the XRD results the amount of portlandite that is still present in the sample after 28 days is fairly similar for the four kaolinitic clays as proven by the similar intensities at 47.4, 51 and 54.6 °2θ. For the smectitic and illitic clays, S2 contains the least portlandite followed by S1, I1 and then S3. These results show the difference in intensity of the portlandite reflections for the eight clays is in consistence with the portlandite consumption determined quantitatively by TGA at 28 days. This indicates that despite of the preferred orientation that portlandite often faces, still a semi-quantitative interpretation based on the differences in peak intensities can be done.

Regarding the newly formed hydration products no remarkable differences could be found between the four kaolinitic clays and all contain stratlingite (C_2ASH_8) , the AFm phase C_4AH_{13} and minor amounts of C-S-H. The formation of these hydration products in kaolinite rich calcined clays is consistent with previous studies (Danner, 2013; Frías and Cabrera, 2001; Gameiro et al., 2012; Silva et al., 2014). Figure 4.15 shows the formation of the hydration products over time for sample K2 calcined at 800°C. The consumption of portlandite over time is confirmed by the decreasing intensity of its peak reflections. In general the amount of newly formed hydration phases increases over the first 28 days. After 56 days the formation of the hydration products and the consumption of portlandite stagnate. Since still an excess of portlandite is present, most likely all calcined kaolinite is already consumed and as a consequence the pozzolanic reaction can no longer continue. The difference in the degree of ordering has no effect on the nature of the formed hydration products, as this is mainly determined by the chemistry of the samples. Nevertheless, the intensity of the peak reflections of the hydration products that are formed differ in the early stage of the reaction according to the degree of ordering of kaolinite.

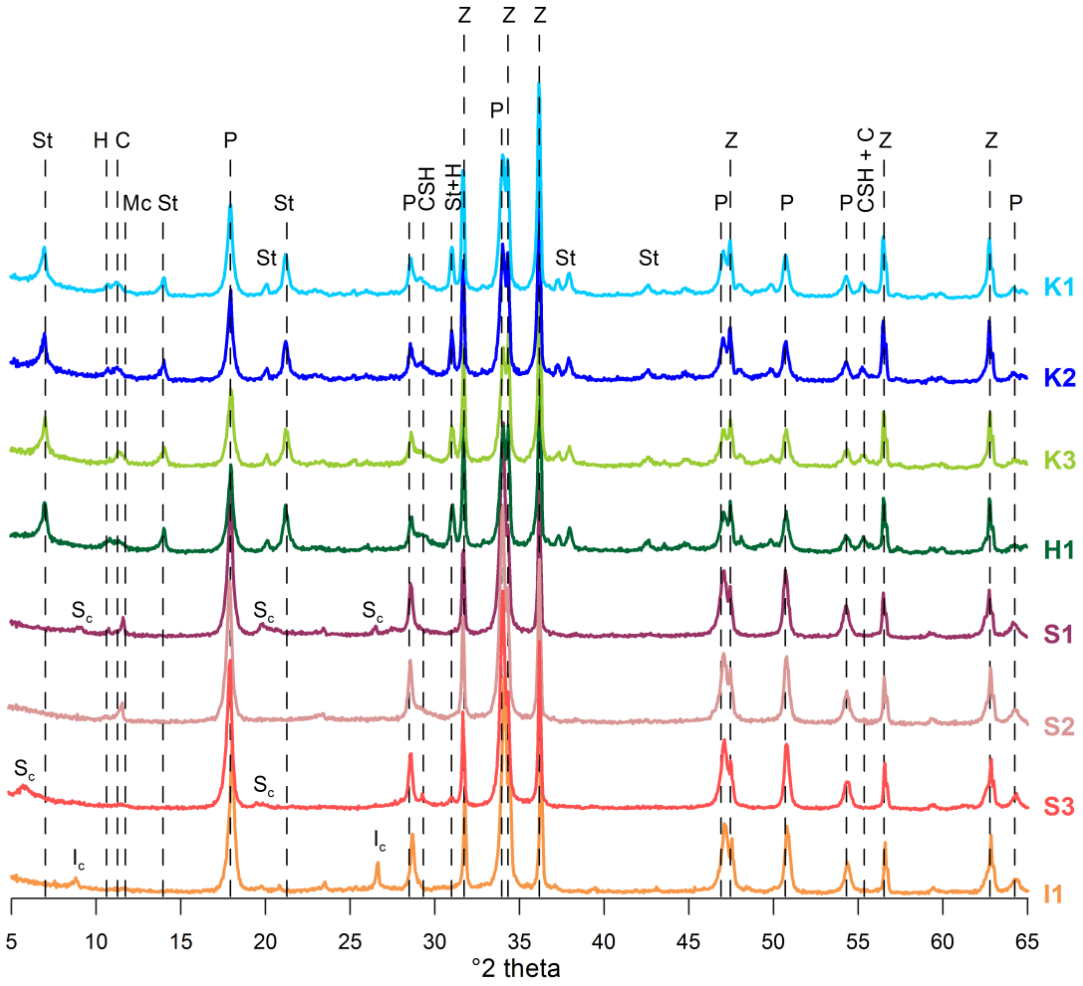

Figure 4.14: *XRD patterns of 28-day hydrated pastes of the clays calcined at 800°C and I1 at 900°C. The phases are indicated: Z: zincite (internal standard), S_c: calcined smectite, I_c: calcined illite, P: Portlandite, St: strätlingite, H:hemicarboaluminate, Mc: Monocarboaluminate, C: tetra calcium alumina hydrate (C_4AH_{13}) and CSH: calcium silicate hydrates*

Strätlingite is the dominant crystalline hydration product with its most pronounced 003 reflection at 7.0 °2θ. Strätlingite is only formed after three days of curing as no peak reflections are visible in the 3 day curing pattern. Between 7 and 28 days the peak intensity increases rapidly. In the past some authors (Ding et al., 1995; Heikal et al., 2004) indicated strätlingite having a positive effect on the mechanical strength and is therefore a favourite hydration phase. The amount of Strätlingite that is formed is clearly influenced by the degree of ordering of kaolinite. All four kaolinites show the presence of Strätlingite only after 7 days. Nevertheless at 7 days the intensity of the 003 strätlingite peak is significantly higher for the K3 and H1 than for K1 and K2. This indicates the formation of strätlingite is more rapid for low and medium ordered kaolinites than for high ordered kaolinites.

The region between 10.5 and 12 °2θ comprises several AFm phases. The most dominant phase that is present is the C_4AH_{13} marked by its reflection at 11.3 °2θ. Previous studies indicate C_4AH_{13} is not stable with aging and already disappears after 28 days (Silva et al., 2014). However even after 90 days C_4AH_{13} can still be detected by X-ray diffraction. Nevertheless some samples do show a slight decrease in the peak intensity of C_4AH_{13}, which confirms its instability over time, however it is not clear to which phase it is transforming, due to the small amount of hydration phases and the overlapping with the formation of new phases.

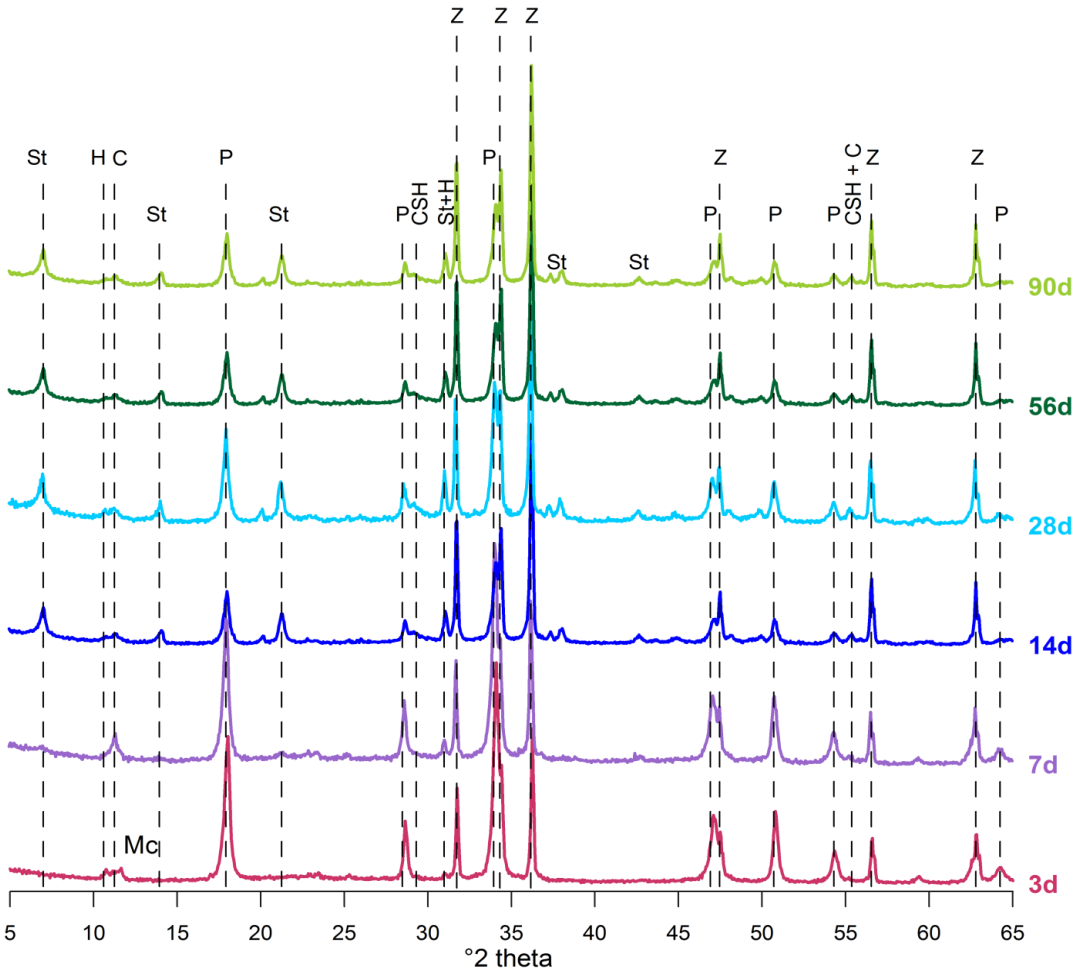

Figure 4.15: *XRD patterns of the K2 paste, calcined at 800°C and cured for 3, 7, 14, 28, 56 and 90 days. Zincite (Z) was added as internal standard. The phases are indicated: P: Portlandite, St: strätlingite, H:hemicarboaluminate, Mc: Monocarboaluminate, C: tetra calcium alumina hydrateC_4AH_{13} and CSH: calcium silicate hydrates*

Other AFm phases that are formed consist of minor amounts of hemicarboaluminate at 10.8 °2θ and monocarboaluminate at 11.7 °2θ. The source of carbon for these phases is not well understood. Several studies report the formation of these carbonate rich phases even though samples are prepared in air-tight circumstances (Gameiro et al., 2012; Silva et al., 2014). Furthermore the quantity of both AFm phases does not increase significantly over time and they are already formed before 3 days. This indicates certainly no infiltration during curing takes place as otherwise samples with a longer curing time would have higher amounts of mono- or hemicarboaluminate. Therefore it is likely that the carbon that is incorporated in these phases originates from contamination of CO_2, which is present in the air, when the sample was prepared. However, there is no evidence that calcium carbonate is formed, which would be expected when CO_2 infiltrates during preparation. This can be explained by the fact that the employed curing conditions and more particularly a relative humidity above 95%, is unfavourable for the formation of calcite as formerly stated by (Gameiro et al., 2012; Silva et al., 2014).

The formation of C-S-H is confirmed by the presence of a broad reflection at 29.4 °2θ. The C-S-H phase is hard to identify as it is a semi-crystalline phase with only a limited amount of rather broad reflections. The C-S-H is already present at 3 days, though in rather limited amounts. Further hydration results in a clear increase of C-S-H up to 28 days. Several authors (Danner, 2013; Serry et al., 1984; Silva et al., 2014) mention the formation of hydrogarnet, which is an unfavourable phase as it decreases the mechanical resistance and therefore also the durability of a mortar or concrete. Up

to 90 days no hydrogarnet can be detected. However, in pastes with a calcined clay lime ratio of 30:70 longer curing times would give rise to the formation of hydrogarnet, as there is a surplus of portlandite and a considerable amount of strätlingite. (de Silva and Glasser, 1993; Massaza, 2009). This problem regarding the excess of portlandite could be tackled by increasing the calcined clay lime ratio to 50:50 or even higher instead of the applied 30:70 to avoid hydrogarnet formation (Silva et al., 2014). Also the selection of the calcined clay cement ratio should be made accordingly to avoid the formation of hydrogarnet.

When the various smectitic and illitic clays are compared the difference in portlandite consumption and the presence of newly formed hydration phases confirm the pozzolanic reactivity that was determined by means of TGA. The main difference between the smectitic and kaolinitic clays is that no strätlingite is formed (Figure 4.14). This can be explained by the lack of sufficient alumina in smectitic and illitic clays, necessary to form strätlingite. The Si/Al ratios of the kaolinitic clays are significantly lower than for the smectitic and illitic clays, which results in the preferential formation of strätlingite. The hydration products that are formed in the smectitic clays S1 and S2 comprises of hemicarboaluminate, monocarboaluminate and C-S-H. Monocarboaluminate is the dominant crystalline hydration phase of both smectitic clays. The intensities of monocarboaluminate in samples S1 and S2, calcined at 800°C and cured for 28 days, are significantly higher compared to the kaolinitic clays. The amounts of hemicarboaluminate that are formed are rather limited, indicating smectitic clays favour the formation of monocarboaluminate over hemicarboaluminate which is logical for an environment that is depleted in aluminium. Figure 4.15 demonstrated that the intensity of monocarboaluminate increases mainly in the first seven days of the reaction. After 14 days there is even a turnover and the percentage of monocarboaluminate is marked by a weak decline. The concentration of hemicarboaluminate, is the highest at long curing times of 90 days. This can indicate monocarboaluminate is partially converted to hemicarboaluminate on the long term. The other hydration phase that is present in the smectitic clays is C-S-H. The intensity of C-S-H increases by aging with the biggest difference between 28 and 56 days. This indicates that the pozzolanic reaction of the calcined smectite-lime still continues with a clear evidence of additional hydration products that are formed, whereas the formation of the kaolinitic clays stagnated. While the amount of mono- and hemicarboaluminate that are formed are comparable for S1 and S2, the quantity of C-S-H differs significantly between S1 and S2. S1 forms less C-S-H as can be seen by the lower intensity of the C-S-H peak reflection at 29.4 °2θ. This phenomenon explains the difference in pozzolanic reactivity as the less reactive S1 produces a smaller amount of C-S-H. Furthermore the background of the S2 paste is more elevated than that of S1, which has a double explanation. First of all S2 was already more amorphous when calcined at 800°C than S1 as visualised in Figure 4.5. This is still visible in the prepared paste of sample S1 by the presence of the remaining reflections of heated smectite (Figure 4.16). Secondly C-S-H phase is semi-amorphous which would enhance the background of S2 even more as it contains more C-S-H. This also gives an explanation why the background of S2 remains rather high, even though during the pozzolanic reaction the background decreases as the calcined smectite is being consumed.

Nevertheless not all smectitic clays do form all three reaction products that are identified in S1 and S2. The low reactive S3 shows no indication of the presence of monocarboaluminate and hemicarboaluminate. This can be explained by the chemical composition that indicates the lack of alumina, that is crucial to form these phases. A weak reflection around 29.4 °2θ indicates C-S-H is present though in limited amounts. For samples I1 and S3 the hydration products are hard to detect based on XRD results. Both samples contain small amounts of monocarboaluminate and C-S-H. However the amounts of these phase are so limited that the reflections are very weak and could only be distinguished when zooming in to the region between 10 and 13 °2θ.

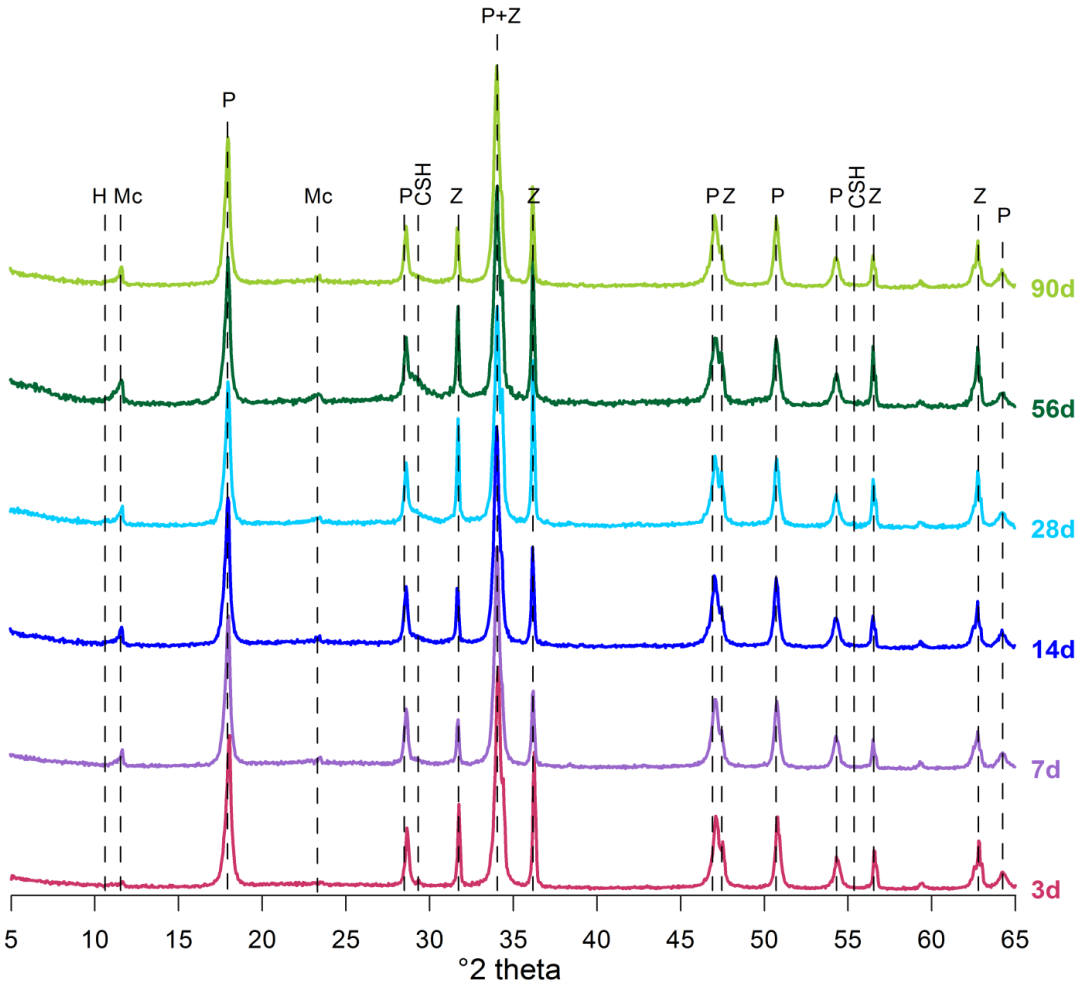

Figure 4.16: *XRD pattern of the pastes of S2 calcined at 800°C and cured for 3, 7, 14, 28, 56 and 90 days. The phases that are presented are indicated: Z: zincite (internal standard), P: Portlandite, H: hemicarboaluminate, Mc: Monocarboaluminate, and CSH: calcium silicate hydrates*

4.4.2 THERMAL ANALYSIS

The reaction products were additionally studied by thermal analyses and the DTG curves of the pastes analysed at 28 days are given in Figure 4.17. Portlandite is decomposed in the temperature range between 350 and 550°C. The portlandite content can be determined more accurately by TGA compared to XRD, since preferred orientation has no influence on the mass loss. Over time the portlandite peak decreases indicating more portlandite is consumed. The mass loss in between 20 and 300°C can be attributed to the loss of chemically bound water of the newly formed hydration products. The temperature at which this occurs is characteristic for each phase and as such the peaks visible in the DTG pattern can be assigned to the various hydration phases. Nevertheless with multiple hydration phases there is too much overlap of the decomposition to quantify the hydration products. However a qualitative observation can be made to verify the XRD results and check whether additional amorphous phases can be detected. Previous studies indicate there is some discussion about the interpretation of the peak position of the DTG or DTA signal of AFm phases. Especially for strätlingite no clear consensus is found regarding its peak positions (Danner, 2013; Gameiro et al., 2012; Silva et al., 2014). The studies (Haha et al., 2012; Okoronkwo and Glasser, 2016) of a pure synthesised strätlingite indicate that strätlingite is marked by double peaks positioned at 170 and 240°C. The DTG curves of K2 at different aging times (Figure 4.18) confirm this hypothesis. K2 clearly shows the development of two peaks at 175 and 235°C from day 7 onwards. The intensity

of both peaks increases over time, corresponding to the XRD results. For the paste of the smectitic clay S2, which does not contain strätlingite, no peaks at that position can be observed.

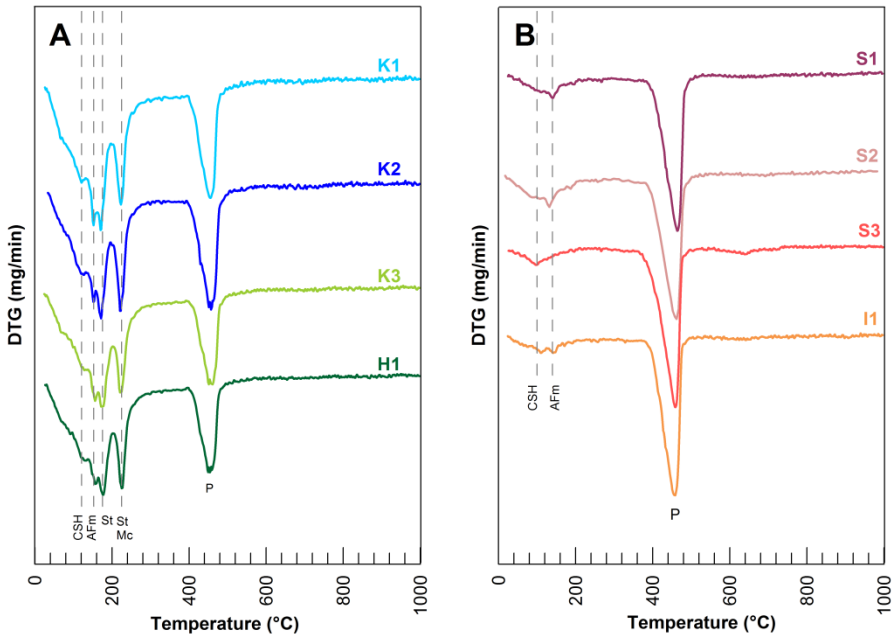

Figure 4.17: *DTG curves of the different clay lime pastes at 28 days of curing, clays were calcined at 800°C and I1 at 900°C.*

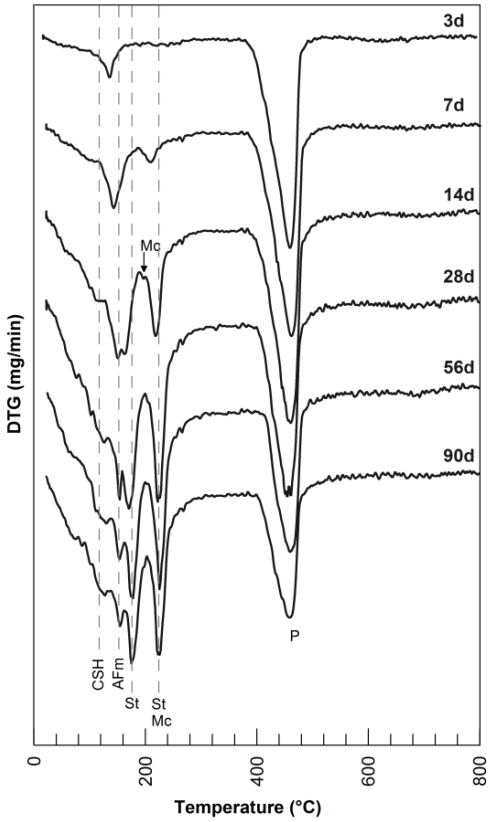

Figure 4.18: *DTG of calcined clay lime paste of K2, calcined at 800°C and cured for 3, 7, 14, 28 and 90 days. The phases are indicated: P: Portlandite, CSH: calcium silicate hydrates, St: Strätlingite, Mc: monocarboaluminate and* C_4AH_{13}.

At the left shoulder of the 235°C peak of strätlingite a small peak can be detected for the kaolinitic clays, especially at short curing times of 7 and 14 days. This peak is also present in the smectitic clays S1 and S2 at 28 days and can be assigned to monocarboaluminate according to previous studies (Gameiro et al., 2012; Silva et al., 2014). The mass loss centred around 140°C can be assigned to the decomposition of C-S-H and the AFm phases C_4AH_{13} and monocarboaluminate (Fernandez, 2009; Gameiro et al., 2012). For short curing times this peak is marked by a left shoulder. Longer curing times result in the bifurcation of the peak whereby the previous left shoulder forms a peak at 120°C and the original peak shifts towards 155°C. Hemicarboaluminate could not be identified separately on the DTG curves as there is too much overlap with other hydration phases.

4.4.3 INFLUENCE OF THE ACTIVATION TEMPERATURE

Since the pozzolanic reaction is influenced by the calcination temperature the question rises whether an effect can also be observed for the hydration products that are formed. The kaolinitic clays show only a significant difference in XRD and TGA results when 500°C is compared to the other calcination temperature. Since higher calcination temperatures do not provoke additional amorphisation both qualification and semi-quantification are similar for calcination temperatures of 700, 800 and 900°C. Kaolinite that is calcined at 500°C produces less strätlingite, especially during the first 14 days of the reaction, while the amount of other crystalline hydration phases like C-S-H, C_4AH_{13} and mono- and hemicarboaluminate is comparable for all calcination temperatures for K2, K3 and H1. Therefore it can be stated that mainly the formation of the alumina rich phase strätlingite is influenced by the chosen activation temperature. Nevertheless the most ordered clay K1 does show a decrease in the amount of all the hydration phases for a calcination temperature of 500°C. When the amount of crystalline kaolinite that remains after calcination is rather high all hydration phases are affected. Another phenomenon that can be observed for K1 and K2 calcined at 500°C, is that the remaining kaolinite reflection at 12.4°2θ weakens over time as shown in Figure 4.19. This indicates the crystalline kaolinite that was still present in the calcined sample is also being consumed during the pozzolanic reaction. However, this reaction is more slowly than for the amorphous phase resulting in a difference in pozzolanic reaction at 28 days for the high ordered K1 and K2. K3 and H1, contained only a limited amount of crystalline kaolinite after calcining at 500°C and as a results this kaolinite has entirely reacted before 28 days resulting in a similar pozzolanic reactivity at 28 days for all calcination temperatures.

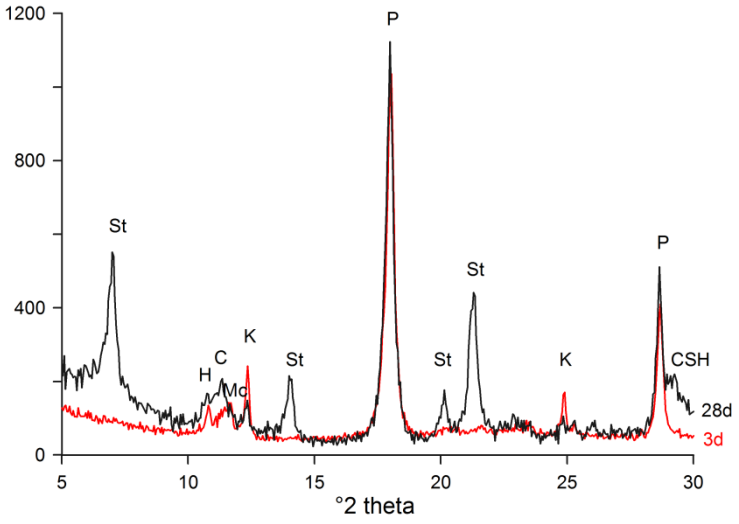

Figure 4.19: *XRD pattern of the K2 lime paste, calcined at 500°C and cured for 3 (red) and 28 (black) days. The phases are indicated: P:portlandite, St: strätlingite, K: kaolinite, C: C_4AH_{13} and CSH: calcium silicate hydrates.*

4.5 CONCLUSIONS

The pozzolanic activity of the 8 clay samples can be summarized as follows: kaolinitic clays (K1, K2, K3 and H1) >> Ca-montmorillonite (S2) > Na-montmorillonite (S1) > illite (I1) > hectorite (S3).

The degree of ordering for the kaolinites is an important parameter that influences the optimal activation temperature. For medium and low ordered kaolinites a calcination temperature at 500°C has been proven to yield fairly good reactivity. High ordered kaolinites, however, do not reach sufficient amorphization at 500°C, resulting in a less pozzolanic reactive material. The degree of ordering and, therefore, also the BET specific surface area of kaolinitic clay, also influences the pozzolanic reaction rate. Medium and low ordered kaolinites tend to consume portlandite more rapidly than high ordered kaolinite. After 28 days most of the kaolinite, calcined at 800°C, has reacted and therefore the differences in reactivity are leveled out resulting in comparable portlandite consumption for all kaolinites. The dominant crystalline hydration phase that is formed is strätlingite, which is formed after 3 days of curing. Additionally C-S-H, mono- and hemicarboaluminate and C_4AH_{13} are formed.

Na- and Ca-montmorillonite (S1 and S2) have a distinct optimum calcination temperature at 800°C. Their reactivity decreases rapidly when higher calcination temperature (900°C) is applied. This is most likely due to enhanced sintering and formation of a new crystalline phase, Mg-Al silicate for S2. At 800°C, Ca-montmorillonite becomes completely amorphous with Al in tetrahedral sites while Na-montmorillonite becomes semi-crystalline, with a shift of the diffraction peaks and with Al is present in less ordered tetrahedral coordination but also in five-fold and octahedral coordination. The difference in thermal behavior can be explained by the octahedral occupancy, cis-vacant montmorillonites have a higher dehydroxylation temperature than mixed cis/trans-vacant montmorillonite. This phenomenon has a direct effect on the pozzolanic reactivity as a cis vacant clay structure was less reactive. Nevertheless the early stage of the reaction is also influenced by the type of exchangeable cation, hereby Ca-montmorillonite tends to consume portlandite more rapidly than Na-montmorillonite. This is also reflected in the higher amount of hydration products, C-S-H, mono- and hemicarboaluminate, for S2 compared to S1.

Also for hectorite (S3) two crystalline magnesium silicate phases, enstatite and a triclinic $MgSiO_3$ phase, are formed and, combined with the lack of aluminum, this results in a poorly reactive clay. The illitic clay's optimal activation temperature is 900°C, nevertheless even at 900°C illite only became partly amorphous and consequently it's reactivity is limited.

CHAPTER 5

CLAY MIXTURES

The pozzolanic properties of pure clays are studied extensively in the past. More particular calcined kaolinite, or metakaolin, seems to yield the highest reactivity followed by smectitic clays. Nevertheless, in nature kaolinite deposits are rarely completely pure. In addition to the mineral kaolinite other clay minerals such as smectites and illites, but also non-clay minerals such as quartz, feldspar, calcite and muscovite are often present in the clay. These less pure clays are economically interesting to be used as SCM, however the effect of the impurities on the pozzolanic activity or/and on the calcinations process is not yet known. Therefore this study will investigate how these impurities affect the pozzolanic reactivity of the calcined clay and whether the optimal firing temperature changes due to the presence of these impurities. To obtain this goal, artificial mixtures were made to assure only the effect of the chosen mineral impurity could be studied without influence of other impurities. An additional objective is to investigate whether the increasing amount of impurity can be linearly correlated to the decrease in the pozzolanic reactivity.

5.1 MATERIALS

To study the effect of various mineral impurities on the pozzolanic reaction of kaolinite rich clay artificial mixtures were made. A selection was made of six different mineral impurities that occur commonly in kaolinite rich deposits. Quartz was used as a reference material since quartz is known to be an inert material, which can be defined as a material that is marked by little to non chemical reaction and as a consequence its contribution to the portlandite consumption is negligible compared to calcined clays. To obtain a material that has a similar grain size as the kaolinitic clay, powdered quartz was used. As a result of this fine grain size quartz may exhibit filler effects since the small quartz particles can act as additional nucleation sites which can speed up the reaction. A second common non clay mineral in kaolinitic clays is feldspar. For this study a combination of 50% kali feldspars and 50% plagioclase was selected consisting of microcline, albite and anorthite. The selected muscovite was ground to a finer grain size by using a coffee mill, as normal milling techniques do not have the desired effect on the grain size due to the platy morphology of this phyllosilicate. Besides non-clay minerals a kaolinite rich deposit often also consist of other clay minerals. Therefore the most common clay mineral smectite and illite were also taken into account. For smectite the reference clay SAz-1 (S2) was used after purification. In chapter 4 it was already indicated that this Ca-montmorillonite possessed the highest pozzolanic reactivity of the examined smectitic clays. The illitic clay comprises the fraction <63 µm of the reference clay Imt-1 (I1) used in Chapter 4. Previous studies indicate the presence of calcite in the original clay can be beneficial for

the reaction process and therefore also calcite was considered as impurity (Danner et al., 2015; Justnes et al., 2011; Østnor et al., 2015). These studies focused on marl, a lime rich mudstone and generally considered as less valuable clay. Furthermore, the addition of limestone to the blended cement can also result in additional formation of hydration products which increase the strength (Antoni et al., 2012; Ghrici et al., 2007; Matschei et al., 2007; Vance et al., 2013).

The kaolinitic clay that was selected as base material was the high ordered Capim (K1) clay, discussed in chapter 4. The six mineral impurities that were considered were blended with kaolinite in different proportions Table 5.1. Quartz, calcite, smectite and illite were blended in the following amounts 15, 30, 45 and 60. Feldspar and muscovite were blended in smaller proportions of 10, 20, 30 and 40% since this resembles better the amount that occurs in natural deposits. After mixing the samples by hand they were further subjected to a 4 hour blending with the turbala mixer to achieve homogenous samples. Afterwards the samples were subjected to a heat treatment in a fixed bedded oven at 700, 800 or 900°C. The calcined samples were ground by a McCrone mill to limit the effect of the grain size and to be able to link the pozzolanic behavior directly to the mineralogy of the impurity.

Table 5.1: *Overview of the composition of the artificial mixtures indicating the amount of impurity added to pure kaolinite (K1 from Chapter 4). For each type of impurity 4 mixtures were prepared.*

Type of impurity					
Quartz	Feldspar	Muscovite	Calcite	Smectite	Illite
15 %	10 %	10 %	15 %	15 %	15 %
30 %	20 %	20 %	30 %	30 %	30 %
45 %	30 %	30 %	45 %	45 %	45 %
60 %	40 %	40 %	60 %	60 %	60 %

5.2 CHARACTERIZATION

5.2.1 MINERALOGY

The mineralogical composition of the uncalcined samples is exactly known as the mixtures were made artificially. The selection procedure of the mineral admixtures was done precisely to guarantee all minerals are as pure as possible. Therefore no extensive qualification and identification by means of XRD was necessary for the initial mixtures. However the calcination process might have an effect on certain minerals resulting in less crystalline phases. Therefore the 30% mixtures, calcined at 800°C were studied by XRD. The diffraction patterns are given in Figure 5.1 and show that kaolinite has become completely amorphous as was expected at the temperature of 800°C. Quartz and feldspar seems to be unaltered by the heating process as the sharp reflections characteristic for these minerals remain. Furthermore, the amorphous hump, which represents the calcined kaolinite, is similar for both mixtures. This indicates the amorphization of kaolinite is not influenced by quartz or feldspar. Quantitatively however there are significant changes when the amount of amorphous material and impurity content of the initial sample is compared to the calcined sample. Initially the quartz sample consists of 30% quartz and 70% of kaolinite. After calcination the quartz content increases up to 39% and the amorphous material comprises 61%. This phenomenon can be explained by the weight loss during calcination of kaolinite due to the dehydration and dehydroxylation. For the used kaolinite, K1, this weight loss encounters 13% as was determined by TGA. Therefore the initial 70% of kaolinite should be decreased by 13% which results in a value after calcination of 61%.

This calculated value corresponds well with the quantitative XRD results. Similar results were found for the feldspar samples.

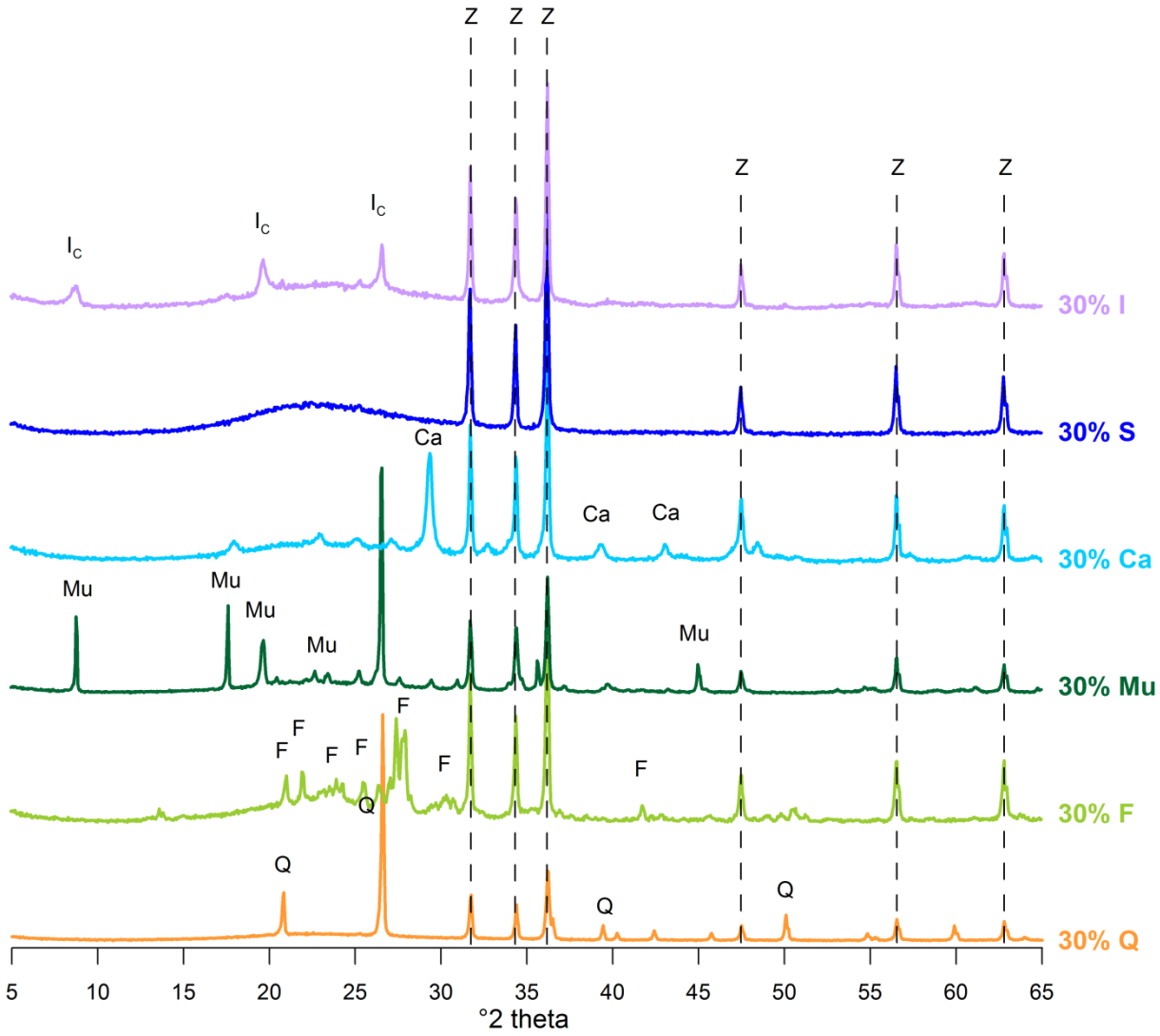

Figure 5.1: *XRD pattern of the mixtures with 30% of impurity and 70% of kaolinite for the minerals Quartz (Q), feldspar (F), Muscovite (Mu), Calcite (Ca), Smectite (S) and Illite (I). Zincite (Z) was added as internal standard.*

The muscovite mixture is also marked by sharp reflections and at first sight muscovite looks unaltered. However the more detailed XRD pattern (Figure 5.2) of the mixtures before and after calcination reveals that some of the muscovite peaks are shifted to lower 2θ values after the calcination process. This effect can be best observed for the reflection at 26.8 °2θ shifting after calcination at 800°C to 26.62 °2θ, but also other reflection peaks are marked by a shift. Important to know is that muscovite dehydroxylates between 700 and 1000 °C. Upon dehydroxylation muscovite undergoes a major phase transition resulting in an expansion of the cell parameters and thereby also the volume of the unit cell (Guggenheim et al., 1987; Mazzucato et al., 1999). As the position of the peak reflections are characteristic for a certain mineral and its cell parameters, the increase of these parameters results in a shift to higher d-values (Guggenheim and van Groos, 2001). The differences in the intensity of the muscovite reflection before and after calcination can mainly be attributed to preferred orientation. The quantification of the amorphous content of the muscovite mixture not possible since some of the muscovite peaks are shifted and as a result no standard pattern could be used.

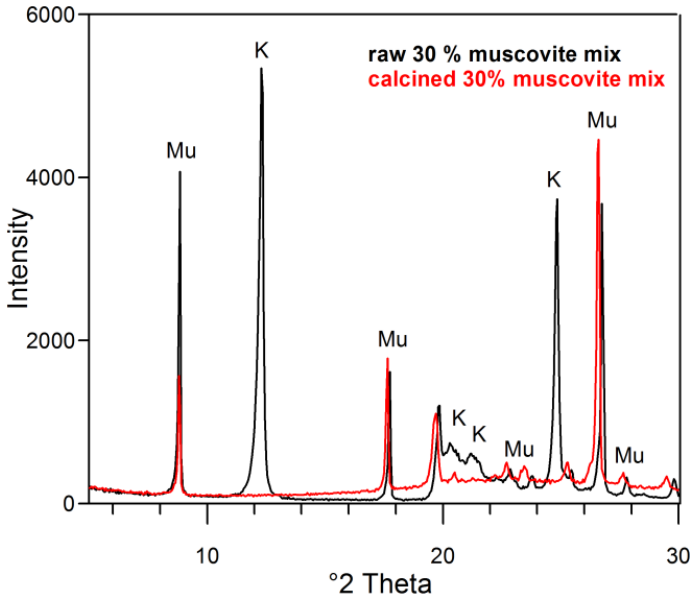

Figure 5.2: *XRD pattern of the 30% muscovite – 70% kaolinite mixture before and after calcination at 800°C. The identified phases are indicated: K: Kaolinite, Mu: muscovite.*

Smectite and illite are altered by the calcination process. The used smectite (S2) becomes completely amorphous and the amount of amorphous material for the 30% smectite sample is comparable with the amount found for the pure kaolinite (K1). Based on XRD no distinction can be made on the type of amorphous material and in total the sample contains 99% of amorphous material. Illite is only partially affected by the heat treatment and the crystalline reflection peaks, characteristic for illite, are shifted. Furthermore, the dome structure between 21 and 32 °2θ, representing the amorphous material, is only slightly elevated compared to the 30% quartz mixture. Only semi quantitative information could be obtained, the alteration of the diffraction pattern of illite makes it impossible to insert a phase that represents the part that is still crystalline.

Also calcite is significantly influenced by the calcination process. The XRD pattern of the 30% calcite mixture calcined at 800°C in Figure 5.1 was measured after exposure to air. As a consequence CO_2, present in the air, was again incorporated in the structure. This phenomenon is shown in Figure 5.3 were pure calcite was measured directly after calcination at 800°C and again after being exposed to the air for 48h. Calcination at 800°C resulted in complete decarbonization of the sample whereby calcite is transformed into CaO and CO_2. However after a certain time the CaO is decomposed again into portlandite, when water is incorporated in the structure. Nevertheless, the formed portlandite is not stable and will partially react with CO_2 present in the air to form calcite. When this newly formed calcite is compared with the original calcite the peak positions are still comparable but the width has changed. The newly formed calcite is characterized by a broader peak indicating the crystallinity and corresponding crystallite size has decreased compared to the original calcite.

Since the decarbonization occurs in the temperature range between 700 and 850°C the structure of calcite was also studied for calcination temperatures of 700 and 900°C. When calcite is only calcined at 700°C the decarbonization process is not yet fully completed and some calcite remains unaltered. Full decarbonization is normally only reached for a temperature above 850 °C. However the long calcination time of 2h also resulted in a complete destruction of calcite already at 800 °C. At 900°C no further changes can be observed. Nevertheless, calcite behaves slightly different upon calcination when Si or Al is available. In the 30% calcite mixture that was calcined at 900°C the decomposition of calcite is accompanied by the recrystallisation of high temperature phases. The Ca of the decomposed calcite reacts with the Al and Si that was made available by the calcination of the clayish matrix to form new Ca-bearing alumino silicates (Tschegg et al., 2009). The newly formed phase

gehlenite could be identified by its main reflection at 31.4 °2θ. Gehlenite is however known as an intermediate phase that is unstable in the presence of quartz or SiO_2 bearing minerals (Duminuco et al., 1998; Trindade et al., 2009). Danner (2013) found that for a smectitic clay rich in calcite besides gehlenite also wollastonite and anorthite formed at a calcination temperature of 850 °C and higher. The presence of quartz triggered the decomposition of gehlenite to wollastonite and anorthite.

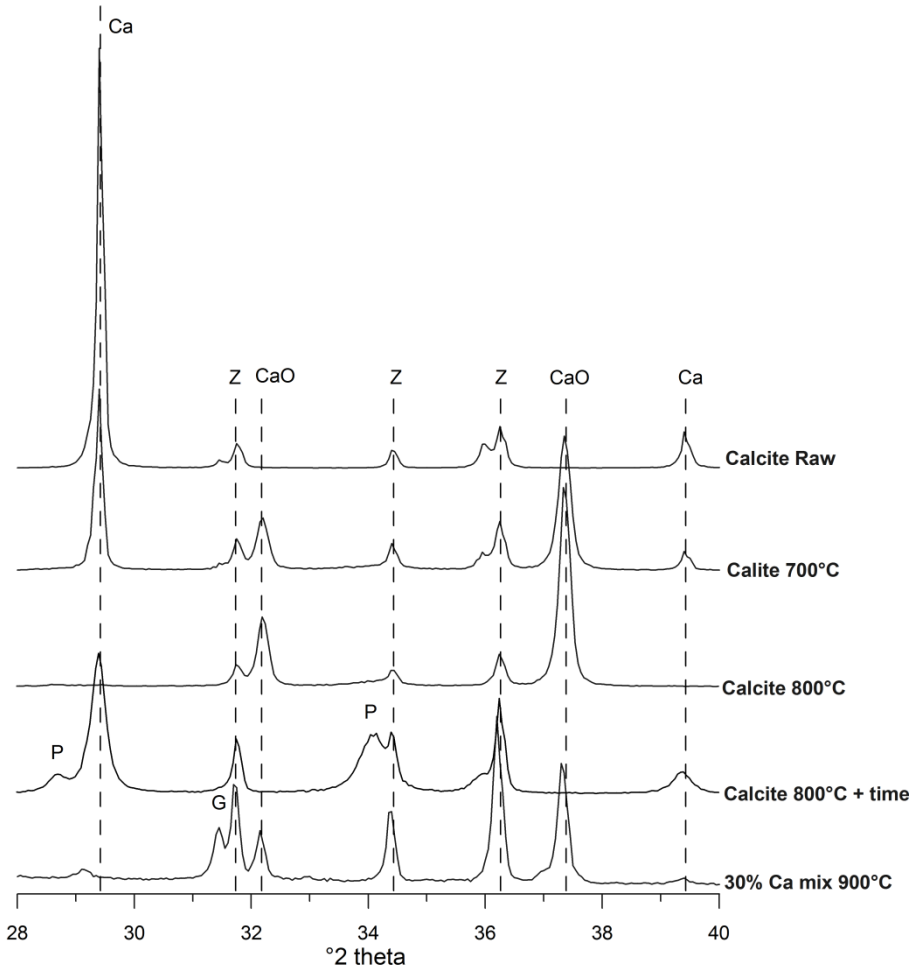

Figure 5.3: *Comparison of the XRD patterns of calcite at different calcination temperatures and rest times afterwards (+time) to allow CO_2 uptake from the air. The 30% Calcite mixture was added to indicate the formation of gehlenite (G). The other indentified phases are: Z: Zincite (internal standard), Ca: calcite, CaO: calcium oxide and P: Portlandite.*

5.2.1 THERMAL ANALYSIS

The thermal behaviour of clay samples can be influenced by the presence of mineral impurities. While some minerals do not undergo changes upon heating others will be marked by dehydration, dehydroxylation, changes to their structure and/or phase transitions. A thermal analysis was used to study the effect of the mineral impurities to the thermal behaviour of the sample. Figure 5.4 shows the TGA curves for the 30% impurity mixtures.

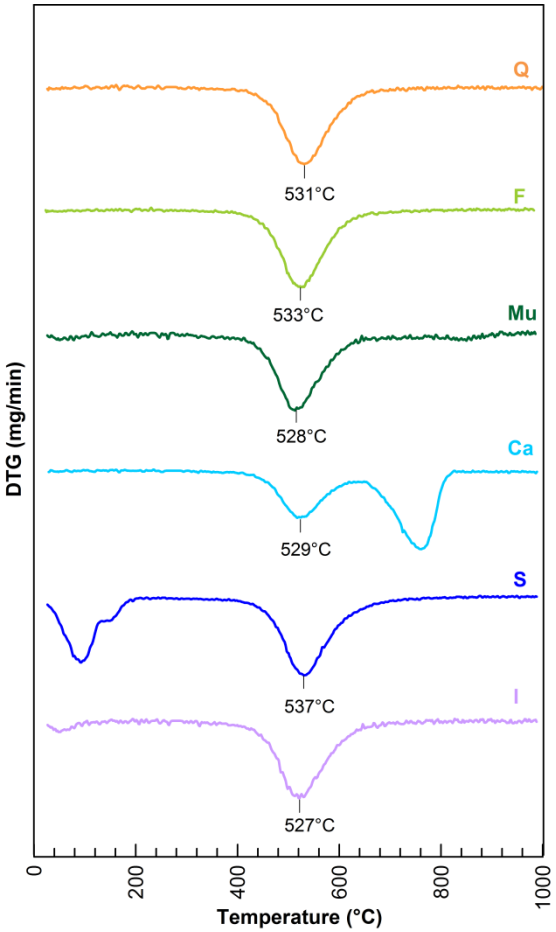

Figure 5.4: *DTG patterns of the 30% impurity mixtures of quartz (Q), feldspar (F), muscovite (Mu), calcite (Ca), smectite (S) and illite (I) in their raw form before calcination.*

The first important thermal reaction that takes place is the dehydration of minerals in the temperature range between 30 and 300°C. Pure well ordered kaolinite does hardly show any weight loss in this temperature range. The addition of non-hydrated minerals like quartz, feldspar and calcite does not contribute to the dehydration reaction. Therefore all three samples are marked by a flat curve without significant weight losses before 300°C. The phyllosilicate muscovite, illite and smectite are however dehydrated and weight loss can be observed. For muscovite and illite this weight loss is limited with values below 1% for a 30% mixture. Smectite, however, contains much more water in the interlayer space that is already released at low temperatures, resulting in a weight loss of approximately 5.5% when 30% of smectite is present. The double peak is an indication that calcium is the dominant exchangeable cation.

Secondly, the dehydroxylation of kaolinite takes place between 400 and 750 °C. For pure ordered kaolinite (K1 chapter 4) the dehydroxylation peak position is 535 °C. The peak positions of the mixtures including the non clay minerals quartz and feldspar at 531 and 533 °C respectively are only slightly lower than for the pure sample. This was expected since the decrease in kaolinite content generally results in a slight decrease of the peak position. Muscovite and calcite lower the dehydroxylation even further dropping below the 530°C. Illite is marked by the lowest peak position at 527 °C, which can be explained by the positive influence of the dehydroxylation of illite itself. The smectite mixture is marked by the highest temperature at 537 °C. The pure smectite (S2, Chapter 4) that was used was marked by a high dehydroxylation temperature of 678 °C. The presence of this smectite increases the dehydroxylation of the entire sample.

One of the other reactions that take place is the change of the crystal structure of quartz whereby α-quartz is inverted to β-quartz at 573°C. However this inversion is only marked by an endothermic reaction and not by any weight loss. Nevertheless, also the differential scanning calorimetric pattern (DSC), which was recorded simultaneously, showed no indication of this process. The dehydroxylation of kaolinite is also marked by an endothermic reaction between 300 and 650 °C and overshadows the inversion of quartz.

The calcite mixture is marked by significant weight loss between 650 and 850 °C which is related to the decomposition of calcite into CaO and CO_2. The weight loss can be directly correlated to the amount of calcite that is present in the sample. Also the muscovite mixture is characterised by weight loss in the range between 700 and 950°C. This weight loss can be attributed to the dehydroxylation of muscovite. During this phase transition alumina changes from 6 to 5 coordination and thereby the Al-sites become more disordered (Guggenheim et al., 1987).

The differences in dehydroxylation behaviour between the 30% mixtures can be observed by looking at the degree of dehydroxylation (Figure 5.5). Three mixtures, including quartz, feldspar and illite, resemble the dehydroxylation curve of the pure kaolinite reference sample. This indicates those admixtures have little influence on the dehydroxylation. The muscovite mixture start similar but at temperatures above 500°C the dehydroxylation rate decreases. This can be related to the late dehydroxylation of muscovite that is only completed at 900°C. Calcite is marked by a total different dehydroxylation curve since the decomposition of calcite interferes with the actual dehydroxylation of kaolinite. Therefore the total weight loss in the temperature range of 300 -1000°C is significantly higher compared to the other mixtures. For smectite the entire dehydroxylation curve is shifted to higher values, which indicates the dehydroxylation temperature is increased when smectite is present in the sample.

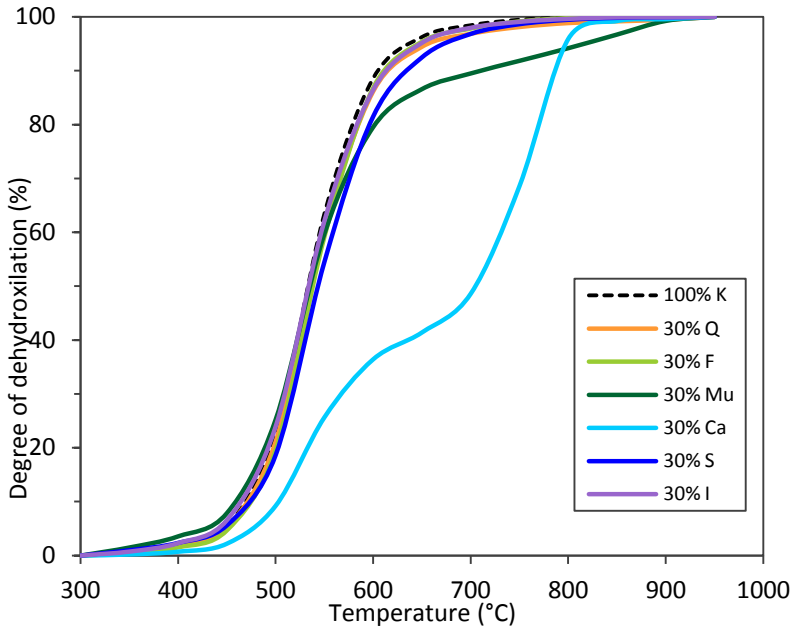

Figure 5.5: *Degree of dehydroxylation of the 30% mixtures in the range between 300 and 1000°C.*

An additional effect on the dehydroxylation peak temperature is the amount of the impurity that is present. The DTG patterns of the quartz mixtures with different kaolinite – quartz ratios shows that in general not only the peak intensity but also the dehydroxylation temperature slightly decreases when more quartz is added. Especially the sample with only 15% quartz shows a 6°C temperature difference with the 30% quartz mixture. For lower amounts, the difference is less obvious. Similar

effects were found for the feldspar, muscovite, calcite and illite mixtures. This indicates the amount of kaolinite can be positive correlated with the peak dehydroxylation temperature. Smectite mixtures were marked by an increase of the dehydroxylation peak temperature when the kaolinite content in the sample decreased. This can be explained by the fact that the influence of the higher dehydroxylation temperature of smectite increases in accordance with its amount.

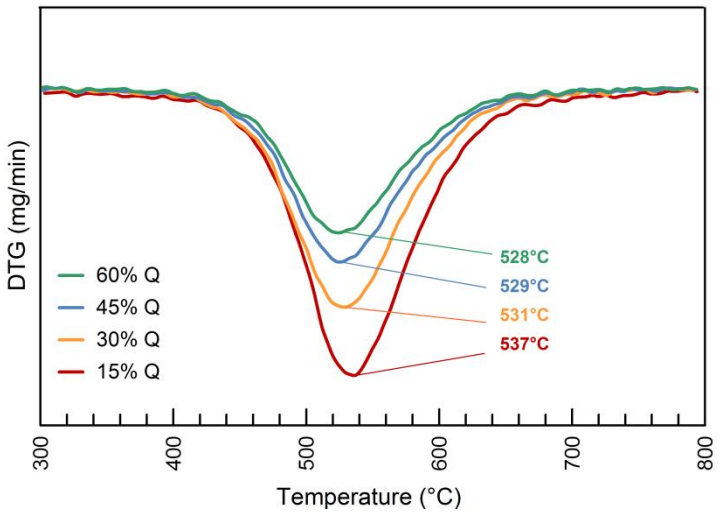

Figure 5.6: *DTG pattern of the quartz kaolinite mixtures with variable quartz content of 15, 30, 45 and 60% in the temperature range of 300 to 800°C.*

5.2.2 GRAIN SIZE DISTRIBUTION

An important parameter that can affect the pozzolanic reactivity is the grain size distribution. Fernandez (2009) indicates that clay minerals are subjected to sintering and agglomeration as a result of the calcination process. The increase of the calcination temperature results in an enhanced sintering effect. This sintering effect is the most intense for smectite, followed by illite and kaolinite. This phenomenon is also reflected in the rapid decrease in specific surface area for smectitic clays. However it is not known whether non clay mineral impurities have an influence on the sintering process. Furthermore, a mixture of several clay minerals can also behave differently than the pure clay.

The effect of the mineral impurities on the calcination process and as such on the grain size was studied by means of laser diffraction. The grain size distribution of the raw mixtures with 30% of impurity and 70% kaolinite was evaluated by making a comparison with a pure kaolinite (Figure 5.7). In general the mixtures are coarser especially when the coarsest 15% of the sample is taken into account. This indicates the admixtures are less finely ground than the kaolinite. Quartz, feldspar, calcite and illite show a similar trend and the increase of the coarseness of the sample is still limited. The mixture that contains muscovite shows however a drastic coarsening of the sample. This increase of the grain size distribution is however not in consistence with the limited amount of muscovite of 30% that was only blended with kaolinite. Most likely the large platy muscovite crystals block the detection of the smaller kaolinite grains, resulting in an overestimating of the grain size.

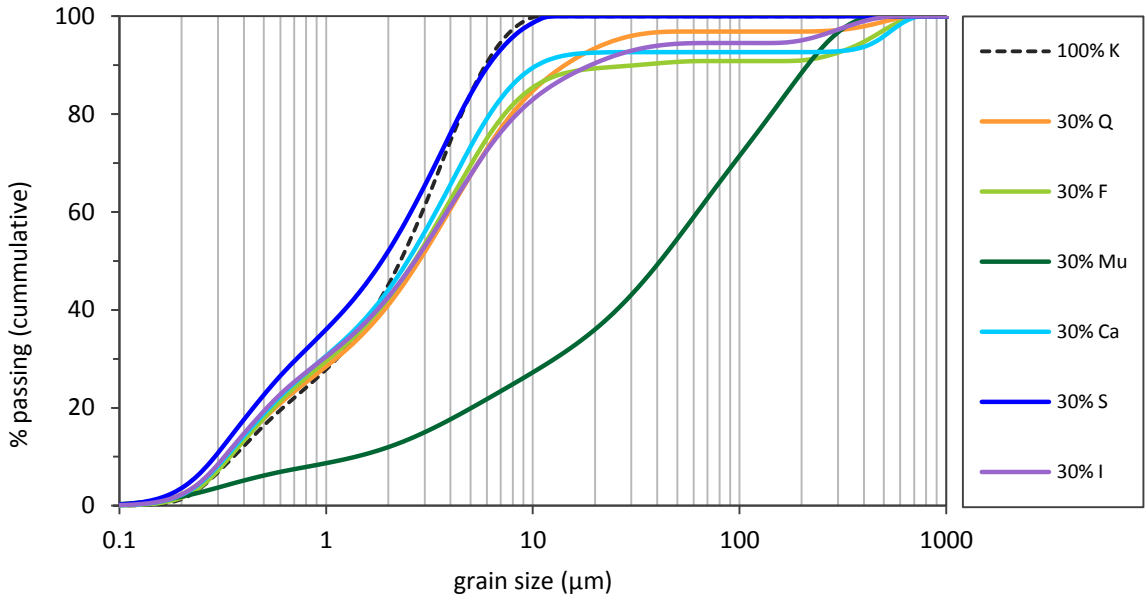

Figure 5.7: *Cumulative grain size distribution of the raw 30% impurity – 70% kaolinite mixtures. The dotted black line represents the grain size of a pure raw kaolinite sample. K: kaolinite, Q: Quartz, F: Feldspars, Mu: muscovite, Ca: Calcite, S: Smectite and I: illite.*

The grain-size distribution of the samples was remeasured after calcining the samples at 800°C. The results, visualized in Figure 5.8, indicate all samples undergo a coarsening of its grain size as a result of sintering and agglomeration. However not all mixtures are affected to the same extent. The mixtures can be subdivided in two groups when their grain size distribution is compared to the 100% kaolinite reference sample. The mixtures that contain quartz, calcite or illite are marked by a finer grain size especially above the third quartile of the sample. This indicates these admixtures provoke less sintering and agglomeration than a pure kaolinite does. This effect might be caused by a shielding effect of non clay minerals like quartz and calcite. The presence of these minerals ensures less kaolinite grains are in contact with each other during the calcination process and can therefore less easily sinter. However, also the mixture with illite is more fine grained than the reference sample even though it is known that pure illite induces significant sintering that is certainly comparable or slightly higher than for pure kaolinite (Danner, 2013; Fernandez, 2009). The plausible explanation is that the calcination temperature of 800°C is still too low for illite to decompose and as a result illite will sinter not to its full extent. When a calcination temperature of 900°C is applied more illite becomes amorphous and as a result additional sintering takes place (Figure 5.8) whereby the illite mixture becomes coarser than the reference sample. This coarsening of the sample can mainly be attributed to illite as kaolinite is only marked by a slight increase in grain size as a result of a calcination temperature of 900°C instead of 800°C.

The second group consists of mixtures containing feldspar, muscovite or smectite and is coarser than the reference sample. The question rises why these admixtures induce additional sintering. For the smectite mixture it was expected that more sintering would take place as pure smectite is marked by the highest sintering effect of all clay minerals. Feldspar was thought to be still inert at the rather low firing temperature of 800°C. However feldspar is a commonly used flux in ceramic industry to lower the vitrification temperature. Nevertheless, at 800°C feldspar is not decomposed as was shown by the XRD pattern Figure 5.1. Furthermore, the results of thermal analysis of the 30% feldspar mixtures did not show any sign of the start of decomposition of feldspar and no endo- or exothermic peaks could be observed. The phase diagrams of Al_2O_3-K_2O-SiO_2 and Al_2O_3-Na_2O-SiO_2 indicate that temperatures of 742 and 730°C respectively can be sufficient to create a liquid phase. However the amount of K_2O and N_2O is rather low in the 30% feldspar mixture, as a result the liquidus temperature considerably increases to temperatures above 1400°C. However the fluxing action of

the active oxides K_2O and Na_2O can already start at lower temperatures of 750 and 860°C respectively (Britt, 2007). Especially potassium rich feldspars can already contribute to the sintering effect. Also muscovite is a mineral rich in K_2O which can enhance the sintering. Furthermore, at a calcination temperature of 800°C, muscovite starts to dehydroxylate as shown by thermal analysis (Figure 5.4) which would explain why muscovite provokes additional sintering. Nevertheless, it is also possible that again muscovite particles block the detection of finer grained particle resulting in an overestimation of the grain size.

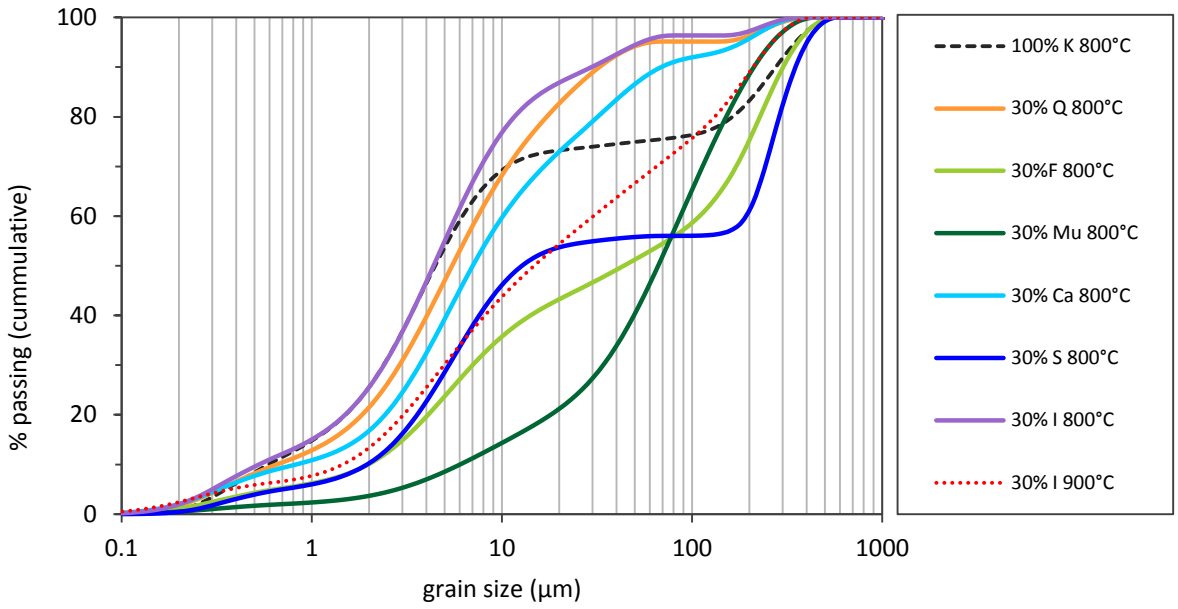

Figure 5.8: *Cumulative grain size distribution of the 30% impurity – 70% kaolinite mixtures calcined at 800°C. The dotted black line represents the grain size of a pure raw kaolinite sample. K: kaolinite, Q: Quartz, F: Feldspars, Mu: Muscovite, Ca: Calcite, S: Smectite and I: illite.*

The milling effect

After calcination of the samples a part was ground by a McCrone Micronizing mill to assure a comparable grain size distribution for all samples. However the milling process was influenced by the type of material. Generally all 30% mixtures showed a bimodal grain-size population with the dominant peak between 4 and 7 µm and a second small peak around 0.4 µm. However the 30% muscovite mixture is characterized by a much coarser grain size distribution with three populations at 0.4, 5 and 40 µm (Figure 5.9). This effect can be caused by the morphology of the muscovite crystals. The flat platy crystals are not easily desegregated by the McCrone during the milling process whereby these crystals remain coarser.

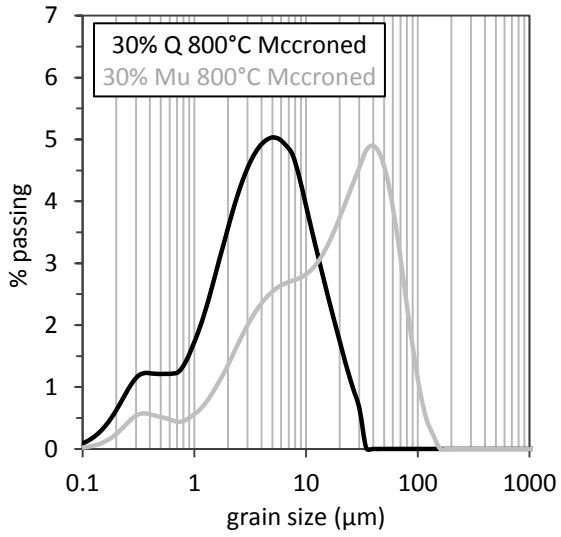

Figure 5.9: *Grain size distribution of the 30% Quartz (Q) and 30% Muscovite (Mu) mixture, calcined at 800°C and wet grinded with a McCrone.*

5.2.3 BET SPECIFIC SURFACE AREA

The specific surface area was determined for the 30% mixtures by means of nitrogen absorbed on the clay according to the BET method. It was demonstrated for natural clays (see chapter 7 and 9) that the milling of the sample has little influence on the BET specific surface area of the calcined samples. Therefore only the samples that were milled with a McCrone after a calcination process to 800°C were analysed. The results, given in Figure 5.10, show the BET specific surface area of all 30% mixtures is fairly similar. The reference sample containing 100% kaolinite has the highest specific surface area of 9.54 m^2/g. The BET specific surface area of quartz, feldspar and calcite is somewhat lower with values of 6.68, 6.19 and 7.56 m^2/g respectively. This small decrease in specific surface area compared to the reference sample is logic since non clay minerals have in general a lower specific surface than clay minerals.

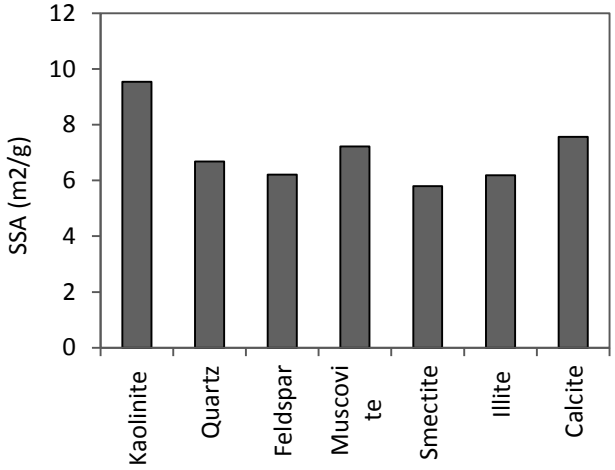

Figure 5.10: *BET specific surface area of a pure kaolinite reference sample and the mixtures containing 30% of impurity and 70% of kaolinite. All samples were calcined at 800°C and milled afterwards with a McCrone.*

Even though the specific surface area of an ordered kaolinite is rather low compared to other clay minerals its values are still higher than for non clay minerals. The smectite and illite mixture have the lowest BET specific surface area values of respectively 5.8 and 6.19 m^2/g. The pure samples of smectite and illite studied in chapter 4 already showed a drastic decrease in the specific surface area upon calcination for smectite and illite while the specific surface area of kaolinite only underwent a very small drop. The 30% of pure smectite or illite that is present in the mixture therefore lowers the BET specific surface area of the sample. The small differences in specific surface area of the various mixtures will normally not have a significant effect on the pozzolanic behaviour of the different admixtures.

5.3 POZZOLANIC REACTIVITY

To study the influence of the presence of impurities on the optimal activation temperature of the clay sample the portlandite consumption at 28 days was determined (Figure 5.11). Three different calcination temperatures of 700, 800 and 900°C were applied to mixtures containing 30% of a mineral impurity and 70% kaolinite. The results of the pure high ordered kaolinite (K1, chapter 3) are included to act as reference sample. Pure kaolinite is marked by a broad range of optimal firing temperatures between 600 and 800 °C with a portlandite consumption varying between 63 and 67%. This phenomenon is also reflected in the 30% mixtures of quartz, feldspar and muscovite. While the portlandite consumption of the 30% quartz and feldspar mixture varies between 52.4 and 55%, muscovite is marked by lower values between 50 and 50.5%. The drop in reactivity between pure kaolinite sample and the 30% mixtures of quartz, feldspar and muscovite can be explained by the dilution effect.

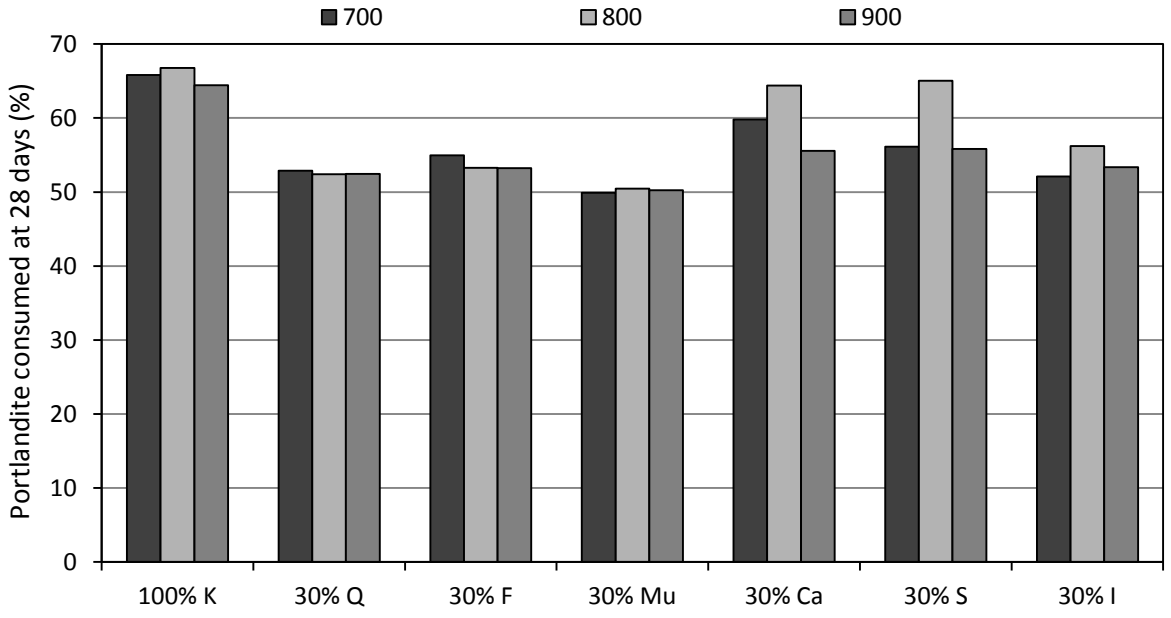

Figure 5.11: *Comparison of the optimal activation temperature and the portlandite consumption at 28 days of the 30% mixtures. The applied calcination temperatures are 700, 800 and 900 °C.*

The XRD and TGA results of the 30% quartz and feldspar mixtures showed that there were no remarkable changes observed as a result of the calcination process. Furthermore, the grinding of the samples after calcination diminished the additional sintering effect that was provoked by the

presence of feldspar. Therefore it can be concluded that both minerals have no direct influence on the calcination temperature. For muscovite, however, the TGA and XRD patterns did show some alteration as muscovite dehydroxylated in the temperature range between 700 and 900°C. Because during this dehydroxylation process alumina gets more disordered in the muscovite structure, it was possible that alumina would react with portlandite and contribute to the pozzolanic reactivity. However even at 900°C, when dehydroxylation of muscovite is completed, no remarkable increase in portlandite consumption could be observed. It is possible that higher temperatures up to 1000°C would activate muscovite, but kaolinite would already recrystallizes to form mullite and loses its pozzolanic potential. Therefore no higher calcination temperatures were examined. So also for muscovite it can be concluded the presence of muscovite does not influence the optimal calcination temperature significantly.

For the calcite mixture the optimal activation temperature is more defined. At 800°C the portlandite consumption is as high as 64.4% while this is only 60 and 55.5% for 700 and 900°C respectively. The decomposition of calcite takes place between 650 and 900°C. At 700°C most calcite is not decomposed yet as indicated by the XRD pattern in Figure 5.3. At 800°C and a resting of 2h no clear signs of calcite could be detected indicating all calcite was transformed into calcium oxide. At 900°C the 30% calcite mixture becomes less reactive again. This can be explained by the formation of gehlenite at a calcination temperature of 900°C by which part of the Si, Al and Ca is already bound in the gehlenite structure and as a consequence are no longer available for the pozzolanic reaction (figure 5.3).

Also for the 30% smectite mixture the optimal activation temperature is 800°C and 65% of the available portlandite is consumed at 28 days. Calcining the sample at 700 or 900°C results in a decrease of the reactivity since only 56% portlandite is consumed. The pure montmorillonite (S2, chapter 4) was classified as medium potential pozzolanic material and will therefore contribute to the total amount of portlandite that will be consumed. To optimize the pozzolanic properties of smectite, a calcination temperature of 800°C should be applied because at this temperature the used smectite becomes completely amorphous. As a result the optimal firing temperature of a kaolinite/smectite mixture is influenced mainly by the optimal activation temperature of the smectite that is present, which is in most cases 800°C.

The optimal calcination temperature of the illitic clay is less distinctive. 800°C has the highest activity with a portlandite consumption of 56.2% while 700 and 900° have a slightly lower consumption of 52 and 53.3% respectively. The optimal activation temperature of pure illitic clay is however 900°C. This indicates the contribution of illite is too low to actually affect the optimal activation temperature of the mixture. Nevertheless, the portlandite consumption of the illite mixture is almost 4% higher than for the 30% quartz mixture, which indicates illite does have some contribution to the reactivity. Therefore another possibility is that the optimal activation temperature of illite is lowered due to the presence of kaolinite as the total dehydroxylation temperature of the sample decreases due to the presence of kaolinite. This could also be seen in the DTG patterns of the raw 30% I mixture, that showed a dehydroxylation peak of only 527°C.

The portlandite consumption was also monitored over time to assess the progression of the pozzolanic reaction (figure 5.12). The 30% impurity mixtures were analysed at 3, 14, 28, 56 and 90 days to see both the effect of the impurity on short and long term. The 30% quartz and feldspar mixtures behave fairly similar and after 28 days the reaction slows down drastically. This is in agreement with the findings of pure kaolinite whereby most of the kaolinite is already consumed at 28 days. The reduced kaolinite content of the mixtures results in a slower reaction rate the first 28 days and lower end reactivity compared to a pure kaolinite sample. At 28 days the average portlandite consumption of the 30% quartz and feldspar mixture is 52.8% while for kaolinite this is 66.8%. The highest value is obtained at 90-day is approximately 54.5% for the two mixtures and 69.6% for pure kaolinite. This indicates that even though the amount of kaolinite decreases with

30%, the pozzolanic reactivity only decreases with 24%. Some authors mention quartz can contribute to the pozzolanic reaction as a result of complex dissolution-precipitation reactions when curing temperatures are high and the particle size is low (Benezet and Benhassaine, 1999). However, at curing temperatures of 25° and a quartz powder with grain size > 5 µm this influence is negligible and in general quartz can still be seen as a chemical inert material, that only exhibit filler effects. The effect that is observed can therefore mainly be assigned to the correlation between the amount of kaolinite and the consumed portlandite, which is not a 1:1 relation.

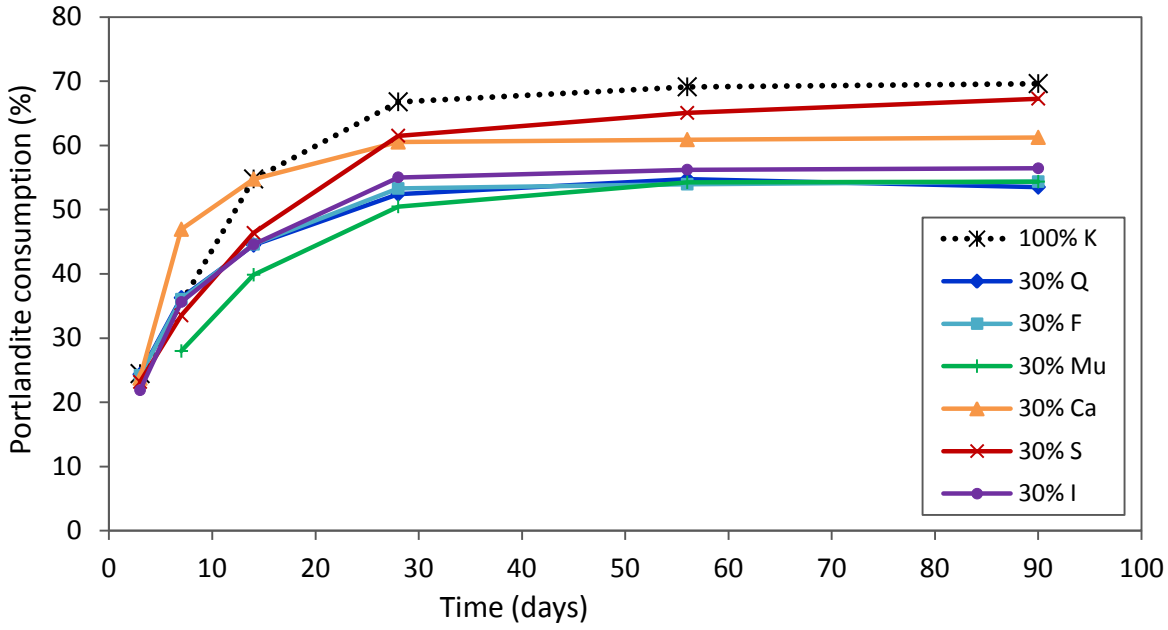

Figure 5.12: *Portlandite consumption after 3, 7, 14, 28, 56 and 90 days measured with TGA for 30% mixtures calcined at 800°. The dotted line represents the 100% kaolinite reference sample. The mean RSD is 1.57%.*

Surprisingly the 30% muscovite mixture is marked by a slower reaction rate compared with the quartz mixture before 56 days of curing. Especially at 14 days of curing the portlandite consumption of 39.8% shows a difference of almost 5% with the quartz and feldspar mixture. From 56 days onward the portlandite consumption is comparable with that of the quartz and feldspar mixture with a maximum value of 54.4% at 90 days. The reason for this lower reaction rate can be found in the difference in grain size. After calcination all mixtures were wet grounded with a McCrone mill to reduce the particle of the sintered samples. In general the particle sizes of the different mixtures became comparable. However the platy morphology of muscovite flakes are hard to grind properly and as a result the particle size distribution remained coarser for the 30% muscovite mixture compared to the other samples. As a consequence the initial reaction surface is smaller and less nucleation sites are available, which explains why the initial reaction rate is slower but a similar reactivity as other chemical inert samples is reached.

The illite mixture starts with a similar reaction rate as the quartz mixture and after 28 days the reaction barely continues. However, the portlandite consumption at 28, 56 and 90 days is approximately 2.5% higher compared to the quartz mixture. This indicates illite actually direct contributes to the pozzolanic reaction, though in limited amount and mainly after the 14 first days of reaction.

The 30% smectite mixture shows a rapid increase of the portlandite consumption up to 28 days. At 28 days the portlandite consumption of 61.5% can be considered as rather good since it is only 5% lower than for pure kaolinite. Moreover, after 28 days the reaction still continues, though at a slower

rate, closing the gap with the kaolinite reference sample. This phenomenon is typical for smectite since pure smectite is also marked by a slower reaction rate that continues steadily even up to 90 days. At 90 days the difference in portlandite consumption is only 2.3%, which indicates that this mixture is highly reactive.

The 30% calcite mixture is marked be a quick start of the reaction. The first 14 days the reaction rate of the 30 calcite mixture even exceeds the rate of pure kaolinite. This indicates the newly formed calcite does not only take part in the reaction but also accelerates the reaction rate significantly. As a consequence the reaction already slows down after the first 14 days and reaches its plateau value of 60.5% at 28 days. After 28 days the reaction continues slowly, with at 90 days a portlandite consumption of 61.3%. While at 14 days the portlandite consumption of the 30% calcite mixture is comparable with the pure kaolinite reference sample, the difference increases in reactivity, especially in between 14 and 56 days. At 90 days the difference in reactivity is more than 8%. Nevertheless, it is possible that the portlandite consumption is slightly underestimated since small amounts of portlandite were detected by XRD in the calcite-kaolinite mixture itself after calcination and exposure to the air. As a result the amount of unreacted portlandite, determined by TGA, can be overestimated. Compared to the 30% smectite mixture the portlandite consumption at 28 days is similar. However at a later stage in the reaction the 30% smectite mixture proofs to be more reactive. This indicated calcite is efficient in increasing the reaction rate in the first days of reaction. Therefore the presence or even addition of calcite to clay can have a positive effect on the low reaction rate in the early stage of the pozzolanic reaction, which is typical for all calcined clays blended cement when compared to ordinary Portland cement due to a combination of the dilution effect and the late start of the pozzolanic reaction. The potential of this ternary blend of calcite, in the form of limestone, calcined clay and Portland cement which is called LC^3 has been demonstrated by numerous authors (Antoni et al., 2012; Damidot et al., 2011; Lothenbach et al., 2008; Sánchez Berriel et al., 2016), indicating calcite additives can certainly be beneficial to the cement properties.

The influence of a variable quantity of a specific impurity was studied in more detail by monitoring the portlandite consumption over time (Figure 5.13). The mixtures of quartz, feldspar and muscovite show a similar behaviour. All samples are the most reactive during the first 28 days and the reaction slows down significantly after 56 days. The difference in portlandite consumption for different replacement levels remains similar after the first 14 days. For each increase of the amount of impurity the percentage of portlandite consumption decreases. However, there is no direct contribution of quartz, feldspar or muscovite to the pozzolanic reactivity as the fluctuation in portlandite consumption mainly depends on the amount of kaolinite that is present in the sample. For all three samples the highest drop in portlandite consumption is between the pure kaolinite and when 15 (Q) or 10% (F and Mu) was added. Afterwards the decrease in portlandite consumption becomes smaller. Up to a replacement of kaolinite by 30% the samples yield a portlandite consumption of 50% or higher at 28 days, which is still acceptable. Several authors have stated that samples with a kaolinite content below 40 to 45% and no additional contributing clay minerals do not show high enough strength and satisfying cementitious properties at 28 days (Fernandez, 2009; Tironi et al., 2014). In agreement with these results it can be stated that at 28 days at least 40% of portlandite should be consumed to be a clayey material with a fairly good pozzolanic potential.

The presence of calcite mainly contributes to the reactivity in the early stage of the reaction. For all percentages the reaction rate is high during the first 14 days and slows down significantly after 28 days. The 15% calcite mixture has similar portlandite consumption as the pure kaolinite reference sample at all curing ages. Also the 30% calcite mixture is characterised by a high portlandite consumption that is only 8% less than the reference sample. The portlandite consumption of the 45 and especially the 60% calcite mixture is however fairly low. These two samples consume similar (45% Ca) or even less (60% Ca) portlandite than the quartz mixture with a similar ratio. This can be

explained since the high amount of calcite in the initial mixture resulting in additional formation of portlandite after calcination and exposure to the air of the calcite-kaolinite mixture. With thermal analyses no distinction can be made between portlandite that was already present in the calcite-kaolinite mixture and the 70% added portlandite. Nevertheless, if additionally formed portlandite would be present the amount of portlandite that is consumed would be underestimated and the sample would in fact be even more reactive.

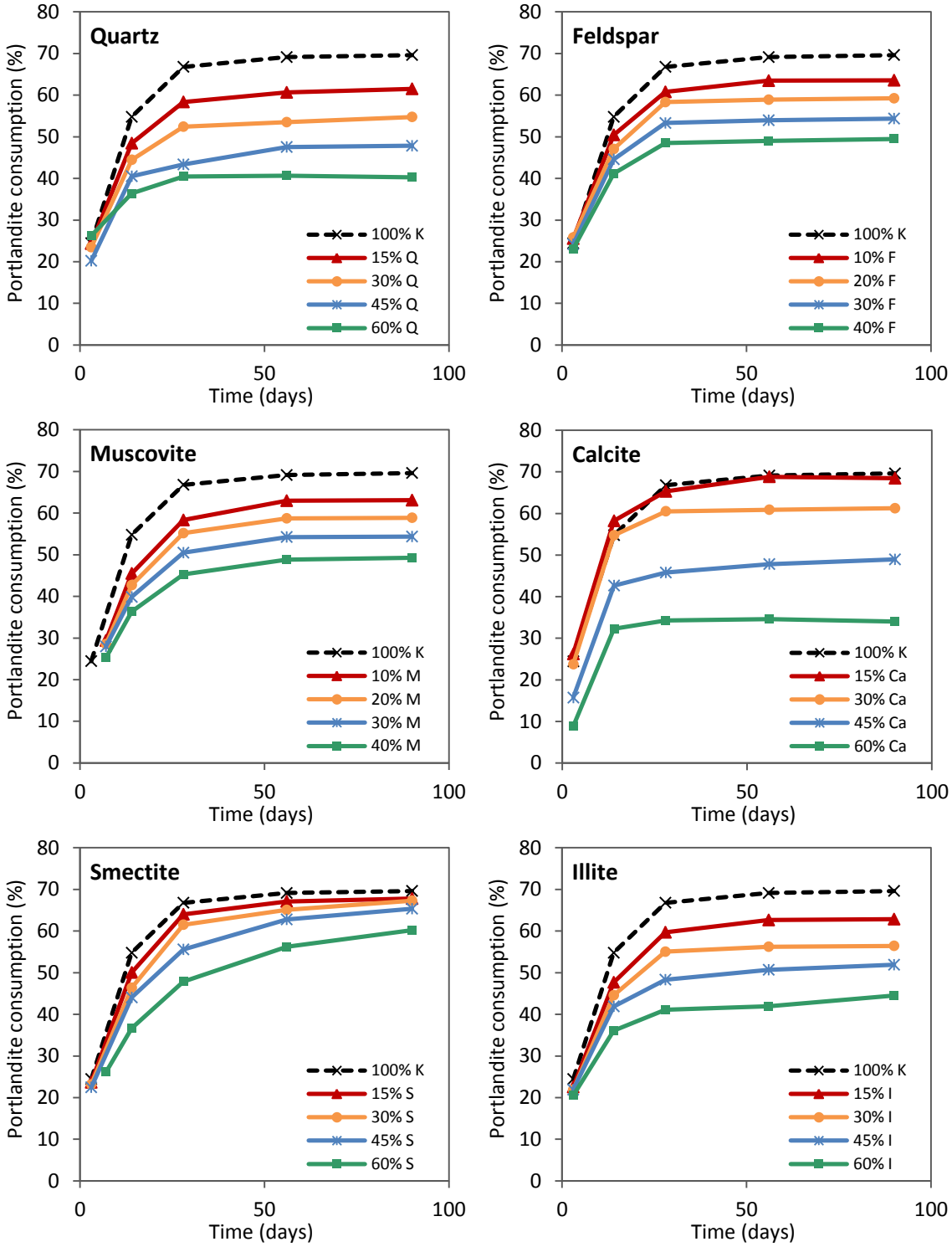

Figure 5.13: *Portlandite consumption over time for different quantities for the six impurities and. As comparison the portlandite consumption of a pure kaolinitic sample (100% K) is included.*

For the smectitic mixtures the reaction is also the fastest during the first 28 days. However, smectite is known to react rather slowly and the portlandite consumption that can be observed after 28 days can mainly be attributed to the presence of smectite. This effect is therefore more distinctive for the mixtures that contain 45 and 60% of smectite. At 56 days the 45% smectite sample almost catches up with the portlandite consumption of the 15 and 30% smectite mixtures. The maximum values are reached at 90 days and can be summarised according to increasing smectite content: 67.8, 67.3, 65.4 and 60.2%. This indicates the reactivity on the long term is comparable between samples containing 15, 30 and 45% of smectite and is slightly less for the 60% smectite sample. At 28 days of curing the portlandite consumption of the 15% smectite mixture is 64%, which is only 2.8% lower than the 66.8% for a pure kaolinite. Furthermore, also the other mixtures with more smectite yield very good reactivity values of 61.5% (30% S), 55.6% (45% S) and 47.9% (60%). All mixtures achieve the threshold value of 40% portlandite consumption and can be seen as potential valuable supplementary cementitious material.

The mixtures that contain illite show a portlandite consumption evolution that is comparable with the quartz mixture. The actual percentages of the illite mixture are generally 2.5% higher than the quartz mixtures at 28, 56 and 90 days. This indicates that even though the illite is not entirely chemical inert, its contribution to the pozzolanic reaction is limited. While the 15 and 30% illite mixtures do not show much change after 56 days the mixtures with higher amount of illite, 45 and 60%, do show an increase in reactivity. This indicates that especially for higher illite concentrations, illite also contributes to the pozzolanic reaction at a later stage. At 28 days all samples have consumed more than 40% of portlandite indicating all samples can be used as potential pozzolan. Nevertheless, the mixture containing 60% of illite has only a consumption of 41.1 which is just above the minimum value. However it is possible that for higher amounts of illite that exceed 30%, the optimal activation temperature of pure illite becomes more important and as a result calcining the samples at 900°C could improve the total reactivity. It will be important to know whether the additional fuel costs are worth the few percentages of extra reactivity.

To be able to predict the portlandite consumption based on the type and quantity of a certain impurity, the amount of impurity is plotted as a function of the portlandite consumption at 28-day (Figure 5.14). This allows determining the relation between the two parameters by formulating a function of the trend line. The functions for each type of impurity are summarized in Table 5.2. For the non clay minerals quartz, feldspar and muscovite this relation can be described by a linear function with a R^2 above 0.97. Quartz and feldspar are much alike, as was expected for these two chemical inert materials. Their functions are representative for all type of mineral impurities that behave in an inert manner. The lower reactivity for muscovite could be explained by the difference in grain size. When a similar curve is made for the results at 56 days, muscovite behaves parallel to the inert quartz. To obtain a more practical and usable function the portlandite consumption was plotted against the kaolinite content which resulted in the following equation with R^2 of 0.95:

$$\%\ Portl.\ Consumption = 0.44 * \%\ kaolinite + 20.97 \qquad (equation\ 5.1)$$

This equation can be used for all kaolinitic clays that only posses inert minerals as impurity.

Also for illite the correlation can be described by a linear function with an excellent R^2 of 0.997. Based on the different curves it can be concluded that indeed the illite mixtures reactivity is slightly higher than for inert materials.

More promising are the smectite mixtures, as they are clearly marked by higher consumption rates for all ratios. The first part of the curve behaves also linear; however, the slope of samples that contain more than 30% of smectite is clearly marked by a sudden steepening. Therefore the entire curve can best be fitted by a polynomial function to obtain a very good fit with R^2 of 0.996. However if one wishes to simplify the calculation process the linear function still gives an acceptable fit with R^2

of 0.941. With a linear fit mainly the reactivity of pure portlandite is overestimated while the 30% smectite mixture is being underestimated.

For calcite a clear difference in portlandite consumption can be defined for samples containing ≤ 30% and samples > 30% calcite. Samples that contain up to 30% of calcite are marked by a relative high pozzolanic reactivity and are highly potential SCMs. However the mixtures that contain 45% or more calcite show a sudden drop in reactivity and are medium to low potential SCMs. Due to this sudden drop in reactivity the function that allows predicting the reactivity has to be polynomial to receive a fit with R^2 of 0.988. When only a linear function would be applied the error of the misfit becomes rather large. However it would be possible to fit the first part of the curve up to 30% with a linear fit.

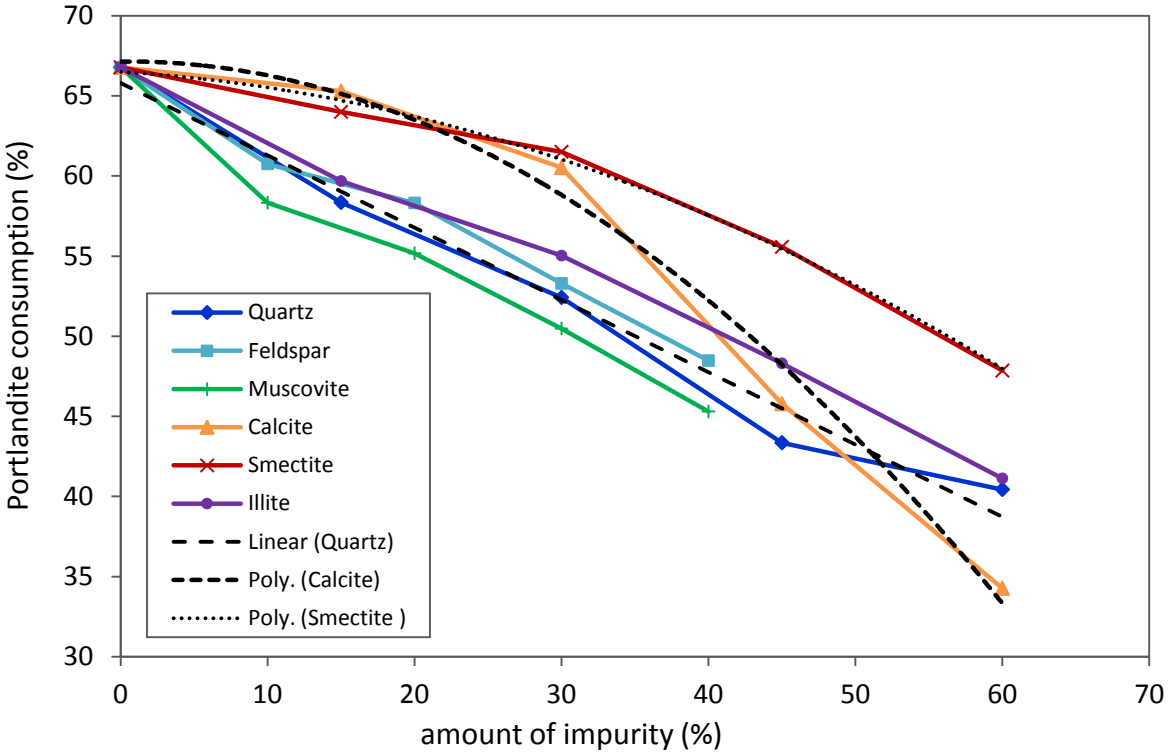

Figure 5.14: *Correlation between the amount of impurity and the portlandite consumption at 28 days. A trend line was made for quartz (linear), calcite and smectite (both polynomial).*

Table 5.2: *Overview of the correlation functions between the amount of impurity (X) and the portlandite consumption at 28 days (Y). The R^2 gives an estimation of the preciseness of the fit.*

Type of impurity	Correlation	Function	R^2
Quartz	Linear	Y= -0.45X + 65.8	0.981
Feldspar	Linear	Y= -0.441X + 66.34	0.988
Muscovite	Linear	Y= -0508X + 65.37	0.977
Calcite	Polynomial	$Y = -0.0095X^2 + 0.008X + 67.15$	0.988
Smectite	Polynomial	$Y = 0.0042X^2 – 0.055X + 66.50$	0.996
	Linear	Y = -0.309X + 68.4	0.941
Illite	Linear	Y = -0.418X + 66.72	0.996

5.4 POZZOLANIC REACTION PRDOUCTS

5.4.1 X-RAY DIFFRACTION

The influence of the type and quantity of the impurity on the pozzolanic reaction products formed was studied by XRD. The diffraction patterns of the 30% impurity mixtures are given in Figure 5.15. Portlandite is still present in all samples as can be observed by its main reflections at 4.9 and 2.63 °2θ. Semi-quantitative determination of the amount of portlandite allows estimating the reactivity of the sample. The 30% mixtures of smectite and illite are marked by the lowest peak intensity at 4.9 °2θ indicating these are the most reactive samples, which is in agreement with the TGA results. The peak intensity of the 30% mixtures of quartz, feldspar and muscovite are comparable. The intensity for the illite mixture is however slightly lower in comparison with the previous samples, which confirms the low pozzolanic reactivity of illite.

The mixtures that contain the pozzolanic inert materials quartz, feldspar and muscovite are characterised by similar reaction products as for all three samples only kaolinite contributes to the reaction. This is confirmed by the presence of strong and sharp reflection peaks for the three types of impurities, Q, F and Mu_c. Strätlingite, with its dominant reflection at 7.0 °2θ, is the main crystalline hydration product and is typically formed in Al-rich environments. Additionally several other AFm phases are formed that can be identified by the broad reflection zone between 10 and 12 °2θ. The C_4AH_{13} phase is marked by a reflection at 11.3 °2θ. Furthermore, hemi- and monocarboaluminate can be detected by their reflections at 10.8 and 11.7 °2θ respectively. Apparently hemicarboaluminate is formed preferably, which indicates carbon is depleted with regard to aluminium as hemicarboaluminate only contains 1 C atom for 2 Al atoms while for monocarboaluminate this ratio is 1:1. The broad reflection around 29.5°2θ is an indication calcium silicate hydrates are present. Since this phase is only semicrystalline, part of the C-S-H phase will only enhance the background. When the three different types of 30% mixtures are compared no differences can be observed in either the enhancement of the background or of the broad reflection of C-S-H. When the hydration products are studied over time it can be concluded that for all three 30% mixtures traces of strätlingite are present from 7 days onwards, nevertheless, the amounts are very low and the 003 reflection peak at 7.0 °2θ is hard to detect but present. The other AFm hydration phases are already detectable at 3 days. Furthermore, mainly the amount of strätlingite and C-S-H is influenced by the amount of impurity, and therefore also the amount of kaolinite that is present in the sample. Even though both strätlingite and C-S-H are formed in all mixtures, the peak intensities decrease significantly when the amount of impurity increases. For the AFm phases C_4AH_{13}, mono- and hemicarboaluminate on the other the peak intensities remain comparable without a clear link with the amount of impurity or with the curing time.

The 30% illite sample shows much resemblance with the mixtures including inert material. The identified reaction products are exactly the same, only the amounts vary slightly based on semi-quantitative interpretations. For the 30% illite mixture the broad reflection of the C-S-H phase at 29.5 °2θ is increased, although to a limited extent. Furthermore, also the background seems more elevated, which can be either due to the presence of additional semi amorphous C-S-H phases or by the non reacted decomposed illite itself. Nevertheless, the higher pozzolanic reactivity of the illite mixtures determined by TGA indicates most likely additional hydration products in the form of C-S-H are formed. Significant differences in the strätlingite content could not be observed. The evolution over time of the reaction products indicate that strätlingite could only be detected in the 30% illite mixture from 14 days onwards. At 7 days no traces of strätlingite could be detected wile for the 30% quartz, feldspar and muscovite some small reflections were already present. For all the illite mixtures that were prepared from 15 -60%, strätlingite could only be detected by XRD from 14 days onwards. This indicates that the presence of illite, even as low as 15%, in the clay sample results in the favouring of the formation of C-S-H above strätlingite during at least the first 7 days of the reaction.

This effect can be assigned to the increased Si/Al of the pozzolan material ratio due to the presence of the more silica rich, partially decomposed illite (figure 2.7, chapter 2).

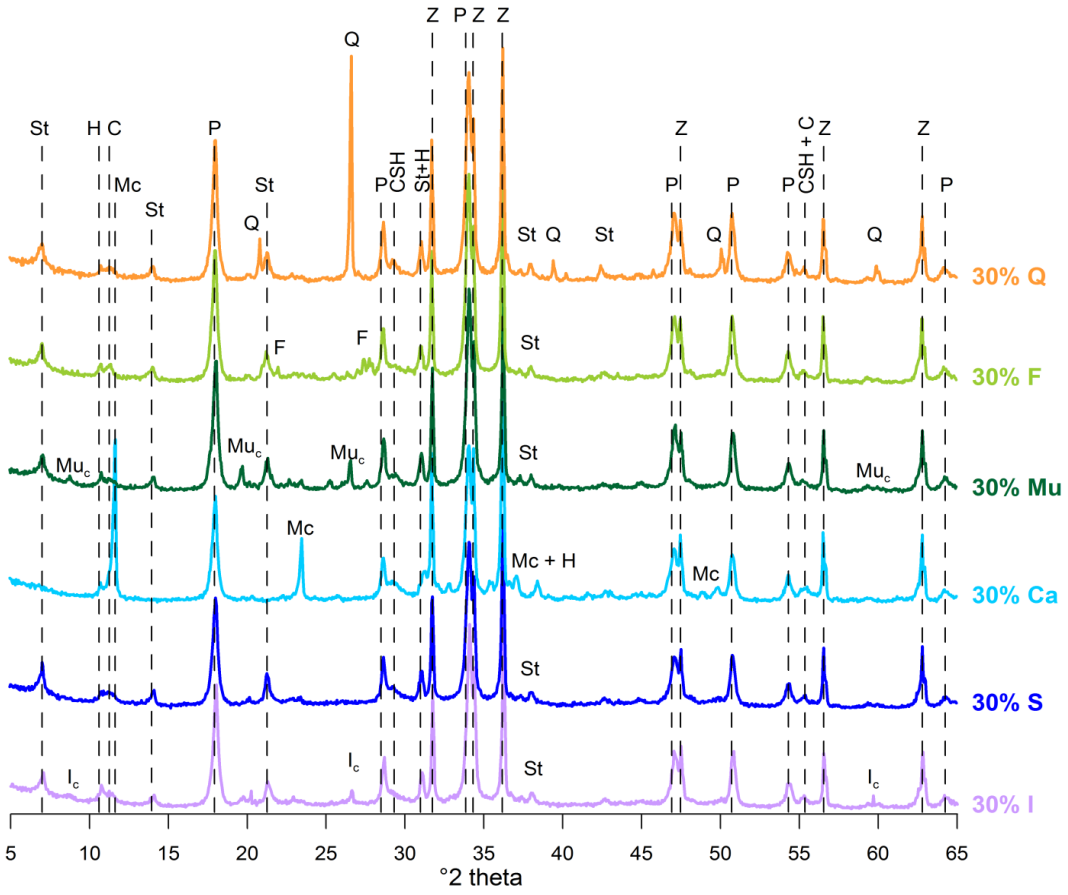

Figure 5.15: *XRD pattern of all pastes of the 30% impurity mixtures calcined at 800°C. The phases are indicated: Z: zincite (internal standard), Mu_c: calcined muscovite, I_c: calcined illite, Q: quartz, Ca: calcite, F: feldspar, P: Portlandite, St: strätlingite, H: hemicarboaluminate, Mc: Monocarboaluminate, C: tetra calcium alumina hydrateC_4AH_{13} and CSH: calcium silicate hydrates.*

At 28 days of curing the 30% smectite sample is marked by the highest intensities of strätlingite and of C-S-H. The high amount of C-S-H and the presence of unreacted amorphous smectite results in a high background. Since smectite is entirely decomposed upon calcination both additional silica and alumina become available. As a result of the higher amount of alumina present in the amorphous material more strätlingite can form, while the extra silica is incorporated in the C-S-H phases. The intensity of the AFm phases, C_4AH_{13}, mono- and hemicarboaluminate are comparable with the 30% mixtures of quartz, feldspar, muscovite and illite. Nevertheless, the Si/Al ratio of the 30% smectite mixture is higher (± 1.53) than for pure kaolinite (± 1.18). As a consequence strätlingite is only detectable in the 30% smectite mixture from 14 days onwards, while for pure kaolinite it was already present at 7 days. Even for the 15% smectite mixture with a Si/Al ratio of ± 1.34, strätlingite could not be detected by XRD at 7 days. This indicates the time of formation of strätlingite is depended on the Si/Al ratio. When different smectite – kaolinite ratios are compared at 28 days of curing, it can be noted that the intensity of the strätlingite peak decreases with an increase of the smectite content since the pozzolan becomes less Al-rich. An opposite effect can be observed for the C-S-H, though this is less explicit.

The 30% calcite mixture differs itself from the other mixtures regarding the formed hydration products (Figure 5.16). Even after 28 days of curing strätlingite is not detectable by XRD indicating that if strätlingite is present the amount is negligible. The main crystalline reaction product is

monocarboaluminate, which can easily be detected by the sharp and well developed peak reflections at 11.7 and 23.5 °2θ. These results are consistent with previous studies that indicated monocarboaluminate was the main reaction product for a Na-smectite with a small amount of calcite (He et al., 1996) and with a calcined marl (Danner, 2013). Furthermore, also higher amounts of hemicarboaluminate compared to other mixtures can be observed. The reason for the formation of these phases is the presence of calcite. Calcium aluminate hydrates will react with the calcium carbonate that is present in the system as reported for cementitious pastes that were blended with limestone (Bonavetti et al., 2001; Bushnell-Watson and Sharp, 1985; Ipavec et al., 2011).

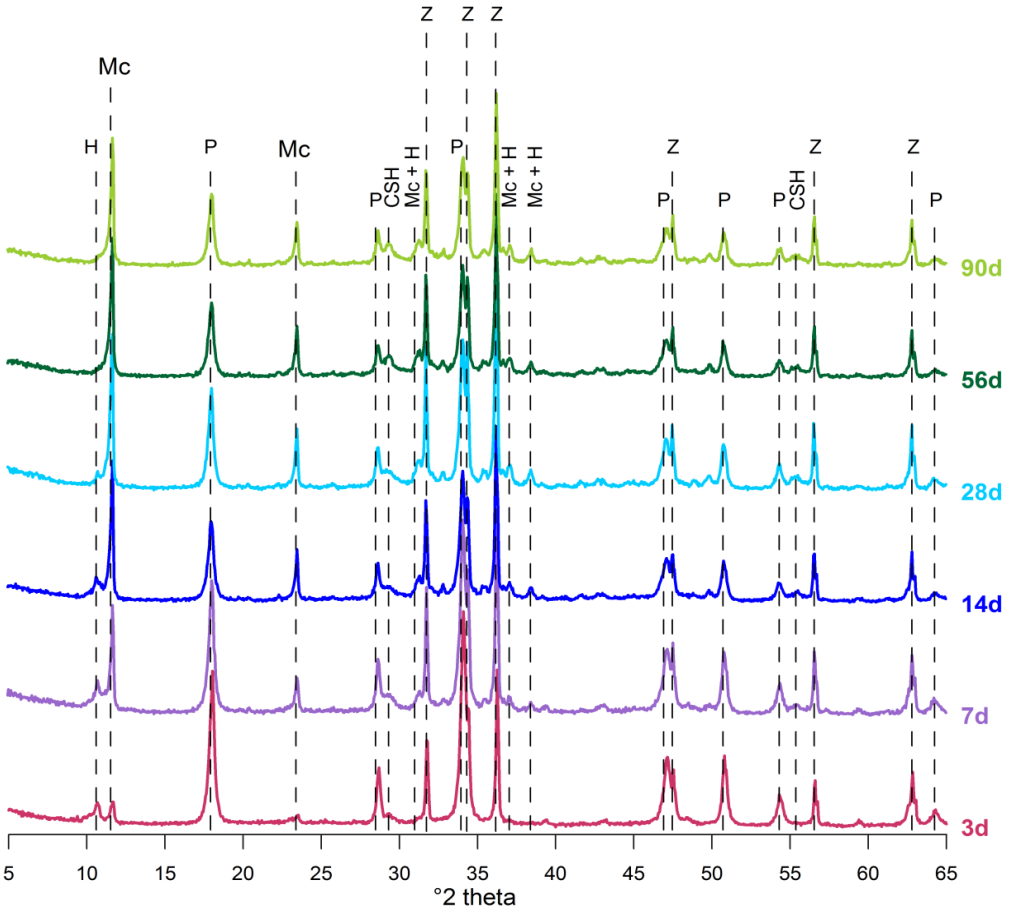

Figure 5.16: *XRD pattern of the 30% calcite mixture, calcined at 800°C and cured for 3, 7, 14, 28, 56 and 90 days. Zincite (Z) was added as internal standard. The phases are indicated: Ca: calcite, P: Portlandite, H: hemicarboaluminate, Mc: Monocarboaluminate and CSH: calcium silicate hydrates.*

After the calcination process of the 30% calcite mixture at 800°C, the formed CaO was transformed again to portlandite and eventually calcite when exposed to air. So indeed calcite was present in the sample and moreover, this newly formed calcite is less crystalline and can react more easily with alumina and silica in the presence of water than the original calcite. As a result this calcite is a source of carbon that can be incorporated in the structure of the newly formed hydration phases. Hereby the formation of monocarboaluminate is favoured over strätlingite. The differences within their chemical composition explains why the calcite mixtures consume more portlandite. The CaO/Al_2O_3 ratio of monocarboaluminate ($C_4A\check{C}H_{11}$) is 4 while for strätlingite (C_2ASH_8) this is only 2, which indicates for a similar amount of alumina available more portlandite is consumed when monocarboaluminate is formed instead of strätlingite. The amount of hemicarboaluminate that is formed is still limited compared to monocarboaluminate. This can be explained by the ratio between C and Al, since hemicarboaluminate only incorporates 1 carbon for 2 alumina atoms and in reality more carbon is available to form monocarboaluminate which has a 1:1 ratio. Previous studies found

however similar amounts of hemi- and monocarboaluminate for their pastes of calcined marls (Danner, 2013). The main differences lie within the original calcite concentration and the amount of CO_2 that was taken up after the calcination process. Hemicarboaluminate is not stable and in the presence of calcite converts to monocarboaluminate (Kuzel and Pöllmann, 1991).

To evaluate this theory the reaction products of the 30% calcite mixture were studied over time. At 3 days of curing the peak intensity of hemicarboaluminate at 10.8 °2θ is comparable to monocarboaluminate. Over time the intensity of hemicarboaluminate decreases rapidly while the amount of monocarboaluminate increases. The time frame of the conversion is comparable with the results of Ipavec et al. (2011). Important to state is that the chosen technique to stop the hydration reaction can have an influence on the detection of hemicarboaluminate. The use of solvents and drying at 35°C result in the conversion of hemi- to monocarboaluminate and hemicarboaluminate would not be detected. Often in-situ XRD on the wet samples is applied (Danner, 2013; Ipavec et al., 2011), but also the freeze drying procedure gives good results for the detection of hemicarboaluminate. The amount of monocarboaluminate increases up to 28 days from which the increase stagnates. Similar effect can be observed for the C-S-H phase.

Another important parameter is the amount of calcite that is present in the sample. The XRD patterns at 28 days curing for the different calcite kaolinite ratios are given in Figure 5.17. The portlandite reflections are lowest for the 15 and 30% calcite mixtures and correspondingly the C-S-H and carboaluminate phases are the highest for these two samples. Hemicarboaluminate could be detected in the mixtures containing 15 and 30% of calcite. For the mixtures that contained more calcite almost no hemicarboaluminate is present as a result of the higher amount of carbon that is available. The calcite in the 45 and 60% mixtures is even in excess as not all calcite has reacted and reflection peaks at 29.4 °2θ can be detected. Higher kaolinite content gives also rise to the formation of strätlingite and when only 15% of kaolinite is replaced by calcite significant amounts of strätlingite are present from 28 days onwards.

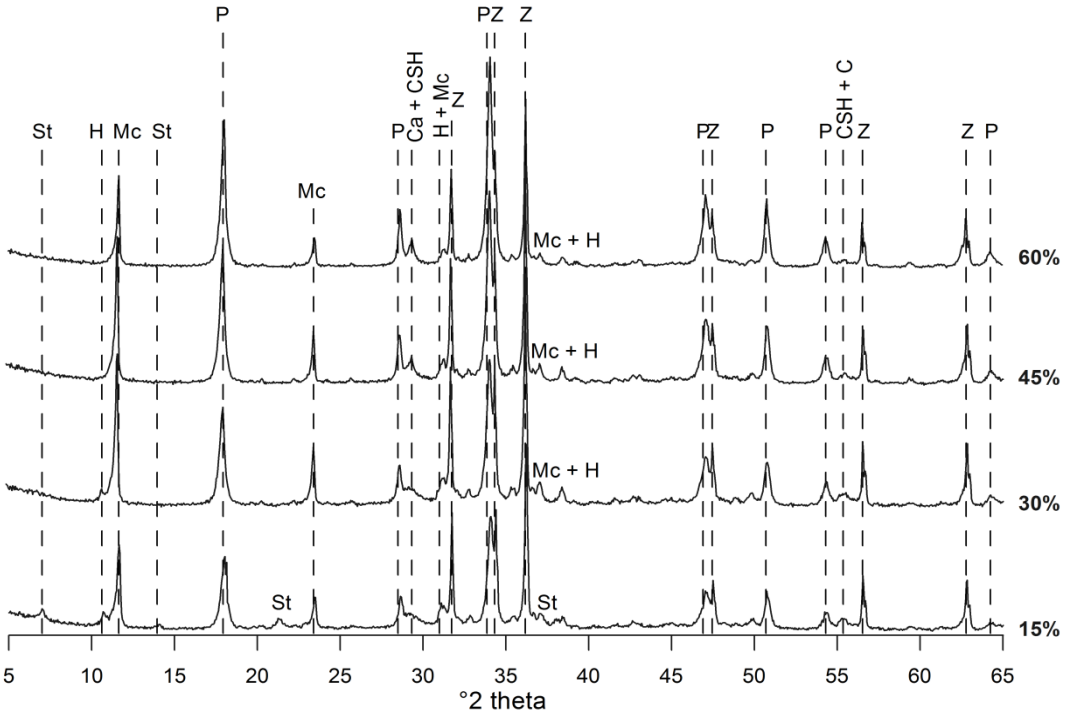

Figure 5.17: *XRD pattern of the paste of the mixtures containing calcite calcined at 800°C and cured for 28 days. The phases are indicated: Z: zincite (internal standard), Ca: calcite, P: Portlandite, St: Strätlingite, Mc: monocarboaluminate and H: hemicarboaluminate.*

5.4.2 THERMAL ANALYSIS

Not only can the portlandite consumption be estimated by means of thermal analysis also the formed reaction products can be identified. Figure 5.18 shows the DTG pattern of the 30% impurity mixtures that were cured for 28 days. The mass loss between 350 and 550°C can be attributed to the portlandite decomposition and was used to determine the pozzolanic reactivity of the sample. Additionally several peaks in the region between 100 and 300°C appear which can be attributed to the newly formed phase. The first peak at 115°C reflects the decomposition of C-S-H phases and can be seen in all 6 types of mixtures. The peak around 150°C can be attributed to the decomposition of AFm phases including C_4AH_{13}, mono- and hemicarboaluminate. For the 30% calcite smectite the monocarboaluminate can be distinguished from the other AFm phases because of existence of a sharp peak at 160°C and a broad peak around 250°C that are both characteristic for monocarboaluminate (Gabrovšek et al., 2008). Additionally strätlingite was found in all samples except for the 30% calcite mixture, which confirms the XRD results. Strätlingite can be recognized by the two peaks at 170 and 220°C. The peak at 170°C can give overlap with the monocarboaluminate peak at 160°C and therefore both phases are indicated for this peak in the pattern.

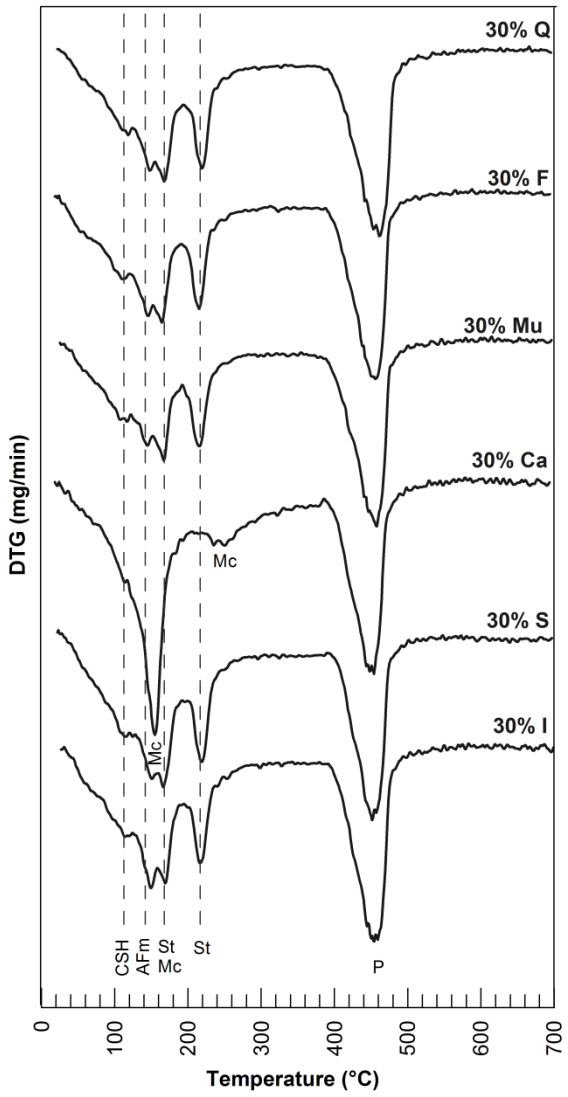

Figure 5.18: *DTG pattern of the lime pastes of the 30% impurity mixtures cured for 28 days. The identified phases are indicated. The identified phases are P: Portlandite, St: Strätlingite, Mc: monocarboaluminate CSH: calcium silicate hydrates and AFm*

An additional benefit of thermal analysis is that the evolution of strätlingite can be monitored more precisely than with XRD. In the early stage of the strätlingite formation, strätlingite can be poorly crystallized and as a result harder to detect with XRD (Fernandez, 2009). For example, for the 30% mixture of smectite, strätlingite could only be detected by XRD from 14 days onwards, while the DTG pattern show that already at 7 days a very small amount of strätlingite is present (Figure 5.18). For the 30% illite mixture no strätlingite was detected in DTG pattern at 7 days. The presence of strätlingite for the 30% quartz, feldspar and muscovite mixtures is also more distinctive by DTG, as XRD showed only very small peak reflections that were hard to distinguish. This indicates strätlingite is not fully crystalline and therefore not detected by XRD when the quantity is low. Longer curing times give rise to further crystallization of strätlingite whereby detectable peaks are formed. Furthermore, the amount and formation time of strätlingite can be negatively correlated with the amount of impurity. The 60% quartz mixtures shows barely any traces of strätlingite while for the 15% Q mix clear strätlingite peaks can be distinguished (Figure 5.19 B).

In general it can be concluded that the amount and timing of the strätlingite formation is related to the amount and type of impurity. The amount of impurity is directly correlated with the amount of kaolinite and therefore also with the total reactivity of the sample. The type of impurity can have an influence on the Si/Al ratio. Reactive type of impurities like illite and smectite the Si/Al ratio of the sample is altered which has a direct effect on the formed hydration products.

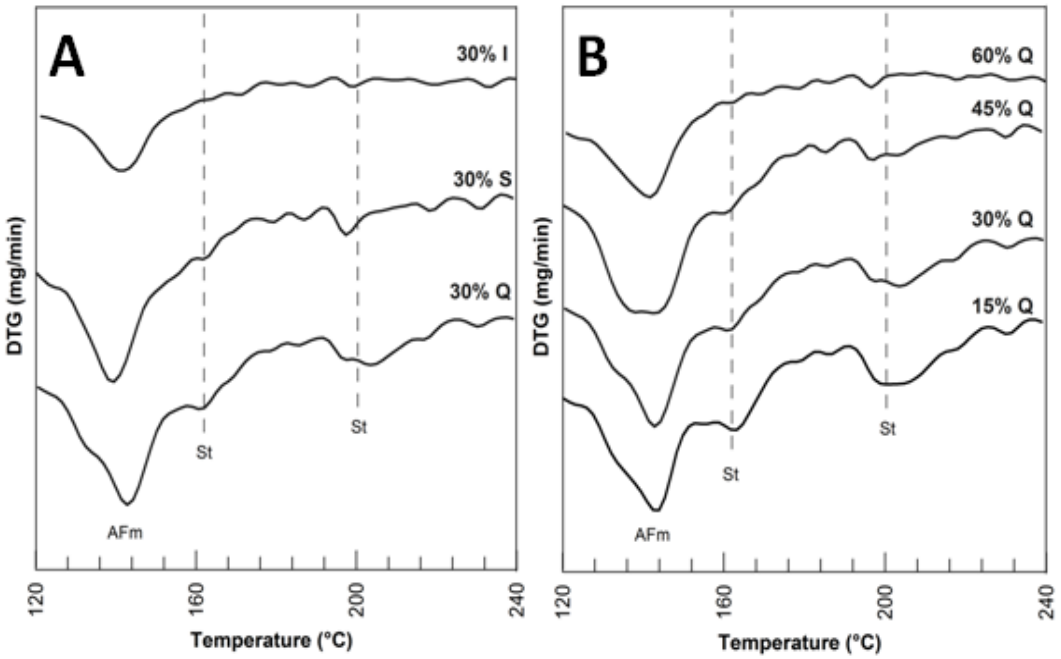

Figure 5.19: *Comparison of the strätlingite formation for A: different type of impurities (30%) and B: different amounts of impurity (quartz) at 7 days by means of a DTG pattern in the temperature range of 120 to 240°C. The identified phases are St: Strätlingite and AFm*

5.5 CONCLUSIONS

Activation temperature

The optimal activation temperature of the mixtures is mainly influenced by the type of the impurity as the amount of impurity has only a limited effect. The activation temperature of the mixtures containing 30% of the inert materials quartz, feldspar or muscovite is not affected significantly compared to pure kaolinite. A broad range of optimal calcination temperatures between 700 and 900°C lead to comparable reactivity.

For the 30% calcite, smectite and illite mixtures, the optimal activation temperature could be appointed at 800°C. Upon calcination of the calcite-kaolinite mixture, calcite was decarbonated and again transformed into a less crystalline calcite when exposed to air, making the calcite more reactive. Further heating to 900°C results in the formation of crystalline gehlenite resulting in a less reactive material. At 800°C smectite becomes completely amorphous and no recrystallisation takes place, so smectite can fully contribute to the pozzolanic reactivity. Even though the optimal activation temperature of illite is 900°C, the negative effect of the additional sintering makes 800°C more suitable.

Type of impurity

The pozzolanic reactivity of the examined mixture is mainly controlled by the type and the amount of the impurity and can be summarized as follows:

Muscovite < Quartz = Feldspar < Illite << Calcite < Smectite

Three types of impurities, quartz, feldspar and muscovite can be considered as chemically inert materials and they do not directly contribute to the pozzolanic reactivity. This is confirmed by the similarity of the reaction phases, strätlingite, C-S-H, C_4AH_{13}, hemi- and monocarboaluminate that were identified. The platy morphology of muscovite makes it more resistant against grinding techniques, which results in a slightly less reactive material during the first 56 days of the reaction compared to quartz and feldspar. Furthermore, some inert materials can have an indirect effect on the pozzolanic reactivity. The presence of muscovite and feldspar provokes additional sintering of the sample during the calcination process (800°C) as a result of respectively partial dehydroxylation and pre-fluxing properties. Due to this sintering effect the grain size increases and without grinding the sample after calcination, this has a negative effect on the pozzolanic reactivity.

The presence of the admixtures of calcite, smectite and illite does influence the pozzolanic reactivity directly in a positive way. The influence of illite to the pozzolanic reactivity is only slightly higher than for the inert minerals. Smectite, however, shows a significant contribution both at 28 days as on the longer time since smectites reaction rate is slower than for kaolinite. Both the mixtures with illite and smectite form similar reaction products as for the inert materials, namely strätlingite, C-S-H, C_4AH_{13}, hemi- and monocarboaluminate. However calcined smectite and illite increase the Si/Al ratio of the amorphous phase and as a consequence the Al-rich phase strätlingite is formed at a later stage in the reaction than for the inert materials.

Also calcite shows a positive effect on the pozzolanic reaction and increases the reaction stage at early ages significantly. The presence of calcite acts as a source of calcium and carbon for the hydration products. As a result monocarboaluminate forms as the main reaction product instead of strätlingite. Hemicarboaluminate was proven to be unstable over time and after 56 days was completely transformed into monocarboaluminate.

Amount of impurity

The amount of the impurity is another important parameter that controls the reactivity. For inert materials like quartz, feldspar and muscovite the reactivity can be linearly correlated to the amount of kaolinite that is present in the sample, resulting in following equation:

*% Portl. Consumption = 0.44 * % kaolinite + 20.97*

Also for illite a linear relation could be found that is fairly similar to the previous equation. The amount of smectite and calcite could only be correlated to the reactivity by a polynomial function. This indicates that a low amount up to 30% of one of these impurities still provides highly pozzolanic materials. For smectite even higher ratios can yield fairly good portlandite consumption but only at a later stage in the reaction.

The pozzolanic reaction products are mainly influenced by the amount of impurity that decreased in accordance with higher amount of impurity. Especially strätlingite and C-S-H are affected while the amount of mono and hemicarboaluminate remain fairly similar. Furthermore, the strätlingite formation is delayed when the impurity amount increased.

CHAPTER 6

NATURAL KAOLINITIC CLAYS

Clay deposits are widely spread over the Earth's crust, however relatively pure and commercially useable deposits are less abundant. Furthermore, these high grade kaolinites are often used in numerous applications like paper, paint, whiteware and refractory industry (Murray, 2007). As a result the availability decreases while the prices increase. This makes these high grade kaolinites less interesting as supplementary cementitious material. However, most clay deposits in nature are mixtures of different clay minerals (kaolinite, illite and smectite) and a large proportion of impurities of non-clay materials, such as quartz, calcite, feldspars, mica, anatase and sulfides. The presence of these hard minerals such as quartz and feldspar increases the abrasiveness of the clay, which is unfavorable when the clay is used as pigment or functional filler (Kogel et al., 2006). Therefore the lower grade kaolinitic clays, that have fewer or no applications, are the economically more interesting clays to be used in blended cements. Previous studies mainly focused on the reactivity and the achieved mechanical strength of blended cements and the full influence of the mineralogy of the SCM is not yet entirely understood (Alujas et al., 2015; Cara et al., 2006; Tironi et al., 2014). Therefore it is important to study these influences from a mineralogical point of view, by determining the effect of variable kaolinite content, the presence of impurities and variable physical characteristics on the pozzolanic reactivity and reaction process of naturally occurring clays. In order to reach this goa,l the sample selection is crucial and it is important to select clays with a variation in both mineralogical and physical characteristics.

6.1 MATERIALS

Seven natural kaolinitic clays were selected based on the kaolinite content of the bulk sample. To guarantee a wide variety in origin, admixtures and physical characteristics, these clays were selected from quarries dispersed over western and southern Europe including France, Germany, Spain and Italy. The pure kaolinitic clay (K1) examined in Chapter 4, was used as a reference material. The colors of the original and calcined clay are given in Table 6.1. The firing colors of most clay samples are pink to orange which indicates that these clays are not suitable for certain applications that require a white firing color such as porcelain ware and white cement. The KA Hostun was received both as raw and calcined material. Since KA Hostun can be classified as waste product of a sand quarry, new applications were taken into consideration. The calcined sample used in this study was fired on lab scale in a fixed bed electrical oven and grinded to a particle size <100 µm.

***Table 6.1**: Overview of the origin and characteristics of the clay samples used in this study*

	Sample	Country	Location	Description	Firing Color
1.	R-KF	Spain	Riodeva	White clay	White
2.	Archichamotas	Spain	Archichamotas	Grey clay with gravel	Light Pink/ orange
3.	KA Hostun	France	Hostun	White clay	Light Pink
4.	R-ALK R	Spain	Alcoroches	White clay	Light Pink/orange
5.	WS35/38	Germany	Schenkenbusch	Grey clay	Crème
6.	Argilla Bianca	Italy	Fossanova	Orange/yellow clay	Dark Orange
7.	CS S	Germany	Christel	Brown/grey clay	Orange/pink

6.2 CHARACTERIZATION

6.2.1 CHEMISTRY

According to the bulk chemical analysis, listed in Table 6.2, all seven calcined clays can be classified as potential good pozzolans, since $SiO_2 + Al_2O_3 + Fe_2O_3 > 70\%$ as stated by the ASTM C618-89 norm. The kaolinitic clays have rather high alumina contents, with a variation between 26 and 40%. The Fe_2O_3 content of the samples Argilla Bianca and CS S is rather high with values of 3.54 and 9.24% respectively. During the calcination process dehydroxylation of the clays takes place and is irreversible. This results in a decrease of the LOI values after calcination. According to the French norm for metakaolin (NF P 18-513) the LOI value should not exceed 4%. Therefore the LOI was determined again after calcining, whereby all values are sufficiently low. For the raw clays, however, a positive correlation ($R^2 = 0.86$) between the alumina content and the LOI exists. This indicates LOI is mainly influenced by the amount of clay minerals present in the sample. The low CaO content also indicates the amount of carbonates, which could influence the LOI, is restricted. To be classified as potential metakaolin for cement replacement, the SO_3% of the calcined clays should be below 1%. This is the case for all samples with values even below 0.06% for most clays and 0.52% for CS S.

***Table 6.2:** Bulk chemical composition of the raw (R) clays. The LOI was additionally determined for the calcined (C) clay. The SO_3 content was not determined for the raw clays (/).*

		Chemical composition%									
Sample		**SiO_2**	**Al_2O_3**	**K_2O**	**Na_2O**	**TiO_2**	**Fe_2O_3**	**CaO**	**MgO**	**LOI**	**SO_3**
R-KF	**R**	51.27	34.62	0.48	0.03	0.21	0.52	0.11	0.18	12.48	/
	C									0.45	0.00
Archi.	**R**	51.04	34.07	1.56	0.04	0.96	0.79	0.05	0.16	11.09	/
	C									0.71	0.06
KA Hostun	**R**	64.40	23.35	0.45	0.03	0.26	0.91	0.22	0.13	8.71	/
	C									0.93	0.03
R-ALK R	**R**	63.44	24.23	4.00	0.14	0.19	0.71	0.10	0.21	6.96	/
	C									0.28	0.01
WS 35/38	**R**	57.57	35.76	1.82	0.14	1.79	1.75	0.51	0.66	13.18	/
	C									1.09	0.04
Fos Bianca	**R**	57.89	25.11	1.97	1.50	0.25	3.54	0.41	0.63	8.40	/
	C									0.86	0.01
CS S	**R**	52.20	33.31	2.61	0.21	1.19	9.24	0.59	0.66	13.37	/
	C									2.05	0.52

6.2.2 MINERALOGY

The bulk mineralogical composition indicates the clays have a broad variation in kaolinite content, varying between 87 and 42% (Figure 6.1). The most pure kaolinite, R-KF, only contains quartz and muscovite as impurities. The XRD patterns of the raw clays (Figure 6.2) show R-KF is marked by three high intensity reflection peaks of kaolinite indicating this is a kaolinite rich sample. The dominant impurities in the Archichamotas clay, containing 68% kaolinite, are quartz (8%) and 2:1 Al clays (19%). Furthermore, some weak reflections of muscovite, phyrophylite, anatase and Fe-oxides, namely hematite, are present. The KA Hostun clay has a kaolinite content of 57% and the highest quartz content of all samples of 37.5%. Minor traces of muscovite, 2:1 Al-clays and anatase are detected as impurities. The R-ALK-R clay with 55% kaolinite contains a high amount, 19%, of feldspar, quartz and traces of muscovite and 2:1 Al-clays. The feldspars consist predominantly of the kali-feldspars microcline and orthoclase. The last three clays, WS 35/38, Fos Bianca and CS S, have a similar kaolinite content of 46, 43 and 42% respectively. However, there is a difference in the total clay amount since the 2:1 Al-clay content differs. WS 35/38 contains 30% of 2:1 Al-clays, CS S contains 18% and Fos bianca only 8%. The presence of the 2:1 Al clays is reflected in the broad diffraction peak at 9 and 17.8°2θ representing the reflections of illite (Figure 6.2). The elevated background around 6°2θ, in WS 35/38 and CS S, confirms the presence of smectite. In addition quartz, muscovite, anatase, Fe-oxides and feldspar are present in all three samples. The feldspar in clay WS 35/38 and CS S is the kali-feldspar microcline, while Fos Bianca consist of both kali-feldspars (microcline) and plagioclase (anorthite and albite), with a reflection peak at 28 and 30.5°2θ. The weak reflection peak at 33.5°2θ corresponds to Fe-(hydr)oxide, mainly goethite. Furthermore, WS 35/38 and CS S show an elevated background in the range between 20 and 30°2θ which corresponds to organic material. This is consistent with grey to brownish color of the raw clays and the higher LOI values.

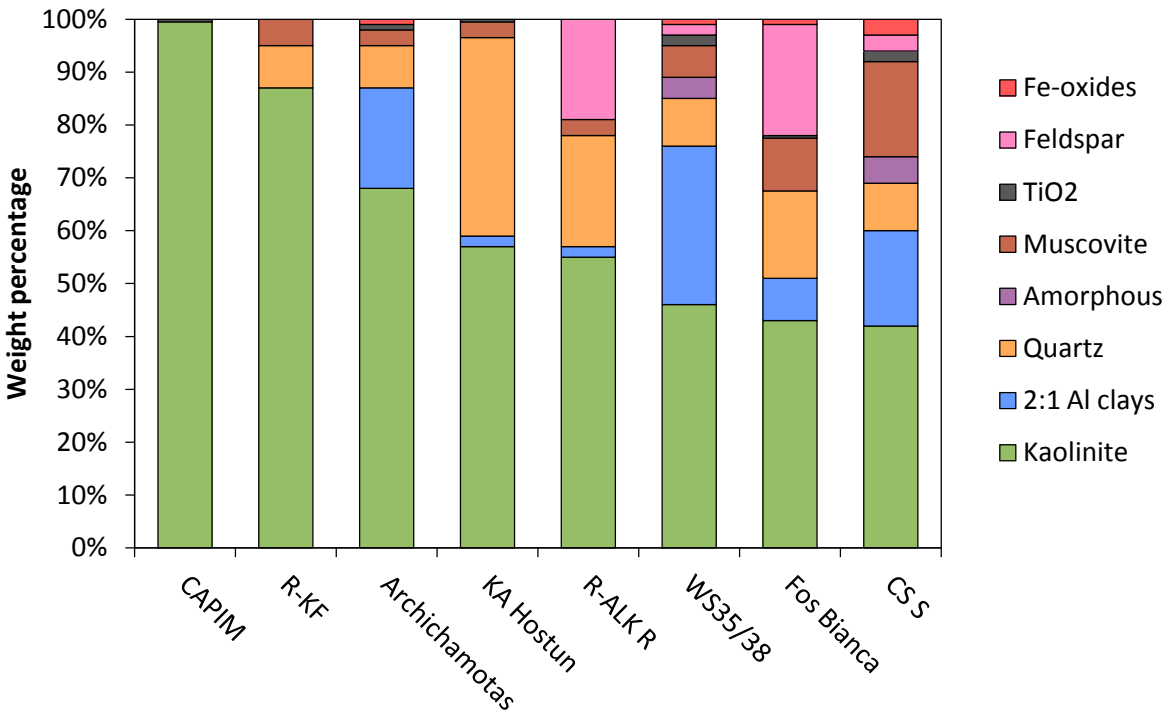

Figure 6.1: *Bulk mineralogical composition of seven kaolinitic clays and one pure reference sample (CAPIM).*

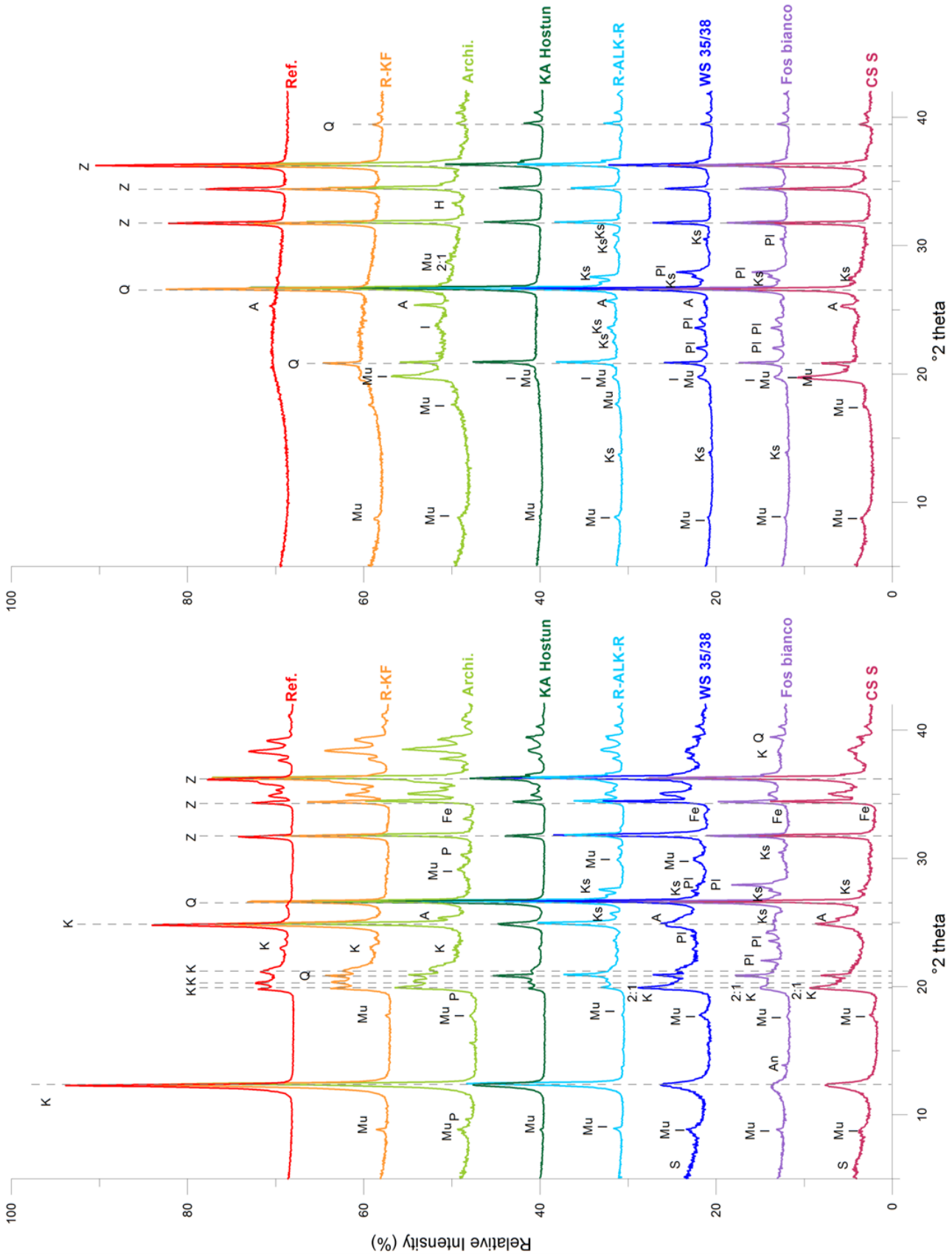

Figure 6.2: *X-ray diffraction patterns of the raw bulk samples and the clays after calcination at 800°C. The main minerals that are present are indicated K: kaolinite, Q: quartz, Mu: muscovite, I: illite, S: smectite, A: anatase, Ks: kali-feldspar, Pl: plagioclase, Fe: Fe-oxides, P: pyrophylite and z: zincite (internal standard).*

Oriented slides of the fraction <2 µm are recorded (Figure 6.3) to get a more detailed picture of the clay mineralogical composition. All clays show clearly the basal reflections of kaolinite with the 001 reflection at 12.4°2θ (7.14 Å) and the 002 reflection at 24.9°2θ (3.58 Å). No shift of the peak position is observed after ethylene glycol treatment. Furthermore, all clays show additional reflections at 8.8° 2θ (10 Å), 17.7°2θ (5 Å) and 26.7°2θ (3.33 Å) corresponding to the 001, the weak 002 and the 003 basal reflection of illite respectively. However the amounts of the clay minerals that are present vary considerable over the samples. A summary of the quantification results is given in Figure 6.4. The pattern of R-KF and KA Hostun shows much resemblance and also quantitatively both clay fractions contain 99% kaolinite and 1% illite. Also Archichamotas contains only kaolinite and illite. However the kaolinite content in the clay fraction is far less with only 27.5% kaolinite present and 72.5% illite. The amount of kaolinite in the fraction <2 µm is fairly low compared to the other samples, certainly when the high kaolinite bulk content of Archichamotas is taken into account. This indicates most kaolinite particles are considerable larger than 2 µm. The R-ALK-R clay contains some illite-smectite mixed layers with a ratio of 80:20 additionally to kaolinite and illite. The presence of I/S results in a small shift in between 7 and 8 °2θ when the glycolated and air dried pattern are compared. The Fos Bianca sample is marked by a rather low kaolinite content of 35.3%. This can be explained by the fact that part of the kaolinite is not entirely pure but partially exists as a mixed layer of kaolinite smectite with a ratio of 78:22. The presence of the K/S is indicated by the small shift of the shoulder to the right of the 001 reflection of kaolinite at 12.4°2θ. WS 35/38 and CS S are the only two samples that contain smectite besides the clay minerals kaolinite, illite and I/S with ratio 70:30 in their clay fraction. The most distinctive smectite reflection is that of the 001 basal plane at 6°2θ (14.5 Å). Since smectite is an expandable clay mineral, a shift of the 001 basal plane to 5.4°2θ (16.36 Å) is observed in the glycolated pattern.

Based on the mineralogical composition and findings of Chapter 4, an optimal calcination temperature was chosen for each sample. Samples that contained pure smectite (WS 35/38 and CS S) are calcined at 800°C in order to activate the smectite, while all others were calcined at 750°C.

After calcination of the samples at 750 or 800°C, the clays are dehydrated and dehydroxylated. As a result the reflections corresponding to kaolinite have disappeared indicating kaolinite is completely transformed to its amorphous higher temperature phase metakaolin. Especially clays with originally a higher kaolinite content indicate the presence of amorphous material by the presence of a dome structure between 15 and 35°2θ (Figure 6.2). Accessory minerals, quartz, feldspar, anatase and muscovite are unaltered by the calcination, moreover, the intensity of their reflections is enhanced indicating their contribution to the total amount of crystalline material increases. Also the structure of illite remains intact. The calcination temperature of 800°C is still insufficient to decompose illite, since the amorphization of illite only takes place from 1000°C (see Chapter 4). The additional activity provided by the amorphization of illite is however negligible compared to kaolinite and smectite. Therefore the samples are not calcined at higher temperatures. At 800°C, the basal planes of smectite can collapse and the 001 plane shifts to the position of illite (12.3 Å) or smectite can become completely amorphous. For CS S only a slight enhancement of the background at 6°2θ can be observed which is lower compared to the raw sample. The 001 reflection of illite at 8.8°2θ (10 Å) is not enhanced indicating most of the smectite has become amorphous. The reflections of phyrophylite at 9.6 and 19.3 °2θ, which were presented in the raw Archichamotas clay, are not observed in de calcined clay indicating the decomposition of pyrophylite to a less crystalline or amorphous phase.

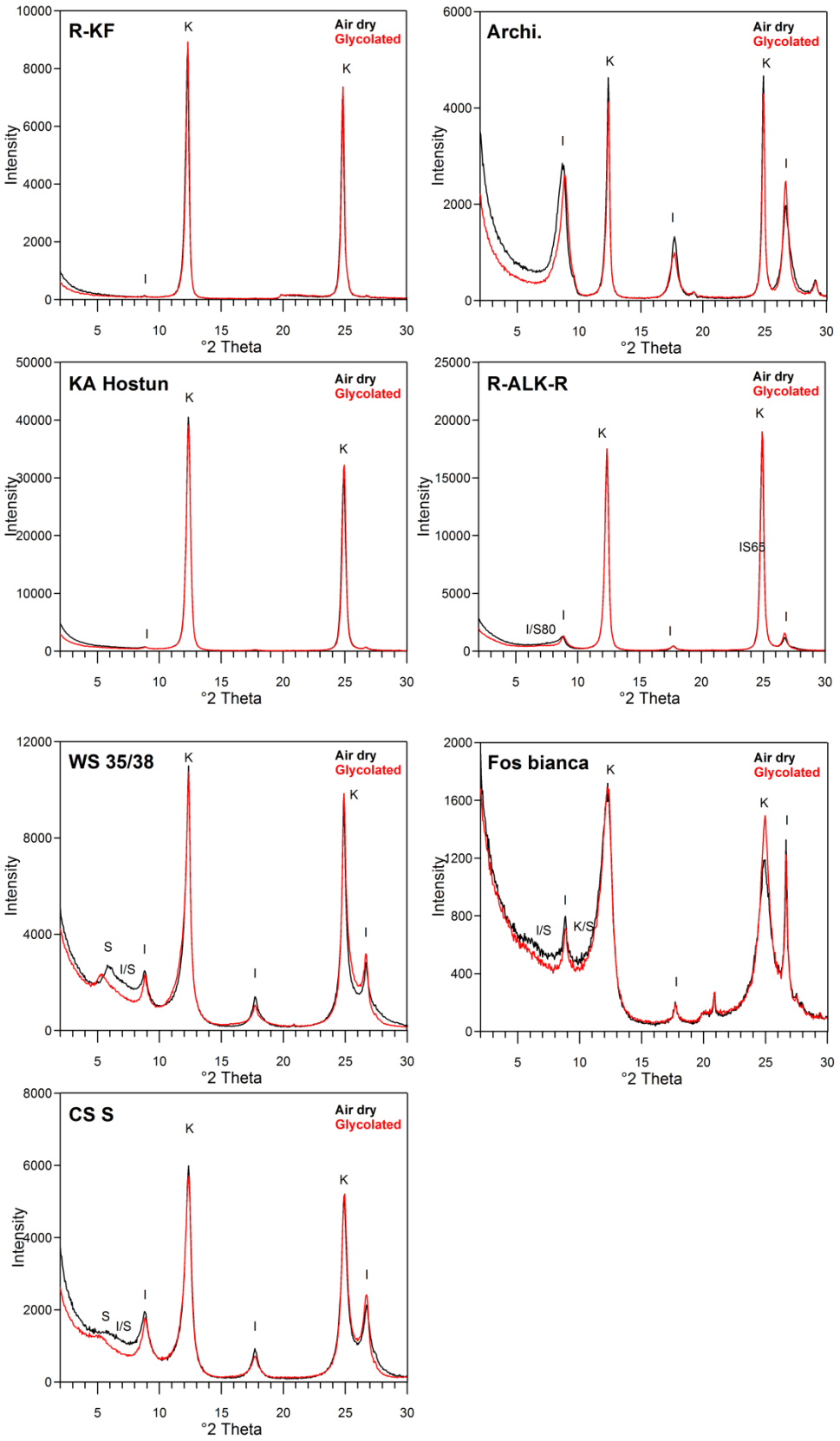

Figure 6.3: *XRD patterns of the fraction <2 µm in air dry and glycolated state. The identified phases are indicated: K: kaolinite, S: Smectite, I: illite, I/S: illite-smectite mixed layer, K/S: kaolinite-smectite mixed layer.*

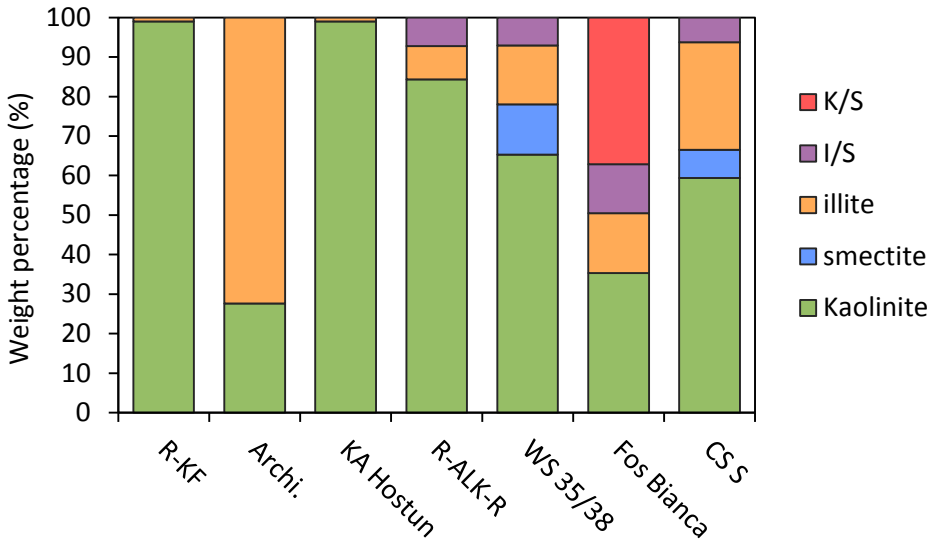

Figure 6.4: *comparison of the mineralogical composition of the clay sized fraction < 2 µm. Sample R-ALK-R contains 80:20 I/S while the other samples contain 70:30 I/S. 78:22 K/S is only present in the Fos bianca sample..*

6.2.3 CORRELATION BETWEEN CHEMISTRY AND MINERALOGY

The Al_2O_3 content is important in the cement industry because free alumina can react with Ca in the cement to form typical aluminates and silicate aluminates hydration phases. Since most alumina is present in the clay minerals the correlation between kaolinite and Al_2O_3 was checked (Figure 6.5). This resulted however in a very poor correlation with R^2 below 0.1. The reason is that some clays contain, besides kaolinite, 2:1 Al-clays like smectite and illite which contribute to the total amount of Al_2O_3 in the bulk sample. Furthermore, the quantity of the 2:1 Al-clays cannot be related to the amount of kaolinite since it is random because of the different localities of the samples. Additionally is should be mentioned that there are actually two distinct groups in the sample set, one with Al_2O_3 concentration above 30% and the other group <30%. This makes that no proper correlation can be made because lack of data in between the two groups. The relation between the sum of clay minerals and the Al_2O_3 content is already more promising nevertheless due to the presence of other Al-rich minerals like muscovite the data points are still spread out. When also muscovite is included the data point plot more closely to each other. However the two existing groups become even more distinct. The Fe_2O_3 content can more easily be related to the mineralogical composition. The Fe_2O_3 – rich samples CS S and Fos Bianca contain the Fe-oxide goethite which turns to hematite after calcination resulting in a red firing color. The high K_2O amount in sample R-ALK-R can be linked to the high amount (19%) of feldspars that is present. However Fos Bianca contains a similar amount of feldspars and its K_2O percentage is significantly lower. This phenomenon is related to the type of feldspar that is present. As already indicated by the XRD results, the feldspars in R-ALK-R consist of the potassium rich microcline and orthoclase ($KAlSi_3O_8$). For sample Fos Bianca the feldspars are a combination of microcline, albite ($NaAlSi_3O_8$) and some minor amount of anorthite ($CaAlSi_3O_8$). This is reflected in the higher amount of sodium compared to R-ALK-R. However also samples with a small percentage of feldspars like CS S, show an elevated K_2O percentages. This can be correlated to the high amount of muscovite that is present. The higher TiO_2 values of samples WS 35/38 and CS S can be explained purely by the elevated levels of anatase present in the bulk sample.

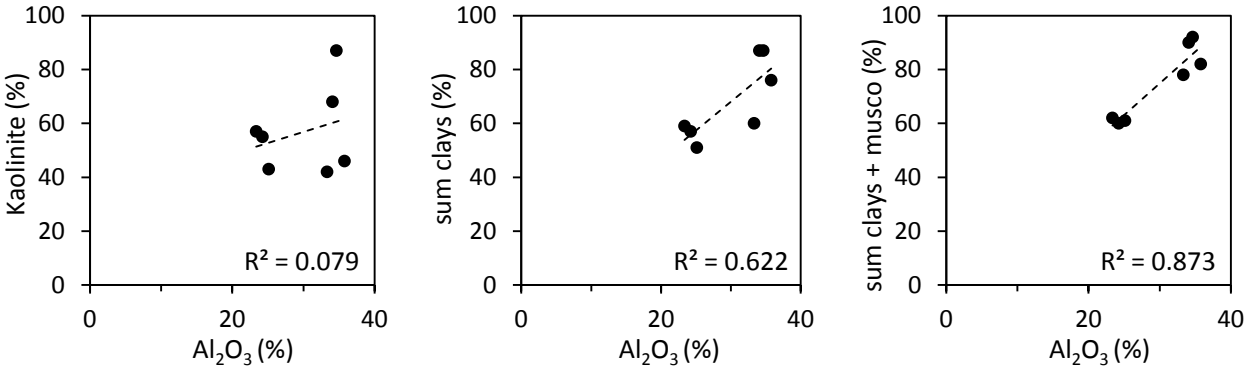

Figure 6.5: *Correlation plots of Al_2O_3 versus kaolinite, sum of clays and sum of clay and muscovite.*

6.2.4 DEGREE OF ORDERING

The degree of ordering of kaolinite can be estimated qualitatively according to the number of peak reflections of kaolinite and their intensity on the XRD pattern. The patterns of the raw clays (Figure 6.2) shows three well-defined sharp reflection peaks of kaolinite in the range of 19 -22° 2θ for R-KF, indicating this is a high ordered kaolinite. However when the kaolinite content is lower and/or other minerals mask the kaolinite reflection, it is hard to estimate the degree of ordering correctly. Therefore the degree of ordering can be determined in a more quantitative way by means of the Hinckley index (HI) and Lietard index (R2). The high ordering of R-KF kaolinite is confirmed by a HI of 0.79 (Table 3.6). For the KA-Hostun sample the kaolinite reflection peaks in the range of 19-22°2θ are rather distinctive, however, the high amount of quartz and its corresponding reflection at 20.7°2θ mask the 111 kaolinite reflection peak which results in a less accurate determination of the Hinckley index. Furthermore, it is hard to determine the HI for kaolinitic clays that have a low degree of ordering like sample WS35/368. The 110 and 111 reflection peaks of kaolinite are not developed adequately whereby almost no separate reflection peaks can be determined. This phenomenon is less distinctive for the R2 index and it was therefore possible to determine it. The classification according to the HI versus the R2 is slightly different. For both methods the kaolinite rich sample R-KF is described as a high ordered sample. KA Hostun however is indicated as high ordered with the HI and medium/low with R2. The R2 index state that R-ALK-R is high ordered, while the HI classifies it as medium ordered. The samples WS 35/38, Fos Bianca and CS S are marked by both methods with low values regarding ordering.

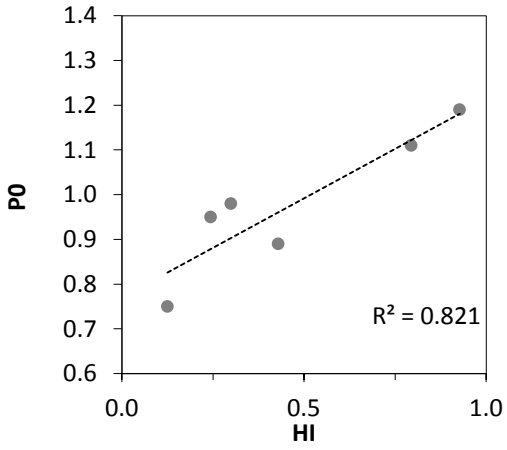

Figure 6.6: *Correlation plot of the Hinckley index (HI) and the P_0 factor determined by FTIR. Sample R-ALK-R was not included.*

The degree of ordering was also analyzed by FTIR by applying the P_0 factor that allows to perform quantitative determination (Bich et al., 2009). The results listed in Table 6.3 show a rather broad range varying between 0.75 and 1.19. The data from the FTIR confirm the results obtained from the HI, samples R-KF and KA Hostun contain high ordered kaolinite while the others are medium ordered. Since the P_0 factor is not influenced by the presence of quartz, the estimation of the degree of ordering for KA Hostun, based on the HI, was still adequate despite the high quartz content of the sample. Furthermore, a fairly good correlation between the HI and the P_0 factor was found, with a R^2 of 0.82 (sample R-ALK-R was not taken into account as it was not measured with FTIR due to technical reasons).

***Table 6.3**: Overview of the degree of ordering of kaolinite. The values qualified as high ordered according to that technique are marked in bold.*

Clay	Ordering HI	Ordering R2	Ordering P_0	Ordering	SS_{BET} (m^2/g) raw	SS_{BET} (m^2/g) Fired at 800°C
Capim	**0.85**		**1.58**	High	8.86	9.54
R-KF	**0.79**	**0.73**	**1.11**	High	13.80	12.47
Archichamotas	0.43	0.67	0.89	Medium	10.09	7.52
KA Hostun	**0.93**	0.61	**1.19**	High	11.09	9.40
R-ALK-R	0.58	**0.76**	n.d.	Medium	6.67	5.86
WS 35/38	0.13	0.37	0.75	Medium	44.94	39.95
Fos bianca	0.24	0.29	0.95	Medium	41.03	31.00
CS S	0.30	0.42	0.98	Medium	50.12	45.44

6.2.5 THERMAL ANALYSIS

Thermal analysis was performed to validate the thermal behavior of the clay mineral and verify the temperature that is needed to guarantee full dehydroxylation of the clay minerals present in the sample. Information about the kind of clay mineral can also be retrieved based on the fact that the decomposition phenomena are characteristic for a certain clay type (Emmerich, 2011). The DTG pattern are given in figure 6.7. The dehydration of the clay minerals takes place in the region between 30 to 240 °C. The DTG pattern of the kaolinite rich sample R-KF is marked by a limited mass loss in this region which is typical for kaolinite. This weight loss can be related to the loss of the absorbed water. WS 35/38, Fos Bianca and CS S have a more pronounced weight loss in this region caused by the present of smectite. The swelling behavior of these clays results in a higher water uptake in the interlayer space. The exchangeable cation influences the dehydration process. Bivalent cations, like Ca^{2+} exhibit a double peak while monovalent cations, like Na^+ or K^+, have only a single thermal peak (Earnest, 1988; Todor, 1976). For all three samples a double peak can be observed indicating the exchangeable cation is divalent. If the amount of 2:1 Al-clays is negligible the dehydration of the clay can be directly related to the specific surface area since kaolinite has no interlayer water. A higher amount of dehydration corresponds to a higher specific surface area. This theory is confirmed by sample R-ALK-R which has the lowest dehydration and correspondingly the lowest BET specific surface area compared to RR-KF and Archichamotas (Table 6.3). For the samples CS S and Fos Bianca an additional peak around 300°C can be observed, which can be related to the release of CO_2 associated with the decomposition of organic materials.

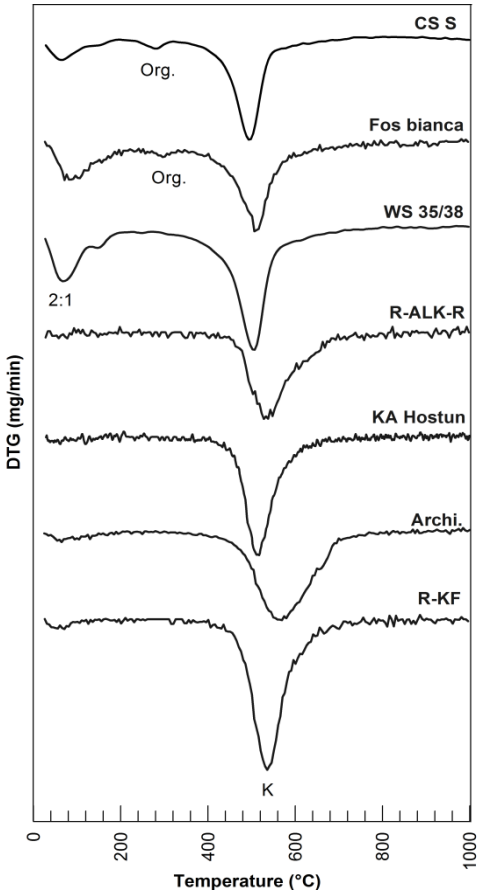

Figure 6.7: *DTG pattern of the raw kaolinite clays with indication of the main phases: K: kaolinite, 2:1: 2:1 Al-clays and Org.: Organics.*

The other important thermal characteristic of clays is the dehydroxylation whereby the structural water is removed to form metastable clay. This phenomenon takes place in temperature range between 400 to 800 °C. Kaolinite has a typical dehydroxylation peak at 480 to 630 °C, while montmorillonite can have a much broader range of dehydroxylation temperatures depending on its structure and octahedral occupancy (Emmerich, 2011). The clay R-KF is marked by a sharp peak at 530 °C that reflects its high kaolinite content. The shoulder around 720 – 800 °C can be assigned to the presence of muscovite. A similar trend can be observed for sample R-KF, nevertheless, the kaolinite dehydroxylation peak is less intense. The Archichamotas DTG curve shows a wide peak at 560 °C with a broad shoulder towards higher temperatures. Herby the dehydroxylation of kaolinite is significantly influenced by the presence of 2:1 Al clays, shifting the peak position to higher temperatures. KA Hostun is marked by a peak dehydroxylation temperature of 618°C. The shoulder to the right can be attributed to the presence of a limited amount of 2:1 Al-clays and muscovite. The WS 35/38 and CS clays have both a well developed intense peak at 505 and 497 °C respectively. Even though both clays contain considerable amounts of 2:1 Al-clays it is not clearly reflected in the dehydroxylation peak. This indicates the 2:1 Al-clays present in those clays have a rather low dehydroxylation temperature similar to that of kaolinite, resulting in an intensifying of the dehydroxylation peak. Sample CS S exhibits an additional mass loss between 250 and 350 °C that can be associated to either organic material or to the dehydration of hydroxides. The goethite present in the raw sample suggests most mass loss in this region can be linked to the decomposition of goethite to hematite. According to these results hematite was present in the calcined sample and resulted in a deep red firing color of the clay. Similar phenomena, dough in more limited extent, can be observed for samples Fos Bianca and WS 35/38. Fos Bianca clay has mainly a weak dehydroxylation peak at 511 °C with a shoulder towards lower temperatures caused by the 2:1 Al clays.

To compare dehydroxylation behavior of the different samples, the degree of dehydroxylation was plotted in Figure 6.8. The dehydroxylation of the more kaolinite rich clays, R-KF, Archichamotas, KA Hostun and R-ALK R, start at higher temperatures. The 2:1 Al-clays present in the other clays have clearly a rather low dehydroxylation temperature which results in the fact that higher degrees of dehydroxylation are already reached at lower temperatures. The optimal activation temperature of 2:1 Al-clays is general at a temperature when at least 95% of the dehydroxylation is completed. At 750°C the degree of dehydroxylation exceeds 95% for all clays and was therefore chosen as good calcination temperature and is also sufficient for the samples containing 2:1 Al-clays.

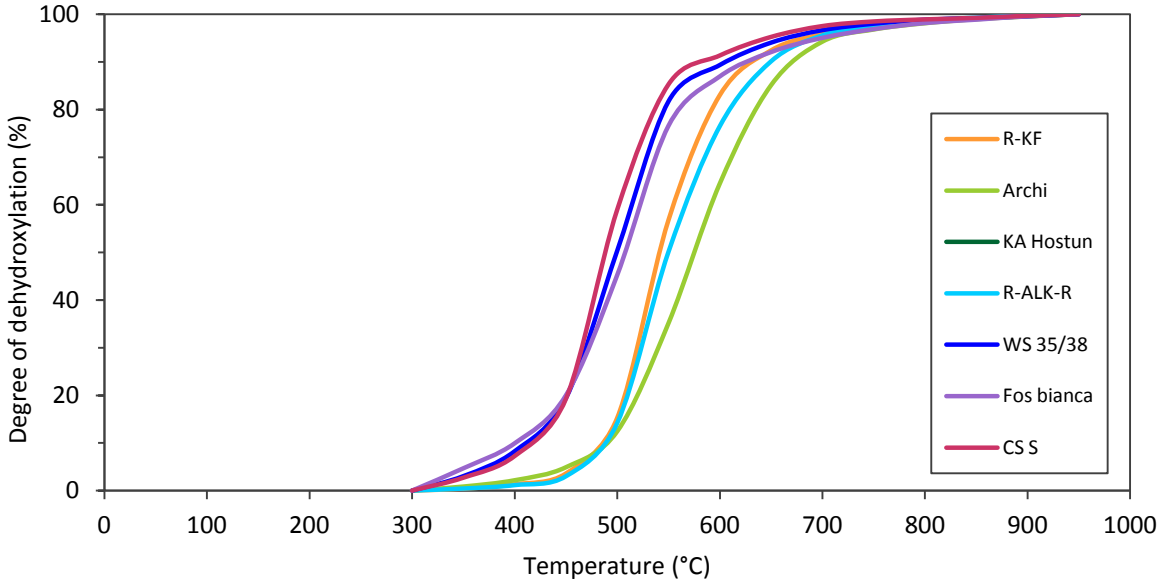

Figure 6.8: *Degree of dehydroxylation determined by thermal analysis*

6.2.6 BET SPECIFIC SURFACE AREA

The BET specific surface area was measured for the raw and the calcined clays (Figure 6.9). The values for the raw sample can be divided into two groups. The first group with a BET specific surface area between 6.5 and 20.5 m^2/g is marked by a kaolinite content above 50% and include the sample R-KF, Archichamotas, KA Hostun and R-ALK-R. The specific surface areas of the second group are much higher ranging between 41 and 51 m^2/g. The samples of this group including WS 35/38, Fos Bianca and CS S have a kaolinite content below 50% and contain a considerable amount of 2:1 Al-clays. After calcination of the samples the specific area decreases for all samples. However samples that contain 2:1 Al-clays (Archichamotas, WS 35/38, Fos Bianca and CS S) are characterized by a more drastic decrease than samples that contain mainly kaolinite as clay mineral (R-KF, KA Hostun, R-ALK-R). This phenomenon can be assigned to the increased sintering effect caused by the presence of the 2:1 Al-clays. The influence of other mineral impurities like feldspar and muscovite is negligible for this sample set. The difference in the specific surface area is for reference sample more pronounced than for the samples that contain kaolinite as main clay mineral (R-KF, KA Hostun and R-ALK-R). Most likely the accompanying non-clay minerals, like quartz, that are present in group 1 cause a filler effect whereby kaolinite grains are less easily sintered together. The presence of other minerals like kaolinite also makes it impossible to correlate the specific surface area of the sample to the degree of ordering of kaolinite. However it is clear that the samples with high kaolinite content of group 1 have in general a low specific surface area and a higher degree of ordering according to HI and P_0.

Nevertheless, this effect is associated with the fact that medium to low ordered kaolinite often contains more impurities of other clay minerals than high ordered clay minerals.

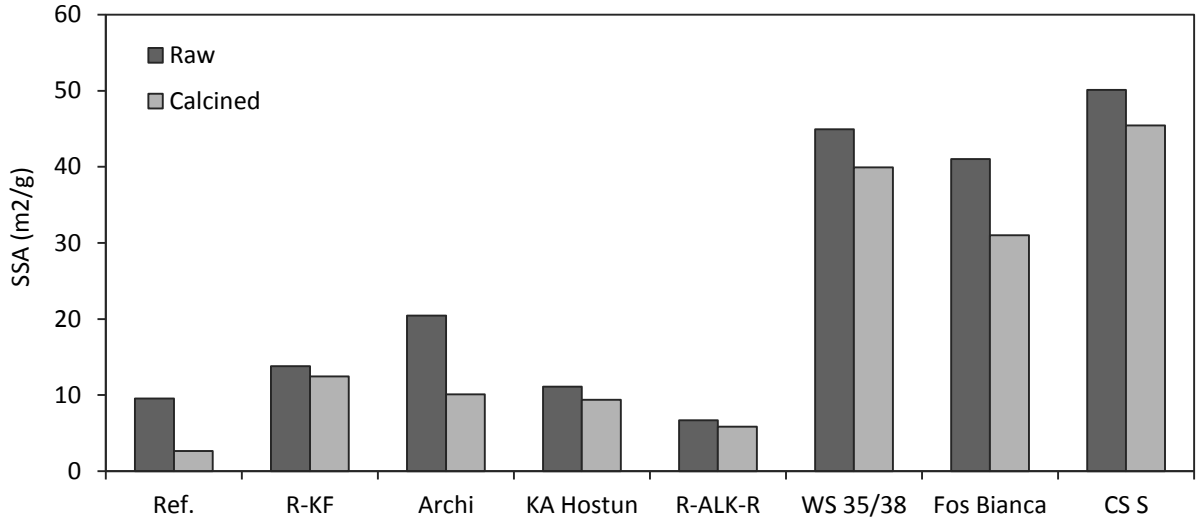

Figure 6.9: *Difference in BET specific surface area of the raw and calcined kaolinitic clays.*

6.2.7 GRAIN-SIZE DISTRIBUTION

The grain-size distribution was determined by laser diffraction for both the raw and calcined samples to study the effect of the calcination process. The results for the raw samples, Figure 6.10, show that almost all samples have a multimodal distribution but vary in fineness and therefore three main groups can be made. The first group consists of sample R-KF and MK Hostun; both samples contain a fine grained distribution with d50 of 5.68 and 5.88 µm respectively (Table 6.4). The distribution is mainly multimodal and is somewhat coarser compared to a pure kaolinite sample. KA Hostun contains however considerably higher amount of quartz to be equally fine grained as R-KF. This indicates that the quartz that is present in the raw sample is very fine grained. The degree of ordering for both samples is high, resulting in somewhat coarser kaolinite that can resemble the very fine grained quartz even more.

Table 6.4: *Overview of the d10, d50 and d90 values of the grain-size distribution of the raw and the calcined clays. Samples were pre sieved to pass through a 1 mm sieve.*

Clay		**Raw**	**(µm)**		**Calcined**	**(µm)**
	d10	**d50**	**d90**	**d10**	**d50**	**d90**
R-KF	0.49	5.68	25.85	2.09	37.71	367.58
Archichamotas	0.49	7.50	200.81	0.85	36.85	275.48
KA Hostun	0.55	5.88	34.98	1.46	6.77	33.99
R-ALK-R	2.58	14.49	73.14	3.06	20.37	139.45
WS 35/38	0.31	2.45	10.68	3.89	88.54	316.09
Fos bianca	0.88	9.76	139.75	1.99	96.68	351.21
CS S	0.31	2.70	20.27	2.07	65.43	294.92

The second group contains the finest clays, WS 35/38 and CS S, with a d50 value of 2.47 and 2.55 µm respectively and with its main population peak positioned around 5 µm these clays are much more fine grained than those of group one. This can be explained by the mineralogical composition since both clays contain 18 (CS S) to 30 %(WS 35/38) of 2:1 Al-clays. The 2:1 Al-clays, especially smectite are known for their fine grain size <2 µm. Furthermore, the kaolinites are only medium ordered and are therefore also finer than the high ordered kaolinites from group one.

The third group is the coarsest and contains the samples Archichamotas, R-ALK-R and Fos bianca. Archichamotas has the lowest d50 value of 7.5 but is marked by a sudden grain size increase resulting in a high d90 of 200 µm. This sudden increase can be explained by the coarse quartz grains that are present with sometimes even the size of fine gravel. Moreover, part of the coarse fraction had to be sieved off before grain size analysis was possible. Approximately 9% of the Archichamotas sample was >1mm. This means that the sample is actually even coarser than the grain-size distribution reflects. R-KF shows a more constant grain size increase with a d50 of 14.49 µm and a d90 of 73.14 µm. This is the only sample that has a more or less bimodal distribution. The presence of quartz or feldspar results in a somewhat coarser grain size. Sample Fos Bianca has a broad distribution and a d50 of 9.76 µm and d90 of 139.75 µ.

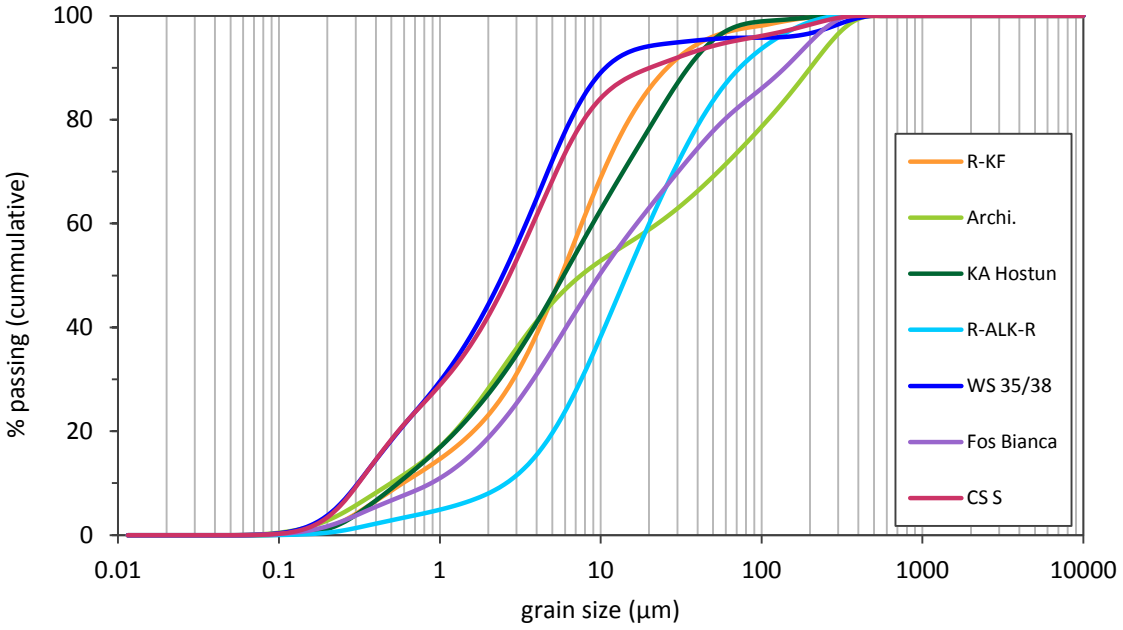

Figure 6.10: *Cumulative grain-size distribution of the raw clays. Samples were pre sieved at 1 mm.*

After calcining the samples the grain-size distribution changes drastically (Figure 6.11) which is also clear from the variation in the d50 values listed in table 6.4. The fine grained samples of group 2 have become much coarser. A reasonable explanation is the increased sintering effect as a result of the high 2:1 Al-clay content. The sample KA Hostun of group one are the finest samples after calcination with a d50 of 6.77 µm. This can be explained by the fact this was received grounded after calcination and no sample of the ungrounded calcined clay was available. The other sample of group one, R-KF, becomes however much coarser with a d50 of 37.71 µm. A possible explanation for this difference can be the higher amount of muscovite, which provokes additional sintering, in sample R-KF combined with the filler effect of the fine grained quartz present in KA Hostun, which obstruct the sintering of kaolinite grains. This coarsening was even more distinctive for the Archichamotas sample as 24% of the sample was >1 µm. This phenomenon is caused by the sintering of the clay particles and the formation of a crust over the coarser non-clay particles which enlarges their diameter. The

sample R-ALK-R becomes coarser and induces double as much sintering upon calcination when compared to the changes of KA Hostun with similar kaolinite content around 56%. This is due to the effect of the mineral impurities. The major difference is the presence of feldspar in R-ALK-R, which enhances sintering. The other clay with feldspar is Fos bianca, which is marked by an intense coarsening of the sample with a d50 of 96.68 µm. Besides feldspar this sample also contains muscovite and 2:1 Al-clays that contribute to the sintering of the sample

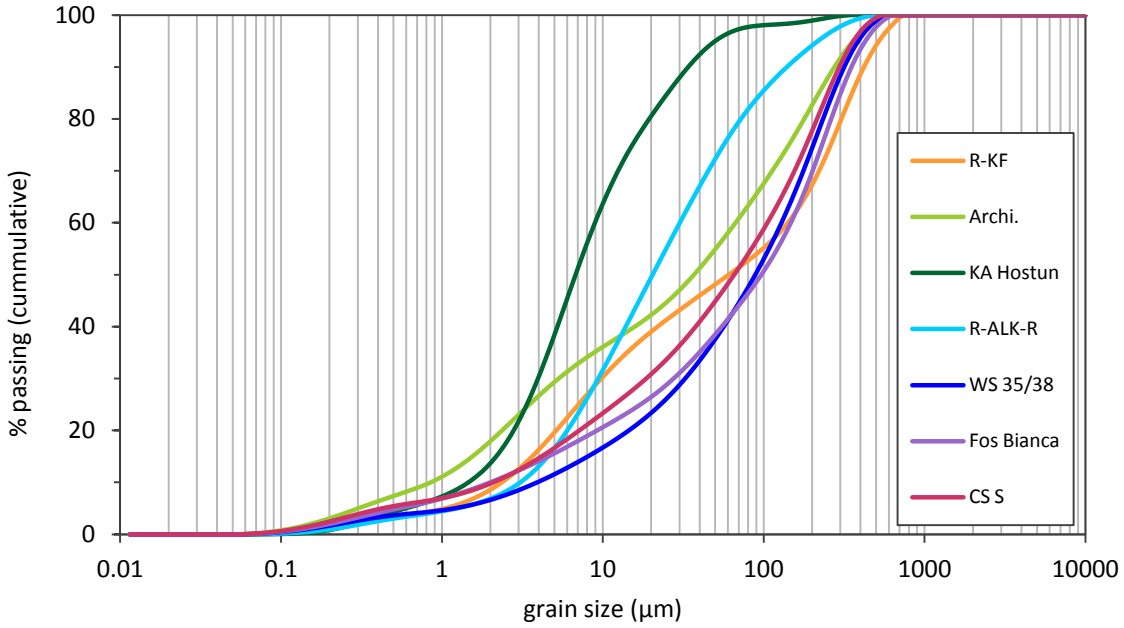

Figure 6.11: *Cumulative grain-size distribution of the calcined clays. Samples were pre sieved at 1 mm.*

6.3 POZZOLANIC REACTIVITY

6.3.1 CHAPELLE TEST

The pozzolanic reactivity was estimated by means of the Chapelle test, thermal analysis (TGA) and strength tests. The Chapelle test allows ranking the sample according to their pozzolanic reactivity. However, in Chapter 3, it was demonstrated that the Chapelle test is not always reliable for natural clay deposits. The pozzolanicity of clays that contain 2:1 Al-clays is overestimated if compared to results of TGA at day 28. Furthermore, it is possible that also the presence of feldspars enhances the amount of portlandite that is fixed by the clay. The more detailed results can be found in Chapter 3.

6.3.2 CALCINED CLAY LIME PASTES

To have a more quantitative approach TGA was performed on calcined clay lime paste samples after different curing times (Figure 6.12). For all clays the reaction evolves the fastest in the first 14 days. After 28 days most of the kaolinite is already consumed and the reaction slows down. The reaction curve of the Archichamotas clay distinguishes itself from the other clays since the reaction speed between 3 and 28 days is rather similar and moreover, the clay continues to consume a considerable amount of portlandite between 28 and 56 days. The reaction rate for the Archichamotas clay is however rather low compared to other clays like R-KF and KA Hostun. The R-KF clay is marked by the highest portlandite consumption and after 28 days 57.5% of portlandite is already consumed which

results in a clear gap in reactivity with the other clays. The R-ALK-R, CS S and Fos Bianca calcined clays behave rather similar, especially at longer curing times. At 90 days the portlandite consumption of all three clays is comparable with values of 43.56, 43.16 and 42.19 % respectively. The R-ALK-R clay reaches its plateau value at 56 days while the other two clays still consume portlandite, though rather limited, between 56 and 90 days. The WS 35/38 clay is also marked by an increase of reactivity between 56 and 90 days indicating not all calcined has reacted. This clay has slightly higher portlandite consumption at 90 days of 47.7%, indicating this clay has a higher pozzolanic potential.

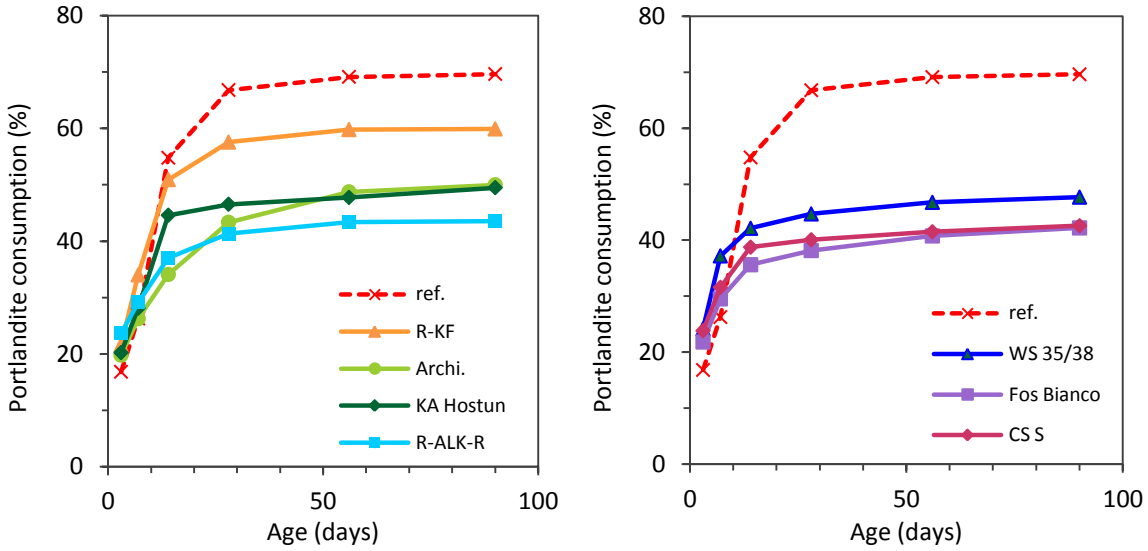

Figure 6.12: *Portlandite consumption of seven calcined clays at different curing times of 3, 7, 14, 28, 56 and 90 days. Left: calcined clays with a kaolinite content > 55%. Right: clays with a kaolinite content < 46%. The dotted line in both figures represents a reference pure kaolinitic clay (K1 of chapter 3).*

Nevertheless, the pozzolanic potential of a calcined clay is best evaluated on day 28. A comparison of the portlandite consumption of the calcined clays at 28 days is given in Figure 6.13. The R-KF is a high reactive clay with at 28 days a portlandite consumption of 57.5 % indicating this has the highest pozzolanic potential. The other six clays have a portlandite consumption that is more comparable. The two clays KA Hostun and WS 35/38 are still good reactive with values of 46.5 and 44.7 % respectively. Archichamotas, R-ALK-R and CS S are marked with portlandite consumption between 43.5 and 40.0 % and can be seen as medium reactive clays. The only clay that consumes less than 40% of portlandite after 28 days is Fos Bianca, which only has a low pozzolanic potential.

The pozzolanic potential of the seven calcined clays can be summarized as follows:

R-KF >> KA Hostun > WS 35/38 > Archi. > R-ALK-R > CS S > Fos bianca

Whereby R-KF has a high pozzolanic potential, Fos Bianca a poor potential and the other samples a medium potential.

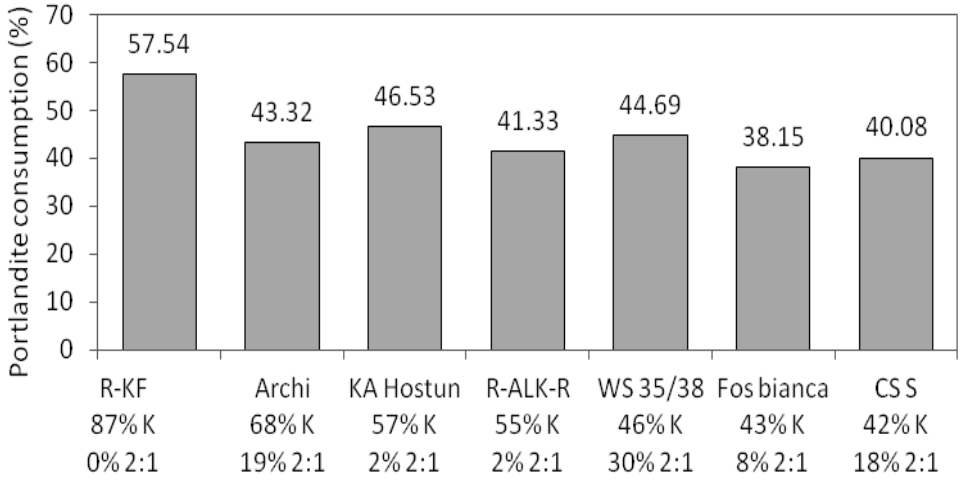

Figure 6.13: *Portlandite consumption at 28 days for 7 calcined clays. The kaolinite (K) and 2:1 Al-clay (2:1) content of the raw bulk sample is given for each sample.*

6.3.3 EFFECT OF GRAIN SIZE

The effect of the grain size on the pozzolanic reaction was estimated by preparing additional lime mixtures of the un-ground calcined clays. This procedure was done for five of the seven clays, as the raw Archichamotas clay was to coarse and KA Hostun was only available ground. The clay contains some particles >1 mm which are not easily homogenously spread over the small sample tubes. This would give unreliable results and proper interpretation would be impossible. To eliminate the effect of the mineralogy and the calcination process the clay sample was split after calcination whereby one part was milled, which reduced the particle size below 50 µm, and the other part was used un-ground. Also the effect of the specific surface area is minimal as the error margin on the BET specific surface area measurements is greater than the difference in specific surface area of the same clay ground and un-ground.The difference in portlandite consumption between the ground and un-ground calcined clay samples at curing times of 7, 14 and 28 days is visualized in Figure 6.14.

The results show that the un-ground samples tend to consume less portlandite than the samples that were ground with a McCrone. Especially at the early stage of the reaction the difference in portlandite consumption is more pronounced with values up to 40 % (CS S). After 28 days the ground and un-ground samples of the R-KF clay has a similar reactivity, with only a variation around 2.5 %, indicating the grain size has less influence on the pozzolanic reaction from 28 days onwards. For the other clays there still exists dissimilarity in reactivity at 28 days; however the gap becomes smaller with percentages of difference of 9.7 % (R-ALK-R), 15.5% (Fos bianca), 15.7% (WS35/38) and 23.5% (CS S). So also for these samples the influence of the grain size of the sample decreases over time. Nevertheless, at 28 days the grain size cannot yet be neglected as the difference in reactivity are still significant.

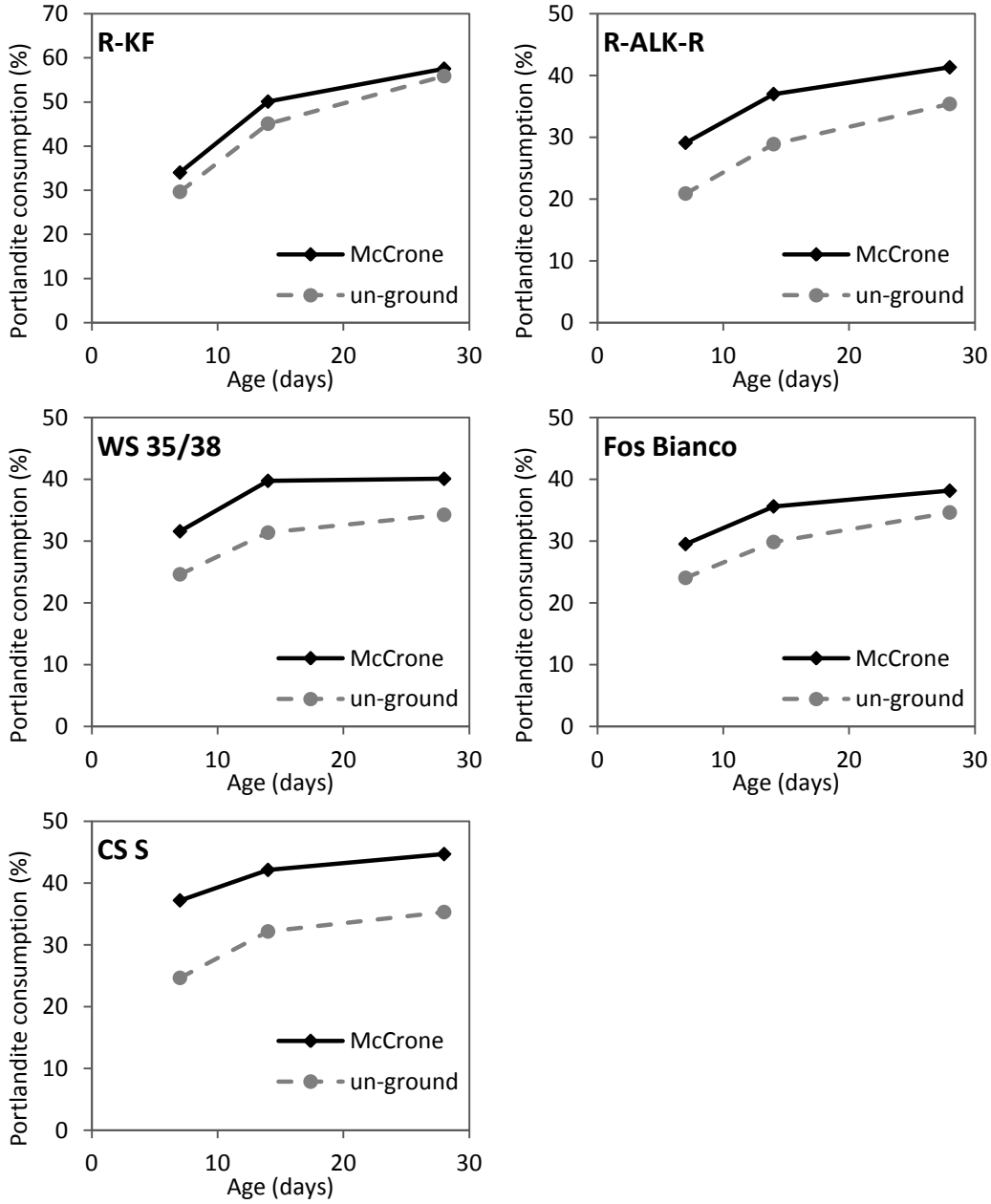

Figure 6.14: *Comparison of the portlandite consumption over time (7, 14 and 28 days) for the calcined clays ground with a McCrone and un-ground calcined clay samples to estimate the influence of the grain size.*

6.3.4 STRENGTH ACTIVITY INDEX

A third method was used to determine the pozzolanic activity of the calcined clays, namely the strength activity index test. In this test the compressive strength of a calcined clay cement mortar beam is determined and compared to the reference of cement mortar. The mortars were prepared in accordance with the standard NF P 18-513 by blending 85% cement (CEM I 52.5N) with 15% of calcined clay, while the reference sample consists of 100% cement. The calcined clays were directly used after calcination without any grinding process. Standard sand (0-2mm) was added in a cement/sand ratio of 1/3. A water/cement (cement + calcined clay) ratio of 0.5 was used for all samples. Even though the blended cement pastes were less plastic than the reference mortar, similar W/C ratio was applied in order to compare the final strength results. The consistency was tested by the plunger penetration test (NF P 18-513, 2013). Hereby the penetration depth of the plunger of the

samples should reach at least a penetration depth of 13 mm. If necessary the superplasticizer glenium ACE 456 was added to improve the consistency of the mortar and reach this goal. Maximum 0.2% superplasticizer was added in relation to the cement mass. Since the amount of superplasticizer and the mortar consistency is not maintained simultaneous for all samples, the reaction kinetics of the cement mixtures can slightly be affected. The details of the mortars set up, the consistency and the amount of superplasticizer that was added can be found in Table 6.5.

Table 6.5: *Overview of water cement ratio (W/C), the amount of the super plasticizer Glenium ACE 456 that was added and the consistency of the 15:85 calcined clay cement mortars compared to a reference sample. The strength activity index was determined after 48 hours and at 28 days of curing*

Sample	Cement (g)	Calc clay (g)	Sand (g)	W/C	Superplasticizer	Consistency	Strength activity index	
							48 h	28 days
100% OP Cem.	450	0	1350	0.50	0.0 g	25 mm	/	/
R-KF	382.5	68.5	1350	0.50	0.9 g	18 mm	0.91	1.12
Archichamotas	382.5	68.5	1350	0.50	0.0 g	18 mm	0.74	0.88
KA Hostun	382.5	68.5	1350	0.50	0.0 g	13 mm	0.89	1.11
R-ALK-R	382.5	68.5	1350	0.50	0.7 g	15 mm	0.87	1.04
WS 35/38	382.5	68.5	1350	0.50	0.6 g	14 mm	0.77	1.02
Fos bianca	382.5	68.5	1350	0.50	0.5 g	15 mm	0.80	0.99
CS S	382.5	68.5	1350	0.50	0.9 g	15 mm	0.82	0.97

According to these results, the mortars consistency was sufficient for the clays Archichamotas and KA Hostun an no superplasticizer needed to be added. Most likely this can be explained by the coarse grain size of the Archichamotas clay which has a positive effect on the water demand. For KA Hostun the particle size distribution of the calcined clay was very fine compared to the other clays since the KA Hostun was ground after calcination. Nevertheless, the high amount of quartz present in this sample and still rather low BET specific surface area might explain the reason why the addition of superplasticizer was not necessary. The R-KF sample contains considerable high amount of kaolinite and in agreement with the behavior of a metakaolin, which has a greater fineness compared to cement, the mortars consistency needed to be improved (Si-Ahmed et al., 2012). The clays WS35/38, Fos Bianca and CS S have a significant decrease of mortars consistency, even after the addition of superplasticizer. This can be is associated with the high BET specific surface area values > 30 m^2/g which can be related to the presence of 2:1 Al clays. The mortars consistency of the R-ALK-R clay is more surprisingly as the clay has a low BET specific surface area, a medium amount of kaolinite and no significant amount of 2:1 Al-clays. The grain-size distribution after calcination indicates a rather fine material, nevertheless, it is still coarser than KA Hostun which has a good consistency. The main difference between R-ALK-R and KA Hostun is the degree of ordering of kaolinite and the presence of feldspar in R-ALK-R. High ordered kaolinite, such as KA Hostun, tends to have a lower water demand than a medium ordered kaolinite, as R-ALK-R. Furthermore, the two feldspar rich clays R-ALK-R and Fos Bianca need the addition of superplasticizer, indicating the feldspar might also have a negative effect on the mortars consistency. However it is hard to draw conclusions based on the results of only two feldspatic rich samples. The use of calcined clays as SCM has a significant negative influence

on the water demand. This effect will be further influenced when calcined clay is also ground after the calcination process or when calcination temperature is reduced to lower fuel costs. However, smaller grain size of the sample is beneficial for the pozzolanic reaction as more reaction surface and nucleation sites are present. Therefore it is also important to select the appropriate calcination temperature and processing steps in function of the mortars consistency of the blended cement and not only look at the reactivity of the calcined clay.

The compressive strength of the cement samples was analyzed after 48 h and after 28 days. Each time the average strength value of three mortar beams was taken for each sample. The average value of each sample is given in Figure 6.15. The strength activity index (SAI) was calculated according to the following equation:

$$SAI = \frac{average\ compressive\ strength\ of\ the\ test\ mixture}{average\ compressive\ strength\ of\ the\ reference} \qquad \textit{(Equation 6.1)}$$

According to the French standard for metakaolin (NF P 18-513), two different kinds of metakaolin can be defined. Type A are high active metakaolins that posses a SAI ≥ 1.00 at 28 days. Type B are classified as medium active metakaolins with a SAI ≥ 0.90 at 28 days. In comparison the SAI of a cement mixture containing 15% of ground quartz has a SAI of 0.72 – 0.82.

The compressive strength of all blended cements at 48h (Figure 6.15) is lower than for the reference sample resulting in an activity index < 1. This phenomenon can be related to the dilution of the cement by 15% and the late start of the pozzolanic reaction. First the cement hydration takes place whereby portlandite is formed. Only afterwards this portlandite can react with the calcined clay and the pozzolanic reaction can start. In general the contribution of the pozzolanic reaction of calcined kaolinites to the strength is the greatest between 7 and 28 days. Therefore the values at 28 days are more significant for the actual strength of the blended cement.

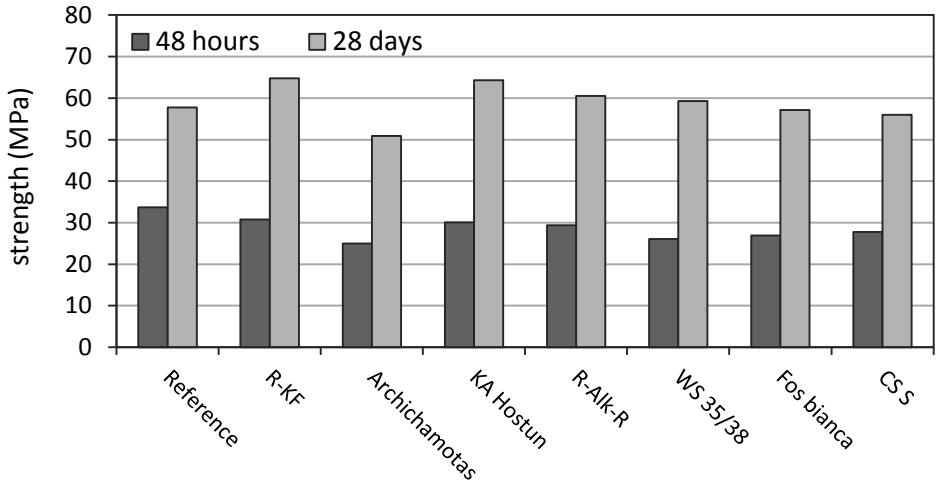

Figure 6.15: *Average compressive strength of the reference and mixture of calcined clay and cement mortar beams at 48 hour and 28 days.*

At 28 days, R-KF is marked by the highest compressive strength of 64.8 MPa resulting in an activity index of 1.12. In comparison the reference sample consisting of 100% Portland cement developed an average compressive strength of 57.8 MPa. According to the NF P 18-513, the R-KF can be classified as an A type of calcined kaolinite regarding strength. Also two other rather kaolinite rich clays, KA Hostun and R-ALK-R can be marked as high active, A type metakaolins with strengths of 64.3 and 60.5 MPa and an activity index of 1.11 and 1.04 respectively. The activity index of WS 35/38 of 1.02 and strength of 59.3 MPa, is only just above the minimum requirement to be classified as A type clay.

The medium reactive or B type calcined clays are Argilla Bianca and CS S. The Argilla Bianca has an activity index of 0.99 and strength of 57.1 MPa, while for CS S this is 0.97 and 56.0 MPa. The least reactive clay is Archichamotas with only an activity index of 0.88 and strength of 50.9 MPa, whereby this clay does not reach the requirements to be classified as B type. According to their compressive strength and their SAI the calcined clays can be arranged accordingly: R-KF > KA Hostun > R-ALK-R > WS 35/38 > Fos Bianca > CS S > Archi.

6.3.5 CORRELATION BETWEEN POZZOLANIC REACTIVITY, COMPRESSIVE STRENGTH AND CLAY CHARACTERISTICS

The pozzolanic reactivity of the different kaolinitic samples varies considerably and therefore it is crucial to understand which parameters contribute to the reactivity. The most important parameter is by far the mineralogical composition of the sample. Since the samples were chosen on behalf of their various kaolinite content, the correlation between the kaolinite content and the portlandite consumption was determined and the correlation plot is given in Figure 6.16. At 28 days the amount of kaolinite allows already to predict the corresponding reactivity rather well, with a R^2 of 0.87. At longer curing times the prediction of the regression line becomes even better with an R^2 around 0.92 at 56 and 90 days. Determination of the bulk mineralogical content of the raw sample therefore provides an excellent measure of the eventual pozzolanic reactivity. The question rises whether chemical analyses can also provide insight in the reactivity of the sample. The amount of Al_2O_3 present in the bulk sample was plotted against the portlandite consumption. However the measured points are widely dispersed and R^2 is only 0.34. The reason for this poor correlation is the presence of several alumina rich minerals besides kaolinite, as was already demonstrated by the weak correlation between the amount of kaolinite and Al_2O_3 in Figure 6.5. Some of these mineral are inert, like muscovite and feldspar, or hardly reactive like illite. As a consequence these minerals enhance the Al_2O_3 concentration of the samples without significant contribution to the pozzolanic reactivity. Since the amount of these minerals is variable among the different samples, Al_2O_3 cannot be used to estimate the reactivity. Also other chemical components like SiO_2 are too much influenced by non reactive minerals like quartz and feldspars, to act as an indicator of the pozzolanic reactivity.

Besides kaolinite the most reactive material that was present in the clay samples is smectite. Therefore the correlation between the portlandite consumption and the sum of the amount of kaolinite and smectite in the bulk sample was made. At 28 days this correlation can be considered as very good with R^2 of 0.91. At longer curing times the correlation further improves to R^2 of 0.96 at 56 and 90 days. This indicates that the use of the total amount of kaolinite and smectite in the bulk sample allows an optimal prediction of the reactivity, which is even better than when only kaolinite is taken into account. However the determination of the amount of smectite by XRD in the bulk composition is much more time consuming and therefore less favorable to have a quick estimation tool of the pozzolanic reactivity. Therefore also the correlation of the sum of all clay minerals including kaolinite and the 2:1 Al clays was made. The R^2 of 0.63 at 28 days however indicates the amount of kaolinite has a greater influence on the reactivity. This can be explained by the presence of illite that only possesses low reactivity. As a result the amount of kaolinite is the easiest method that gives a reliable estimation of the portlandite consumption of kaolinitic rich calcined clay.

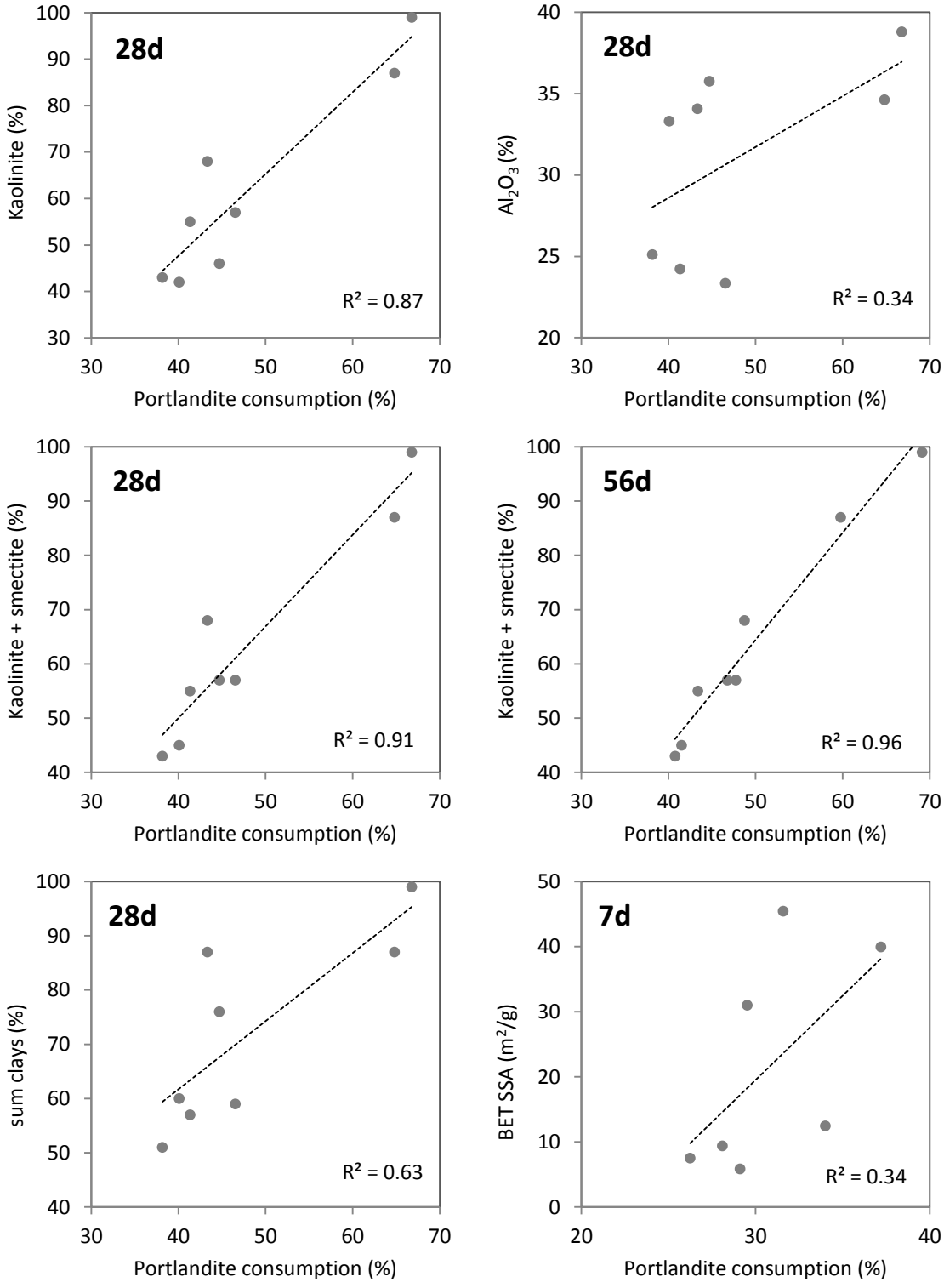

Figure 6.16: *Correlation plots to validate the parameters that influence the portlandite consumption of the sample.*

Even though the amount of kaolinite is a good starting point there can be additional influence of other parameters, listed in Table 6.6. In the studied sample set two samples show clearly a deviated reactivity considering their kaolinite content. The first sample is WS 35/38 that has a higher reactivity than would have been expected based on the kaolinite content. This can be explained with the

presence of 11% of smectite in the bulk sample. The smectite was turned completely amorphous upon calcination and will take part in the pozzolanic reaction which increases the total amount of portlandite that will be consumed. The second sample, Archichamotas, is marked by rather low portlandite consumption at 28 days of 43.3%. The BET specific surface area and degree of ordering (HI) are comparable with samples KA Hostun and R-ALK-R. The main striking difference is the low amount of kaolinite of only 27.5% that is present in the clay fraction <2 µm although the bulk contains a considerable amount of 68% kaolinite. Furthermore, the other clay samples that are less rich in kaolinite have higher amounts of kaolinite present in their clay fraction. This indicated that a large part of the kaolinite of Archichamotas is present as clay plates larger than 2 µm. The importance of the grain size of the reactive particles regarding the portlandite consumption was already demonstrated in paragraph 7.3.3. As a result the initial reaction surface is smaller and the reaction is slower. This effect can be seen in Figure 6.12 whereby Archichamotas has a slow reaction rate especially the first 28 days of the reaction.

Table 6.6: *Overview of the chemical, mineralogical and physical characteristics of all kaolinitic samples listed according to decreasing kaolinite content. The reactivity and strength activity index (AI) are determined after 28 days. The values that are notable are indicated in bold.*

Sample	Kaolinite (%)	Sum clays (%)	Smectite bulk(%)	Kaolinite +K/S <2µm (%)	Reactivity (%)	SAI	Al_2O_3 (%)	BET (m^2/g)	HI
R-KF	87	87	0	99	64.8	1.12	34.62	12.47	0.79
Archi.	68	87	0	**27.5**	**43.32**	**0.88**	34.07	7.52	0.43
KA Hostun	57	59	0	98	46.53	**1.11**	23.35	9.40	0.93
R-ALK-R	55	57	0	84.5	41.33	1.05	24.23	5.86	0.58
WS 35/38	46	76	**11**	65.5	**44.69**	1.02	35.76	39.95	0.13
Fos bianca	43	51	0	72.5	38.15	0.99	25.11	31.00	0.24
CS S	42	60	3	59.5	40.08	0.97	33.31	45.44	0.30

After 56 days the reactivity of Archichamotas becomes more comparable with KA Hostun. The presence of this rather coarse kaolinite could however not be derived from the physical properties like grain size or BET specific surface area since these parameters are also influenced by the presence of all other minerals.

The correlation between the BET specific surface area and the portlandite consumption is not really promising as the best fit that could be found was at 7 days and gave only a R^2 of 0.34. This poor correlation can mainly be explained by the influence of low or medium reactive minerals on the SSA values. The presence of 2:1 Al clays tend to enhance the SSA, even after calcination, however these minerals are not as reactive as kaolinite with low SSA. As a result no proper correlation can be derived.

Besides the portlandite consumption also the strength activity index (SAI) was determined for these samples. The SAI is also largely influenced by the amount of kaolinite that is present in the original sample. Nevertheless, the strength is additionally defined by the fraction of solid/pore volume. Higher porosity will give rise to lower strength of the sample. For this reason the initial grain size will have a significant effect on the strength, since it affects the porosity. Furthermore also the specific reaction kinetics and the amount of hydration phases that are formed will influence the pore volume.

The KA Hostun was marked with a rather high SAI, because this was the only sample that had been ground after calcination. Furthermore, also the fairly low SAI of Archichamotas can be explained by the grain size of the sample. The calcined Archichamotas clay was marked by a very coarse grain-size distribution with 24% of the particles that are >1 µm. As a result the pore spaces are less filled and the strength of the sample decreases unrewarding the high kaolinite content of the sample. Grinding after the calcination process will certainly enhance the pozzolanic properties of this sample. The portlandite consumption of the unground samples can be related to the strength activity index at 28 days (Figure 6.17); However, the correlation is not ideal with a R^2 of 0.66, which indicates not only the pozzolanic reaction but also other parameters like for example the pore volume and amount of solids will influence the eventual strength of the mortar. This theory is confirmed by sample R-ALK-R which was rather fine grained after calcination and did not suffer a great deal of sintering. Even when the positive effect of the fine grains on the pozzolanic reaction is taken into account, the SAI is still higher than would have been expected due to the influence of other parameter like the solid/pore volume ratio and the reaction kinetics. As a result the SAI cannot entirely be estimated based on the portlandite consumption only and additional parameters should be taken into account.

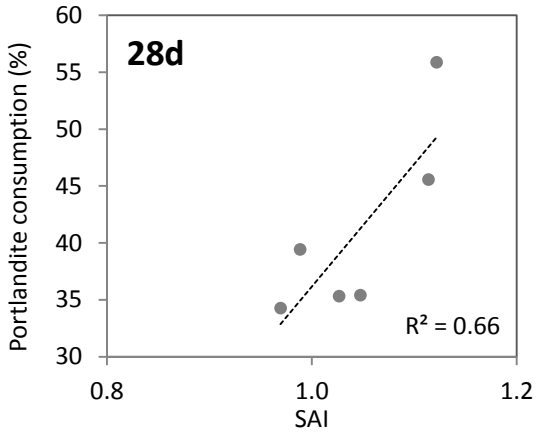

Figure 6.17: *Correlation plot of the strength activity index versus the portlandite consumption of the unground samples at 28 days.*

6.4 POZZOLANIC REACTION PRODUCTS

To study the reaction products in the calcined clay - lime system, pastes were measured by TGA and XRD at different curing times of 3, 7, 14, 28, 56 and 90 days. The TGA results at 28 days are shown in Figure 6.18 for all seven samples. The mass loss due to the decomposition of portlandite between 350 and 550°C has the highest intensity peaks for the Fos Bianca clay and the lowest for sample R-KF. This visually confirms the results of the determination of the pozzolanic reactivity. The hydration phases that can be identified are in consistence with the pure kaolinite samples examined in chapter 4 and consist of strätlingite (C_2ASH_8) around 180 and 240°C, AFm phases (C_4AH_{13}, mono- and hemicarboaluminate) at 140°C, an additional peak of monocarboaluminate at 160°C and a more broad spread C-S-H phase between 80 and 140°C. Strätlingite can be detected in all samples from 7 days onwards while the other two hydration products are already present at 3 days. The difference in bulk mineralogy and especially in kaolinite content has clearly no effect on the nature of the formed hydration products. The amount of hydration products, determined semi-quantitative, are formed consistent with the reactivity of the sample. The least reactive clay forms generally also a smaller quantity of the three hydration products, strätlingite, C-S-H and C_4AH_{13}.

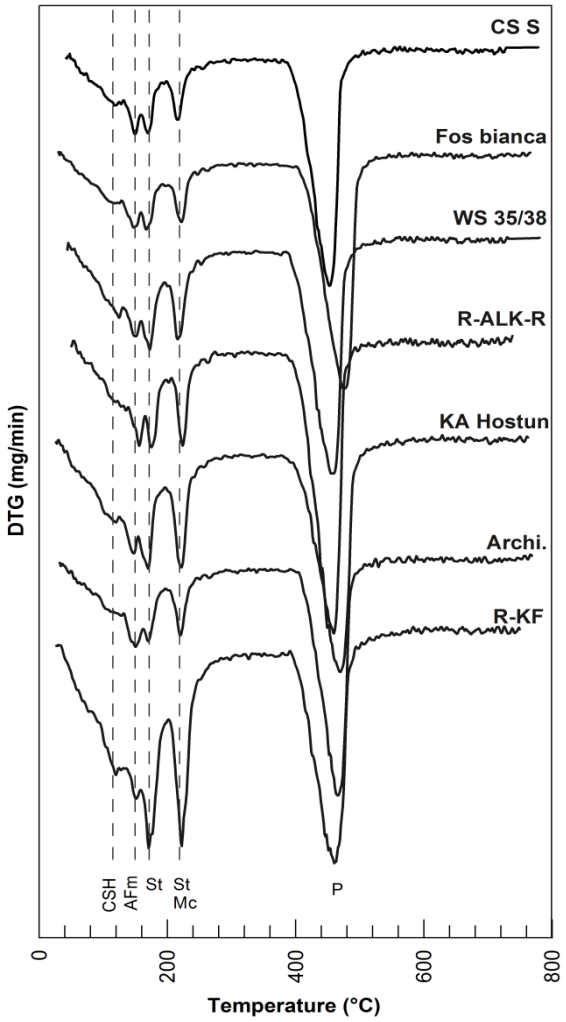

Figure 6.18: *DTG pattern of the calcined clay lime pastes at 28 days. The formed hydration products are indicated: P: Portlandite, St: Strätlingite, Mc: monocarboaluminate, AFm (including C_4AH_{13}, mono- and hemicarboaluminate) and CSH: calcium silicate hydrates.*

The effect of the grain size on the formed hydration products was also analyzed. Figure 6.19 shows the paste of CS S cured for 28 days in both the McCroned and ungrounded state. It is remarkable that the intensity of the AFm phase peak is comparable for both samples, while the amount of strätlingite and C-S-H is clearly smaller for the coarser sample. This indicates that the AFm is less influenced by the grain size than the other hydration phases. AFm phases generally already formed early in the hydration reaction and could be detected in both pure kaolinite samples and the kaolinite rich clays at 3 days. This indicates the AFm phases, including C_4AH_{13}, mono- and hemicarboaluminate forms more easily than strätlingite. In general C_4AH_{13} is preferably formed over strätlingite when the solution is more silica rich (Taylor, 1997). A possible theory is that the more coarse grains of the ungrounded sample make the dissolution of Si and Al in the early stage of the reaction harder and less nucleation sites are present. Also the other calcined samples and especially those that are less rich in kaolinite like WS 35/35 and Fos Bianca had a clear difference in reactivity between the ground and ungrounded sample, showed similar results.

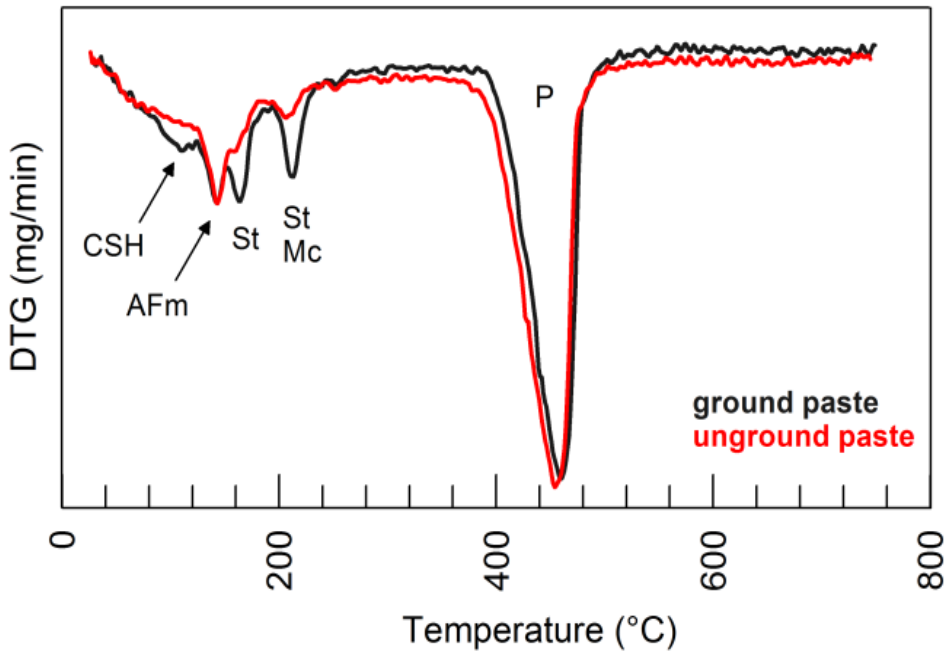

Figure 6.19: *DTG curve of the calcined lime paste at 28 days of sample CS S, both ground after calcination and ungrounded. The formed hydration products are indicated: p: Portlandite, St: Strätlingite, Mc: monocarboaluminate, AFm and CSH.*

Based on the XRD patterns of the pastes similar reaction products can be found as for TGA (Figure 6.20). The dominant crystalline hydration phase is clearly strätlingite for all samples. Strätlingite is present after 7 days of curing and the formation time is not influence by the amount of kaolinite present in the original sample. The other identified hydration products consist of C-S-H and AFm phases. C_4AH_{13} can be identified based on the weak reflections around 11°2θ. Additionally also mono- and hemicarboaluminate are present, visible by the reflections at 11.65 °2θ and 10.8 °2θ respectively. The quantity of all hydration phases systematically increases according to measured reactivity of each sample. The kaolinite content therefore does not influence the type of reaction products that are formed. There is no significant influence detectable of accompanying mineral impurities. The patterns of the pastes of the feldspar rich R-ALK-R and Fos Bianca, are marked by unaltered feldspar reflections in the region between 27.0 and 28.5 °2θ. For all samples also the sharp reflections of quartz are visible at 20.8 and 26.7 °2θ. The 2:1 Al-clay rich sample WS 35/38 is marked by a higher quantity of C-S-H compared to KA Hostun, while the amount of strätlingite is lower for sample WS 35/38. This indicates the calcined 2:1 Al-clays mainly contribute to the formation of the C-S-H phase and not to the formation of the aluminum rich strätlingite. The differences in the other AFm phases are hard to detect and no conclusion on the formed quantities in relation to the presence of 2:1 Al-clays can be made.

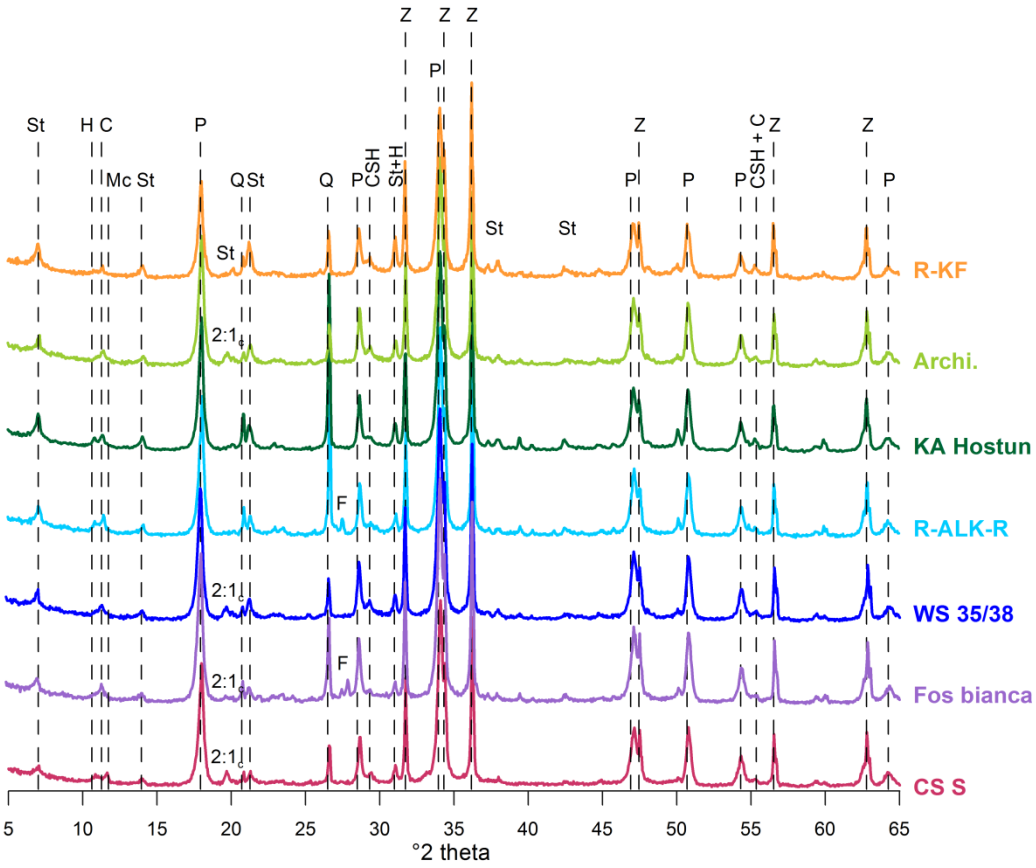

Figure 6.20: *XRD pattern of the calcined clay lime mixtures at 28 days of curing. The identified phases are indicated: Z: zincite (internal standard) Q: quartz, F: Feldspar, 2:1$_c$: calcined 2:1 Al-clays, P: Portlandite, St: Strätlingite, Mc: monocarboaluminate, h: hemicarboaluminate, C: C_4AH_{13} and CSH.*

6.5 CONCLUSION

The pozzolanic reactivity of the ground calcined kaolinite rich clays can be summarized accordingly:

R-KF >> KA Hostun > WS 35/38 > Archi. > R-ALK-R > CS S > Fos Bianca

This indicated that clays that only contain around 40% of kaolinite can still be considered as a pozzolanic material. The main controlling parameter of the pozzolanic reactivity is proven to be the mineralogical composition. The amount of kaolinite present in the bulk raw sample can act as an excellent marker to estimate the pozzolanic reactivity of natural kaolinite rich clay deposits. For a more accurate approximation the bulk smectite content should be included as well. However determination of the bulk smectite content by XRD is much more time consuming and asks for more specialized analyzing and interpretation techniques since normal bulk analyses only quantify the amount of 2:1 Al clays in total. However, other techniques like sorption tests with methelyene blue are extensively used to estimate the smectite content of a sample in geotechnical engineering (Alther, 1983; Boxill, 2011; Chiappone et al., 2004). Even though this method is less accurate than XRD results it might allow a better estimation of the pozzolanic reactivity of the sample than when only the kaolinite content is used as parameter (Panna, 2014). Especially for kaolinitic clays that are still rich in smectite, the pozzolanic reactivity would otherwise be underestimated.

Besides the influence of the mineralogy also the physical characteristics of the calcined clay will

contribute to the reactivity at 28 days. Especially the processing of the sample after the calcination process has a huge impact on the actual portlandite consumption. Coarser grain-size distribution of ungrounded samples will lead to less reaction surface and less nucleation sites. As a consequence the reaction rate drops significantly compared to the same sample that was ground after calcination. Especially clays that contain a considerable amount of 2:1 Al clays are affected to a greater extent, since they are marked by a higher degree of sintering. Because the grain size is an important controlling parameter of the portlandite consumption, also the size of the reactive kaolinite particles can play a major role. Kaolinite rich clays that have less kaolinite present in the clay fraction <2 µm and consist of rather coarse kaolinite particles possess an inferior pozzolanic reactivity in comparison to their kaolinite content. The size of the kaolinite particles is often correlated to the degree of ordering. Nevertheless, no correlation between the reactivity and the degree of ordering could be found. The specific surface area was too much influenced by the mineralogical composition that no conclusive correlation could be made and will be important during the first 7 days of the reaction.

Also the strength activity index is not only influenced by the amount of kaolinite but also the grain size plays a major role. For very coarse kaolinite rich samples, like Archichamotas, the achieved strength will be insufficient in correlation to the kaolinite content. Therefore the grinding of the samples after the calcination process can have a major positive effect on the strength because both the pozzolanic reaction is improved and the pore size will be reduced. Nevertheless, smaller grain sizes will have a negative effect on the water cement ratio of the blend and additional super plasticizer will be needed. Therefore both positive and negative aspects should be taken in consideration.

CHAPTER 7

NATURAL SMECTITIC CLAYS

In the past most studies have focused on kaolinite rich clays and demonstrated their potential as supplementary cementitious material. It is known that the calcination of kaolinite rich clays form a metastable phase, metakaolin, that is highly reactive. However to know the full potential of calcined clays in general, other clay minerals should also be considered. Natural clay mixtures dominated by 2:1 clays and in particular by the swelling clays like montmorillonite, are rarely studied in detail. The limited studies that were done are performed on calcined montmorillonite in its pure form and all conclude that both Ca- and Na-montmorillonite are fairly good pozzolans (Danner, 2013; Fernandez, 2009; He et al., 1996). More recently also NMR studies of Garg and Skibsted (2014, 2015) on pure montmorillonite samples confirmed these results. The limited occurrence of pure montmorillonite clay and more premium application asks for more economical alternatives. For this reason recently one research group focused on the use of calcined marl (Danner, 2013; Danner et al., 2015; Justnes et al., 2011; Østnor et al., 2015). These calcareous montmorillonite rich clays tend to have good pozzolanic properties and could replace up to 55% of clinker material in Ordinary Portland cement. To summarize, montmorillonite rich clays can indeed have good pozzolanic potential but due to the complexity of the mineralogy and structure of montmorillonite and the overshadowing of the highly reactive kaolinite, they are not always taken into account. Therefore in this chapter special attention has been given to natural montmorillonite rich clay mixtures to asses their potential as SCM on behalf of the clays raw characteristics such as chemistry, mineralogy and physical properties.

7.1 MATERIALS

The clays that were used in this study were collected by representative sampling of different clay deposits and drill cores located in Belgium, France and Italy. The selection of the samples was made based on the estimated content of smectite and the presence of certain non clay impurities in the bulk sample to assure a broad variation in mineralogical composition. The clay samples from Belgium and France belong to the Eoceen-Oligocene interval and more particular to the marine deposits of Kortemark, Orchies and Zomergem and the continental Goudberg section. The Italian clay is more calcareous rich and was therefore added to the sample set. An overview of the samples is given in Table 7.1.

Table 7.1: *Sample overview with location and brief description.*

Sample	Country	Location	Description	Firing Color
1. SM1	Belgium	Hoegaarden	Goudberg section	Brown
2. SM2	Belgium	Kallo	Kortemark	Brown
3. SM3	Italy	Colombara (Bologna)	-	Brown/orange
4. SM4	France	Orchies Tuillerie	Orchies Clay	Dark brown
7. SM5	Belgium	Sint-Katelijne Waver	Zomergem clay	Red brown

7.2 CHARACTERIZATION

7.2.1 CHEMISTRY

The bulk chemical composition of the unfired clays is reported in Table 7.2. The alumina content of smectitic clays is in general rather low compared to kaolinite rich clays. The alumina content varies between 16.39 and 9.76%. Even though all calcined samples would classify as potential good pozzolan according to the ASTM C618-89 norm, stating that $SiO_2 + Al_2O_3 + Fe_2O_3 > 70\%$, not all silica, alumina and iron in the samples is available to take part in the pozzolanic reaction. The CaO content of SM3 is rather high, with a value of 11.14%, and was one of the reasons to select this clay. The rather low concentrations of Na_2O compared to CaO for all samples, reveal that the dominant exchangeable cation of smectite is more likely to be Ca^{2+}. Nevertheless XRD and thermal analysis will give more conclusive results. The iron contents that vary between 2.0 and 6.6% explain the brown – reddish firing colors.

Table 7.2: *Bulk chemical composition of the untreated smectitic clays.*

% Weight	SiO_2	Al_2O_3	Fe_2O_3	CaO	MgO	K_2O	Na_2O	TiO_2	LOI
SM1	58.66	15.19	6.57	2.45	1.81	0.63	0.01	3.40	11.23
SM2	60.94	16.39	3.64	3.61	1.72	1.89	0.39	0.90	10.05
SM3	47.31	14.07	6.45	11.14	4.01	2.66	1.05	0.62	12.61
SM4	63.23	13.01	4.07	1.43	2.48	2.66	0.04	1.20	8.89
SM5	73.75	9.76	2.02	2.15	0.97	2.35	0.20	0.58	6.83

7.2.2 MINERALOGY

The mineralogical composition of the samples was analyzed by XRD. The results of the bulk composition (Figure 7.1) demonstrate that the amount of 2:1 Al-clays has a good spread between 28 and 85 %. The XRD patterns of the raw and the calcined samples are shown in Figure 7.2. The presence of montmorillonite in the raw clay samples is visible by the broad 001 reflection peak at 5.7 °2θ. This reflection peak is most pronounced for sample SM1, which has the highest 2:1 Al-clay content of 83 %. The position of the 001 peak can also be related to the dominant exchangeable cation. The diffraction peak at 5.7 °2θ is typical for a Ca-rich montmorillonite while a Na-rich montmorillonite would reflect at higher 2θ angle. For the samples SM3, SM4 and SM5 it is harder to derive the dominant exchangeable cation as the reflection peak is less developed due to the lower amounts of montmorillonite in these samples. Nevertheless the broad peaks are more situated

around 5.7 °2θ indicating Ca is most likely the dominant cation. The amount of 2:1 Al-clays further decreases according sample number with 55% for SM2, 46.5% for SM3, 41% for SM4 and only 29% for SM5. Regarding other 2:1 Al-clay minerals besides montmorillonite, the presence of illite can normally be confirmed by its 001 reflection at 9.9 °2θ and a rather sharp reflection at 19.84 °2θ. If only montmorillonite would be present, this second reflection would be much broader. However also muscovite has got a reflection at both positions and therefore it is hard to estimate the presence of illite in the samples. Moreover, due to the limitation of the quantification software Quanta (© Chevron) illite and montmorillonite cannot be quantified separately based on the bulk XRD pattern. A more quantitative distinction of the 2:1 Al-clays will be made based on the oriented slides of the fraction <2 µm. Muscovite, however, can already be quantified in the bulk composition since this mineral has more reflection peaks that can be distinguished at 5, 3.87, 3.73 and 3.20 °2θ. The presence of muscovite was only confirmed for SM2 (8%) and SM3 (4%). Additionally SM3 contains 3% of the mica biotite (In Figure 7.1 only the sum of mica's is given). Furthermore, the clays contain some other clay and certainly non-clay minerals besides the 2:1 Al-clays, which can be seen as impurities. The iron rich chlorite, ripidolite, can be found in samples SM2, SM3 and SM4 with its primary 002 reflection at 12.4 °2θ. The additional reflection at 18.76 °2θ confirms indeed chlorite is present and not only kaolinite, of which the 001 reflection overlaps with chlorite at 12.4 °2θ. All five samples contain a minor amount of kaolinite varying between 2 and 6%.

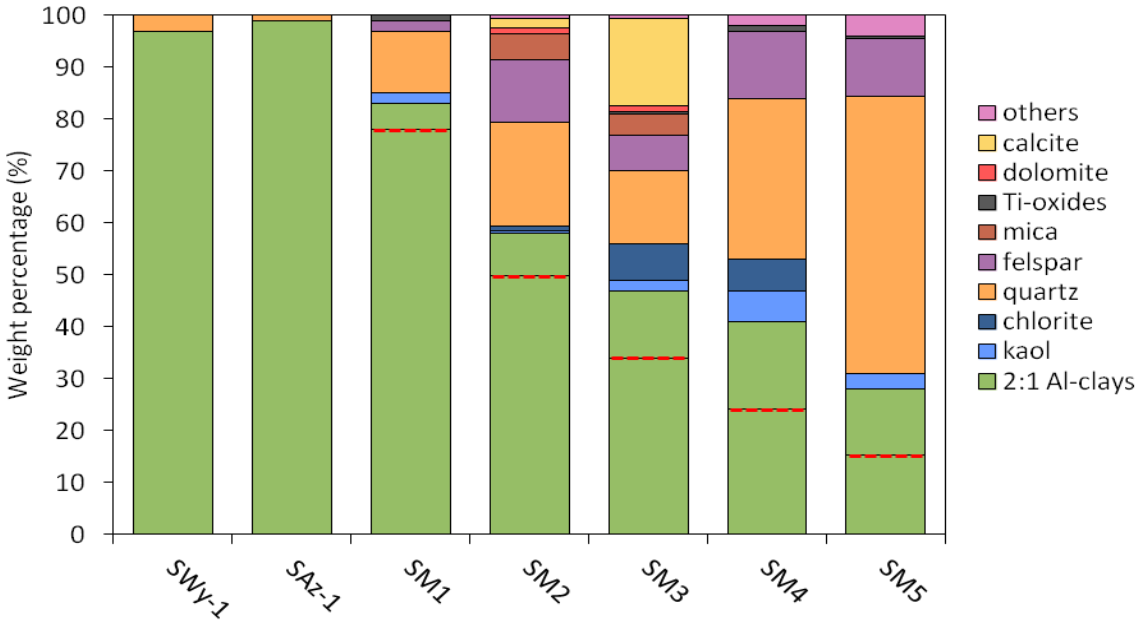

Figure 7.1: *Bulk mineralogical composition of five smectitic clays and two pure reference samples SWy-1 and SAz-1.The red dashed line represents the amount of smectite present in the bulk natural clay sample determined after analyzing the fraction <2 µm..*

Quartz is the dominant non-clay mineral in the samples. SM1 contains only 12% of quartz while SM5 has the highest quartz content with 52.5%. In general the quartz content increases when 2:1 Al-clay content decreases, resulting in a more silty clay. Only sample SM3 has somewhat lower quartz content of 14% compared to the other samples. The high intensity and sharp reflection in sample SM3 at 29.46 °2θ can be assigned to calcite. This high amount of calcite explains why the quartz content was lower. SM3 is the only clay with a significant amount of calcite, which can be beneficial for the pozzolanic reaction (Justnes et al., 2011). SM2 also contains calcite; nevertheless, since it is only 1% no clear effect is expected. Both clays SM2 and SM3 contain 1% of dolomite as shown by the reflection at 31 °2θ. The range between 27 and 28 °2θ is marked by multiple reflections of feldspar. Both kali-feldspar and plagioclase are present in all samples in various quantities, ranging between 2 (SM1) and 11% (SM4 & 5). Only small amounts (0.4 - 1%) of the Ti-oxide anatase, characterized by a

reflection at 25.28 °2θ, are present in all samples except SM2. The reflection peak at 11.64 °2θ in samples SM4 and SM5 represents gypsum, 2 and 4% respectively. Traces of pyrite (0.2 – 0.5%) were identified in samples SM2 and SM3 based on the reflection at 33.12 °2θ.

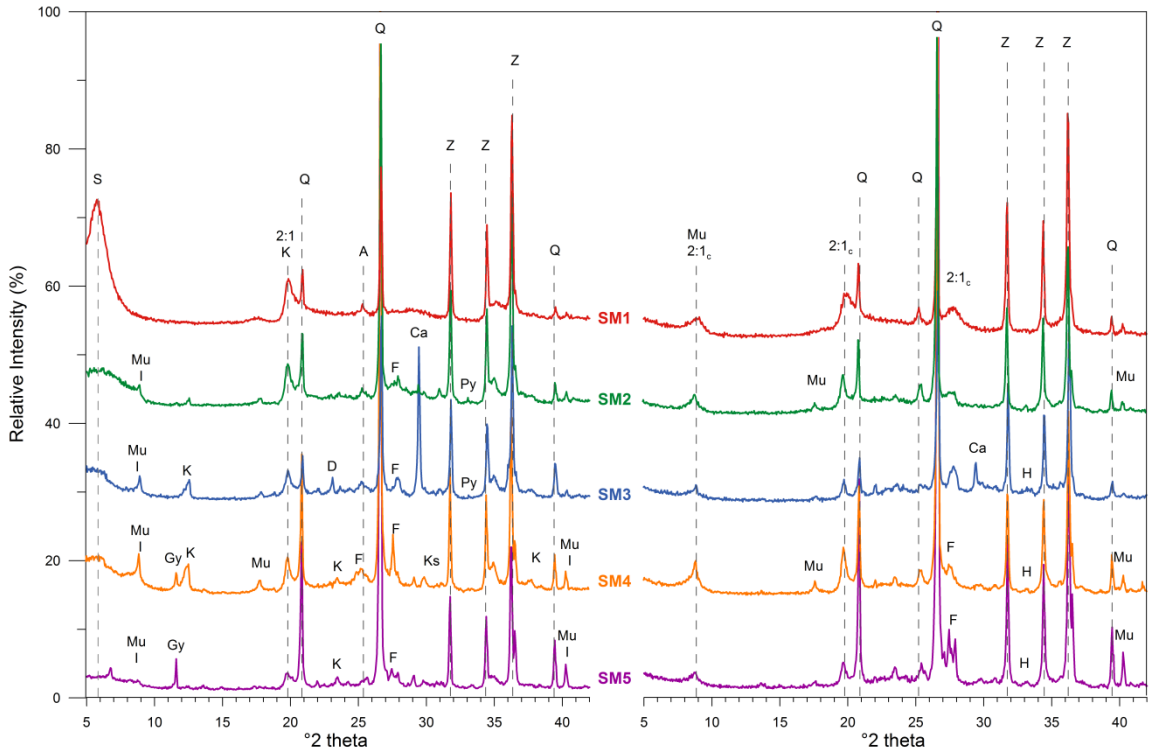

Figure 7.2: *XRD patterns of the raw (left) and calcined (right) smectitic clays. The identified phases are indicated: Z: zincite (internal standard), Q: quartz, S: smectite, I: illite, 2:1: 2:1 Al-clays, 2:1$_c$: calcined 2:1 Al-clays, K: kaolinite, Mu: muscovite, F: feldspar, Ca: calcite, D: dolomite, Gy: gypsum, Py: pyrite and H: hematite.*

The detailed clay mineralogy allows distinguishing different clay minerals within the 2:1 Al-clay group. The air dry and ethylene glycolated patterns are given in Figure 7.3. All samples include the clay minerals smectite, illite-smectite mixed layer and kaolinite. However the quantification results, shown in Figure 7.4, are variable between samples. The <2 µm fraction of SM1 is dominated by 93% smectite, which can be identified by the shift of its 001 reflection from 5.88 to 5.10 °2θ when glycolated. The illite-smectite mixed layer can be identified by the presence of a reflection at 10.24 °2θ in the glycolated pattern. The ratio of I/S that was found after modeling is 66:34 and is randomly oriented (R0). The amount of kaolinite is even less with only 1%, the reflection of kaolinite at 12.20 °2θ is very weak. SM2 is marked by a slightly lower amount of smectite of 85%. The I/S comprises 9% and has a ratio of 70:30 and has Reichweite R0. Again only traces of kaolinite (1%) could be detected. The presence of pure illite could be identified by the presence of a reflection at 8.94 °2θ in both the air dry and glycolated pattern. SM3 contains besides the same clay minerals as sample SM2, also 2.5% of chlorite, which has a characteristic reflection at 18.78 °2θ. The smectite content of SM3 is 68.5%. Sample SM4 is characterized by a higher kaolinite content in the clay fraction of 7.5% and additionally 1% of K/S mixed layer. SM4 has also the lowest smectite content of 53.5% and as a consequence the illite and 66:34 I/S (R0) amounts are higher with values of respectively 15.5 and 22%. SM5 contains 54.5% of smectite, 9% illite, a high amount of 36% of 66:34 I/S (R0) and traces (1%) of kaolinite. In general it can be seen that a decrease of the 2:1 Al-clays in the bulk composition is accompanied with a decrease of the amount of smectite in the clay fraction <2 µm. As a consequence the amount of illite and I/S increases. The smectite content in the bulk composition was determined by recalculations and is indicated by the red dotted line in Figure 7.1.

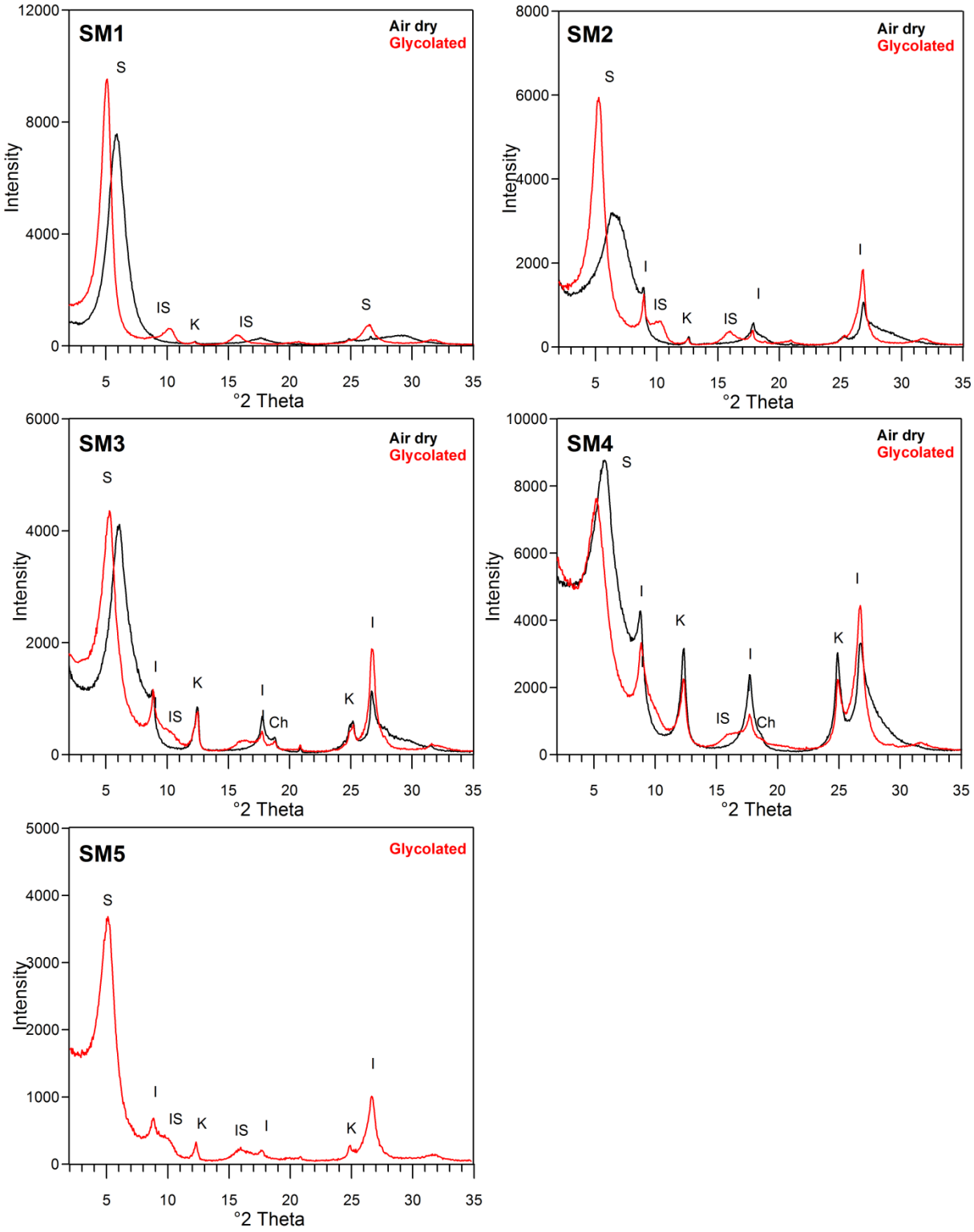

Figure 7.3: *XRD patterns for air dry and ethylene glycolated state of the oriented slides of the clay fraction <2µm of the smectitic samples. The phases that are present are indicated: K: kaolinite, S: smectite, I: illite, IS: illite smectite mixed layer and Ch: chlorite.*

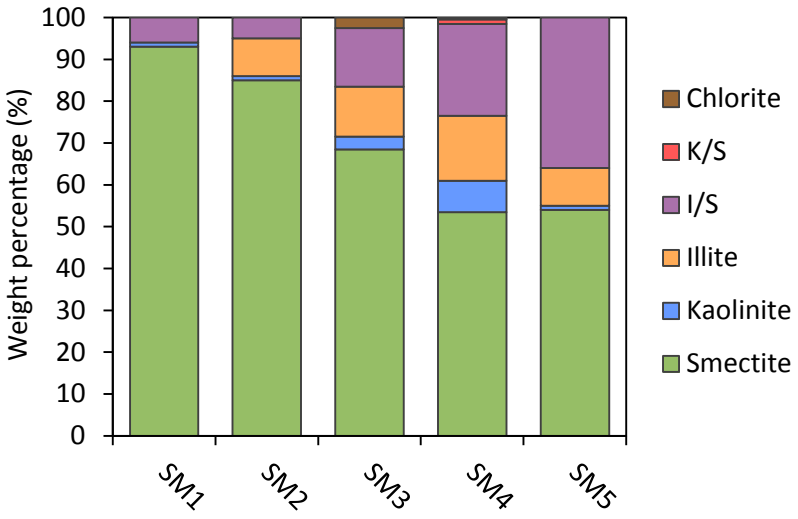

Figure 7.4: *Comparison of the mineralogical composition of the clay fraction <2 µm. I/S represents the R0 illite smectite mixed layer with a ratio of 66:34 for SM1, SM4 and SM5 and 70:30 for SM2 and SM3. The kaolinite smectite mixed layer (K/S) has a ratio of 85:15.*

During the calcination process the clays are dehydroxylated and the structure of montmorillonite collapses partly or entirely. The XRD patterns after calcination are shown in Figure 7.2. The basal 001 reflection of smectite is clearly affected due to the heating. For sample SM1 the peak is shifted from 5.70 to 8.84 °2θ and the intensity of the reflection is decreased significantly. This peak position after calcination reflects that of the illite structure, indicating the montmorillonite is only collapsed partially. This is further confirmed by the appearance of an additional peak upon calcination at 27.86 °2θ. This behavior is similar to that of the pure S1 (SWy-1) in Chapter 4, whereby also the smectite reflections remained, dough shifted, after calcining at 800 °C. For SM2 the broad peak between 5 and 8 °2θ disappears completely after calcination. However there is no peak shift as the reflection at 8.8 °2θ, present in the calcined pattern, shows no difference in intensity or broadness with that of the raw sample. This indicates the reflection at 8.8 °2θ in the calcined pattern can be entirely assigned to muscovite and illite, already present in the raw material, while montmorillonite has become completely amorphous. The total amorphisation of montmorillonite at 800 °C was also observed for sample S2 (SAz-1) in chapter 4. SM3 and SM4 also have mica and/or illite present in their raw sample which provokes a reflection at 8.8 °2θ. After calcination the reflection remains fairly similar with only very little broadening of the peak. This again indicates almost a complete amorphisation of montmorillonite. For SM5 the main peaks of montmorillonite collapse, due to the rather low 2:1 Al clay content of SM5 (29%) no conclusive decision can be made whether the changes around 8.8 °2θ are significant enough to conclude that partial or complete amorphization took place.

A second important change during the calcination process is the dehydroxylation of kaolinite and chlorite. This phenomenon is most clearly observed by the disappearance of the 001 basal reflection of kaolinite and the 002 reflection of chlorite at 12.46 °2θ upon calcination at 800 °. This can best be observed in sample SM4 since it has the highest amount of both minerals but also the other samples are marked by this disappearance. In general the peak reflections of non-clay minerals like quartz, feldspar, muscovite and anatase are unaltered and, moreover, are often intensified. However not all mineral impurities are inert and some do alter upon heating. An example is the hydrated gypsum present in sample SM4 and SM5. Already at low temperatures (90 °C) gypsum is dehydrated and converted to anhydrite. Temperatures up to 800 °C, however, result in further disintegration of anhydrite. Also pyrite is oxidized to hematite during calcination and the small reflection at 28.5 and 33 °2θ (sample SM2 and SM3) disappears. The presence of hematite in the calcined sample is

confirmed by the reflection at 33.16 °2θ. Calcite, present in SM3, is marked by decomposition between 700 and 900°C whereby $CaCO_3$ is converted to CaO and CO_2. Since its decomposition process is not yet fully completed at a calcining temperature of 800 °C, the reflection peaks still remain visible but the intensity is weakened significantly. Furthermore, less calcite was present directly after calcination and similar to the calcite mixtures studied in chapter 5, new calcite is formed when the calcined sample is exposed to CO_2 present in the atmosphere.

7.2.3 THERMAL ANALYSIS

To predict the thermal behavior and the structure of the smectitic clays thermal analysis was applied. The DTG patterns of the five samples are compared in Figure 7.5. The dehydration is an important thermal reaction for smectites and occurs in the temperature range between 20 and 250 °C. Based on the shape and especially the amount of dehydration peaks the charge of the dominant exchangeable cation can be determined. For all samples a double peak is present, indicating the exchangeable cation is dominant divalent, like Ca^{2+}. Nevertheless the two peaks are not always very distinctive. Especially for SM4 and SM3 one peak is dominant and only a shoulder at the right of this peak can be distinguished. Even though all samples were pretreated in a similar way by heating the sample to 60°C to assure similar dehydration of the sample, the dehydration peaks cannot be directly related to the amount of smectite. A possible explanation is that the difference in humidity was significant to cause these intensity variations.

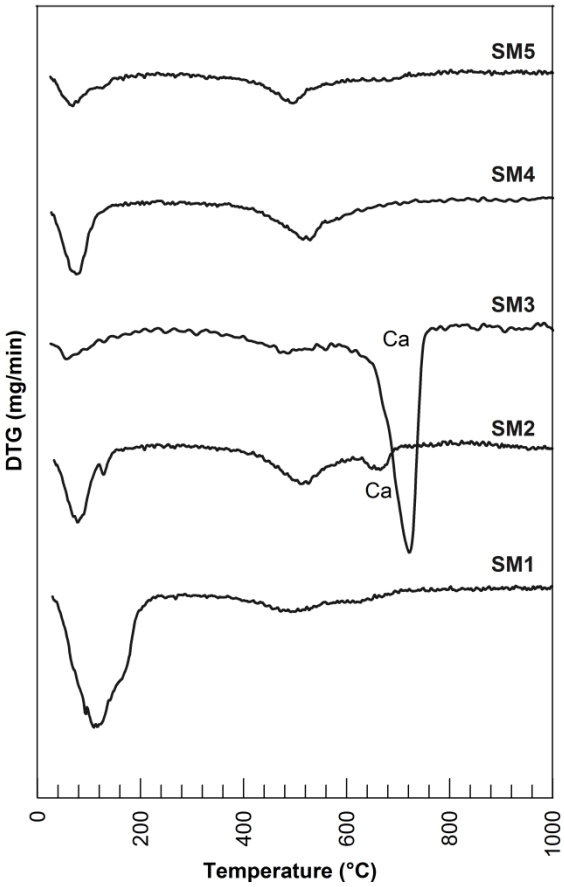

Figure 7.5: *DTG curves of the smectitic samples. The peak of calcite (Ca) is indicated.*

The dehydroxylation for smectitic clays occurs between 400 and 800 °C and is far less intense than for kaolinitic clays. SM1 is marked by a broad dehydroxylation that continues up to 800°C and two broad peaks can be distinguished at respectively 492 and 627 °C. The low temperature of 492°C can

be associated with trans vacant smectite. However the presence of the second peak, which is higher than 600°C indicates also smectite with cis vacant structure is present. For SM2 the dehydroxylation peak temperature was set at 511°C, indicating the clay is predominant trans vacant. It is however possible that a second dehydroxylation exists, however the presence of calcite, with a decarbonization peak at 665°C would mask this peak. The XRD results that indicated SM2 becomes fully amorphous upon calcination support the theory of a low dehydroxylation temperature and mainly trans vacant smectite. For SM3 dehydroxylation occurs at 486°C indicating the clay is trans vacant. The high calcite content of this sample is confirmed by an intense peak at 721°C representing the release of CO_2 of the calcite structure. The dehydroxylation temperature of SM4 is slightly higher at 529°C; Furthermore, the shoulder to the right might indicate the presence of some cis vacant smectite. Nevertheless, the dehydroxylation temperature, even when the shoulder is included, remains below 600 °C, indicating this clay is dominantly trans vacant. However the bulk smectite content of this clay is rather low and other clay minerals that are present like illite and illite/smectite mixed layer will influence the dehydroxylation temperature significantly. The combination of no traces of high temperature dehydroxylation and the fact that smectite became amorphous after calcination at 800 °C, strongly suggests the smectite is dominant trans vacant. The dehydroxylation of SM5 is situated at 496 °C and can be seen as mainly trans vacant. The degree of dehydroxylation did not reveal any significant difference between the dehydroxylation behavior of the samples as calcite masked the actual temperature at which 90% of the dehydroxylation was completed.

7.2.4 GRAIN SIZE DISTRIBUTION

The grain size of the raw and calcined samples was measured with laser diffraction. The results of the d10, d50 and d90 values for both raw and calcined samples are listed in Table 7.3. The samples vary somewhat in fineness whereby SM2, SM3 and SM4 are rather fine grained with a d50 of 10.31, 7.52 and 8.91 µm respectively. The samples SM1 and SM5 are coarser, especially sample SM5 with d50 value of 22.21 and 29.40 µm. However as the grain size distribution of the sample is not just mono modal the d50 value does not give all the needed information. Based on the cumulative results shown in Figure 7.6 and the d90 value of 134.43 µm it can be concluded that SM3 has a significant proportion coarse grains >100 µm. SM1 evolves rather continuously with a d90 of 83.23 µm.

Table 7.3: *Overview of the d10, d50 and d90 values of the grain size distribution of the raw and the calcined clays.*

Clay	**Raw (µm)**			**Calcined (µm)**		
	d10	**d50**	**d90**	**d10**	**d50**	**d90**
SM1	1.87	22.21	83.23	6.20	50.72	128.95
SM2	2.19	10.31	52.79	4.90	69.60	304.02
SM3	0.96	7.52	134.43	0.35	5.11	18.37
SM4	1.47	8.91	42.45	4.23	151.36	519.46
SM5	2.44	29.40	243.21	21.84	169.88	482.70

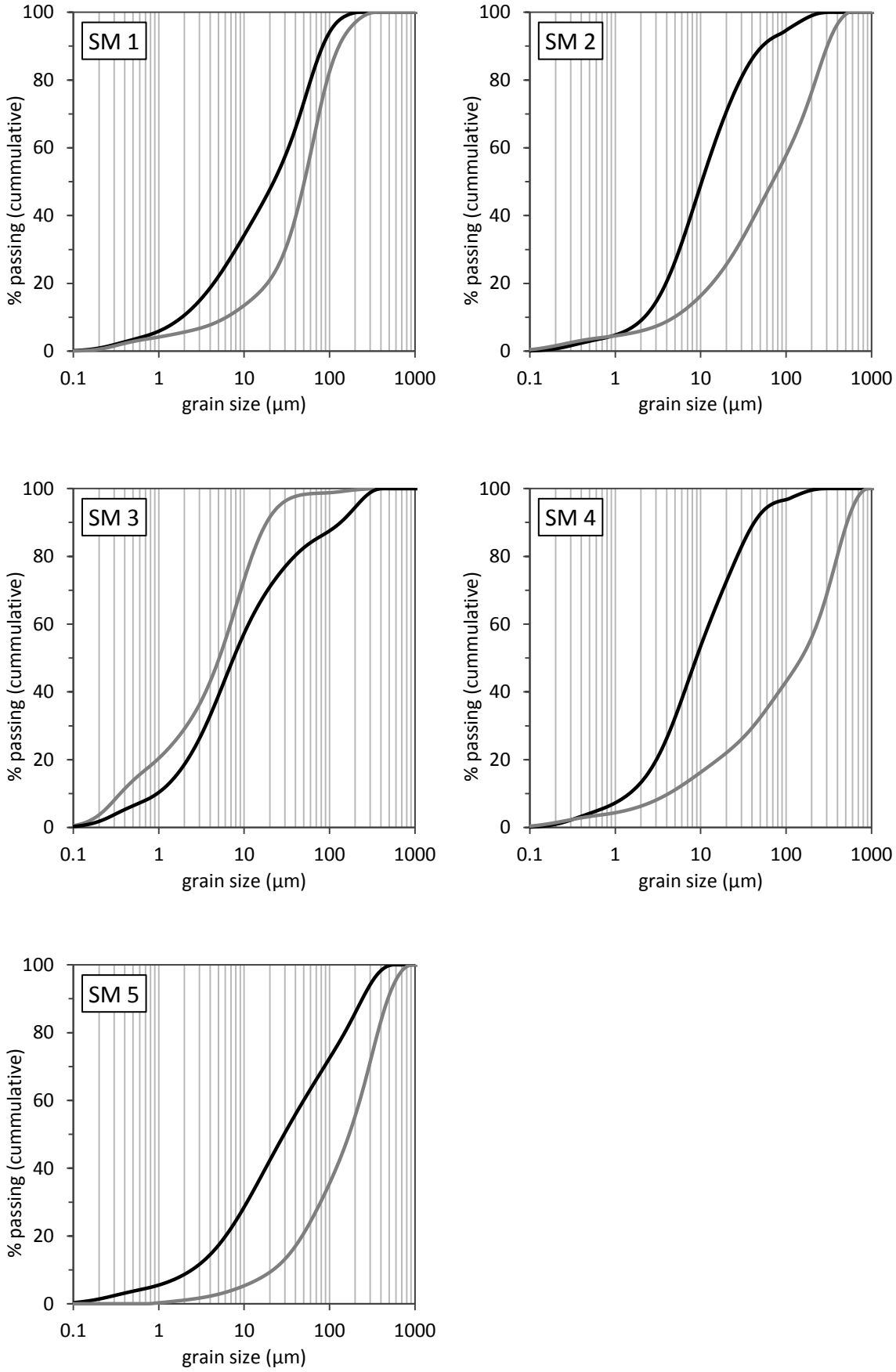

Figure 7.6: *Cumulative grain size analysis of the five raw (black line) and calcined at 800°C (grey line) smectitic clays.*

The grain size distribution of the samples was also determined after calcination to study the sintering effect caused by a heating temperature of 800°C. The cumulative results, shown in Figure 7.6, indicate that in general the samples coarsen during calcination except for sample SM3. Furthermore, the extent of this coarsening is not equal for all samples and is mainly controlled by the grain size distribution and the mineralogical bulk composition of the raw sample. SM1 is characterized by a coarsening mainly of the smaller clay fraction, indicating the individual clay particles are more sintered which results in a shift to the right of the bottom of the grain size curve and a significant increase (x3.3) of the d10 value. For SM2 also the larger grain size fraction (>50 µm) increases which can be the result of the sintering of non-clay minerals like feldspar and mica. SM3 is the only sample that does not show a coarsening of the sample. Upon calcination the grain size decreases. A possible explanation for this behavior can be that calcite has a significant influence on the grain size. In the raw sample calcite is most likely present in the silt or sand fraction between 10 and 100 µm. The calcination of calcite at 800°C results in a decomposition of calcite whereby the coarse calcite grains are no longer present. Instead CaO, with generally a very fine grain size, is formed. The proportion of smaller particles becomes therefore larger. Nevertheless the clay particles also sinter but apparently the sintering effect is not sufficient. SM4 is marked by a clear coarsening especially of the particles above 1 µm which results in a drastic increase of the d50 and d90 values to 151.36 µm and 519.46 µm. SM5 is marked by an overall coarsening of the sample. The presence of a substantial amount of non-clay minerals is not sufficient to limit the sintering.

7.2.5 BET SPECIFIC SURFACE AREA

The results of the BET specific surface area analyses for both the raw and calcined clays are visualized in Figure 7.7. The BET specific surface area of raw smectitic clays can vary a great deal. This is demonstrated by the difference of the two reference smectites S1 and S2 with a value of 23.36 and 87.26 respectively (see chapter 4). Therefore it is hard to draw conclusions or link mineralogy to the BET specific surface area of the raw clays. Upon calcination, the BET specific surface area of smectitic clays changes drastically due to sintering of the clay plates. Compared to kaolinitic clays the effect of the calcination is much more pronounced indicating smectitic clays sinter more than kaolinitic clays. A general trend can be observed that the effect of the calcination process declines with a decreasing smectite content. The most smectitic rich clay SM1 is marked by a drop from 63.07 to 1.45 m^2/g. This clay has the lowest BET specific surface area after calcination compared to the other samples. The change in SM2 can also be attributed to the smectite that is present and in minor amount to feldspar. After calcination the specific surface area is still somewhat higher with 9.11 m^2/g. The buffer effect of impurities that are present like quartz might explain the higher specific surface area after calcination compared to the more smectitic rich SM1. SM3 has a somewhat lower raw specific surface area of 36.39 m^2/g. This can be the result of the presence of coarser calcite, nevertheless it is also possible the smectite present in the raw sample has a smaller specific surface area. The BET specific surface area of SM4 changes from 39.71 to 17.4 m^2/g, which is the highest value after calcination. This is most likely the result of the presence of kaolinite and chlorite whose specific surface area does not alter much upon calcination on one hand and the presence of inert impurities on the other hand. SM5 has already a very low specific surface area to start, 10.75 m^2/g due to the high amount of non-clay minerals. Upon calcination the specific surface area decreases as low as 3.54 m^2/g. When the difference in percentage is taken into account this sample only has a minor decrease in specific surface due to low amount of clay minerals.

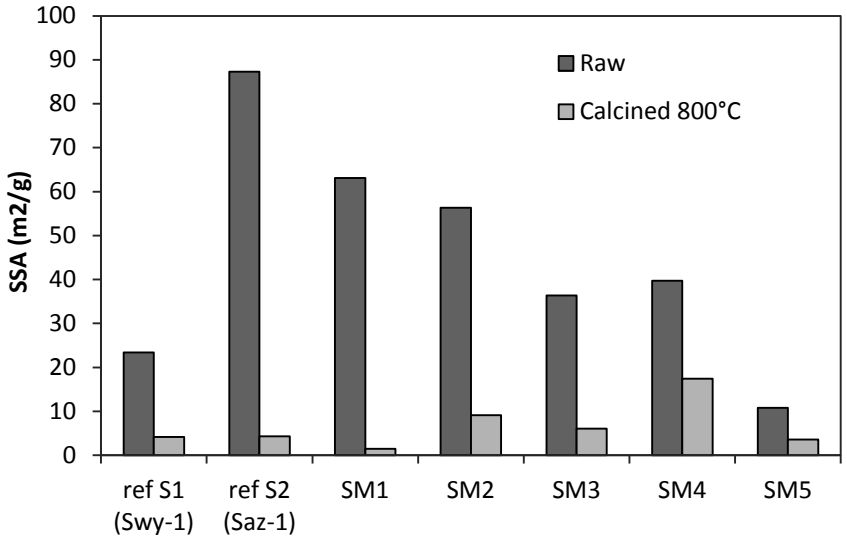

Figure 7.7: *BET specific surface area of raw and calcined smectitic clays. The two reference samples S1 and S2 were discussed in more detail in Chapter 4.*

7.3 POZZOLANIC REACTIVITY

7.3.1 CALCINED CLAY LIME PASTES

The evolution of the pozzolanic reaction was studied by measuring the amount of portlandite that was consumed by the calcined clay at certain curing times by means of thermal analyses. The results are given in Figure 7.8 and as reference two pure montmorillonites, SWy-1and SAz-1, studied in chapter 4 were included. All smectitic samples are marked by a rather slow reaction rate, whereby SM2 is marked by the highest reaction rate in the first 28 days. While SM1, SM3 and SM4 have comparable reaction rates the first 28 days, SM5 reacts somewhat slower.

In comparison with kaolinitic samples, whereby their action is almost completed after 28 days, the smectitic clays still continue to consume portlandite up to 90 days. Nevertheless the reaction rate between 56 and 90 days seems to differ significantly between the samples. SM1 and the two reference samples seem to have the highest reaction rate. For SM5the reaction seemed to be stagnated between 56 an 90 days and most likely most smectite is already consumed. The other three samples SM2, SM3 and SM4 are characterized by an intermediate reaction rate that is only slightly lower than that between 28 and 56 days.

Nevertheless for calcined clays that contain less than 20% of smectite in their bulk composition like sample SM5, the reaction rate decreases considerably after 56 days to a speed of only 0.1 % portlandite/day. Between 56 and 90 days SM1 and the two reference samples seem to have the highest reaction rate. These three samples contain more than 75% of smectite in the original sample and have a reaction rate of approximately 0.16 % portlandite/day. The intermediate samples, SM2, SM3 and SM4 have an average rate of 0.1 % portlandite/day. It can be concluded that the reaction rate at later stage of the reaction, >56 days, is controlled by the amount of smectite that is present in the sample and is not influenced by the actual reactivity. The rate at the beginning of the reaction is however controlled by multiple parameters and determines the actual reactivity at 28 days.

When the actual reactivity is compared, SM2 is the most reactive sample with a portlandite consumption of 32.2% at 28 days (Figure 7.9). This makes SM2 a moderate pozzolanic material. For the other clays the portlandite consumption at 28 days is fairly comparable and ranges between 24.0

and 27.2 %. It is only at longer curing times that the difference in reactivity increases. This effect is the result of the rather slow pozzolanic reaction that is typical for smectitic clay. The reactivity at 28 days is comparable with the 25.7% portlandite consumption of illitic clay calcined at 900°C (chapter 4). Illite was however considered as a poor pozzolanic material and also these smectites, SM1, SM3-SM5, have a low pozzolanic potential.

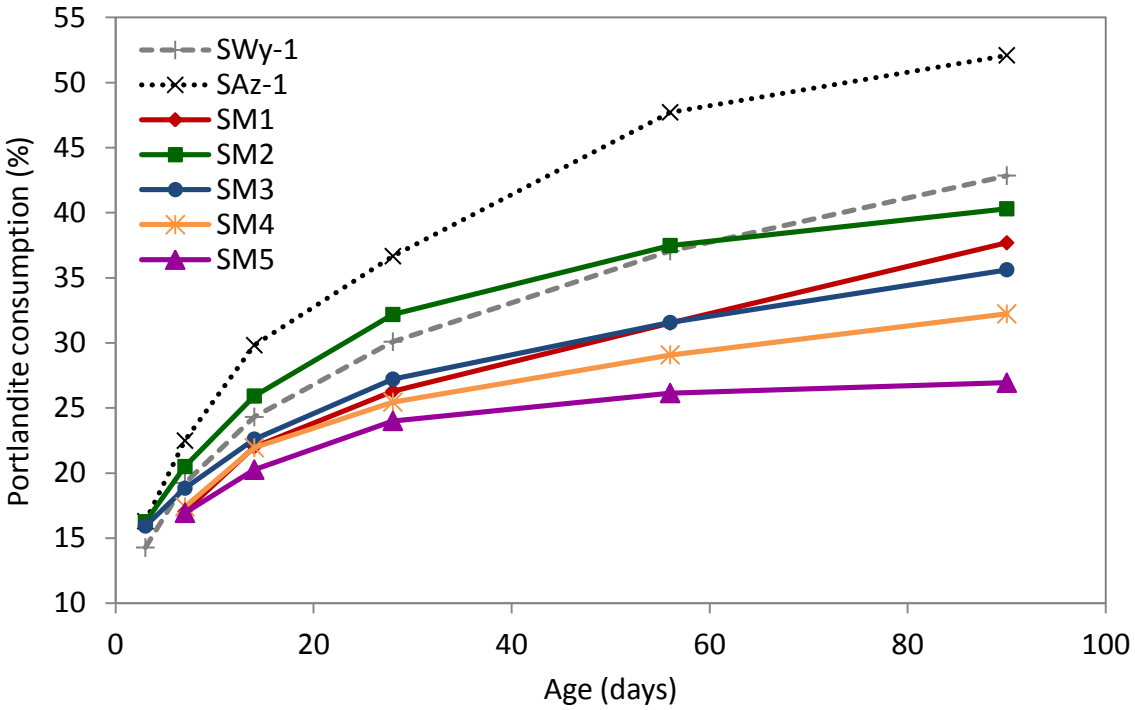

Figure 7.8: *Portlandite consumption over time for the different smectitic clays and two pure smectite reference samples SWy-1 and SAz-1.*

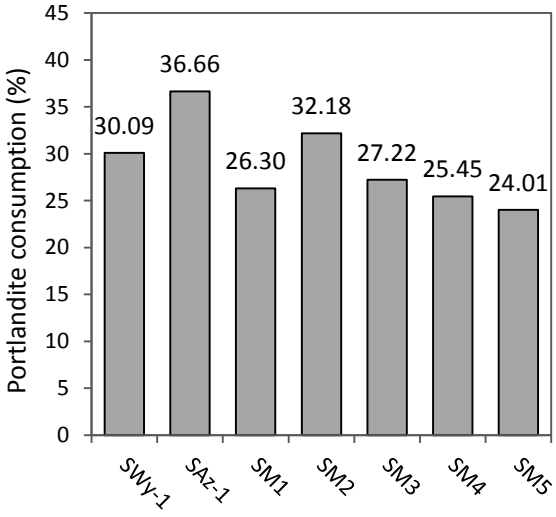

Figure 7.9: *Comparison of the portlandite consumption at 28 days of curing for the smectitic samples and two reference samples SWy-1 and SAz-1.*

7.3.2 CORRELATION BETWEEN REACTIVITY AND CLAY CHARACTERISTICS

The variation of the initial reaction rate of the smectitic samples is controlled by multiple parameters. SM1 has the highest smectite content but shows a rather slow start of reacting which is similar to SM4. This can be ascribed to the very low specific surface area of 1.45 g/m^2 of SM1. This low specific surface area results in less available reaction surface and slows down the initial start of the pozzolanic reaction. SM4 has a somewhat higher specific surface area of 17.4 g/m^2 which improves early portlandite consumption even though the smectite content is limited. Nevertheless this difference in specific surface area can also be partially related to the amount of smectite that is present in the sample, as higher smectite content will provoke additional sintering which leads to a lowering of the specific surface area.

Also the reaction rate at longer curing time is affected by the amount of smectite present in the sample. For calcined clays that contain less than 20% of smectite in their bulk composition, like sample SM5, the reaction rate decreases considerably after 56 days to a speed of only 0.02 % portlandite/day. Samples that contain more than 75% of smectite like SM1 and the two reference samples seem to have the highest reaction rate between 56 and 90 days of approximately 0.16 % portlandite/day. The intermediate samples, SM2, SM3 and SM4 have an average rate of 0.1 % portlandite/day. It can be concluded that the reaction rate at a later stage of reaction, >56 days, is mainly controlled by the amount of smectite that is present in the sample and is not influenced by the actual portlandite consumption, since SM1 is less reactive than SM2 at 28 days.

Not only the reaction rate but also the differences in portlandite consumption can be explained by the clays features. The dominant controlling parameter is the quantity of smectite that was present in the bulk sample. Similar to the kaolinitic samples, in general an increase of the amount of the reactive clay type results in an increase of the pozzolanic reactivity. This effect could clearly be observed in sample SM2 to SM5 that showed a decrease in the portlandite consumption at 28 days according to their lower smectite content (Figure 7.9). Remarkable is that the type of other impurities seems to have very little effect on the portlandite consumption. This is especially surprising for the calcite rich sample SM3, as no clear effect of calcite on the reactivity can be observed. This can be explained by the combined effect of the reduced clay quantity and the finesse of the material. Furthermore, SM1 was marked by the highest smectite content of 78%, but at 28 days both SM2 and SM3 prove to be more reactive. The main reason for this difference can be found in the thermal behavior of the smectite species. The XRD patterns of the calcined SM1 indicated that this smectite did not become entirely amorphous upon calcination at 800 °C and could be considered as semi-crystalline. For the other samples the amorphisation process was entirely complete with little evidence of remaining crystalline parts. As a consequence less Si and Al is present in the amorphous phase of SM1 and the actual portlandite consumption decreases accordingly. The cause of this incomplete amorphisation of SM1 could be found in the thermal analysis results. SM1 was marked by a rather high and broad dehydroxylation temperature, which indicates that besides trans vacant also cis vacant smectite layers are present, resulting in a delay of the amorphisation process. Figure 7.10 demonstrates the effect of the octahedral occupancy on the correlation between the amount of smectite and the portlandite consumption. When all samples are taken into account a rather poor correlation with R^2 of 0.50 was found. However when the clays are subdivided according to their octahedral occupancy two groups can be identified. The first comprises the dominant trans vacant clay that was marked by a complete amorphisation of smectite upon calcination. Within this group a linear correlation with R^2 of 0.941 is present. The second group of dominant cis vacant smectites only consists of two samples, SM1 and the reference sample SWy-1. These two samples lie parallel to the linear regression line of group one. This suggests that a similar amount of smectite results in less pozzolanic reactivity for cis vacant smectitic clays compared to group one. However with only two samples no meaningful correlation can be made.

To be classified as a moderate pozzolanic material, a dominant trans-vacant smectitic clay should contain at least 50% of smectite. When the smectite content is below 50%, the portlandite consumption can be compared to that of an illitic clay calcined at 900°C and is classified as a poor pozzolanic material. However, when mainly cis-vacant smectite is present, the clay is less reactive, since cis-vacant smectites are marked by a higher dehydroxylation temperature and consequently a lower degree of amorphisation compared to trans-vacant smectite when calcined at 800°C. Therefore 50% of cis-vacant clay is insufficient to obtain a moderate pozzolanic material. Moreover even a clay containing 80% of cis-vacant clay only produces a poor pozzolanic material after calcination. As a result cis-vacant smectites are less favorable to be used as a pozzolanic material.

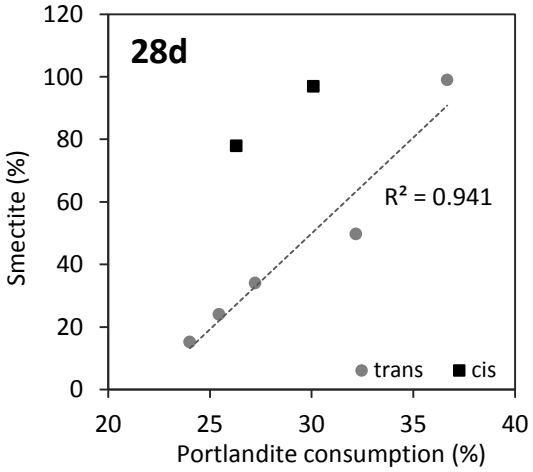

Figure 7.10: *Correlation of the portlandite consumption and the amount of smectite that was preset in relation to the octahedral occupancy, cis or trans vacant, of smectite of the five smectitic clays and the two reference samples. For trans-vacant clay a linear correlation with R^2 of 0.941 was found.*

7.4 POZZOLANIC REACTION PRODUCTS

The reaction products were characterized by thermal analyses and XRD and are similar to the typical reaction products formed in smectite rich clays examined in chapter 4. The DTG patterns in Figure 7.11 show that at 28 days still a considerable amount of portlandite is present. Between 50 and 120 °C the decomposition of C-S-H takes place. C-S-H could be identified in all samples, however the quantities differ considerably according to the reactivity of the sample. As a consequence the most reactive samples, SM2, are marked by the largest C-S-H peak around 100 °C. The AFm phases comprising C_4AH_{13} and mono- and hemicarboaluminate, are decomposed around 136 °C. Since their decomposition temperature largely overlaps for most samples, no clear distinction between these phases can be made. SM3 is marked by a high intensity peak at 147 °C that can be assigned to monocarboaluminate. The formation of this phase can be related to the 17% of calcite that was present in the sample and act as carbon source during the pozzolanic reaction. Nevertheless not all calcite that was present in the calcined clay is consumed at 28 days, since a mass loss due to the decarbonation of the remaining calcite can be detected around 685 °C. In chapter 5 it was demonstrated that kaolinitic clay that contains 15 or even 30% of calcite was also marked with the formation of monocarboaluminate. However at 28 days, all calcite was already consumed and no traces of calcite could be found. For SM3 a longer curing time of 56 days also resulted in the full consumption of calcite and consequently an increase of the amount of hemicarboaluminate. The phenomenon confirms the slow reaction of smectite whereby the consumption of not only portlandite but also of the calcite mixture takes more time. This was also indicated in the study of

Danner (2013) whereby a calcined marl with 18% of calcite had unreacted calcite present in the sample up to 6 months of curing and the amount of monocarboaluminate increases over time.

The results of thermal analyses are confirmed by performing XRD on the calcined clay-lime pastes that were cured for 28 days. The results are visualized in Figure 7.12. Monocarboaluminate and C-S-H could be identified for all samples with reflections at respectively 11.7 and 29.3 °2θ. For the most reactive sample SM2, the presence of C_4AH_{13} at 9.9 °2θ and hemicarboaluminate at 10.8 °2θ is more distinctive than for SM1 and SM5 that only show weak reflections. The high intensity peak of monocarboaluminate for the calcite rich sample SM3 confirms the TGA results. Furthermore, XRD shows the amount of hemicarboaluminate that is formed is negligible. This indicates monocarboaluminate is preferentially being formed, most likely due to the presence of sufficient alumina and surplus of carbon. The lower alumina content of a calcined smectite compared to calcined kaolinitic clay would also further explain the slower rate of the calcite consumption for that was observed for the smectitic clay SM3.

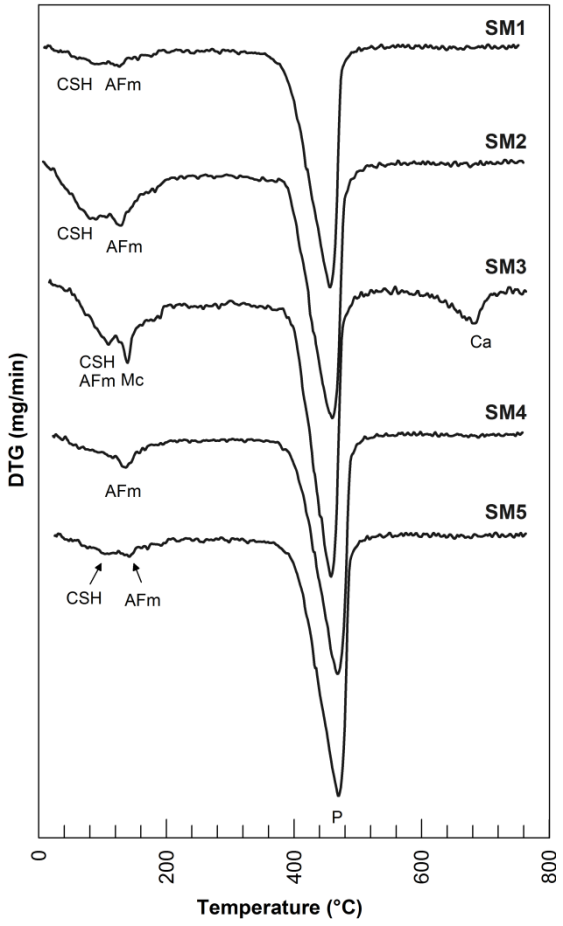

Figure 7.11: *Comparison of the DTG patterns at 28 days of curing. The identified phases are indicated. P: portlandite, CSH: calcium silicate hydrates, Mc: monocarboaluminate, Ca: calcite and AFm phases.*

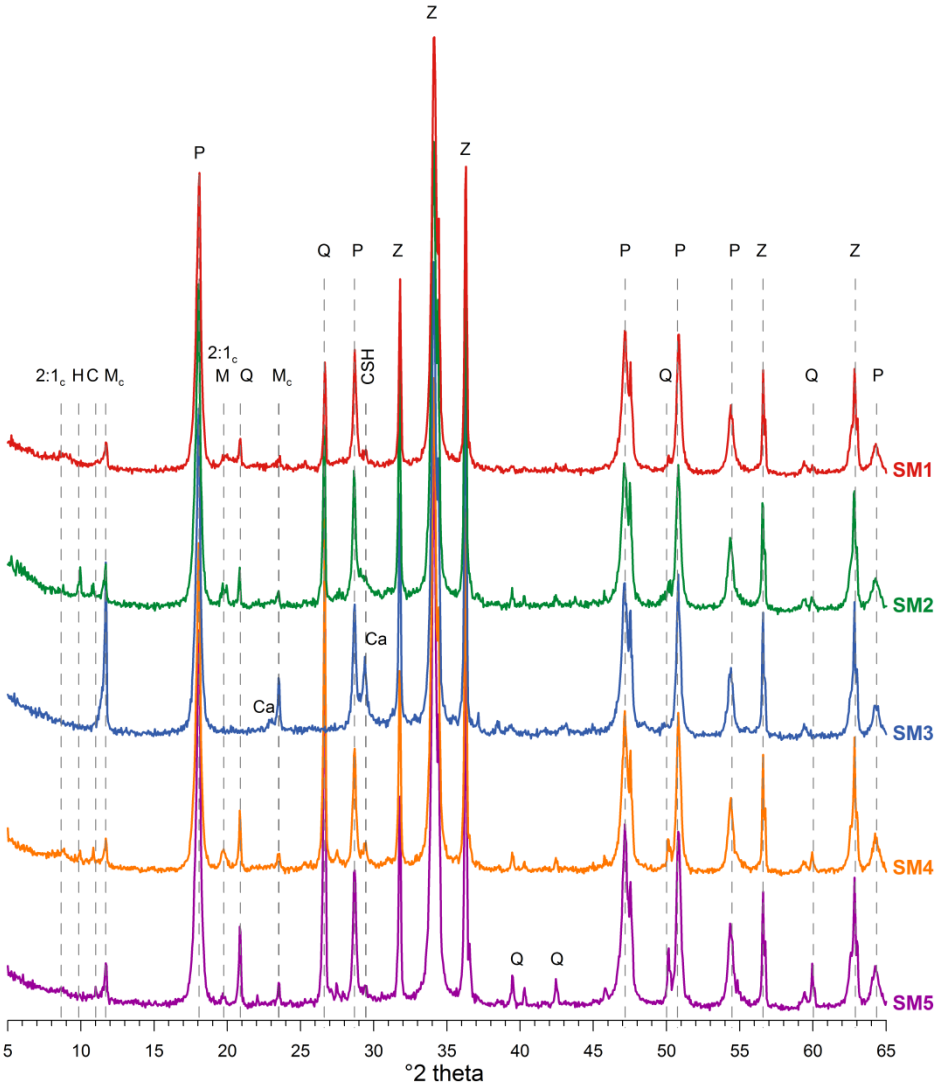

Figure 7.12: *XRD pattern of the calcined clay lime mixture at 28 days of curing. The identified phases are indicated: Z: zincite (internal standard) Q: quartz, 2:1$_c$: calcined 2:1 Al-clays, Ca: calcite, P: Portlandite, Mc: monocarboaluminate, H: hemicarboaluminate, C: C_4AH_{13} and CSH.*

7.5 CONCLUSION

The octahedral occupancy has a major influence on the dehydroxylation temperature of the smectitic clay and as a consequence also on the degree of amorphisation upon calcination. Cis vacant clays become only semi crystalline at 800 °C, resulting in a less reactive material than the fully amorphous trans vacant smectites. In general the portlandite consumption of cis vacant smectite is 7% lower than for trans vacant. Nevertheless it should be taken into account that only two cis vacant smectites were analysed.

Furthermore, for trans vacant clays a good correlation between the percentage of smectite and the reactivity was found. Natural clays with a smectite content of ≥50% provide calcined clays that can be classified as a medium potential pozzolanic material. The contribution to the pozzolanic reactivity of additional parameters is negligible. Nevertheless smectite rich clays are marked with severe sintering

upon calcination, which results in a coarsening of the particle size distribution and decrease of the specific surface area. Without grinding processes, the reactivity drops to low values.

The reaction rate of smectitic clays is rather slow compared to kaolinitic clays and reaction continues up to 90 days. The amount of smectite that is present has a remarkable influence on the reaction rate at longer curing times, 56 – 90 days. Samples that contained >75% smectite reacted 1.6 time faster than samples that contained between 30 and 50% smectite. As a result, a higher smectite content can be of importance when additional strength at a later stage is required.

The reaction products that were formed are fairly similar for all samples and consist of: C-S-H, monocarboaluminate and some minor amount of C_4AH_{13} and hemicarboaluminate. Calcite rich samples produced a higher amount of monocarboaluminate, but the reaction was also rather slow to have a significant effect on the pozzolanic reactivity at 28 days.

It can be concluded that to obtain a medium pozzolanic material it is best to select trans vacant smectitic clays that contain at least 50% of smectite. Clays with a lower amount of smectite should be combined with kaolinite rich clay to assure a faster reaction rate in the early stage of the reaction and still obtain an intermediate pozzolanic material.

CHAPTER 8

CASE STUDY: CLAYS OF THE LATNESKOYE DEPOSIT

Natural clay deposits are widespread and abundantly available with large reserves and variable compositions. To optimize the sustainability and the ecologic effect of mixed cements by using calcined clays as a cement replacement, it is best to use local reserves to minimize transportation distances. Several countries already started to investigate the pozzolanic potential of their local clay resources, especially in the vicinity of the cement industry (Alujas et al., 2015; Badogiannis and Tsivilis, 2009; Cara et al., 2006; Castillo et al., 2010; Chakchouk et al., 2006; Fernandez, 2009). Furthermore, special attention is given to waste products and clays that are less pure since those resources are economically more feasible and can already yield fairly good results regarding their achieved strength and their potential as SCM (Snellings et al., 2016). The use of local clays is most likely one of the best ways to lower the energy cost of the cement production and diminish the amount of CO_2 that is emitted. The kaolinite rich clays of the Latneskoye deposit are marked by a broad variety in mineralogical composition, especially regarding the proportion of clay minerals like kaolinite and smectite, resulting in several distinguishable clay grades. The large reserves and the presence of a nearby cement industry makes this deposit suitable to provide a sustainable future for the local cement industry. Furthermore, some of the clay deposits are covered by a thick layer of chalk that can also be used in the cement production process. Since clay deposits are complex regarding mineralogy, chemistry and the structure of the individual clay minerals, research is necessary to understand the reaction mechanism of these materials. Therefore the main goals for this case study are:

- *Clarify the effect of the calcination process*
- *Identify the parameters that control the pozzolanic reaction*
- *Determine the pozzolanic potential of the Latneskoye deposit*

8.1 GEOLOGICAL SETTING

The Latneskoye clay deposit is located in the west of the European part of Russia in the Voronezh Oblast, a district of the Russian Federation. The Voronezh oblast district is located 470 km south - South east of Moscow and approximately 180 km west from the Ukrainian border (Figure 8.1). The main city Voronezh is located 15 km east of the operating clay sites. The commercial production, which started in the beginning of the 20th century, mainly focused on the manufacturing of refractory

ware and ceramics (Muzylev et al., 2006). The low iron and sulphur content and high plasticity makes these clays ideal for the production of ceramics, porcelain and faience ware (Levitskaya et al., 2002). Other areas of application are the use of these clays in the production of white Portland cement to enhance the whiteness of the cement and to control its chemical composition. Moreover, the presence of coal can act as fuel and thereby the consumption of gas during the production process of Portland cement can be reduced by 15 – 20% (Muzylev et al., 2001). The clay deposit occupies approximately 20 km^2 and occurs along both sides of the Devitsa river. The deposit is characterized by horizontal clay lenses, which are a couple of hundred meters wide and change rapidly in thickness and occurrence, resulting in lateral heterogeneity. The thickness of these clay bodies fluctuates between 1 to 4 m and the average overburden is 35 to 50 m. The clays can be characterized as kaolinitic clays with kaolinite percentages varying between 70 and 90% (Bortnikov et al., 2012).

Figure 8.1: *Map of Russia with indication of the Voronezh oblast and the study area. Moscow is marked with an asterix (Van Den Heuvel, 2015).*

The Cretaceous layers, which include the mined Latnekoye clays, were deposited discordant on the Devonian and Carboniferous layers. The formation of the Latneskoye kaolinitic clays can be related to the geological evolution in the Early Cretaceous. After a period of uplift and intense weathering, the denudation plain was largely replaced by alluvial, lagoon-deltaic and shallow marine plains, grading northwards (Bortnikov et al., 2011). During the Aptian, the Latneskoye area was situated in the middle of the northern slope of the Voronezh anticline and the environment was dominated by alluvial floodplains with lacustrine-swampy facies Figure 8.2. The weathered Devonian crust covered 80% of the surface and acted as a primary source for the kaolinite clays. Denudation, transportation over more than 300 km and redeposition of the weathered crust material resulted in mechanical disintegration of the kaolinite clay. These phenomena provoke changes in grain size, crystal morphology and in the degree of ordering of the structure (Bortnikov et al., 2013). The clays can be marked as monogenetic terrigenous redeposits. Simultaneously authigenic kaolinite was formed due to partial dissolution of terrigenous kaolinite during diagenesis. This process was driven by the presence of organic material, since organics control the chemical environment and act as a matrix for pseudomorphous replacement by aluminosilicate minerals (Bortnikov et al., 2012). This formation of

kaolinite happens in several phases. The original illite present in the Devonian crust is replaced by montmorillonite, after which it is replaced by mixed layer montmorillonite-kaolinite. The latter is replaced by kaolinite and sometimes gibbsite (Bortnikov et al., 2012). The combination of these two formation processes make the Latneskoye clays a polygenetic material with a polymineral composition dominated by kaolinite.

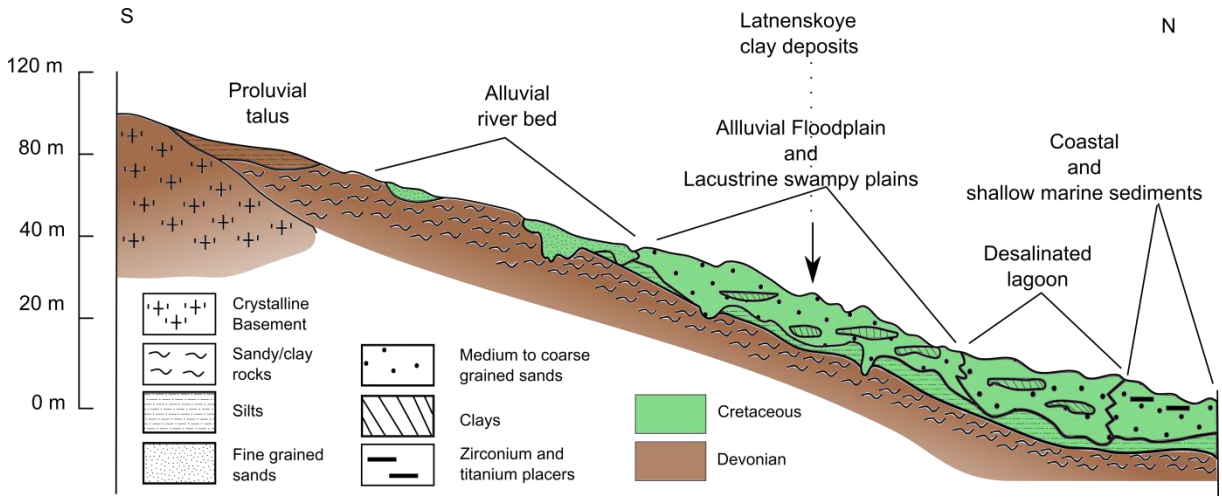

Figure 8.2: *South to North paleofacies profile of the Voronezh anticline during the Aptian stage. The different depositional environments and the location of the Latneskoye clays are indicated on the figure (modified after Sirotin et al., 2005).*

Table 8.1: *Lithostratigraphy and geological sequence of the Voronezh Oblast. The thickness and brief description of each sequence is added. The Latneskoye clays belong to the refractory clays of the Aptian.*

AGE		LITHOLOGY	THICKNESS (meters)	DESCRIPTION
QUATERNARY		Topsoil, moraine, clays & loam	1 - 26	Brownish yellow loam and moraines with clay material
NEOGENE		Sands & Clays	2 - 4	Reddish brown clay
CRETACEOUS	TURONIAN/ CONIACIAN	Chalk	0 – 22	White chalk with coarse horizontal bedding
	ALBIAN/ CENOMANIAN	Clay band (smectitic)	7 - 25	Greenish clay
		Glauconitic sand & phosphate bands		Greenish grey glauconitic sands containing 2 or 3 phosphate bands
	APTIAN	Nadglinyanaya: White & Yellow Sand	4 - 8	Fine to coarse grained sands. Yellow (Fe) at the bottom and is more white at top.
		Refractory clay: Kaolinitic Clay	2 - 4	Clay sequence is sandier at base, with higher alumina clays in the centre & carbonaceous at the top.
		Podglinyanoy : Sand & Gravel	15	Very coarse angular sands and gravel with fining upwards trend

The Aptian deposits can be subdivided in three main layers (Table 8.1): Podglinyanoy, the horizon underneath the refractory clays, the refractory clays and Nadglinyanaya, the layer above the refractory clays. The thickness of the refractory clay layers is variable due to wavy bedding, intercalation of sand lenses and thinning towards the south strike. The clays are light grey/cream to black depending on the carbon content.

After the Albian a transgression resulted in a change of depositional environment. The continental deposits were covered rapidly by shallow marine sediments which were deposited in a calm hydrodynamic regime. The stage was marked by sands with horizons rich in glauconite. In the Cenomanian the basin deepened resulting in an increase of silty and clayey material. This resulted in a succession of glauconite sands followed by green clays rich in both glauconite and muscovite (Sirotin et al., 2005). In the Neogene – Pliocene alluvial sediments were deposited which consist of reddish brown clay with carbonate concretions of iron and magnesium hydroxides (Muzylev et al., 2001).

8.2 SAMPLING AND MATERIALS

The Latneskoye clays were studied and sampled in four different Sibelco quarries and green fields in the framework of the master thesis of Caroline Van den Heuvel (Van den Heuvel, 2014). The location of these areas is indicated on Figure 8.3. The results of the fieldwork show that there is a clear difference in the lithological sequence of the clay benches when those 4 quarries are compared (Figure 8.3). The Belly Kolodets A quarry is characterized by two separate clay benches with a more coarse sand layer in the middle and a yellow iron-rich clay at the bottom. The Belly Kolodets B quarry comprises a continuous clay package. The Belly Kolodets Souteast area is marked by high clay content and minor sand. The clay bench in the Sredny quarry, which is located the most north, contains a sand layer at the bottom and has a lignite layer at the top. In total 17 clay samples were collected and analyzed in order to reflect the vertical and lateral discontinuity, since the clays are deposited as lenses. The difference in mineralogy within the refractory clay bench was taken into account and 15 samples were chosen to cover the different clay qualities that are present. During sampling, an estimation of the clay quality was made based on the quartz content. Furthermore, 2 samples of clay-rich overburden, namely a green clay of the Cenomonian and a red clay of the Neogene, were sampled. An overview of the collected samples is given in Table 8.2.

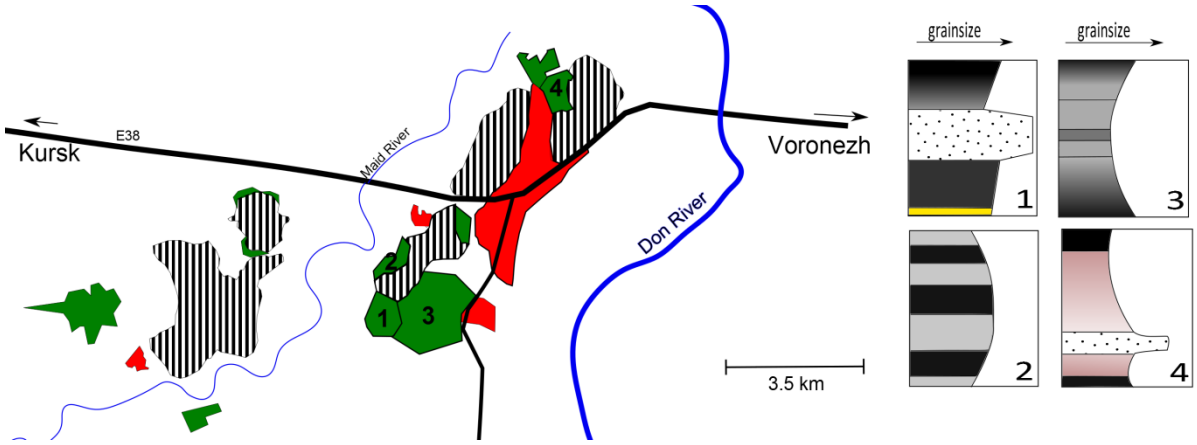

Figure 8.3: *Overview of the Latneskoye deposit with the quarries and reserves (green), resources (red) and mined out areas (hatched pattern). The characteristic general sequence of visited and sampled quarry is given, 1: Belly Kolodets A, 2: Belly Kolodets B, 3: Belly Kolodets South East and 4: Sredney (adapted from* Van Den Heuvel, 2015*).*

Table 8.2: *Sample list with locations (BK SE: Belly Kolodets Southeast, SR: Sredney, BK B: Belly Kolodets B and BK A: Belly Kolodets A), age, brief description and clay qualities (discussed in section 9.4.1).*

	Sample nr	Location	Age	Description	Clay quality
1.	VO14CV15	BK SE	Aptian	Grey clay	LTK
2.	VO14CV18	BK SE	Aptian	Black clay	LT2
3.	VO14CV19	BK SE	Aptian	Brown clay iron rich	LT0
4.	VO14CV22	BK SE	Aptian	Light grey clay	LT0
5.	VO14CV24	BK SE	Aptian	Grey clay	LT1
6.	VO14CV25	BK SE	Aptian	Grey clay	LT1
7.	VO14CV27	BK SE	Aptian	Dark grey clay	LT3
8.	VO14CV29	BK SE	Aptian	Dark grey to black clay with sand layers	LT2
9.	VO14CV30	BK SE	Aptian	Grey clay with sand layers and pyrite	LTPK
10.	VO14CV33	BK SE	Aptian	Organic rich dark grey clay with pyrite	LTPK
11.	VO14CV35	SR	Aptian	Lignite clay	LTU
12.	VO14CV37	SR	Aptian	Grey clay with pyrite	LT1
13.	VO14CV41	SR	Aptian	Light grey sandy clay	LTPK
14.	VO14CV48	SR	Cenomanian	Green to red glauconite clay	Overburden
15.	VO14CV52	BK B	Aptian	Light grey clay	LTU
16.	VO14CV71	BK A	Aptian	Brown to yellow clay	LTKj
17.	VO14CV78	BK A	Neogene	Red clay	Overburden

8.3 CHARACTERIZATION

8.3.1 CHEMISTRY

The elements measured are visualized in box plots (Figure 8.4), since box plots give information on the quartiles (boxes), median (middle line), the maximum and the minimum (whiskers) and the outliers (cross). The box plots for SiO_2 and Al_2O_3 are both right skewed distributed and extend over a fairly broad range, especially SiO_2. The outliers of the Al_2O_3 distribution are the two overburden clay samples (CV48 and CV78). Both clays are sandier and contain less clay, resulting in lower Al_2O_3 contents. The LOI has almost a normal distribution, the elongated whisker indicates the presence of some organic and lignite rich clays with high LOI values. The box plot of Fe_2O_3 shows a right skewed distribution indicating most samples have a rather low Fe_2O_3 content of around 1.1%. This is also confirmed by the long top whisker caused by three samples with a rather high Fe_2O_3 concentration, namely the two overburden clays, the red colored clay CV78 and the green glauconitic clay CV48, with concentrations around 5.3%. Also the brown yellowish clay CV71 is iron rich (±4%). The amount of TiO_2 is concentrated around 1.8% and is normal distributed without outliers. CaO is distributed almost normal with two outliers, the overburden sample CV78 and the lignite clay CV35. The distribution of MgO and K_2O shows a rather narrow concentration range, between 0.1 and 0.6%, with both two clear outliers with higher concentration. These two samples are again the two overburden

samples CV48 and CV78. Also the amount of Na_2O and P_2O_5 for these two clays provokes outliers. The distribution of MnO is very narrow with all samples having a concentration of 0.01 or 0.02%, only sample CV78 has a higher concentration of 0.32%. For all clays the MgO and alkali content (expressed in Na_2O equivalent) does not exceed the top border of 4% which is necessary to be qualified as an economic potential metakaolin deposit.

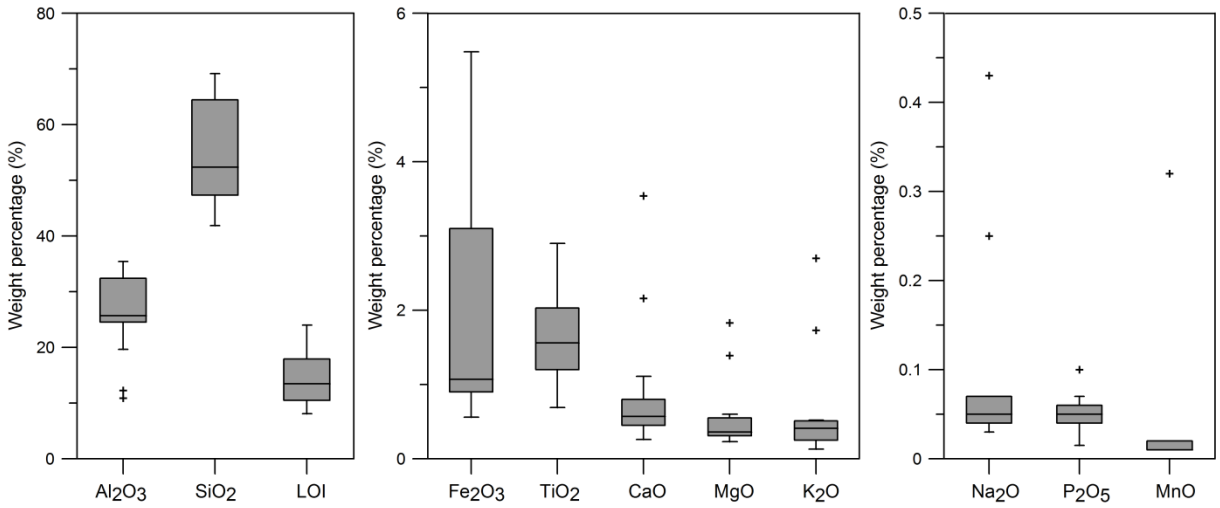

Figure 8.4: *Box plots of the main chemical elements (Al_2O_3, SiO_2, Fe_2O_3, TiO_2, CaO, MgO, K_2O, Na_2O, P_2O_5 and MnO) and the LOI.*

The clay quality can be determined on the basis of the bulk chemical composition. The combination of three main parameters is decisive for each clay quality (Table 8.3). The first factor is the Al_2O_3 content which is related to the plasticity of the clay. The Fe_2O_3 content is taken into account due to the influence of iron on the firing color. Normally the Fe content varies between 0 and 2 % in the Latneskoye clays with an exception of one quality, LTKj, with values above 6%. The last parameter is the LOI value which reflects both the amount of clay and the amount of organic material that are present. For most clay qualities both a light and a dark, organic-rich variety exists. The lignite-rich clay, LTU, with LOI values between 20 and 40% is classified as a separate clay quality. In total there are thirteen different clay qualities that can be distinguished in the Latneskoye clay deposit when light and dark varieties are included. Since the Al_2O_3 and Fe_2O_3 content to determine the clay quality is estimated both in literature and by Sibelco on the fired clay after the LOI was determined, results were recalculated so that the results can be correlated to the different clay qualities.

Table 8.3: *The thirteen Latneskoye clay qualities as determined by Sibelco on fired clays* (Muzylev et al., 2006)*. The dark variant is indicated in bold*

	LT0	**LT1**	**LT2**	**LT3**	**LTPK**	**LTK1**	**LTK3**	**LTKj**	**LTU**
$\%Al_2O_3$	≥ 39	37 to< 39	33 to< 37	28 to< 33	23 to < 28	15 to < 23	15 to <23	15 to <23	≥ 28
$\%Fe_2O_3$	≤ 1.5	≤ 2.0	≤ 2.0	≤ 2.5	No spec	< 2.0	< 2.0	< 6.0	≤ 3.5
% L.O.I.		≤ 14	≤ 18	≤ 14	≤ 14	≤ 10		≤ 14	≤40
	≤ 15	**≤ 18**	**≤ 20**	**≤ 20**	**≤ 18**		**≥10**		

The three quality determining parameters are plotted in a bubble plot (Figure 8.5), with Al_2O_3 and LOI on the axes and the Fe_2O_3 content represented by the size of the bubble. There is a positive correlation between Al_2O_3 and the LOI. This indicates the LOI is mainly influenced by the amount of clay present in the sample, which increases the Al_2O_3 content. This can be explained since clays are dehydrated and dehydroxylated, which results in a mass loss. However, four samples with high LOI content are not following the main trend. These samples are marked in the sample description as dark grey to black, lignite rich clays and are classified as the dark variety of that clay quality or as LTU, a lignite rich clay. Therefore the amount of organics that is present in these samples influences the LOI significantly and a clear distinction between organic rich and organic poor clays can be made. Nevertheless, also decarbonation can influence the LOI and a positive correlation between CaO and LOI can be found. However the amount of CaO that is present in the clay is for most (except for CV35 and CV78) samples rather low, around 0.6% and the influence is negligible. The Fe_2O_3 is the determining factor for the LTKj clay quality which has similar Al_2O_3 content and LOI compared to the surrounding samples. The appropriate clay grade assigned to each sample is listed in Table 8.2.

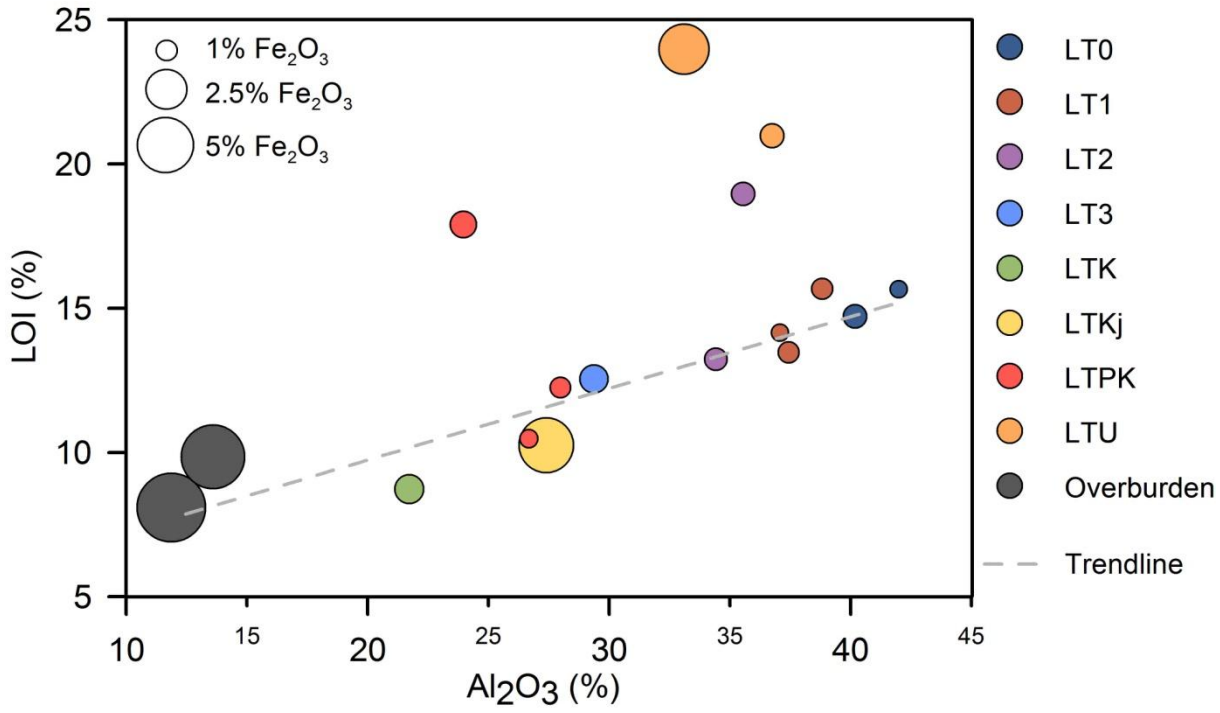

Figure 8.5: *Bubble plot of the three main parameters Al_2O_3 content, LOI value and Fe_2O_3 content, indicating the different clay qualities*

8.3.2 MINERALOGY

The bulk mineralogical composition of all 17 samples was analyzed. The qualitative composition of the clays is fairly similar, consisting predominantly of kaolinite, quartz, and 2:1 clay. The box plot in Figure 8.6 indicates however that quantitatively there is a broad range of compositions. Both quartz and kaolinite are right skewed distributions with limited whiskers. The kaolinite distribution varies between 46 and 70% and contains two outliers CV78 and CV48, which are the two overburden samples. The distribution of the 2:1 clays is normal and much more narrow ranging between 9 and 17%. All samples of the kaolinite clay bench contain only aluminum rich 2:1 clays. The two overburden samples contain besides 2:1 Al-clays, also 2:1-Fe clay which resulted in higher total 2:1 clay concentrations of 32 and 28% respectively.

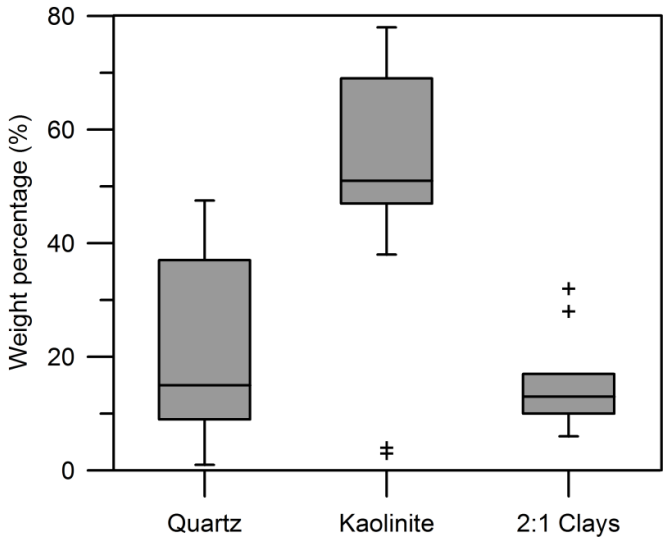

Figure 8.6: *Box plot of the three main mineral components Quartz, Kaolinite and 2:1 clays, including Al- and Fe-2:1 clays. Outliers are marked with a cross.*

The mineralogical composition is visualized in the bar chart, Figure 8.7. The variation in the kaolinite content of the samples is clearly visible. Most samples contain a significant amount of amorphous material which represents the presence of organics. The lignite rich clays CV35 and CV52 contain the highest quantity of amorphous material, of 13 and 17% respectively. In general the darker grey clays like CV27, CV29 and CV33, have high amorphous content between 8 and 11%. Other impurities that are present are muscovite, Ti-oxide (mainly anatase), feldspar, Fe-(hydr)oxides (hematite and goethite) and the Al-hydroxide gibbsite. The presence of gibbsite can be attributed to the formation process of these clays as gibbsite is additionally formed during the decomposition of kaolinite-smectite mixed layer to kaolinite (Bortnikov et al., 2012). The overburden sample CV78 also contains 4% calcite.

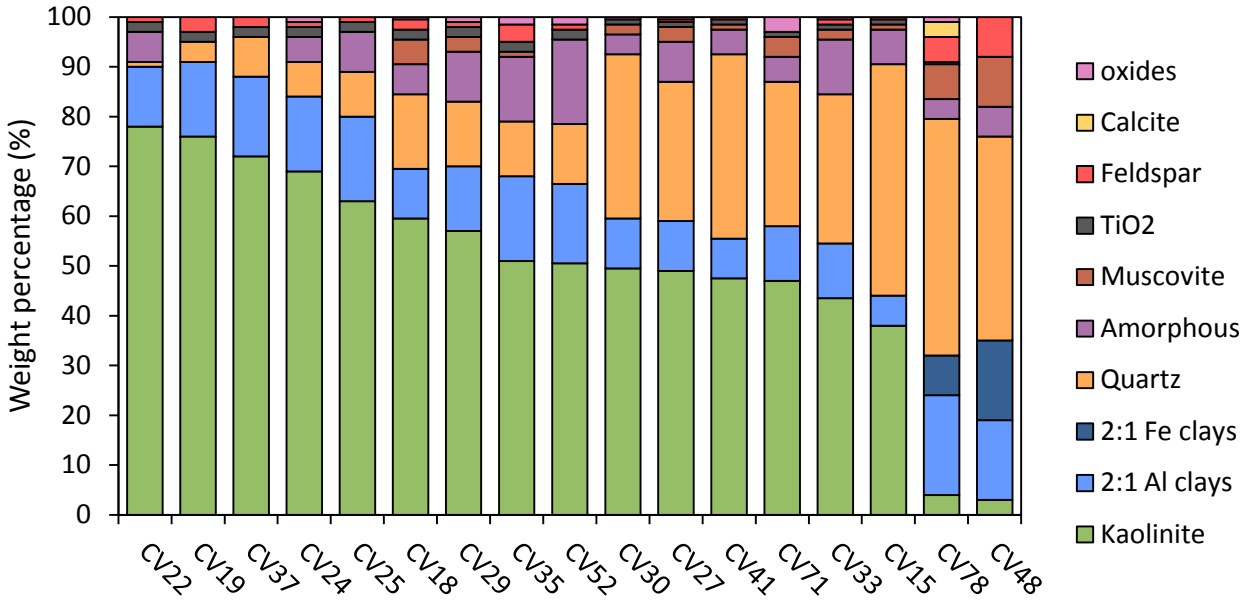

Figure 8.7: *Mineralogical bulk composition of the 17 clay samples expressed in weight percentage.*

The clay fraction (<2 µm) was separated in order to gain a more detailed clay mineralogy (Figure 8.8). Two typical diffraction patterns of the kaolinitic bench (CV25 and CV35) are given in Figure 8.9. Three distinctive basal reflections of kaolinite are present at 7.2 Å (001), 3.6 Å (002) and 2.4 Å (003). In the two example samples, CV25 and CV35, respectively 49 and 67% of kaolinite is present in the clay fraction. Smectite can be identified by the shift of the 001 reflection 14.2 from to 17 Å when glycolated due to its swelling behavior. Sample VC25 also contains a minor amount of illite, as shown by the 001 and 002 reflections at 10 and 5 Å. Chlorite was only detected in a small amount (2%) in sample CV33.

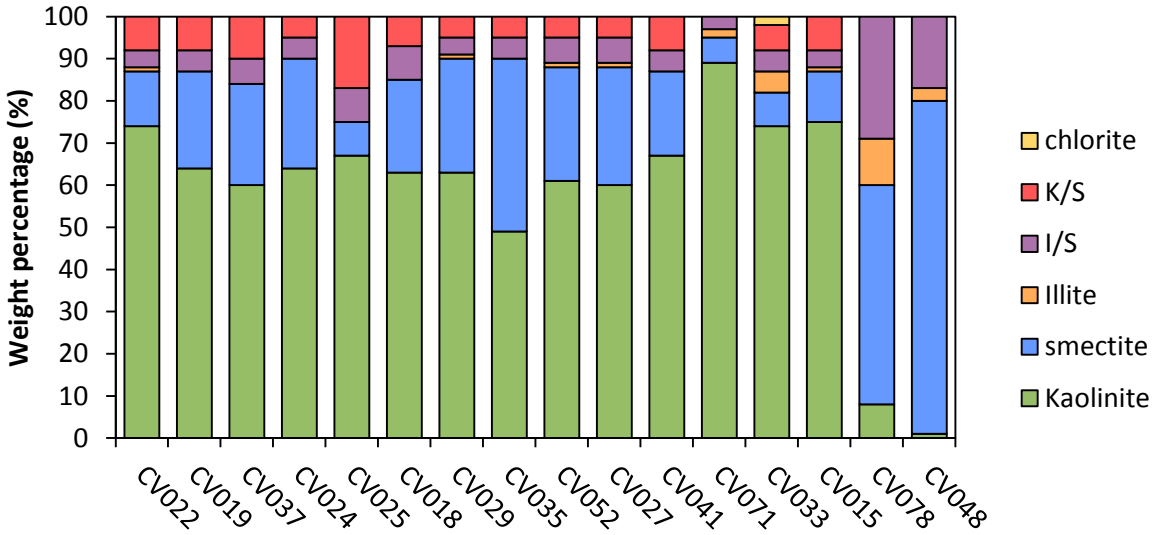

Figure 8.8: *Overview of the mineralogical composition of the clay fraction <2 µm. The samples are ordered according to the decreasing amount of kaolinite in the bulk composition.*

The differences between the air dried and the ethylene glycolated pattern at 3 - 3.4 Å indicate the presence of mixed layer clay minerals. This is an illite-smectite mixed layer with a ratio of 30:70 and a Reichweite R=0, which indicates the layering is random. A broader shoulder next to the 001 reflection of kaolinite is identified as kaolinite-smectite mixed layer, with a ratio of 73:27. The content of this K/S layers varies between 5 to 17% in the clay bench samples.

The XRD patterns of the overburden samples vary from those of the clay bench samples and are given in Figure 8.9. The glauconite rich clay CV48 consists mainly of smectite (79%) and RO illite-smectite 65:35 (17%) in the clay fraction. Minor amounts of illite (3%) and kaolinite (1%) are present. The red clay CV78 has the same dominant clay minerals smectite (65%) and RO illite-smectite 65:35 (29%). The content of illite (8%) and kaolinite (11%) is slightly higher than for CV48.

The distribution of the clay minerals present in the samples is shown in Figure 8.10. Kaolinite in the clay fraction shows a similar right skewed distribution as in the bulk sample. Kaolinite is present in all clay samples with a mean value of 67%. The two outliers are the overburden samples (CV48 and CV78). The left skewing distribution of smectite is opposite to that of kaolinite. This is confirmed by the fact that a negative correlation between kaolinite and smectite exists. Illite is only present is some samples in a limited amount between 1-3% and has therefore a narrow distribution with CV33 as outlier.

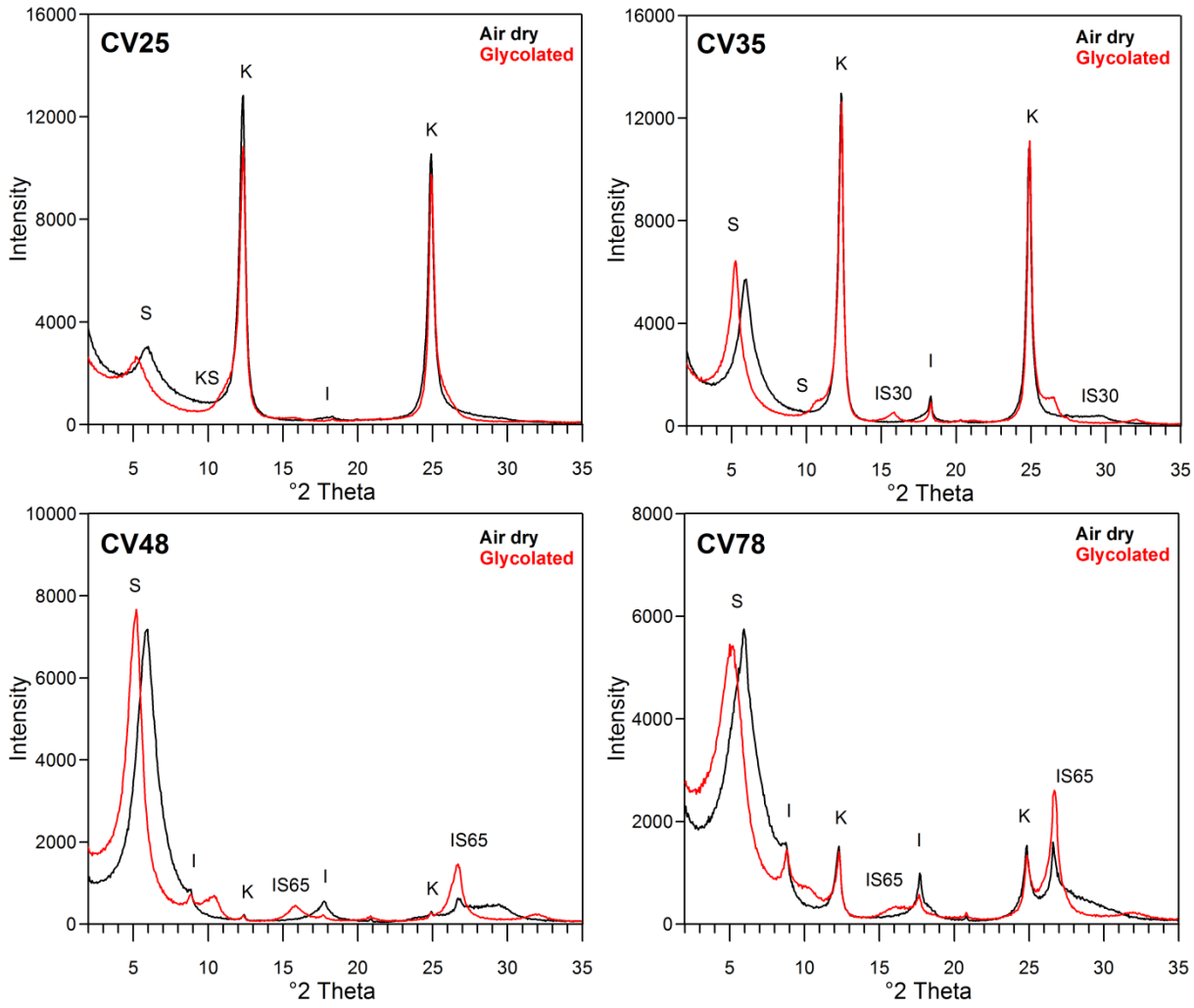

Figure 8.9: *XRD patterns for air dry and ethylene glycolated state of the oriented slides of the clay fraction <2µm of samples CV25, CV35, CV48 and CV78. The phases that are present are indicated: K: kaolinite, S: smectite, I: illite, KS: 73:27 kaolinite smectite mixed layer, IS30: 30:70 illite smectite mixed layer and IS65: 65:35 illite smectite mixed layer.*

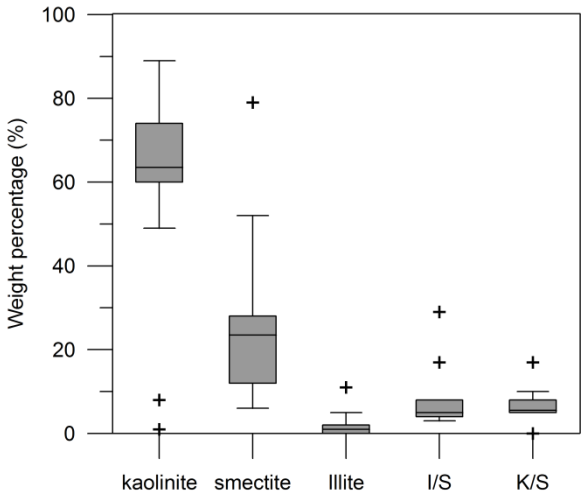

Figure 8.10: *Box plots showing the distribution of the mineralogical composition of the clay fraction (<2µm).*

8.3.3 DEGREE OF ORDERING

Besides qualitative and quantitative information of the bulk mineralogical composition, XRD patterns can give an estimation of the degree of ordering of kaolinite. The pattern of the most kaolinite rich sample CV22 shows that in the region of 19 to 22°2θ the kaolinite reflection peaks are not that well developed. This indicates the degree of ordering is rather low, because a well ordered kaolinite would have three distinctive reflection peaks. For a more quantitative approach two different methods were applied, the Hinckley index (HI) and the index of Lietard (R2) (Table 8.4).

Both the HI and R2 are fairly similar for all kaolinite bench samples. The kaolinite content of the overburden samples CV48 and CV78 was too small to determine the degree of ordering. Since the HI is influenced by the amount of quartz that is present in the sample it was not possible to determine the HI correctly for the quartz rich samples CV15 and CV41. The R2 is less influenced by the presence of impurities and could still be defined. The HI for the clay bench samples varies from 0.14 to 0.25, with sample CV71 as an exception with an index of 0.82. This indicates most samples are disordered or low ordered kaolinitic clays with exception of CV71. The R2 index confirms the similarity in the degree of ordering ranging between 0.36 and 0.49 for most clays. Sample CV71 has again the highest value of 0.60 indicating this clay is more ordered than the others. However, values of R2 should be higher than 0.7 to be classified as ordered and can therefore best be classified as medium ordered.

Table 8.4: *Hinckley index (HI) and index of Lietard (R2) to estimate the degree of ordering of kaolinite in the clay samples. For some samples the HI or R2 could not be determined (n.d.)*

Sample	HI	R2	Sample	HI	R2
CV15	n.d.	0.49	CV33	0.19	0.49
CV18	0.23	0.48	CV35	0.14	0.45
CV19	0.24	0.46	CV37	0.15	0.44
CV22	0.25	0.44	CV41	n.d.	0.36
CV24	0.16	0.45	CV48	n.d.	n.d.
CV25	0.20	0.45	CV52	0.24	0.45
CV27	0.24	0.42	CV71	0.82	0.60
CV29	0.18	0.38	CV78	n.d.	n.d.
CV30	0.25	0.43			

8.3.4 CORRELATION BETWEEN CHEMISTRY AND MINERALOGY

In the previous paragraph each sample was assigned to a certain clay quality depending on the Al_2O_3, Fe_2O_3 content and LOI values. The Al_2O_3 content is influenced by the amount of kaolinite present in the clay. Other minerals rich in alumina are the additional clay minerals illite, smectite, mixed layer minerals and muscovite. Due to the domination of kaolinite as clay mineral the Al_2O_3 content can, however, be directly correlated to the kaolinite content (Figure 8.11) with a correlation coefficient R^2 of 0.95. Regarding the clay quality the high Al_2O_3 clay grade LT0 also contains the highest amount of kaolinite and the kaolinite content decreases according to the grade Table 8.5.

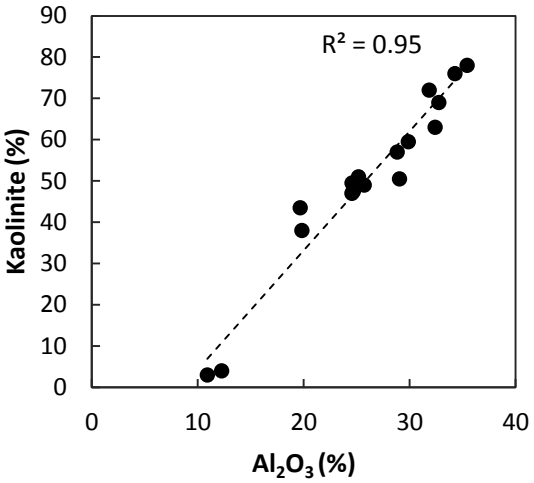

Figure 8.11: *Correlation between kaolinite and Al_2O_3 %. The dashed line represents the regression line with the regression coefficient R^2 of 0.95 %.*

Table 8.5: *Overview table of the average bulk mineralogical composition of each clay grade. The number of samples per grade is given in the second column.*

Quality	# Samples	Kaolinite	2:1 Al clays	Quartz	Amorphous	Muscovite	Anatase	Feldspar	Oxides
LT0	2	77	13.5	2.5	3	0	2	2	0
LT1	3	68	16	8	4.3	0	2	1.4	0.3
LT2	2	59	11.5	14	8	4	2	0.75	0.75
LT3	1	49	10	28	8	3	1	0	1
LTPK	3	48.5	9	33.3	5.7	1.7	1	0.5	0.3
LTK	1	38	6	46.5	7	1	1	0.5	0
LTU	2	50	16.5	11.5	15	0.5	2	2.25	1.5
LTKj	1	47	11	29	5	4	1	0	3

Mineralogical changes upon calcination

During calcination the clay minerals are dehydrated and dehydroxylated resulting in a transformation to high temperature phases like the conversion of kaolinite to metakaolin. Depending on the structure of the clay minerals the decomposition and amorphization process can be different. The XRD pattern of sample CV35 shows the pattern before and after calcination at 800°C. Non-clay minerals like quartz, anatase and feldspar remain unaltered while the reflections of the clay minerals are changed. Kaolinite has become completely amorphous and no reflections are visible in the calcined pattern. Instead an amorphous bump between 20 and 30°2θ is visible. The 2:1 Al-clays are also decomposed, as visible by the disappearance of the 001 basal reflection. The 2:1 Al-clays of CV35 consisted of smectite, K/S 73:27 mixed layer and I/S 30:70 (Figure 8.8). This indicates the smectite present in the sample becomes completely amorphous at 800°C. The amount of illite that is present in the sample is derived from the I/S 30:70 and is therefore very limited. Since illite does not decompose entirely at 800°C, a small enhancement of the background at 8.7°2θ might indicate the presence of some unaltered illite in the calcined sample. For the overburden sample CV78, which is

richer in illite, the remaining reflection of illite are clearer, especially the 001 reflection at 8.7°2θ. Another transformation that can be observed in the iron rich samples is that goethite is transformed to hematite upon calcination or hematite is formed additionally.

The calcination temperature has a major influence on the degree of dehydroxylation and amorphization of the clay sample and therefore it will also influence the pozzolanic potential of the sample. Therefore two samples (CV22 and CV25) were calcined at two different temperatures, 800°C and 650°C. The calcination temperature of 800°C is required in order to assure smectite is decomposed and optimally activated, as was shown in Chapter 4. Kaolinite dehydroxylates in the temperature range of 530°C to 630°C, so 650°C is sufficient to have made all kaolinite present in the sample amorphous. Both samples consist of a mixture of kaolinite, smectite and K/S 73:27. However CV25 contains more 2:1 Al-clays while CV22 is more kaolinite rich. The differences in the mineralogical changes during calcination at different temperatures of sample CV22 are visualized in the XRD pattern Figure 8.12. In general the pattern of the clay calcined at 650°C and of that at 850°C does not differ substantially. However the 2:1 Al-clays clay reflection in the region around 5 – 10°2θ is more pronounced for the sample calcined at 650°C. Moreover, this region is not much changed when the raw bulk sample and the calcined (650°C) are compared. Therefore the calcination process has not yet influenced the structure of the 2:1 Al-clay considerably. By increasing the calcination temperature to 800°C the structure of smectite is altered and the amorphous content of the sample increases. This is reflected by the increase of the hump between 21 and 25°2θ. Similar results were found for sample CV25

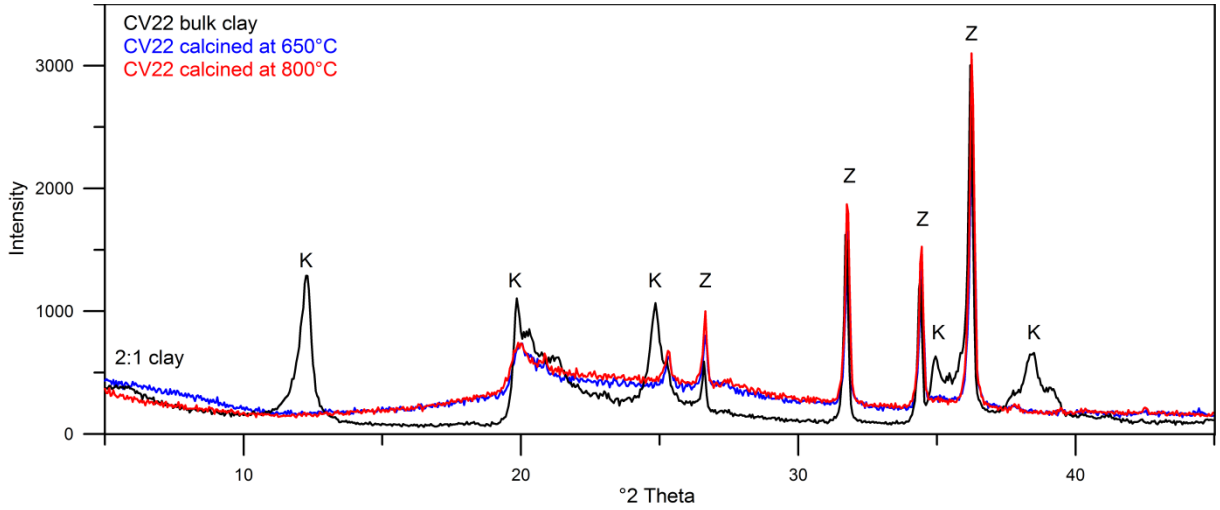

Figure 8.12: *XRD pattern of sample CV22 of the raw bulk sample, calcined at 650°C and at 800°C. K: kaolinite, Z:zincite, 2:1: 2:1-Al clays.*

8.3.5 GRAIN SIZE ANALYSIS

The grain size distribution was determined by laser diffraction for all clays in both the original and calcined state. For the raw samples two different groups can be subdivided according to their grain size distribution (Figure 8.13 and Figure 8.14). The first group, group 1, consists of a polydisperse particle distribution with multiple peaks around 0.2, 10, 50 and 200 µm. This grain size distribution group consists of the samples CV15, CV27, CV30, CV33, CV35 and CV71. Sample CV27 represent the typical grain size distribution of this group and its grain size distribution is given in Figure 8.14. The second group (2) is bimodal with the two population peaks around 0.4 and 6 µm and is more fine grained compared to the first group. The samples CV18, CV19, CV22, CV24, CV25, CV29, CV37 and CV52 belong to this group. Regarding their mineralogical composition it is understandable that the clays of group 2 are finer grained as they contain less impurities and higher amounts of clay minerals.

There are also three samples that do not belong to one of these groups, namely CV41 and the two overburden samples CV48 and CV78. The overburden samples are more coarse grained and contain a limited clay fraction (<2 µm). CV41 has a broad grain size distribution which differs slightly from group 2. This difference is clearly visible for the grain size >10 µm (Figure 8.13), indicating the coarse fraction is different compared to other samples of group 2.

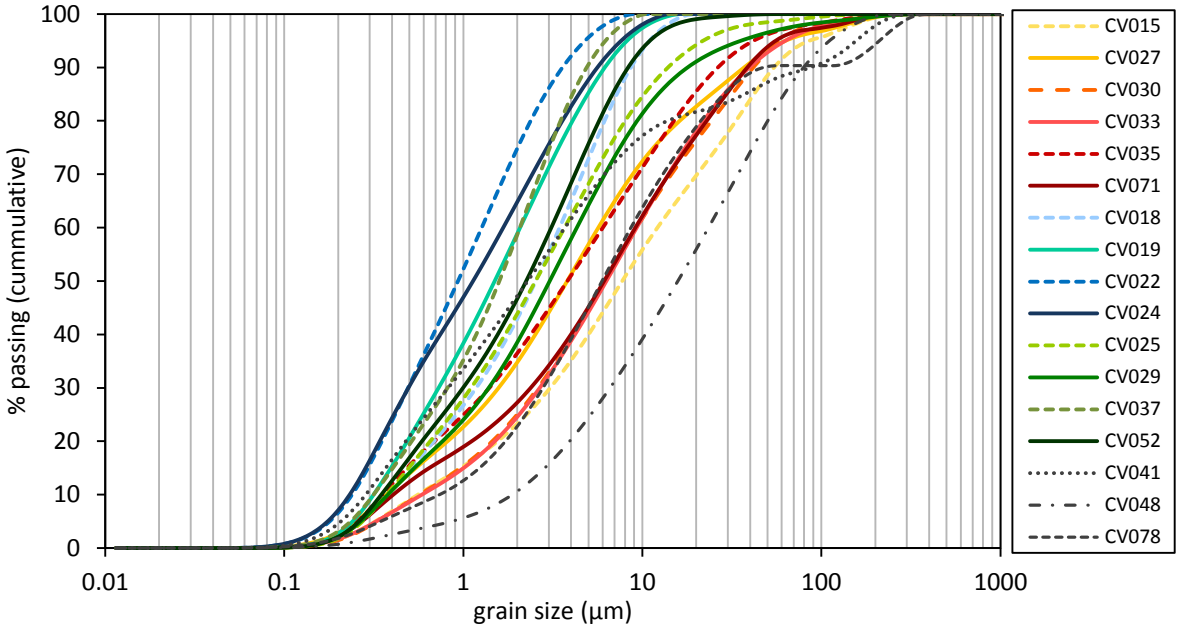

Figure 8.13: *Cumulative grain size distribution for all samples. Samples of group 1 are shown in yellow – red colors while samples of the finer grained sample of group 2 are green – blue. Three samples CV41, CV48 and CV78 cannot be grouped.*

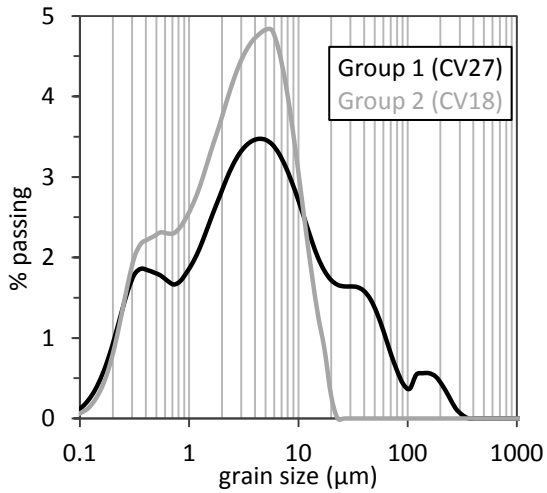

Figure 8.14: *Example of a typical multi modal grain size distribution of group 1, represented by sample CV27 and of the finer grained, bimodal distribution of group 2 embodied by sample CV18.*

The calcined samples can also be subdivided in two major groups (Figure 8.15 and Figure 8.16). The first group, group 1, consists of the same samples as for the raw samples namely CV15, CV27, CV30, CV33 and CV71 and is marked by a asymmetric grain size distribution with peak populations around 0.5 and 5µm and a large peak between 70 and 160 µm. Due to technical problems, the calcined sample of CV35 was not measured and is therefore not included in group 1 of the calcined samples. For the second group the coarse peak around 120 and 200 µm is much narrower and has a wavy left limb. A second population can be found around 0.3 µm. This group contains the samples CV18, CV19,

CV22, CV24, CV25, CV29, CV37, CV52, CV25, which is similar to group 2 of the raw samples. Additionally sample CV41 can be added to this group as it has a similar distribution after calcination. The overburden samples CV48 and 78 have a more spread out distribution compared to the clays in group A and B.

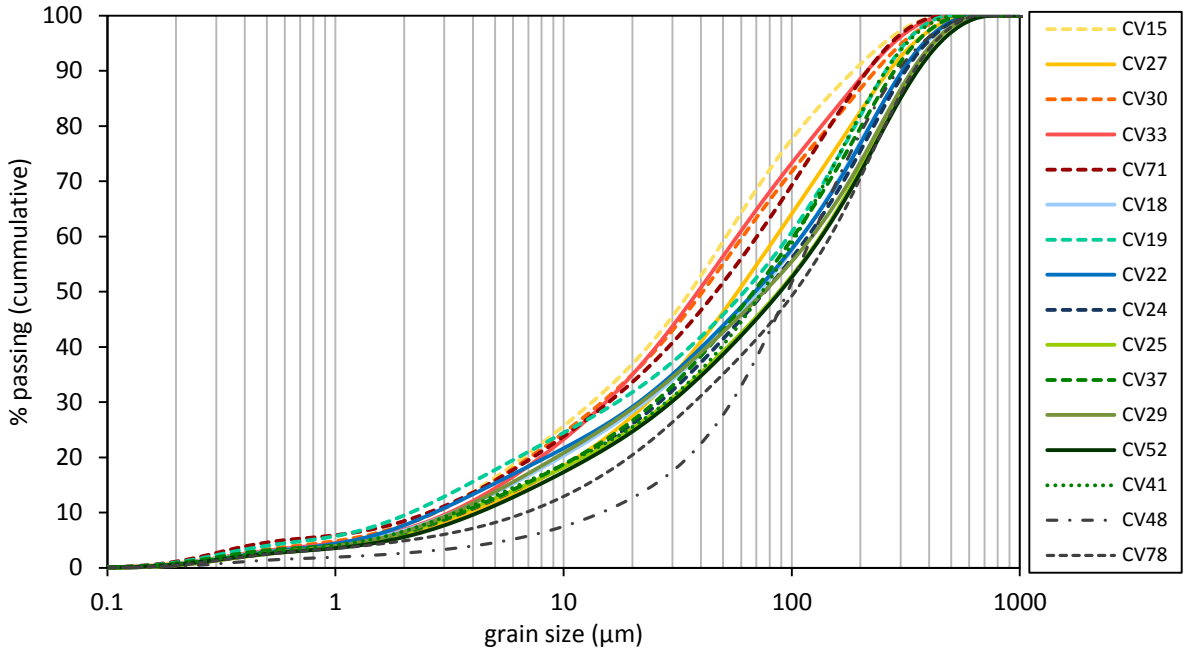

Figure 8.15: *Cumulative grain size distribution for all samples calcined at 800°C. Samples of group 1 are shown in yellow – red colors while samples of the finer grained sample of group 2 are green – blue. Sample CV41 can be added to group 2 while samples CV48 and CV78 are coarser and do not correspond to the characteristics of one the two groups.*

When the cumulative distribution of the raw and the calcined samples are compared it can be seen that the two groups are opposite to each other; for the raw clays group 2 is the finest while for the calcined samples group 1 is more fine grained. This effect can be explained by the mineralogical composition of these samples. During the calcination process part of the clay becomes amorphous. This heating process leads to an enhancement of the agglomeration and sintering phenomena, resulting in larger grain size. The quantity of sintering depends largely on the mineralogy of the sample as demonstrated in chapter 5. The samples of group 1, with initial a larger grain size, all contain less than 50% of kaolinite, more than 27% of quartz and the sum of clays is below 60%. Group 2 consists of samples with a kaolinite content above 50%, less than 15% of quartz and the total sum of clays is above 66%. The exception to these boundaries is the sample CV41 which has a bit of both groups with a kaolinite content equal to 52.5% it would belong to group 2, however the high quartz content of 37% and the sum of clays of 58.5% are characteristic of group 1.

It can be concluded that calcined clay samples with a high clay content and low non-clay fraction tend to be more affected by the combined effect of agglomeration and sintering resulting in coarser material compared to less clay rich calcined samples (Figure 8.16). This is opposite to the original samples whereby more clay rich samples have smaller grain sizes.

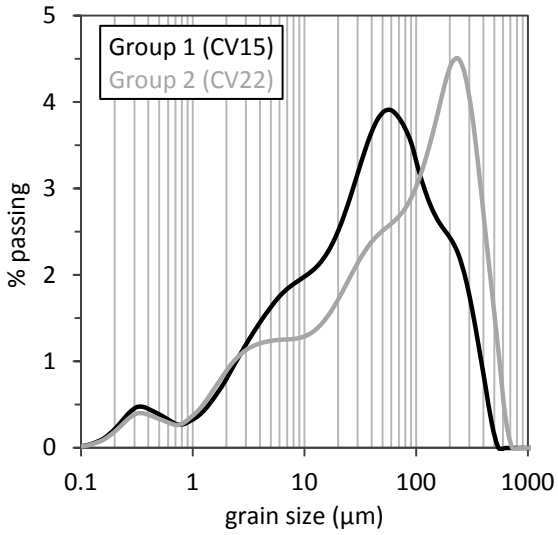

Figure 8.16: *Example of a typical grain size distribution of the calcined clay sample of group 1 (CV15) with a low clay content and of group 2 (CV22) which is more clay rich.*

Furthermore, the calcination temperature will also influence the grain size. This is demonstrated in figure 8.17 where the cumulative grain size distribution of the original sample of CV25 is compared with its calcined product heated at 650 and 800°C. A higher firing temperature will provoke additional sintering. At 650° kaolinite is already amorphous and will have induced agglomeration, however, at 800°C also the smectite present in the sample will contribute to the sintering process. After grinding the sample with the McCrone the particle size is again reduced (Figure 8.18). The grinding step with McCrone results in a similar particle size distribution for all calcined clay. On average, the main peak of the McCroned calcined clay samples is situated around 5.2 µm accompanied by a smaller peak at 0.32 µm with a standard deviation of 1.3 and 0.03 respectively. Therefore, it is possible to minimize the influence of the grain size on the pozzolanic reactivity by McCroning the sample.

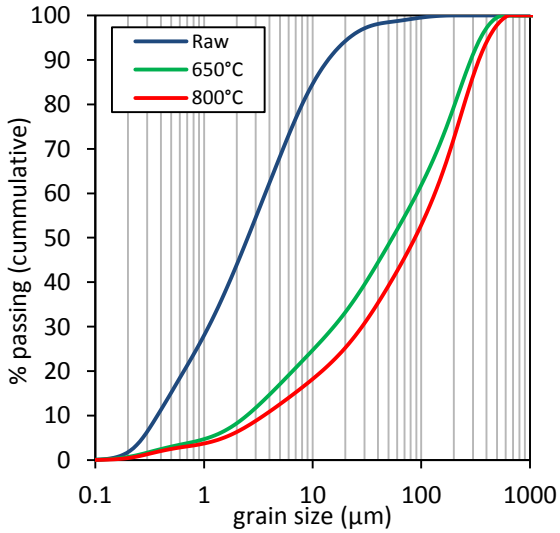

Figure 8.17: *Cumulative grain size distribution to indicate the effect of the calcination process on the grain size of sample CV25 measured raw, after calcination at 650°C and after calcination at 800°C.*

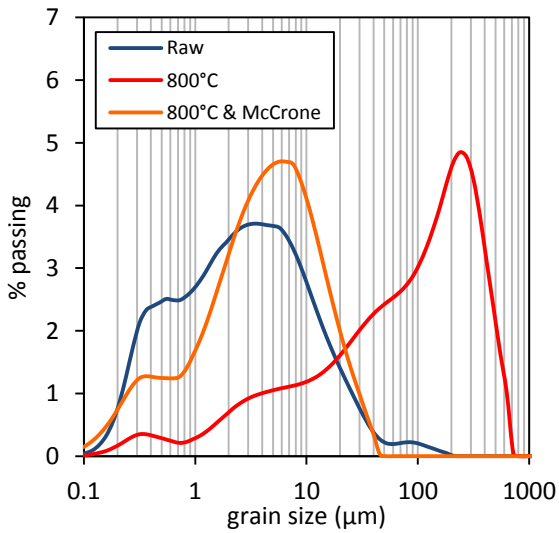

Figure 8.18: Grain *size distribution of sample CV25 to demonstrate the effect of calcination and grinding with a McCrone Micronizing mill.*

8.3.6 BET SPECIFIC SURFACE AREA

The BET specific surface area (SSA) was measured for the original and ground calcined (800°C) samples (Figure 8.19). For the raw samples of the kaolinite bench, the BET SSA varies between 13 and 37 m^2/g. A general declining trend can be witnessed when the samples are arranged according to a decreasing kaolinite content. However the amount and type of 2:1 Al-clays that are present can also influence the BET SSA. The smectitic rich sample CV35 has a higher smectite content compared to the other clays, resulting in a higher SSA than what would have been expected according to its kaolinite content.

After calcination the BET SSA of the kaolinite bench samples is on average 18.5% lower than for the raw sample due to the combination of agglomeration and sintering phenomena. No direct link between the mineralogy and the decrease of the BET SSA upon calcination can be found. The drop in SSA for sample CV78 is rather remarkable due to its relative low clay content.

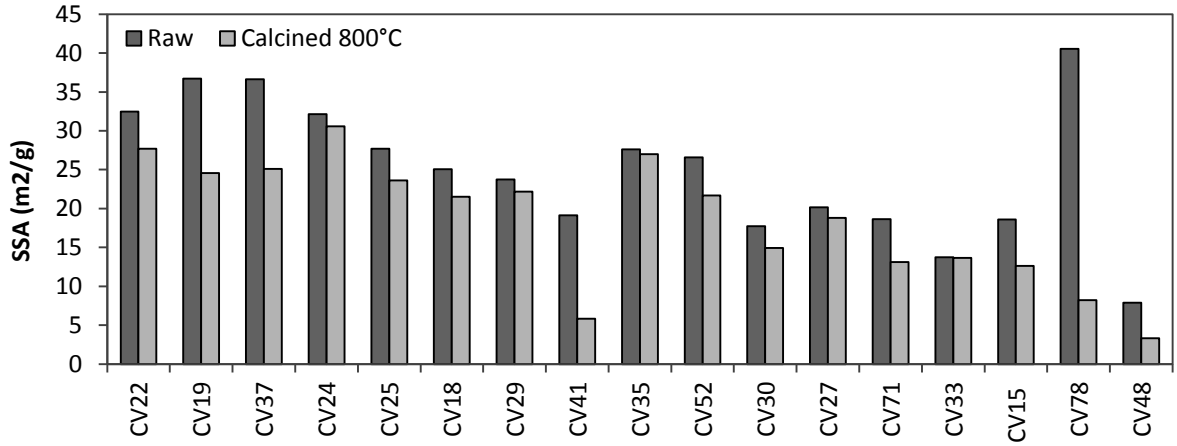

Figure 8.19: *BET specific surface area of the original and ground calcined clay samples.*

The changes upon calcination were studied in more detail for the samples CV22 and CV25 (Figure 8.20). The original and ground samples, calcined at 650°C and 800°C were measured. Calcining the samples at 650°C resulted in a decrease of the specific surface area of approximately 18%. (5.67 m^2/g for sample VC22 and 5.13 m^2/g for samples VC25). Further calcination to 800°C resulted in a small increase around 3.5% of the specific surface area.

The dehydroxylation of clay minerals causes a collapse of the structure and results in a less ordered phase with higher SSA. For pure well ordered kaolinite this decrease is situated in the temperature range between 500 and 600°C as demonstrated in Chapter 4 and in the study of He et al. (1994). However, these clays are disordered kaolinitic clays with the presence of other clay minerals including smectite. Smectitic clay has a higher dehydroxylation temperature and therefore the less ordered phase, which is accompanied by an increase in SSA, is only formed at higher temperatures. This explains why the increase of the SSA takes place in the temperature range between 650 and 800°C. Furthermore, the SSA of smectitic clays is initially more sensitive to heat treatment (Chapter 4). The steeper decrease in SSA of samples CV22 and CV25 compared to a pure disordered kaolinite KGA-2 can therefore be explained by the presence of smectite in the sample.

Additional tests were performed in order to analyze if there is a significant difference in the BET SSA of the McCroned and the non-ground calcined samples. For CV22 calcined at 880°C, the McCroned sample had a SSA of 27.71 m^2/g and for the non-ground sample the SSA was 27.67 m^2/g. The difference of 0.04 m^2/g is limited and even smaller than the average error range of 1.0 m^2/g. This was confirmed for sample CV25 with a difference of 0.86 m^2/g (800° & McCrone: 22.79 m^2/g and 800°: 23.55 m^2/g).

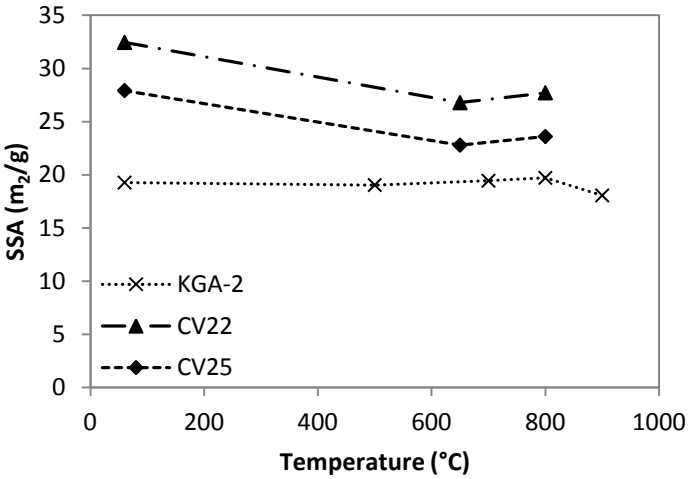

Figure 8.20: *Evolution of the BET specific surface area upon calcination of the clay samples CV22 and CV25. The pure disordered kaolinite sample KGA-2 was added as reference.*

8.4 POZZOLANIC REACTIVITY

8.4.1 CALCINED CLAY LIME PASTES

The pozzolanic potential of the different clay qualities was analyzed by means of thermal analysis. The portlandite consumption of the ground clays calcined at 800°C was studied over time and visualized in Figure 8.21. Reaction is faster during the first 14 days and after 28 days the reaction slows down as most calcined clay is already consumed. The two clays of the LT0 quality show a similar portlandite consumption starting at 26% at day 3 evolving to 62.5% at day 90. The trend of the three LT1 clays is also comparable with portlandite consumption around 24% at 3 days and 57% after 90 days. For the LT2 clays the initial portlandite consumption is similar, with a value of 24% at day 3. However, after 14 days, sample CV29 consumes less portlandite compared to sample CV18 with values at 90 days of 49 and 54.3% respectively. The three clays from the LTPK quality show more variable portlandite consumption compared to the other grades ranging between 43% and 50% at 90 days. The LTU clays CV35 and CV52 have a clear difference in portlandite consumption, with values of 50 and 55% respectively at 90 days. For the other clay qualities, LT3, LTK and LTKj only one sample was analyzed with a consumption between 44 and 47% at 90 days.

To compare the clay qualities relative to each other the amount of portlandite that was consumed after 28 days was plotted in Figure 8.22. The Al_2O_3 rich LTO and LT1 have the highest portlandite consumption around 58 and 55% respectively. LT2 and LTU have medium portlandite consumption with a clear difference between the different samples of the same grade. The remaining clay qualities LT3, LTPK, LTK and LTKj have a low Al_2O_3 content (<23%), which is reflected in a decrease in the portlandite consumption with a value below 48%.

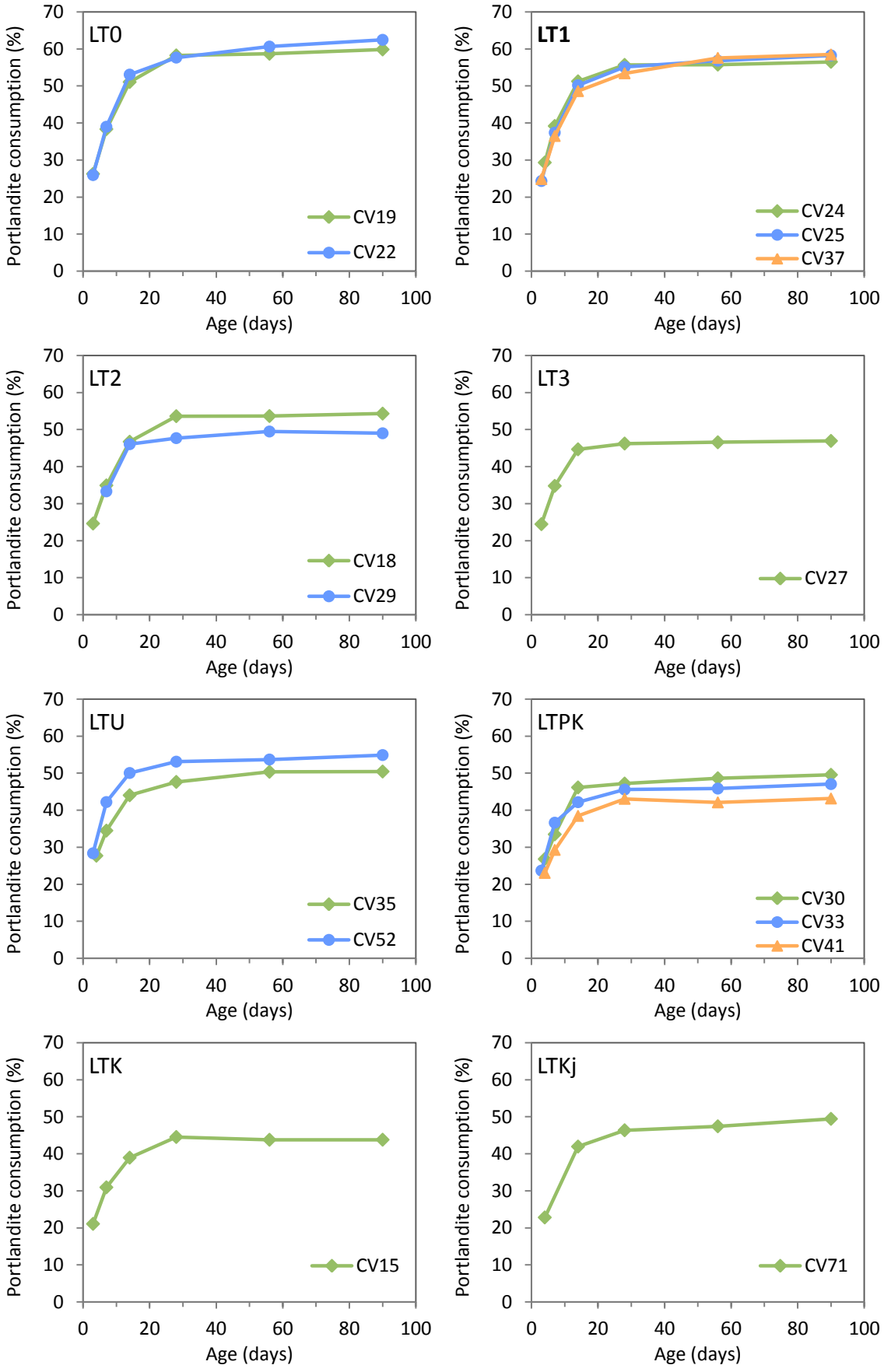

Figure 8.21: *Portlandite consumption over time for the different clay grades from the kaolinite bench. All samples were calcined at 800°C and milled afterwards.*

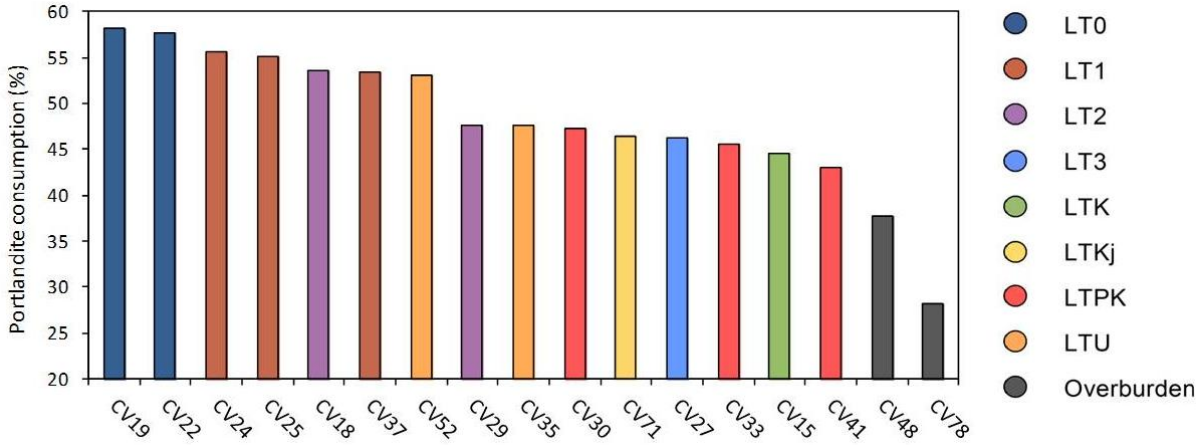

Figure 8.22: *Portlandite consumption of the different clay grades at 28 days. Samples were calcined at 800°C and milled with a McCrone afterwards*

The portlandite consumption of the two overburden samples was also determined and the results are shown in Figure 8.23. The portlandite consumption of both samples is fairly low with a value of 37.75 %for CV48 and 28.2 % for CV78 at 28 days compared to a kaolinite rich clay bench sample. This is also reflected in the low reaction rate of the overburden samples in the early stage of the reaction (before 14 days). The low clay content of both samples explains this major difference. However there is also a clear difference in the reactivity between the two samples. Since the kaolinite content is negligible (3 and 4 %) and the smectite content in the bulk samples is comparable for both clays, 12.8 and 11.3 % respectively, the difference should be correlated to the amount of other clay minerals. The most important difference is the amount of 2:1 Fe-clays present in both samples. For the glauconite rich sample CV48, the amount of 2:1 Fe-clays is 16% while it is only 8% for the red CV78 clay. This explains the difference in portlandite consumption of on average 9% (for the 28 and 56 days).

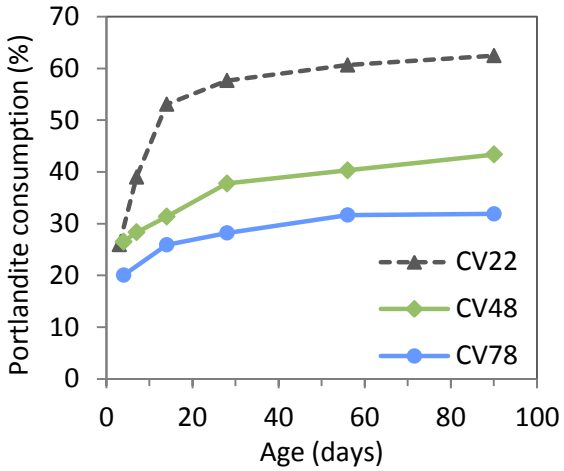

Figure 8.23: *Portlandite consumption of the overburden samples CV48 and CV78 calcined at 800°C and milled. As reference the kaolinitic sample CV22, also calcined at 800°C is added.*

8.4.2 EFFECT OF THE CALCINATION TEMPERATURE

For two samples CV22 and CV25 the influence of the activation temperature on the pozzolanic reactivity was tested for the calcination temperatures of 650° and 800°C. The plots of the portlandite consumption (Figure 8.24) show that for both samples the lower calcination temperature of 650°C results in a slightly less reactive material. At 28 days the difference in reactivity is for sample CV22 3.2% and for sample CV25 2.5%. A longer curing time of 56 days results in a further increase of the reactivity difference of 4.3% for sample CV22, while the difference for sample CV25 remains similar. At 90-day curing also CV25 shows a lower reactivity when only calcined at 650°C. This variation in reactivity, especially at longer curing times, can be related to the fact that 2:1 Al clays such as smectite, illite and illite/smectite mixed layer do not fully contribute when the sample is calcined at lower temperatures (650°C) since smectitic clays have a higher activation temperature around 800°C. The difference in reactivity further increases when longer curing times are taken into account. This can be explained by the fact that and 2:1 Al-clays have a slow reaction rate that continues steadily after 28 days. The smectitic clays therefore mainly affect the longer term pozzolanic reaction.

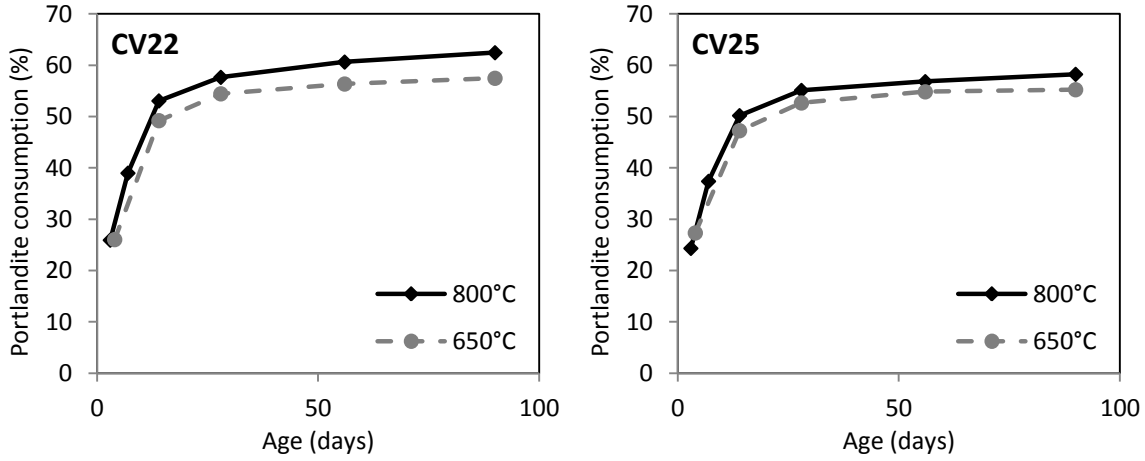

Figure 8.24: *Portlandite consumption over time of samples CV22 and CV25 calcined at two different temperatures of 650°C and 800°C.*

8.4.3 EFFECT OF THE GRAIN SIZE

The influence of the grain size on the pozzolanic reactivity was analyzed for sample CV25. As the sintering upon calcination can change the grain size significantly, one part of the sample was milled with a McCrone after calcination to reduce the sintering effect while for the other part no additional treatment or milling after the calcination process was applied. The same clay sample and calcination temperature of 800°C was investigated to avoid influence of the mineralogy or the chosen calcination temperature. The reactivity plot (Figure 8.25) shows the difference in portlandite consumption is already significant at the beginning of the reaction, certainly when it is taken into account that CV25 McCroned was measured at 3 days while CV25 course was measured only after 4 days. If both samples would have been measured at 3 days the difference would even be greater. At 28 days the difference in portlandite consumption amounts to 11.3 %. After 28 days the gap between the two samples becomes smaller since the McCroned sample has reached almost its maximum reactivity while the non-milled sample reacts much slower. The outer reaction surface of the McCroned sample is much larger, resulting in a high initial reaction rate while the non-milled sample is still reacting at day 56 and still hasn't reached its plateau. These results indicate that the milling of the calcined sample can alter the pozzolanic reactivity drastically in a positive manner.

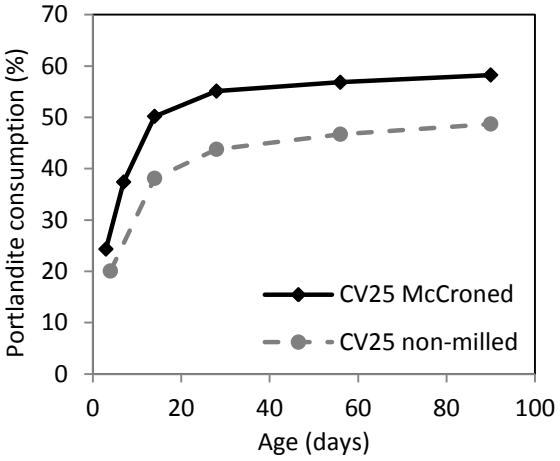

Figure 8.25: *Portlandite consumption over time of sample CV25 calcined at 800°C to clarify the effect of the grain size on the pozzolanic reaction.*

8.4.4 CORRELATION BETWEEN REACTIVITY AND CLAY CHARACTERISTICS

It is known that kaolinite is a dominant controlling parameter regarding the pozzolanic reactivity. However five samples (CV27, CV30, CV35, CV41 and CV52) with a similar kaolinite content varying between 47 and 52.5% have a rather broad range (43 -53.5%) of portlandite consumption (Table 8.6). The reactivity of these samples follow a general decreasing trend with declining kaolinite content indicating that the kaolinite content is an important parameter that influences the pozzolanic reactivity. However, some samples do not follow this trend and have a higher (CV52) or lower (CV41) reactivity than expected based on their clay mineralogical composition. Therefore other parameters also contribute to the overall reactivity. For the highly reactive sample CV52 it can be seen that the Al_2O_3 content is rather high compared to the other samples. Since the kaolinite and 2:1 clay content is similar to the other clays, alumina must be present in the other mineral phases. This sample has also a high amorphous content of 17% and even though it is lignite rich the LOI is lower (20%) than for sample CV35 (23%). This indicates that the amorphous phase might include additional alumina that is free to react with portlandite and thereby increasing the clays reactivity. Furthermore, the lignitic material will decompose during the calcination process resulting in relatively higher kaolinite content for this sample. Another parameter which can have an effect, is the coarseness of the kaolinite present in the sample. Even though the variation in the degree of ordering (HI and R2) of kaolinite and of the BET specific surface area is not significant, sample CV52 contains more fine grained (<2 μm) kaolinite than CV35 as the kaolinite content in the clay fraction is 61 and 49 % respectively (see Figure 8.8). The effect of smaller grain size of kaolinite explains the more rapid increase in reactivity of sample CV52 compared to CV35. At a later stage of the reaction, 56 days and more, the reactivity of both samples becomes more equal. Sample CV71 has also a rather high reactivity in relation to the other clays. In this case the most important difference is the presence of an iron rich phase in the bulk mineralogy namely 3% of goethite. This excess of iron can react with portlandite to form more Fe-rich cement phases. The third exception CV41 has a lower pozzolanic reactivity; this can be explained by the low specific surface area of 5.83 m^2/g of the McCroned calcined clay.

Table 8.6: *Overview of the chemical, mineralogical and physical characteristics of 6 kaolinitic samples listed according to decreasing kaolinite content. The reactivity is determined after 28 days. Exceptional values are indicated in bold.*

Sample	Kaolinite (%)	Reactivity (%)	Al_2O_3 (%)	Fe_2O_3 (%)	LOI (%)	Amorphous (%)	sum clays (%)	smectite bulk (%)	Kaolinite <2µm (%)	BET (m^2/g)	HI
CV35	51	47.64	25.16	3.1	23.98	13	68	15.2	49	27.01	0.14
CV52	50.5	**53.11**	**29.03**	1.07	20.98	**17**	66.5	12.7	61	26.58	0.24
CV30	49.5	47.20	24.55	0.89	12.25	4	59.5	7.1	62	14.94	0.25
CV27	49	46.23	25.7	1.57	12.55	8	59	8.0	60	18.80	0.24
CV41	47.5	**43.07**	24.68	0.72	10.48	5	58.5	6.4	67	**5.83**	n.d.
CV71	47	46.36	24.54	**4.06**	10.25	5	58	6.0	89	13.11	0.84

To explain the differences in portlandite consumption between and within the different clay grades more accurately, the correlation of the pozzolanic potential with chemistry, mineralogical composition and physical characteristics is made. The correlation of these parameters is studied for six different time spans (3, 7, 14, 28, 56 and 90 days) to see if the influence is time dependent. The first parameter, which can influence the pozzolanic behavior, is the Al_2O_3 content (Figure 8.26). At 3 and 7 days the correlation between Al_2O_3 and the pozzolanic reactivity is negligible with values for the correlation coefficient R^2 of 0.22 and 0.53 respectively. However, after 14 days the correlation becomes much better, with R^2 of 0.89. After a longer time span the correlation coefficient slightly decreases with a value of 0.81 after 90 days. This indicates the Al_2O_3 content influences the reaction from 14 days onwards. This influence decreases again after a longer curing time of 56 and 90 days. Since it was shown in Figure 8.11 that there is a good correlation between Al_2O_3 and kaolinite, a similar trend was found for kaolinite (Figure 8.27). The first 7 days the correlation with the reactivity is poor ($R^2 < 0.44$). The highest correlation coefficient for kaolinite is found at 14 days, with R^2 0.87. In general the values of the correlation coefficient are somewhat lower for kaolinite than for Al_2O_3. This can be explained by the participation of other clay minerals like smectite and mixed layer kaolinite/smectite in the pozzolanic reaction. Therefore also the sum of clay minerals was plotted against the reactivity (Figure 8.28) . From day 14 the correlation coefficient becomes sufficiently high with a R^2 of 0.84. In contrast to the decreasing trend of the correlation coefficient of Al_2O_3 and kaolinite at later time spans, R^2 of the sum of clays is increasing at 28 and 56 days to 0.86 and 0.91 respectively. At 90 days the correlation becomes again less good than at 56 days with R^2 of 0.88. This confirms the fact that non-kaolinitic clay minerals, like smectite, react much slower and will influence the reaction mainly in a later stage around 56 days while the presence of kaolinite is important between 14 and 28 days.

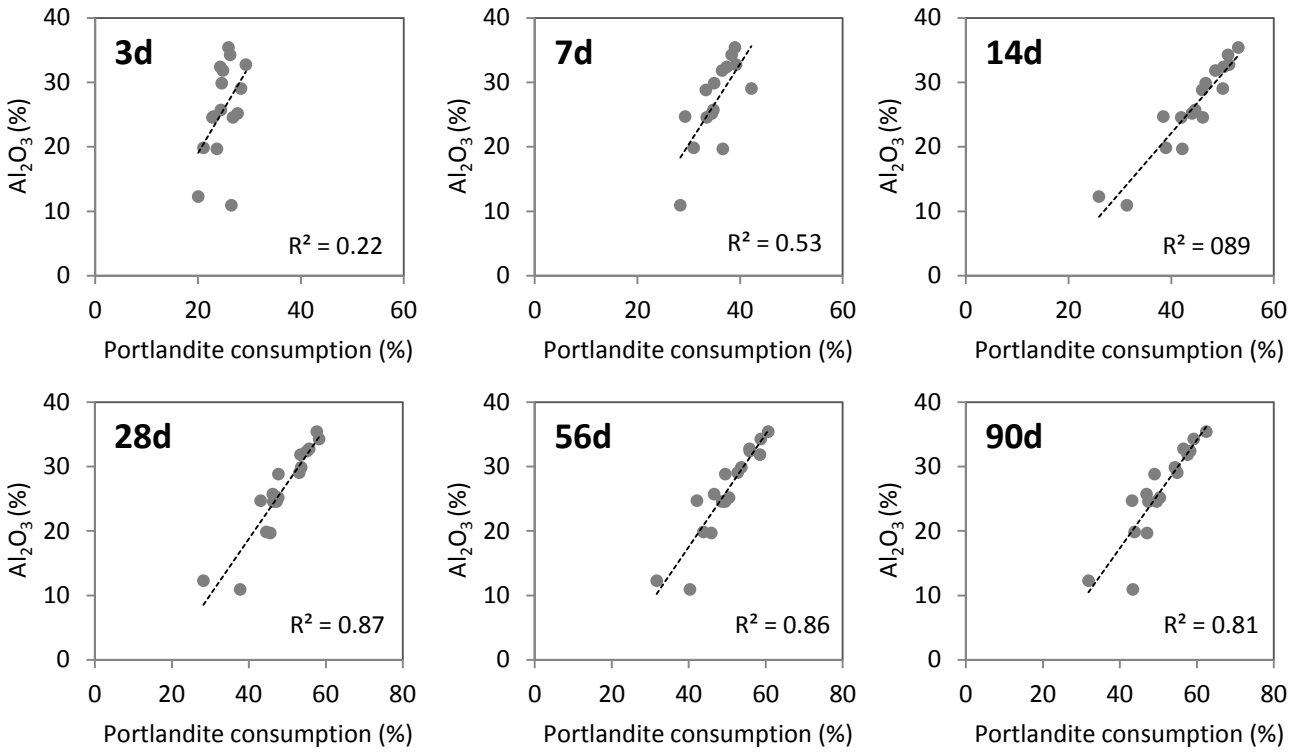

Figure 8.26: *Correlation plots of the portlandite consumption in function of the Al_2O_3 content at different hydration times.*

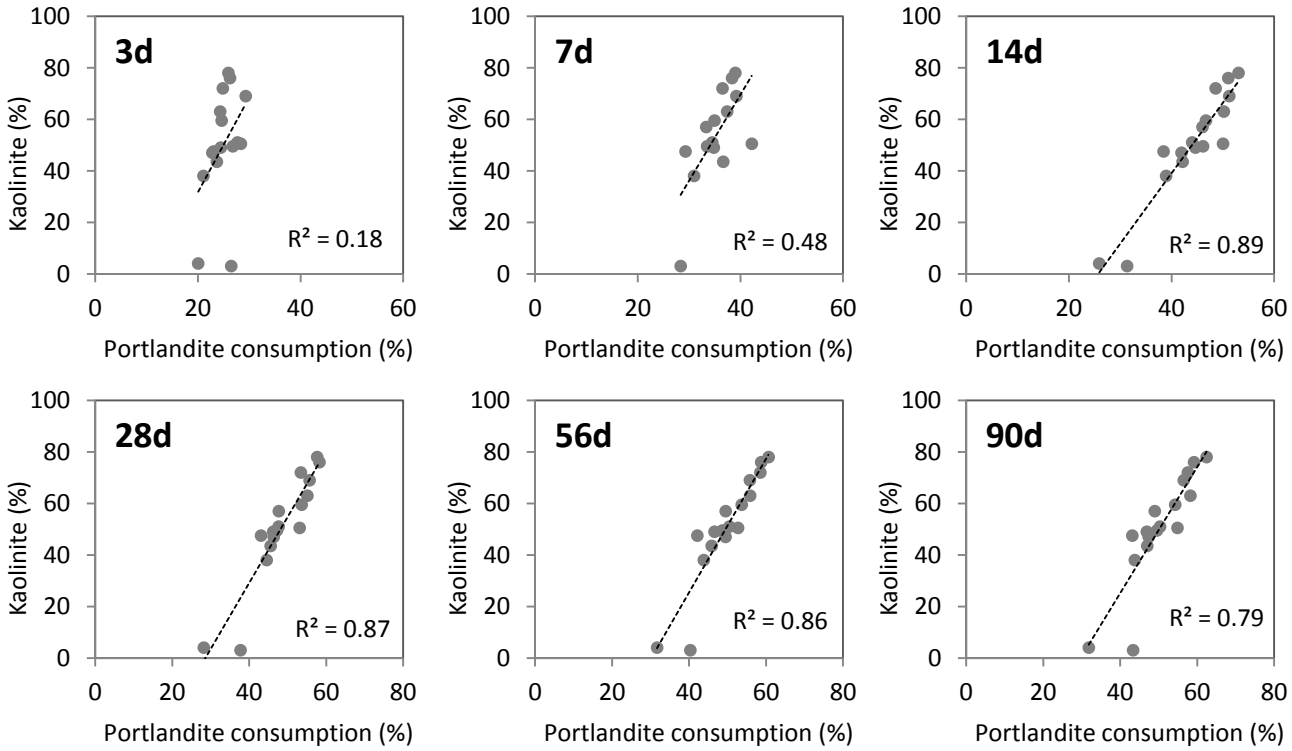

Figure 8.27: *Correlation plots of the portlandite consumption in function of the kaolinite content at different hydration times.*

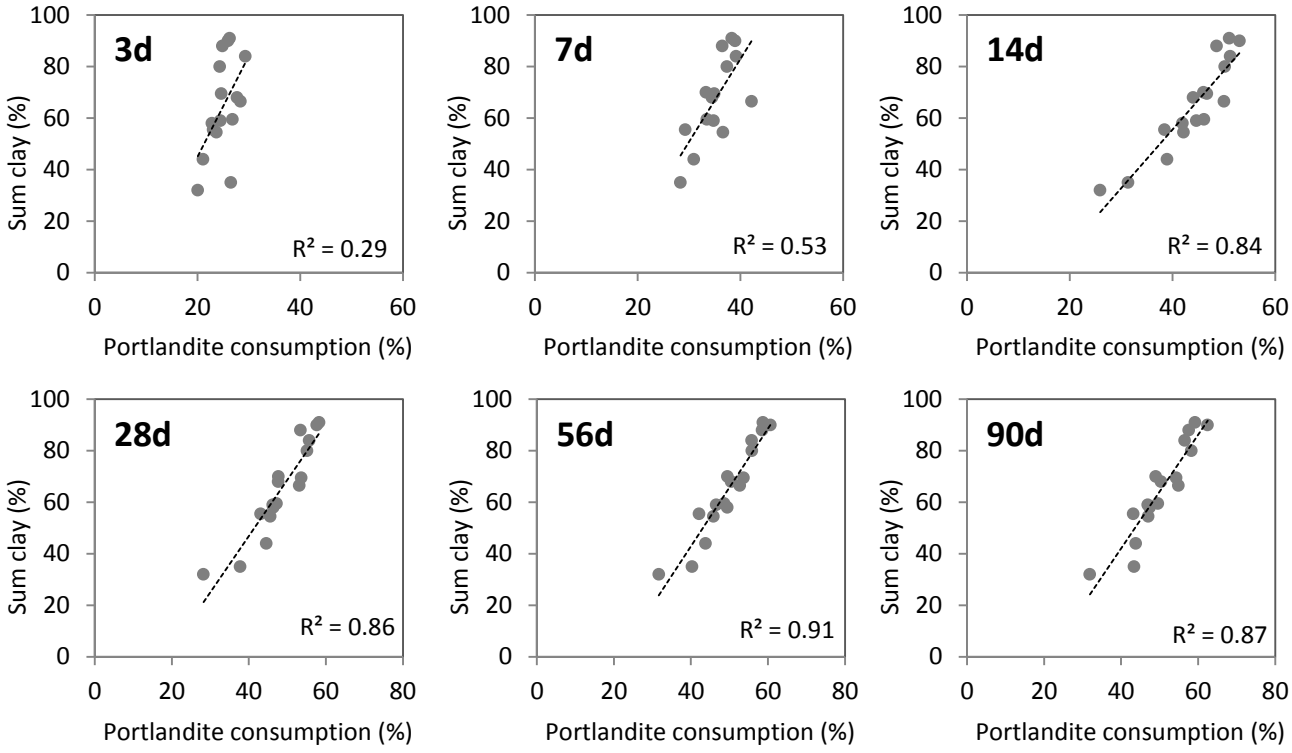

Figure 8.28: *Correlation plots of the portlandite consumption in function of the sum of clay content of the sample at different hydration times.*

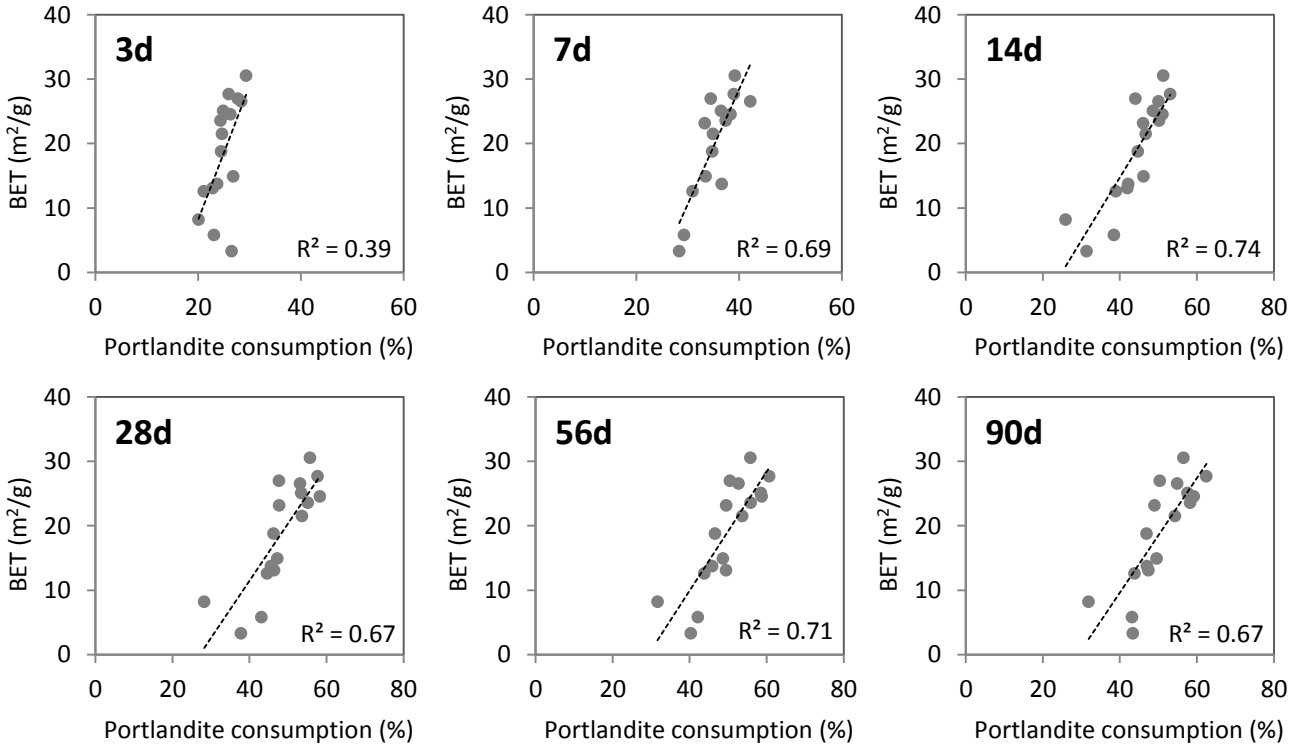

Figure 8.29: *Correlation plots of the portlandite consumption in function of the BET specific surface area at different hydration times.*

Another parameter influencing the pozzolanic reactivity is the BET specific surface area (Figure 8.29). The correlation plots indicate that the BET specific surface area is correlated, though limited, from 7 days onwards. At 7 and 14 days the correlation coefficient is higher compared to other time intervals with R^2 of 0.70 and 0.75 respectively. Even though this correlation coefficient is rather low compared to the good correlation (R^2>0.83) of the other parameters, at 7 days the R^2 of the BET SSA is the highest. At 56 days the correlation between the BET SSA and the reactivity increases again to R^2 = 0.73. This can be clarified by the presence of a positive correlation between the BET SSA and the smectite content (R^2 = 0.73). The controlling influence of the 2:1 Al clays, and thereby also of smectite, is greatest at 56 days this is also reflected in the SSA – reactivity correlation but is actually caused by the 2:1 Al clays. This demonstrates that the BET specific surface area is more relevant in the early stage of the reaction. After 14 days the correlation decreases again and SSA becomes less important.

8.4.5 POZZOLANIC POTENTIAL OF THE LATNESKOYE CLAYS

To estimate the pozzolanic potential of the Latneskoye clays the portlandite consumption at day 28 is taken into account since this is the most important day in concrete technology. Since the different clay qualities are determined on the Al_2O_3 content and there is a good correlation between the reactivity and the Al_2O_3 and kaolinite content at day 28, it is possible to rank the clay qualities according to their potential:

$$LT0 > LT1 > \frac{LT2(high\ Al_2O_3)}{LTU(high\ Al_2O_3)} > \frac{LT2(low\ Al_2O_3)}{LTU(low\ Al_2O_3)} > \frac{LTKj > LT3 > LTK}{LTPK} > glauconite\ clay \gg Red\ clay$$

The clay qualities with the highest Al_2O_3 content have also the highest potential as pozzolanic material. This is because the Al_2O_3 content is related to the amount of kaolinite and even more the total sum of clays that is present in the sample. The LT0 clay grade has a kaolinite content above 70% and a sum of clay minerals around 90%. The LT1 are also high potential clays with a kaolinite content above 60% and a sum of clays ≥ 80%. LT2 and LTU are the following clay qualities. Both grades extend over a similar and broad Al_2O_3 range (between 33 and 37% for LT2 and above28% for LTU). This results, however, in a broad range of mineralogy with also a wide variety in pozzolanic reactivity, especially for LTU. Therefore, these two grades are split in low and high Al_2O_3 clays. The high Al_2O_3 clays within these grades are high potential clays, while the low Al_2O_3 clays are marked with a clear drop in reactivity below 50% and can be seen as semi-potential. The clay grades with lower Al_2O_3 content, LTPK, LTKj, LT3 and LTK, are characterized by similar portlandite consumptions in the range of 44 to 47 % and this can be seen as semi to low pozzolanic potential. The exception is the LTPK sample CV41 with a reactivity of 43 % which can be classified as low pozzolanic clay. Regarding the overburden samples the glauconite rich sample still resembles the activity of the low Al_2O_3 kaolinite bench clays when the reactivity at 56 days is taken into account. However, both the glauconite as the red clay are not sufficient reactive at 28 days resulting in low portlandite consumption rates.

For the Latneskoye clay deposit a first good estimation of the pozzolanic potential can be made based on the bulk chemical composition of the sample. Especially the Al_2O_3 content allows to accuratly predict the pozzolanic reactivity. However there are always some exceptions since other parameters like the grain size, the detailed clay mineralogy including the smectite content can influence the pozzolanic reaction significantly. Furthermore, the prediction on behalf of the Al_2O_3 content works for this deposit because there is also a good correlation between the kaolinite content and Al_2O_3, so actually the mineralogy is taken into account. For kaolinitic clay deposits that contain additional Al-rich phases like illite or more feldspar, the pozzolanic reactivity would be estimated incorrectly.

8.5 POZZOLANIC REACTION PRODUCTS

8.5.1 CALCINED CLAY-LIME SYSTEM

The hydration products that were formed during the pozzolanic reaction of the calcined clay lime pastes were analyzed by thermal analysis and XRD. The differential of the TGA (DTG) of the kaolinite rich CV22 sample calcined at 800°C is shown in Figure 8.30. The DTG pattern is marked by a mass loss between 350 and 550°C caused by decomposition of the portlandite that has not yet reacted. The portlandite decomposition peak intensity shows a decreasing trend over time which reflects the portlandite consumption. This mass loss was used to calculate the pozzolanic reactivity of the sample in the previous paragraph. A second mass loss in the region of 50 to 300°C can be correlated to the decomposition of the newly formed hydration products. The reaction products that can be identified are typical for a kaolinite rich deposit and the intensity of these peaks increases over time. Three main mineral phases can be distinguished namely strätlingite (C_2ASH_8) around 180 and 240°C, monocarboaluminate at 140°C and a more broad spread C-S-H phase between 80 and 140°C. At 3 days of curing the dominant phase recognizable by TGA is monocarboaluminate. Several studies indicate the presence of this phase in calcined clay/lime pastes despite the lack of a proper carbon source other than contamination by CO_2 from the air when drying the sample to stop the reaction. Strätlingite is formed from day 7 onwards as visible by the increase of its peak around 190°C. At day 7 some overlap is present with the decomposition peak of monocarboaluminate afterwards the strätlingite peak is subdivided in two peaks. Also the C_4AH_{13} phase is present from 7 days onwards. Due to the overlap of the hydration phases no quantitative results can be obtained.

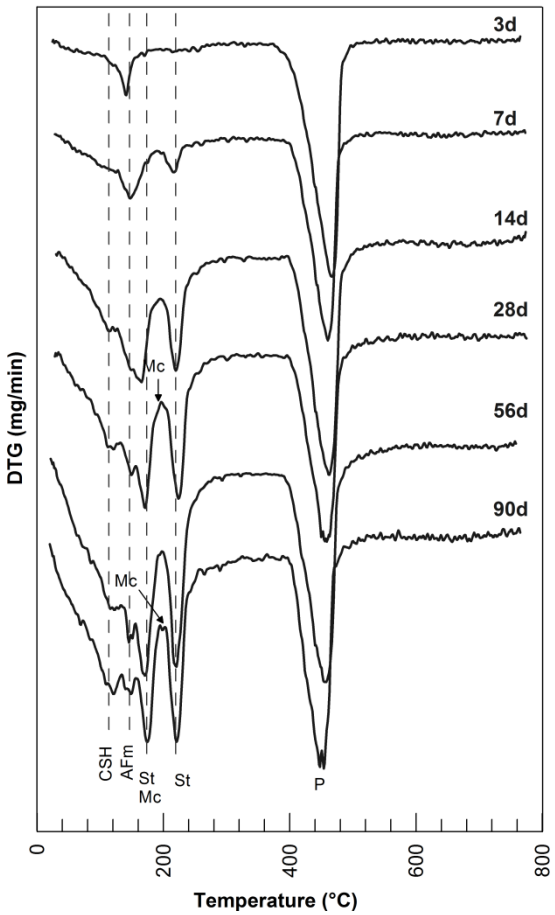

Figure 8.30: *DTG curve of the calcined clay lime paste of sample CV22 cured for 3, 7, 14, 28, 56 and 90 days. The hydration products are indicated: P: Portlandite, St: Strätlingite, Mc: monocarboaluminate, C_4AH_{13} and CSH.*

XRD patterns confirm the TGA results and similar reaction products are found. The diffractograms at different curing ages for sample CV22 are shown in Figure 8.31. The (semi) heat resistant minerals in the clay like muscovite, quartz, anatase and illite (if present) remain their characteristic reflections. The presence of portlandite (CH) is marked by the peak reflections at 17, 27, 34, 47 and 51 °2θ. The intensity of the reflections decreases rapidly during the first stage of the reaction (up to 14 days) and stabilizes at 56 and 90 days. This is in agreement with the results of the reactivity test indicating that after 28 days most of the calcined kaolinite is already consumed. The preferential formation of AFm phases when calcined clay pastes are made is demonstrated by the reflections at 7, 14, 20, 21,31 and 39 °2θ of the Al- and Si-rich phase strätlingite. This is the most abundant newly formed crystalline phase that is present from 7 days onward. It appears that some reflections at 20 and 21°2θ are already present at 3 days. These are however the reflections of muscovite which overlap with the strätlingite peak position. Nevertheless, it is possible that small amounts are already present but are too low to be properly detected by XRD or TGA as suggested by Gameiro et al. (2012). The region between 10 and 12 °2θ comprises a mixture of different AFm phases. In general the intensities of the peaks in that region is rather stable over time. Monocarboaluminate is characterized by a weak reflection at 11.65 and 23 °2θ. Furthermore, some hemicarboaluminate might be present with a reflection at 10.8°2θ. The C_4AH_{13} phase, around 11°2θ seems to be a minor phase in XRD which confirms the TGA interpretation on strätlingite has two decomposition peaks in the DTG analysis. The study of Silva et al. (2014) already indicated that the C_4AH_{13} phase is marked by rather weak reflections.

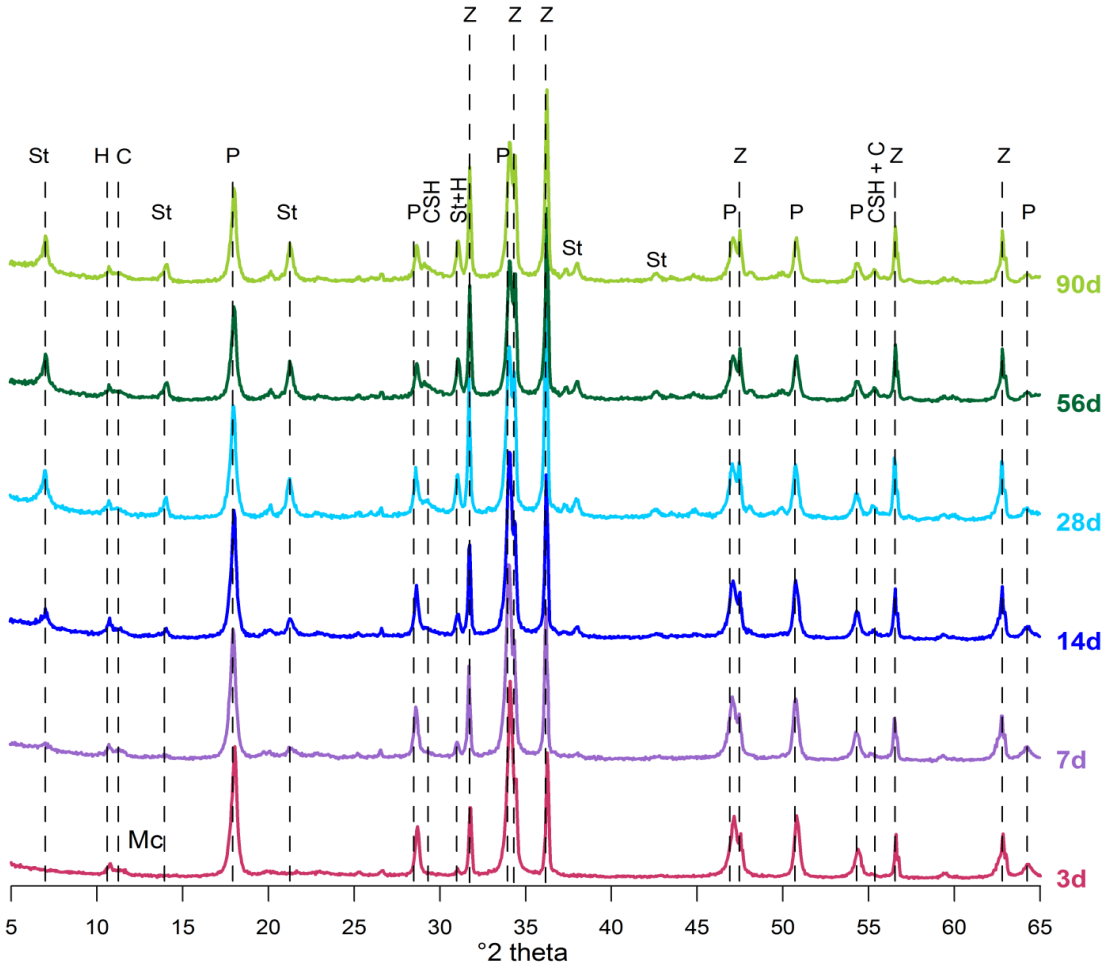

Figure 8.31: *XRD pattern of the calcined clay lime mixture of CV22 calcined at 800°C at different curing times. The hydration products are indicated: Z: zincite (internal standard) P: Portlandite, St: Strätlingite, Mc: monocarboaluminate, C: C_4AH_{13} and CSH.*

Figure 8.32 shows the amount of the Al-rich Strätlingite phase declines with a decreasing amount of kaolinite. This is normal since kaolinite is the most important source of the alumina in the pozzolanic reaction. Nevertheless, sample CV15 with the lowest Al_2O_3 content of 21.72% (fired clay), a kaolinite content of only 38% and a Si/Al ratio of 3.4, still forms strätlingite. For the two overburden samples, which are kaolinite poor (<4%), no strätlingite is formed at 28 days of reaction. The glauconite rich clay CV48 main hydration phases are monocarboaluminate and C-S-H phase. The red clay CV78 has additionally formed hemicarboaluminate whereby less CO is implemented in the structure compared to monocarboaluminate. The reactivity difference can most likely be linked to the difference in the amount of C-S-H formed. The more silica rich CV48 (69.1%) has a more elevated background/peak around 29.5°2θ where the reflection of the C-S-H is situated. CV78 has less silica in its bulk composition and, moreover, has a larger amount of quartz and lower amount of clays. Therefore more silica is trapped in the inert quartz resulting in less C-S-H phase that can be formed in CV78.

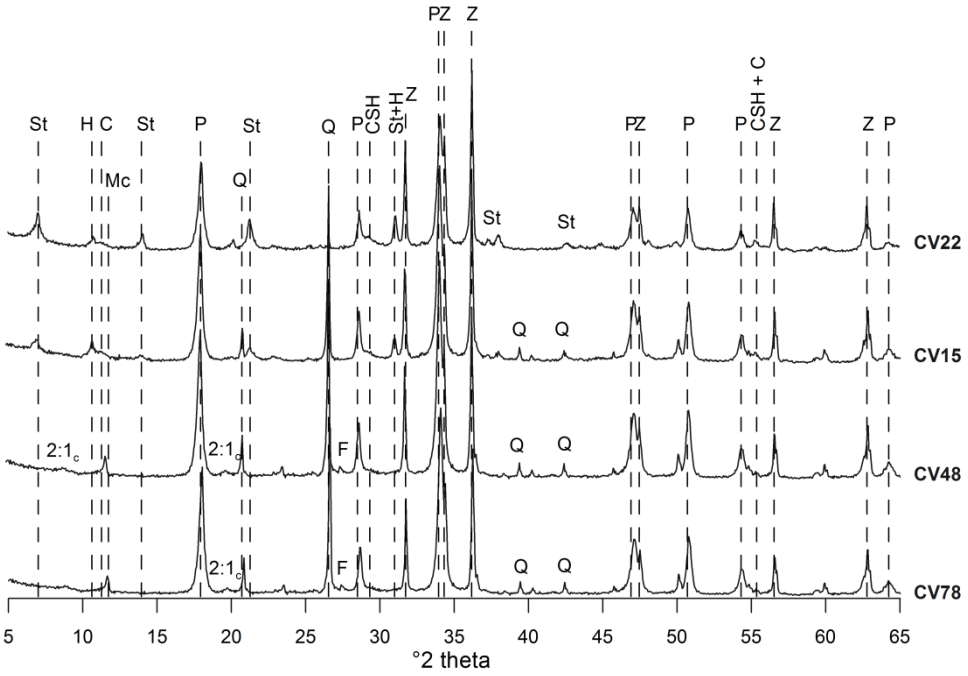

Figure 8.32: *XRD pattern of the calcined clay lime pastes of CV22, CV15, CV48 and CV78 calcined at 800°C and cured for 28 days. The phases are indicated: Z: zincite (internal standard) P: Portlandite, St: Strätlingite, Mc: monocarboaluminate, H: hemicarboaluminate, C: C_4AH_{13}, CSH, $2:1_c$: calcined 2:1 Al-clays, Q: Quartz and F: feldspar.*

8.5.2 CALCINED CLAY PORTLAND CEMENT SYSTEM

Besides the calcined clay-lime paste a paste with Ordinary Portland cement (OPC) was made for sample CV22, CV25 and CV35. The pastes are prepared in 1:5 calcined clay – cement ratio and water to solid ratio of 0.5. An OPC of the type CEM I 52.2, indicating the strength after 28 days is 52.5MPa, was used. OPC pastes were prepared according to a similar sample preparation maintained for the lime paste (see Chapter 3).

The thermal analysis patterns after different curing times (3, 7, 14 and 28 days) are visualized in Figure 8.33. The peak around 450°C confirms the presence of portlandite. Portlandite is formed during the first step in the reaction when the cement containing free lime (CaO) reacts with water to form portlandite ($Ca(OH)_2$). This is observed in the DTG by an increase of the amount of portlandite up to day 14. The formation of portlandite triggers the pozzolanic reaction whereby the calcined clay

reacts with the newly formed portlandite. In the first stage of the reaction the hydration and formation of portlandite is faster than the consumption of portlandite by the calcined clay. After 14 days the amount of portlandite in the paste decreases rapidly indicating the pozzolanic reaction has become more dominant. The amount of hydration products increases over time. The C-S-H phase forms an important component and decomposes between 50 – 200°C. However in the same temperature range the AFt phase ettringite also decomposes with its main peak around 130°C. The decomposition of the AFm phases can have some overlap with the C-S-H phase but are centered more towards 190°C instead of 130°C for C-S-H (Fernandez et al., 2009). The presence of strätlingite is indicated by the appearance of the second peak around 220°C at 28 days. The peak at 550 and 650°C can be related to the decomposition of calcite ($CaCO_3$). The presence of this phase can be due to carbonation whereby CO_2 from the air reacts with the Ca in the sample, or because carbonates where originally presented in the OPC. However this last option in not likely since there is almost no indication that at day 3 and 28 carbonates are present.

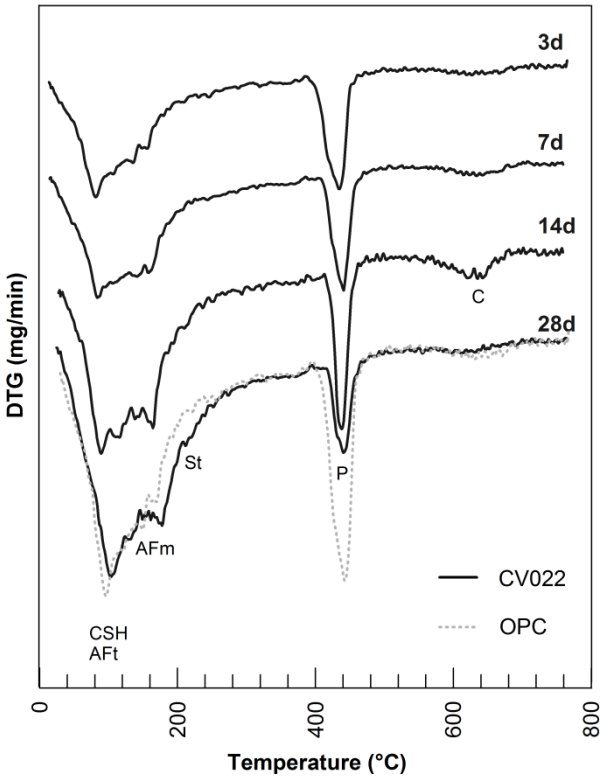

Figure 8.33: *DTG pattern of the calcined clay cement mixture for sample CV22 calcined at 800°C and the reference Ordinary Portland cement paste (OPC). The hydration products are P: portlandite, St: strätlingite, C: calcite, CSH, AFm phases and AFt phases.*

To examine the additional hydration products present due to the pozzolanic reaction, the difference between a pure OPC and blended calcined clay – OPC paste was examined by XRD (Figure 8.34). The results indicate that typical hydration phases are portlandite, the C-S-H phase, alite (C_3S) and belite (C_2S). The AFm phase monocarboaluminate is formed in both the pure OPC paste as in the blended paste. Regarding the pozzolanic reaction, strätlingite is already formed at 14 days, dough the reflection peaks are rather weak indicating the amount of strätlingite is still minor. However at 28 days the peak intensities have increased significantly indicating the pozzolanic reaction is contributing more. In the OPC paste no signs of formation of strätlingite at 28 days can be seen. Nevertheless, at 28 days the amount of portlandite is also clearly lower compared to the pure OPC paste.

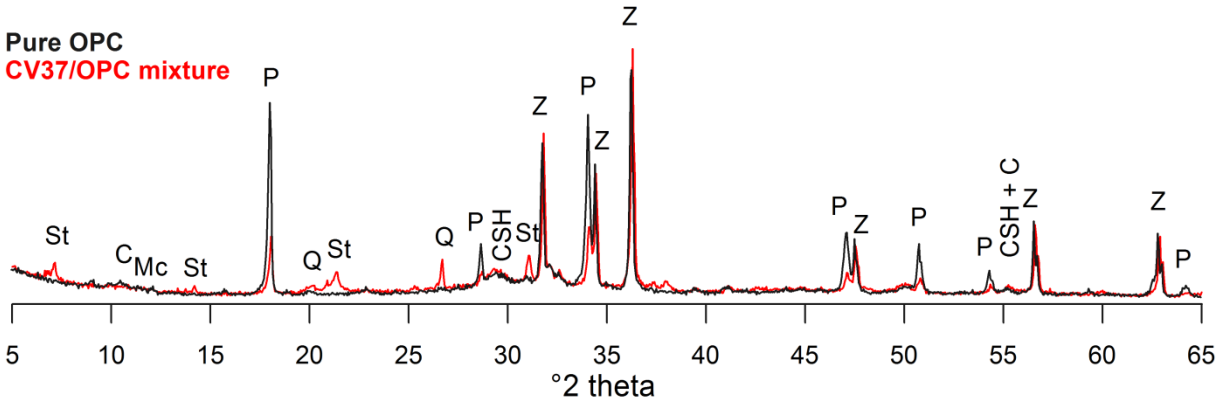

Figure 8.34: *XRD pattern of pastes cured for 28 days of the pure OPC and of CV37 calcined at 800°C and blended with OPC. The phases that are present are indicated: Z: zincite (internal standard) P: Portlandite, St: Strätlingite, Mc: monocarboaluminate, C: C_4AH_{13}, CSH (C-S-H containing hatrurite C3S and larnite C2S) and Q: Quartz.*

8.6 CONCLUSIONS

The Latneskoye clay deposits contain a variety of kaolinitic clays with fluctuating kaolinite content. The most abundant clay minerals, which are present in the samples are kaolinite, smectite, kaolinite-smectite mixed layer and illite-smectite mixed layer. The dominant non-clay impurities consist of quartz, anatase, amorphous material, muscovite and feldspar. Calcination of the clays results in the amorphisation of kaolinite while the 2:1 Al-clays only became partially amorphous. Especially at low firing temperatures of 650°C still reflections of the 2:1 Al clays were visible by XRD. Higher calcination temperature of 800°C resulted in a further decomposition of the 2:1 Al-clays.

Furthermore, the grain size was affected by the calcination process. The sintering and agglomeration process was more pronounced for clay rich samples resulting in more coarse calcined clays while the grain size of more silty samples was less influenced. In general the BET specific surface area was only slightly influenced by the heating process resulting in a decrease of the specific surface area. Nevertheless, pure kaolinite is only marked by a small increase of the specific surface area upon calcination and similar behavior was found for natural kaolinite rich clays.

The TGA measurements of the calcined clay – lime pastes that were prepared and analyzed at various curing ages show the reaction rate is the highest during the first 14 days of the reaction. At 28 days the reaction slows down and reaches a plateau value at 56 days. The main hydration products that are formed are qualitatively comparable for all samples and consist of strätlingite, mono- and hemicarboaluminate, C_4AH_{13} and C-S-H. Due to the lack of kaolinite and therefore alumina, in the overburden samples, the Al-rich phase strätlingite was not formed. The same hydration phases were formed for the calcined clay – OPC mixtures that include alite and belite.

The pozzolanic reactivity of the Latneskoye clays is mainly influenced by the mineralogy. Since there is good correlation between the kaolinite content and the Al_2O_3 percentage the pozzolanic reactivity at 28 days can be estimated based on their Al_2O_3 content according to the following formula:

$$\%\ Portl.\ Consumption = 0.87 * \%\ Al_2O_3 + 15.95$$

This provides an easy tool to quickly assess the pozzolanic potential of a certain kaolinitic clay grade of this deposit. Especially in industry, this can be a very time efficient method to make a first selection of potentially valuable clays. Nevertheless, this function cannot be extended directly to

other clay deposits as it only can be applied to kaolinitic rich deposits that contain little or no illite or other inactive alumina rich phases. The correlation between the mineralogical composition and the reactivity, however, can be applied directly to other deposits as well. The best correlation between the kaolinite content and the reactivity can be found at 14 days and the correlation decreases slowly afterwards. However for longer curing times the participation of the 2:1 Al-clay smectite becomes more important. Therefore at 56 days the sum of clays gives the best correlation. Another parameter that influences the reactivity is the specific surface area of the clays. This is most pronounced at 14 days, but also at 7 days the correlation with the reactivity is fairly good, certainly compared to the correlation of the other parameters. This indicates the specific surface area has mainly an influence on the early stage of the pozzolanic reaction where the amount of potential reaction surface is more important. Also the grain size influences the reaction as smaller grains, present in the milled samples, will have a larger reaction surface and can react faster than larger grains. Even though the influence of the grains size decreases over time, the negative effect at 28 days is still rather large and should be taken into account.

The pozzolanic potential of the Latneskoye is mainly depends on the kaolinite content and can be summarized as follows:

$$LT0 > LT1 > \frac{LT2(high\ Al_2O_3)}{LTU(high\ Al_2O_3)} > \frac{LT2(low\ Al_2O_3)}{LTU(low\ Al_2O_3)} > \frac{LTKj > LT3 > LTK}{LTPK} > glauconite\ clay \gg Red\ clay$$

The high kaolinite and smectite content makes the Latneskoye deposit a high potential candidate to be used as SCM. Nevertheless, also the less kaolinite rich clays can yield fairly good pozzolanic properties and can be more interesting from an economic point of view. The two overburden samples, however, have a portlandite consumption <40% at 28 days, which marks them as a poor pozzolanic material. Additional tests in strength and durability are necessary to further confirm these results.

CHAPTER 9

MINERALOGICAL MODEL

Small differences in the calcination process or of the used equipment can already lead to fluctuations in the pozzolanic reactivity. When these external parameters are however maintained constant for the different samples the actual influence of the clay characteristics on the pozzolanic reactivity can be determined. Previous chapters have demonstrated that the mineralogy of the sample is one of the key controlling parameters. Already some correlation could be found with the dominant reactive clay mineral, kaolinite or smectite, and the reactivity of the calcined clay. Nevertheless natural clay deposits are hardly found in entirely pure form and consist of a mixture of several clay and non clay minerals. Furthermore other parameters like the specific surface area and the degree of ordering influence the portlandite consumption at certain curing times in the reaction. Therefore it is crucial to see whether a simple mathematical tool can be developed whereby the pozzolanic reactivity can be estimated based on the characteristics of the clay.

9.1. SET UP

To establish a mathematical model, regression analysis was applied on the gathered data of the clay samples. In the first step the data of the pure reference samples and the artificial mixtures from Chapter 4 and 5 are used to formulate a mathematical function that allows to predict the portlandite consumption (Y) based on the characteristics of the clay (X_1, X_2, …), by including coefficients (a_0, a_1, …) resulting in a regression model of the type:

$$Y = a_0 + a_1*X_1 + a_2*X_2 + a_3*X_3 \qquad \text{(equation 9.1)}$$

The only sample that was not included in the calculation is the smectitic sample S3, since it is the only sample that contains trioctahedral clay and reacts differently compared to the dioctahedral smectitic clay samples. Besides the mineralogy also other clay parameters such as the chemical composition, the specific surface area and the degree of ordering will be taken into account. Since the influence of the different parameters are expected to be time depending, each curing time will have its own individual model. The curing times that are considered are 7, 14, 28, 56 and 90 days. The 3 day curing time is not taken into account since the portlandite consumption of some samples was not determined at 3 days due to technical problems. It was not possible to implement time as a parameter since the pozzolanic reactivity is only determined on certain curing ages and no information in between two curing days is available.

To test whether the independent variables, also referred to as the applied parameters, or the model are significant three important steps are taken into account:

1) formulate the null hypothesis:
   H0: $b = 0$ (the parameter is not significant / there is no regression)
   H1: $b \neq 0$ (the parameter is significant / there is a regression)
2) Determine the significance level: usually a value of 5% is chosen
3) Apply the t-test (parameters) or the F-test (model): If the test result is smaller than the significance level the null hypothesis can be rejected.

For each model the significance of the regression was evaluated by means of the F-test and the quality of the fit was assessed by the correlation coefficient R^2, whereby a value close to 1 indicates a good fit. The significance of the effect of the independent variables was each time determined by performing t-tests. Additionally the model found is only reliable and can be used for prediction, if the model assumptions hold that the residuals are scattered around the average 0 at random, following a normal distribution and with a constant variance. Therefore a graphical analysis of the residuals was performed to verify these assumptions.

In a second phase the model needs to be validated on behalf of natural clay samples. For this purpose the 29 natural clay samples examined in Chapters 6, 7 and 8 were used. The variable clay content of these samples and the inclusion of not only kaolinite rich but also smectitic dominated samples, provide an ideal validation sample set. The measured portlandite consumption should normally correspond to the predicted portlandite consumption determined with the established model and align with the 1:1 ratio line. This was examined by calculating the root mean square error (RMSE) and performing a visual inspection of the predicted and measured portlandite consumption. When needed, correction to the model can be made.

For the configuration and validation of the mineralogical models the statistical software R, extended with the R studio interface, was used.

9.2 MATHEMATICAL MODEL

To estimate which parameters were needed to estimate the portlandite consumption (Y) and establish a mathematical model, a range of parameters were considered, including mineralogy, chemistry and physical properties. To estimate whether a parameter is significant and is actually needed to reconstruct the measured data, the results of the t-test should be <0.05. As example of the different modeling steps that were followed, the result of the performed t-tests for the 28-day of curing are given in table 9.1. The results of the other curing times (7, 14, 56 and 90 days) can be found in appendix. In the first step of the modeling, linear regression was performed on single parameters. Regarding the mineralogical composition the different clay minerals, kaolinite, smectite and illite were taken into account. For the bulk chemical composition the main constituents, namely the Al_2O_3 and SiO_2 content, were tested. Additionally the physical characteristics were tested including the BET specific surface area of both the raw and calcined material and the grain size distribution (d50) of the ground calcined clays. According to the t-test of these parameters, kaolinite provides a low value of $9.24E^{-14}$ and already a decent fit a R^2 of 0.857. This phenomenon can be explained since most of the used samples consist of 40 – 100% of kaolinite, with exception of the pure smectite and illite samples. As a result the significance (t-test) and the fit of the other parameters is considerably less. The bulk smectite content and the amount of SiO_2 both have a t-test value >0.05, indicating the null hypothesis could not be rejected and the parameter is insignificant when used as single parameter. However, even though kaolinite is the dominant influencing parameter, other parameters might also contribute to the total pozzolanic reactivity of the sample.

Therefore the kaolinite content was chosen to further stepwise built the full model. In a second phase one additional parameter besides the kaolinite content was added (table). Nevertheless, the bulk illite and calcite content, the degree of ordering (Hinckley index and P0) and the physical characteristics (d50 and BET SSA) are not significant to explain the portlandite consumption at 28 days of curing. Only the addition of the bulk smectite content is significant with a t-test value of $4.44E^{-07}$, additionally the fit is improved to a R^2 of 0.939. In a third phase, the BET SSA and the illite content were checked as possible third parameter. Both parameter did however not significant contribute to the fit of the model.

Table 9.1: *Overview of the significance of the tested parameters (t-test), the correlation of the fit (R^2) and the reliability of the model (F-test) at different modeling phases at 28 days of curing. When the t-test >0.05 the parameter is insignificant (marked in grey). When the F-test >0.05 the model is not reliable (marked in grey).The best model is marked in bold.*

Function Parameters	**t-test p1**	**t-test p2**	**t-test p3**	**R^2 adj.**	**F-test**
PHASE 1					
K	$9.24E^{-14}$			0.852	$9.24E^{-14}$
S	$6.25E^{-02}$			0.084	$6.25E^{-02}$
I	$3.94E^{-03}$			0.227	$3.94E^{-03}$
Al_2O_3	$2.44E^{-05}$			0.446	$2.44E^{-05}$
SiO_2	$2.75E^{-01}$			0.008	$2.75E^{-01}$
d50	$1.08E^{-02}$			0.176	$1.08E^{-02}$
SSA	$3.91E^{-03}$			0.228	$3.91E^{-03}$
PHASE 2					
K + S	**$<2.00E^{-16}$**	**$4.44E^{-07}$**		**0.943**	**$<2.00E^{-16}$**
K + I	$2.14E^{-12}$	$5.11E^{-02}$		0.866	$2.23E^{-13}$
K + Cal	$2.49E^{-13}$	$3.55E^{-01}$		0.851	$1.00E^{-12}$
K + SSA	$1.16E^{-11}$	$4.67E^{-01}$		0.849	$1.18E^{-12}$
K + d50	$5.47E^{-12}$	$6.35E^{-01}$		0.848	$1.38E^{-12}$
K + P0	$1.07E^{-12}$	$4.59E^{-01}$		0.849	$1.17E^{-12}$
K + 1/P0	$4.37E^{-12}$	$9.32E^{-01}$		0.847	$1.54E^{-12}$
K + HI	$7.13E^{-13}$	$4.62E^{-01}$		0.849	$1.17E^{-12}$
PHASE 3					
K + S + SSA	$3.87E^{-16}$	9.32^{E-07}	$9.18E^{-01}$	0.937	$<2.00E^{-16}$
K + S + I	$3.52E^{-15}$	$3.40E^{-06}$	$4.08E^{-01}$	0.939	$2.20E^{-16}$
PHASE 4					
$Al_2O_3 + SiO_2$	$4.95E^{-05}$	$5.13E^{-01}$		0.435	$1.29E^{-04}$
$AlO_3 + S$	$1.59E^{-04}$	$5.16E^{-01}$		0.435	$1.29E^{-04}$
$Al_2O_3 + K$	$9.13E^{-01}$	$1.66E^{-09}$		0.847	$1.54E^{-12}$
PHASE 5					
K^2	$1.14E^{-11}$			0.794	$1.14E^{-11}$
$K + K^2$	$2.10E^{-03}$	5.34^{E-01}		0.849	$1.27E^{-12}$
$K^2 + S$	$5.43E^{-11}$	$1.67E^{-01}$		0.801	$5.93E^{-11}$
$K + S^2$	$5.84E^{-16}$	$4.27E^{-05}$		0.916	$3.10E^{-16}$
$K+ K^2 + S$	$4.18E^{-09}$	$8.16E^{-02}$	$1.80E^{-07}$	0.944	$<2.00E^{-16}$
$K + S + S^2$	$<2.00E^{-16}$	$1.10E^{-03}$	$1.35E^{-01}$	0.942	$<2.00E^{-16}$

The possibility to estimate the portlandite consumption based on the chemical composition of the sample was examined in a fourth phase. Al_2O_3 was proven to be the best chemical parameter, but the addition of the SiO_2 content did not improve the fit of the model. Other chemical parameters were not tested as they do not take part in the pozzolanic reaction. Also the addition of the bulk smectite content was insignificant and only when the kaolinite content was added the fit improved to a R^2 of 0.847. However this fit is less good than when the kaolinite content is used as single parameter. This indicates the mineralogy of the sample allows a far better estimation of the portlandite consumption of the sample than the chemical composition.

In the fifth phase it was examined whether the inclusion of a quadratic parameter would be preferred above a linear function. However, for most cases the R^2 value is lower and/or the contribution of the additional quadratic parameter cannot be classified as significant. This indicates the linear regression model should be chosen over a quadratic function.

Before accepting the outcome of the linear regression model, its suitability at explaining the data need to be tested. Thereby the difference between the observed value and the predicted value, referred to as the residuals, are visually examined. This allows to validate whether the residual errors are randomly spread and the removal of one sample has no significant impact on the model's suitability. The residual plots for the model Y~ K + S at 28 days are given in Figure 9.1. Graph A shows the residual errors plotted versus their fitted values. The residuals are in general randomly distributed around the horizontal line an the observed trend is limited, which is still a acceptable. Graph B shows each residuals Leverage, which expresses its importance in determining the actual regression model. The contour lines for Cook's distance are superimposed on the plot. A small distance indicate that the removal of the point would have little effect on the result of the regression model. When the distances are larger than 1, the samples are suspicious and suggest a poor model. However, all samples have a cook's distance <1, and only one of the pure smectites, S1, has a value >0.5 (indicated with number five in Figure 9.1 B).

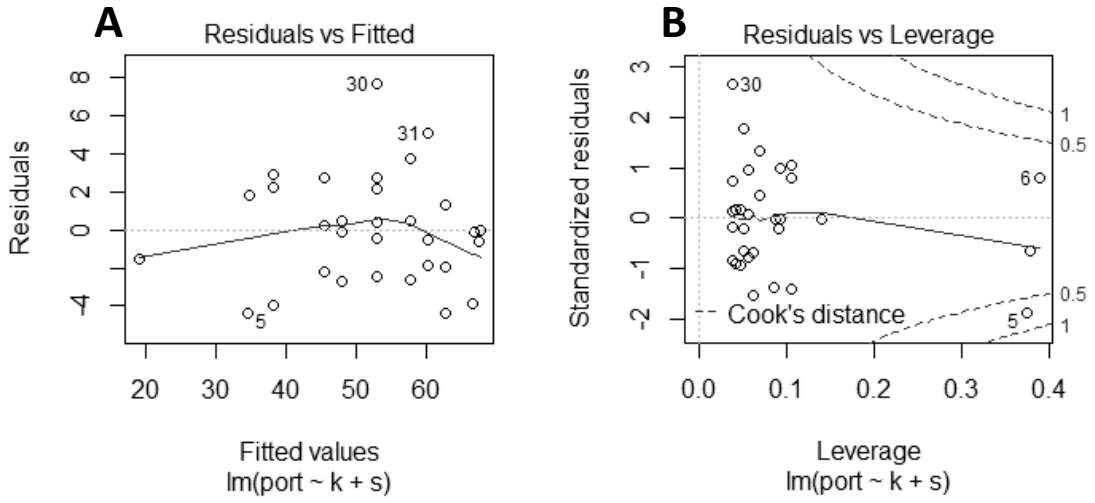

Figure 9.1: *Graphs of the residuals to test the suitability of the model. A: The residual errors are plotted versus the fitted values. B: The residuals are plotted against the leverage of each residual. The dotted lines represent the Cook's distance.*

This modeling procedure was performed for all the different curing ages separately since the influence of each of these parameters on the portlandite consumption can change over time.

The five models at 7, 14, 28, 56 and 90 days are combined in one model a linear combination of the content of kaolinite (K), smectite (S) and the BET specific surface area (SSA) of the calcined clay

resulted in the best fit with the portlandite consumption at a certain curing time t and is expressed according to the following equation:

$$P_t = a_0 + a_1*K + a_2*S + a_3*SSA \qquad \textit{(equation 9.2)}$$

With: P_t = *Portlandite consumption at time t*
K = *Bulk kaolinite content of the uncalcined clay*
S = *Bulk smectite content of the uncalcined clay*
SSA = *specific surface area of the calcined clays*
a_i = *coefficient determined by the regression software*

The coefficients, a_i, that were obtained by the least square method of the regression method are listed for the different curing times in Table 9.2. It is important to note that not all three parameters are included at all curing ages. At 7 and 14 days the amount of smectite (a_2) that is present in the sample hardly contributes to the overall prediction model. The hypothesis that a_2 significantly differs from 0 could not be rejected since the t-test value for the smectite coefficient was > 5%. From 28 days onward the SSA coefficient (a_3) becomes insignificant and is no longer needed to predict the portlandite consumption. However in the early stage of the reaction the SSA has a major influence on the portlandite consumption. In general a large specific surface area results in an increase of the reaction surface and as a consequence the reaction has more starting or nucleation sites. The effect of the SSA decreases over time and become less significant at 14 days while the influence of kaolinite content increases.

Table 9.2: *Coefficients (a_i), correlation coefficient (R^2) and F-test probability for the reactivity model at different curing ages based on 31 clay samples of chapter 4 and 5.*

Time (days)	a_0	a_1	a_2	a_3	R^2	F-test
7	17.96	0.147	0	0.802	0.773	$6.38*e^{-10}$
14	22.77	0.260	0	0.545	0.857	$1.18*e^{-12}$
28	18.59	0.490	0.162	0	0.943	$< 2.20*e^{-16}$
56	22.53	0.460	0.225	0	0.871	$3.82*e^{-13}$
90	24.27	0.439	0.263	0	0.832	$1.40*e^{-11}$

The weight of the smectite coefficient a_2 tends to increase over time and is marked with the highest value at 90 days. The coefficient of kaolinite (a_1) is most important at 28 days, at longer curing times the values of the kaolinite coefficient a_1 become smaller again. This phenomenon reflects the difference in reaction rate between kaolinite and smectite. At 28 days most of kaolinite is already consumed and therefore the kaolinite content does not further contribute significantly to the reactivity. Smectite is marked by a slow reaction rate and as a result after 28 days the reaction still continues. As a result at 56 and 90 days the contribution of the smectite content increases.

The quality of the fit is given by the correlation coefficients that are given in Table 9.2 for the different curing ages. In general the measured data fit close to the fitted regression line with R^2 values ranging between 0.773 and 0.943. The fit of the measured versus the calculated portlandite consumptions at 28 days is visualized in Figure 9.2 and indicate a good agreement of the results. Actually the model at 28 days shows the best fit with the measured values, which is ideal as this day is considered to be important in concrete technology. R^2 is quite high and hence 94% of the variability of the portlandite consumption can be explained through the linear regression on kaolinite and smectite content. Furthermore the regression can be seen as significant since the F-test has values <0.05 for all curing ages. In a last step the residuals are studied to see if they are randomly

spread without certain trends. In general the residuals for all curing ages are randomly spread, with semi normal data. Also the Cook's distance is never larger than 1. This indicates that little effect on the regression results is seen when one of the observation points is removed. Observations points with distances larger than 1 are rather suspicious and would suggest the presence of an outlier or a poor model.

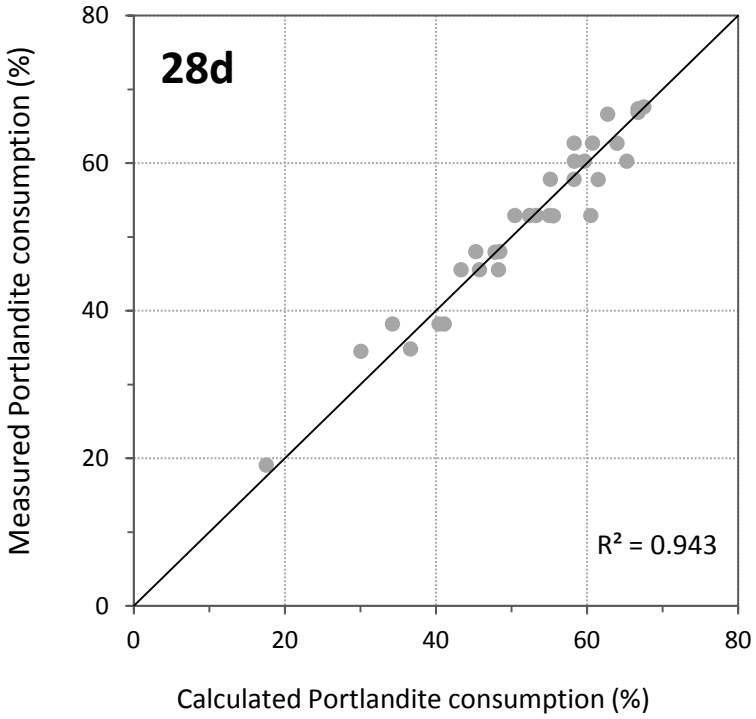

Figure 9.2: *Correlation Plot of the measured and calculated (model based) portlandite consumption of the pure clays and artificial mixtures discusses in Chapter 4 and 5, with exception of sample S3.*

Additionally to the applied parameters other characteristics, including the chemical composition, the illite and calcite content, of the clay were tested, but did not significantly contribute to the fit of the model. The bulk chemical composition of a clay can easily be determined. However, no meaningful regression model could be made that was only based on the chemical composition including Al_2O_3, SiO_2 and Fe_2O_3 content. Regarding mineralogy the addition of the illite or calcite content to the equation did not result in a significant increase of the fit of the model. This is most likely because illite is only a little bit more reactive than the inert phases and its contribution to the total portlandite consumption is too limited. The effect of calcite is most likely balanced out since mixtures that contain <30% calcite are more reactive than inert mixtures, while samples with >30% calcite are less reactive. This phenomenon should be taken into consideration and it is good to know that the portlandite consumption of clay samples with less than 30% calcite is underestimated. The degree of ordering of kaolinite could also not be included into the model since the variation of the samples was too small, with only four different values of the degree of ordering recorded for the pure clay samples. All mixtures contained the same type kaolinite. Nevertheless the difference in the degree of ordering of the kaolinites is also reflected in the specific surface area.

In general it can be concluded that the linear regression model is best fitting for the prediction of the portlandite consumption at 28 days. Furthermore at 28 days only the mineralogical content of the raw sample need to be known while at 7 or 14 days also information about the specific surface area of the calcined clay is necessary to estimate the sample reactivity. Nevertheless the determination of the smectite content in the bulk sample is rather time consuming since the detailed clay mineralogy

of the fraction <2 µm needs to be known. The total amount of 2:1 Al clays in the bulk sample cannot be used as both smectite and illite are included in these clays while their reactivity is significantly different.

9.3 VALIDATION

To validate the accuracy of the prediction of the portlandite samples the formulated model was tested on natural clays with a variable mineralogical composition. For this purpose the natural clays samples studied in the Chapters 6, 7 and 8 were used to obtain a variation of kaolinitic rich clays and also include dominant smectitic clays. The portlandite consumption was calculated using the equation 9.2 and the corresponding coefficient for each curing time listed in Table 9.2.

To validate the model the root mean square error (RMSE) can be calculated as it gives the standard deviation of the difference between the predicted and the measured values, called the prediction errors. The RMSE value should be as small as possible to assure a good prediction can be made based on the proposed model. The RMSD can be calculated according to the following equation:

$$RMSE = \sqrt{\frac{\sum_{i=1}^{N}(P_{p,i}-P_{m,i})^2}{N}} \qquad \textit{(equation 9.3)}$$

With: $P_{p,i}$ *= predicted portlandite consumption for sample i*

$P_{m,i}$ *= measured portlandite consumption for sample i*

N *= number of samples*

The RMSE values that for each curing time are indicated on the graphs in figure 9.3. For 28, 56 and 90 days of curing the RMSE is rather comparable with values of 3.89, 3.55 and 3.42 respectively. This indicated that the predicted portlandite consumption has an average error of 3.6, which is still acceptable when the analytical errors are taken into account. At 14 of curing the RMSE of 6.96 is almost double as high as for 90 days. The highest RMSE value of 28.96 was found for the comparison of the predicted and measured results at 7 days. The predicted model for 14 and especially for 7 days is not well suited and visual inspection can help to estimate whether the model should be adapted or not.

Visually the data can be validated by plotting the measured portlandite consumption in function of the predicted portlandite consumption of each sample (Figure 9.3). In general there is a good correlation between the two variables with the best fit at 56 days (R^2=0.871) and at 14 days the lowest correlation was found (R^2=0.754). Nevertheless, at short curing times the predicted portlandite consumption is marked by significant higher values than the real measured portlandite consumption. At 7 days the predicted values are systematically 30% higher than the actual values. This can also be seen as normally the correlation line should coincide with the 1:1 dotted line, which is the line of best fit, indicated in Figure 9.2. This indicates the mineralogical regression model overestimates the portlandite consumption at low curing times. The systematic overestimation of the portlandite consumption of 30% of portlandite is in agreement with the RMSE value for 7 days of 28.96. For 14 days the fit with the regression line and the 1:1 line is already improved but still the predicted portlandite consumption is slightly overestimated.

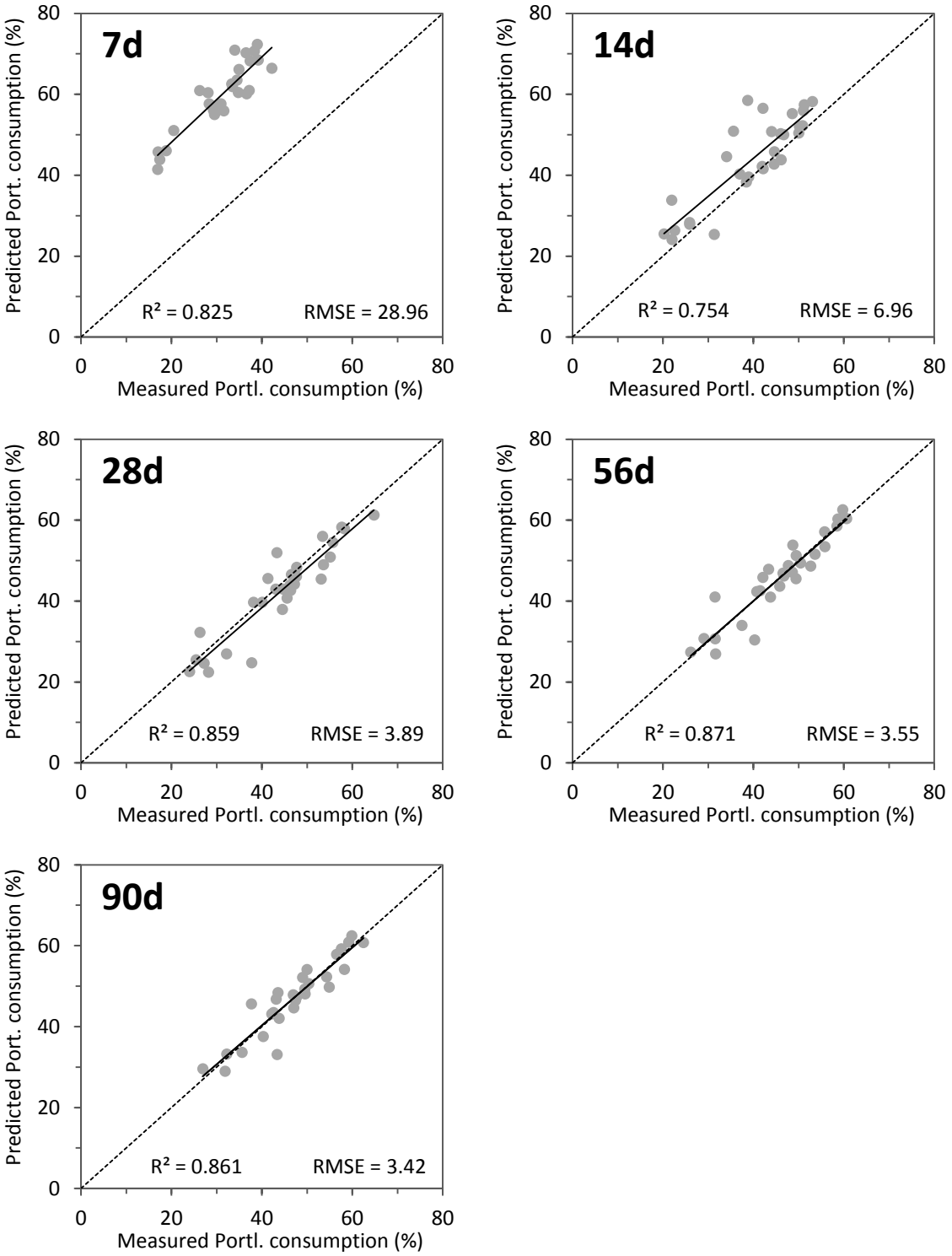

Figure 9.3: *Correlation plots of the measured portlandite consumption in function of the predicted portlandite consumption determined with the model proposed in equation 9.2 and the coefficients in table 9.1 at different curing times. The R^2 gives the correlation of the regression line and the data point. The dotted line represents the 1:1 line (line of best fit) which idealistic should correspond with the regression line.*

An explanation for this phenomenon can be found in the parameters that are incorporated in the model of 7 and 14 days. Besides kaolinite the specific surface area of the calcined clay is an important controlling parameter at low curing times. For the pure clays there was a clear tendency that kaolinite clays were less influenced by sintering processes upon calcination. As a result their BET

specific surface area remained rather high and could be correlated to the degree of ordering of kaolinite. The smectitic and illitic clays experienced much more sintering whereby their initial high specific surface area dropped significantly to values below 5 m^2/g. As a result higher specific surface areas could be directly correlated with an increase in reactivity in the early stage of the reaction. For the mixtures only one type of kaolinite was used and as a result the specific surface area of the different mixtures were fairly similar. For the natural clays however the sintering was much different, since the presence of inert minerals caused a shielding effect whereby less clay particles were sintered. As a result the drop in specific surface area, especially for 2:1 Al rich clay, upon calcination was less distinct. As a consequence when the higher specific surface areas that were determined for the natural calcined clays are inserted in the models equation the estimation of the portlandite consumption will be much higher. Nevertheless the regression line at 7 days runs parallel to the 1:1 line, which indicates a certain correlation exists between the amount of portlandite that is consumed and the percentage of kaolinite and specific surface area. However most likely the coefficient need to be adapted. To improve the mineralogical model on 7 and 14 days the natural samples should be included to establish the model. The new coefficients are given in table 9.2 and can be used in equation 9.2. In general less weight is assigned to the specific surface parameter than originally. The R^2 value slightly drops indicating the fit is somewhat less good as more samples are included and the variation can be greater. Nevertheless the p-value decreases indicating the model becomes more significant.

The predicted portlandite values of this second model are plotted against the measured values in Figure 9.4. At 7 days the correlation between the measured and predicted portlandite values is 0.707. Compared to the first model, with an R^2 of 0.825 at 7 days, this correlation is less, however the data points plot more close around the 1:1 line and more important the RMSE decreases significantly to 4.15, indicating that this model is more suitable. The clay samples that show the highest misfit are medium and low ordered kaolinites. This can be explained because for these samples their degree of ordering was related to a high specific surface area which directly contributed significantly to the portlandite consumption while for clay mixtures this effect is far less. At 14 days the correlation and the misfit regarding the 1:1 line improves significantly and the RMSE value decreases to 3.97. This indicates that when specific surface area is included in the prediction model, it is important to include natural clay mixtures since their SSA is affected in a different way upon calcination than for the pure clays.

From 28 days onward the initial proposed model shows good resemblance and at 56 and 90 days this resemblance further improves and the two lines completely coincide with high correlation coefficients with respectively a R^2 0.871 and 0.861. At 28 days the alikeness between the 1:1 line and the regression line can be further improved when the most misfitted sample, CV48, is not taken into account. The portlandite consumption of CV48 is underestimated with a value of only 24.7% while the actual portlandite consumption is 37.8%. This severe underestimation can be explained by the presence of 2:1 Fe-smectite that participates in the pozzolanic reaction but is not incorporated in the model where only the 2:1 Al-smectite is taken into account.

Table 9.3: *Coefficients (a_i), correlation coefficient (R^2) and F-test probability at 7 and 14 days when all 60 clay samples are taken into account..*

Time (days)	a_0	a_1	a_2	a_3	R^2	F-test
7	18.03	0.198	0	0.257	0.694	$7.09*e^{-15}$
14	22.52	0.299	0	0.227	0.842	$<2.20*e^{-16}$

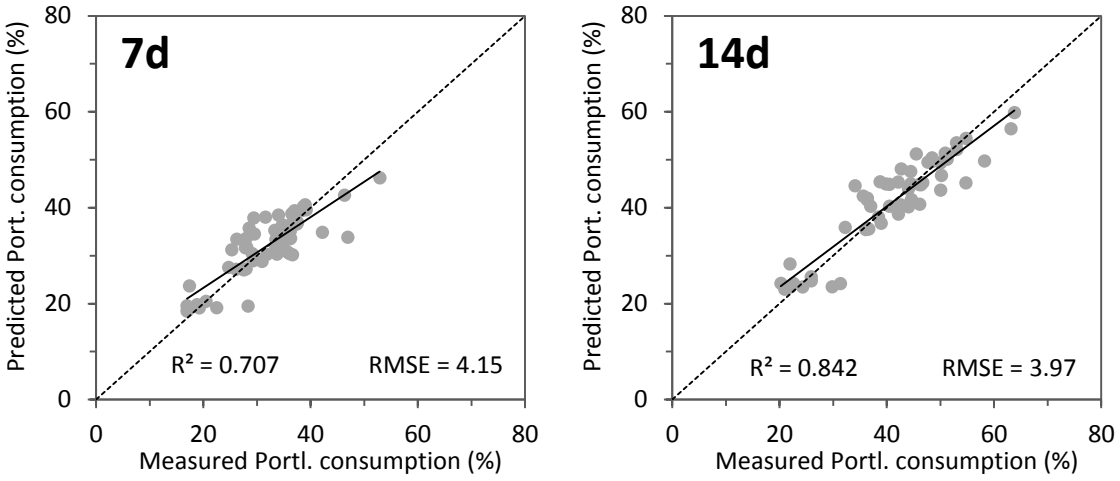

Figure 9.4: *Correlation plots of the measured portlandite consumption in function of the predicted portlandite consumption determined with the model proposed in equation 9.2 and the coefficients in table 9.2 at 7 and 14 days of curing. The R^2 gives the correlation of the regression line and the data point. The dotted line represents the 1:1 line which idealistic should correspond with the regression line.*

9.4 INFLUENCE OF GRAIN SIZE

One parameter that can potentially influence the actual portlandite consumption significantly is the grain size distribution. The samples that were used to establish and validate the previous proposed linear regression model were all ground after calcination. This was done to minimize the effect of the grain size to be able to only see the effect of the mineralogy of the different clays and to be able to compare the samples directly to each other. Nevertheless it was already indicated in chapter 6 and 8 that a more coarse grain size has a negative effect on the reactivity of the sample. This effect is not yet negligible at 28 days, certainly not for clay samples that also contain a significant amount of 2:1 Al clays. To estimate the importance of the grain size distribution a new regression model was made for the six samples of which the portlandite consumption was both determined for the ground and unground sample.

Due to the limited data available, only for the portlandite consumption at 28 days a meaningful regression model could be established. The parameters that influence the reactivity of the sample significantly are the kaolinite content and the 1/d50 of the calcined sample. The achieved model can be summarized in the following equation.

$$P_{28} = 8.31 + 0.568 *K + 22.756*1/d50 \qquad \text{(equation 9.2)}$$

To include the variation in the grain size distribution, the inverse of the d50 value of the calcined sample resulted in the best fit. The R^2 of the model fit was proven to be very good, with a value of 0.917 (Figure 9.5). Also the p-value of $1.407e^{-5}$ is smaller than 0.05 and therefore the regression model is significant. A graphical study of the residuals indicate no trends could be observed and the data are approximately normally distributed. At 7 and 14 days the parameter of K does not significantly contribute to the portlandite consumption. Also the addition of other parameters like the specific surface area of the calcined clay did not improve the model significantly. When only the grain size was taken into account the model only provided a weak fit with R^2 of only 0.307 and the F-test indicated the model was not significant.

This indicates the implementation of the grain size was only meaningful for predicting the portlandite consumption at 28 days. However the number of analyzed samples is rather limited and includes only kaolinite rich samples. Furthermore the model cannot be validated with additional clay samples. Nevertheless it gives a good indication of the importance of the grain size regarding the pozzolanic reactivity and that the grain size of the sample can be represented by the d50 value.

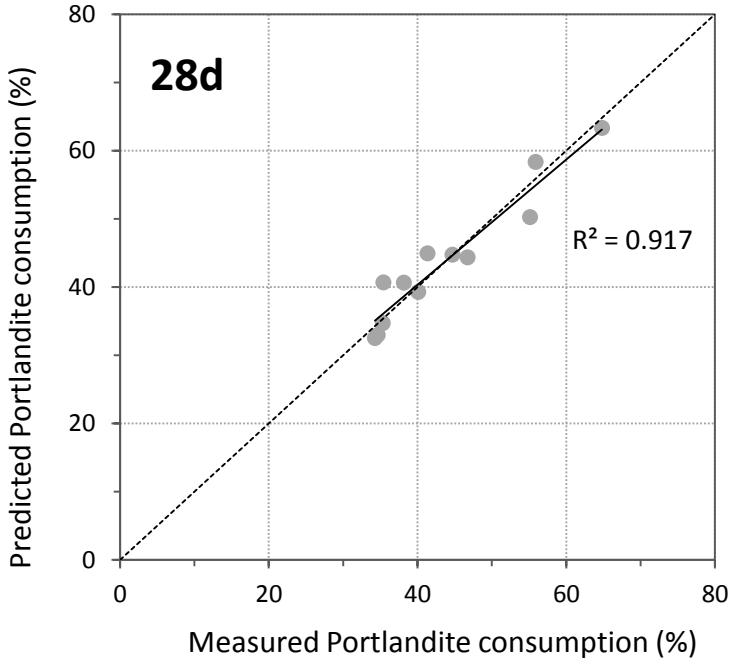

Figure 9.5: *Correlation plot of the measured portlandite consumption in function of the predicted portlandite consumption determined with the model proposed in equation 9.2 at 28 days. The R^2 gives the goodness of the fit of the model. The dotted line represents the 1:1 line.*

9.5 CONCLUSION

The portlandite consumption of a natural clay can be predicted with the established linear regression model that can be summarized in the following equation:

$$P_t = a_0 + a_1*K + a_2*S + a_3*SSA\ (+ a_4*1/d_{50})$$

The parameters that have a considerable effect on the reactivity of the ground calcined clay are the kaolinite content, bulk smectite content and the specific surface area. At early curing ages up to 14 days, the amount of kaolinite and the specific surface are of the calcined clay form the crucial parameters. From 28 days onward the specific surface area becomes less important and the smectite content will gain significance. This allows to give an accurate estimation of the reactivity at 28 days of natural clay based on its clay mineralogy. This indicates that a detail mineralogical characterization of the starting material is of key importance to provide valuable information on the reactivity. Furthermore this model can be applied on different clay deposits that are either kaolinite or smectite rich. Other parameters like the chemical composition can often only be applied to one single deposit site.

The only drawback is that the grain size is not taken into account. Since all samples were ground after calcination, their grain size distribution and d50 values were too similar to be implemented in the

model as a significant parameter. Nevertheless unground samples are marked with a significant drop in their pozzolanic reactivity. Therefore it can be stated that when samples are not ground after calcination the parameter 1/d50 should be implemented in the equation to provide a better estimation of the portlandite consumption.

Furthermore, the influence of the presence of calcite in clay rich samples was leveled out and as a consequence the calcite influence could not be considered as an important controlling parameter. Nevertheless, it is likely that when only clays with a calcite content below 30% are incorporated, the calcite content becomes more significant and will have to be included in the formula.

CHAPTER 10

GENERAL CONCLUSIONS AND PERSPECTIVES

The main aim of this study is to investigate the potential use of calcined clays from a mineralogical point of view by linking the characteristics of the untreated clays to the pozzolanic activity of the calcined clays. The characterization of the raw material and the performance of accurate pozzolanic reactivity tests allowed to estimate the optimal activation temperature, determine the controlling parameters and identify the formed pozzolanic reaction products. This knowledge was combined in a predictive model that allows to estimate the pozzolanic reactivity of a clay based on its characteristics. The general conclusion regarding these topics and opportunities for further research are presented in the following paragraphs.

10.1 CONCLUSION

OBJECTIVE 1: POZZOLANIC REACTIVITY AND OPTIMAL ACTIVATION TEMPERATURE

Determination of the pozzolanic reactivity: To evaluate the pozzolanic reactivity of a clay rich sample it is important to apply an accurate and repeatable test method. In this study two measuring methods that have been applied in previous studies were taken into account. Thermal analyses of calcined clay lime pastes at different curing times have proven to be an effective way to monitor the pozzolanic reaction over time and to determine the pozzolanic reactivity of the sample. Compared to the chapelle test, TGA is more accurate, since the chapelle test tends to overestimate the pozzolanic reactivity of smectitic and illitic clays. Furthermore the repeatability decreases drastically for smectitic clays and for natural clay mixtures which negatively affects the accuracy of the chapelle test. Therefore the TGA reactivity test is favored.

Determination of the optimal calcination temperature: To enhance to pozzolanic properties of a clayey material, the clay is thermally treated. The choice of the applied calcination temperature has a direct influence on the reactivity of the calcined clay and can be related to the type of both the clay minerals and non-clay mineral that are present. The optimal activation temperatures that were found for pure clays confirm previous reported values in literature. Kaolinite is marked by a broad optimal firing temperature between 500 and 900°C. Smectitic clays have a distinct optimum

calcination temperature at 800°C. Their reactivity decreases rapidly when a higher calcination temperature (900°C) is applied. This is due to enhanced sintering and formation of a new crystalline phases. The illitic clay's optimal activation temperature is 900°C, nevertheless even at 900°C illite only becomed partly amorphous.

For kaolinitic clays this study proves that the degree of ordering of kaolinite is an important parameter that influences the optimal activation temperature. For medium and low ordered kaolinites a calcination temperature at 500°C yields a fairly good reactivity. High ordered kaolinites, on the other hand, do not reach sufficient amorphization at 500°C, resulting in a less pozzolanic reactive material.

Additionally the optimal activation temperatures of clay mixtures was studied in detail to clarify the contribution of each mineral phase individually. Even though the amount of impurity only had a limited effect, the type of impurity proved to be have a significant influence on the calcination temperature. For kaolinitic clays that only contain inert minerals like quartz, muscovite or feldspar as impurity the activation temperature is not affected compared to pure kaolinite. When however, calcite, smectite or illite is present a distinct optimal activation temperature of 800°C was found.

The optimal activation temperature of the mixtures is mainly influenced by the type of the impurity as the amount of impurity has only a limited effect. The activation temperature of the mixtures containing 30% of the inert materials quartz, feldspar or muscovite is not affected significantly compared to pure kaolinite. For the 30% calcite, smectite and illite mixtures the optimal activation temperature could be appointed at 800°C. Upon calcination of the calcite-kaolinite mixture, calcite was decarbonated and again transformed into a less crystalline calcite when exposed to air, making the calcite more reactive. Further heating to 900°C results in the formation of crystalline gehlenite resulting in a less reactive material. At 800°C smectite becomes completely amorphous and no recrystallisation takes place, so smectite can fully contribute to the pozzolanic reactivity. Even though the optimal activation temperature of illite is 900°C, the negative effect of the additional sintering makes 800°C more suitable.

OBJECTIVE 2: CONTROLLING PARAMETERS

Natural clay mineral deposits often have a rather complex mineralogy and can consist of multiple clay minerals. Furthermore the chemical and physical properties of natural clays can vary a great deal. Therefore an important part of this study focused on the relation between the characteristics of the clay and its behavior as a pozzolanic material and one of the main objectives was to **determine the controlling parameters (Obj 2).** Previous studies highlight the importance of the clay type, but often neglect additional structural, chemical and physical parameters. These parameters where taken into account in this study that contribute to the pozzolanic reactivity of the calcined clay are discussed in the following paragraphs.

1. *Type of clay mineral*

From literature it is known that kaolinite is the most reactive clay mineral and both smectites and illites only possess mediocre to poor pozzolanic properties. The reactivity tests on pure reference clays confirmed that kaolinite was indeed highly reactive, which can be explained by its total amorphisation that occurs upon calcination. Illite remains semi-crystalline even at high optimal calcination temperatures of 900°, resulting in a low pozzolanic materiall. Di-octahedral smectite-rich clays can be classified as medium potential and depending on their structure full or partial amorphisation takes place. The tri-octahedral clay hectorite was proven to be the least reactive clay due to the lack of alumina atoms and the rapid recrystallisation of Mg-silicate phases. In general the reactivity of pure clays can be summarized as follows: Kaolinite >> Ca montmorillonite > Na montmorillonite > illite > hectorite

2. Cation and octahedral occupancy

The differences in the pozzolanic reactivity of the di-octahedral smectitic clays could be traced back to the octahedral occupancy and the dominant exchangeable cation that is present in the clay. For smectitic clays the dehydroxylation temperature is influenced by the octahedral occupancy. Trans vacant clays tend to dehydroxylate more early and as a consequence they are completely decomposed when calcined at 800°C resulting in more reactive clay. Furthermore, the dominant cation that is present also influences the reactivity whereby Ca-rich montmorillonites are somewhat more reactive than Na-montmorillonites.

3. Degree of ordering

Even though it is know that kaolinite is a highly reactive pozzolan, the differences in reactivity between two kaolinites is not well known. The monitoring of the portlandite consumption over time allowed to make a distinction in the reactivity of kaolinite based on its degree of ordering. High ordered kaolinitic clays tend to have a lower specific surface area than medium or low ordered kaolinite. As a consequence the reaction surface of high ordered kaolinites is smaller and the reaction rate will initially (<28 days) be slower than for medium and low ordered kaolinites.

4. Specific surface area

The specific surface area of the clay is significantly altered upon calcination due to sintering of the clay particles. These changes depend on the calcination temperature and the type of clay mineral. Higher temperatures will reduce the SSA more and 2:1 Al-clays tend to be more affected by the sintering, which decreases their SSA more, than kaolinites. Nevertheless for clay mixtures, inert material provide a shield and inhibit sintering and as a consequence the SSA is less influenced. In the calcined clay lime pastes the SSA plays an important role at short curing times up to 14 days. A higher specific surface area results in more reaction surface and increases the pozzolanic reaction rate. However after 14 days this initial effect is minimized and the SSA becomes less significant.

5. Amount and type of impurities

Inert materials like quartz, feldspar and muscovite have no direct influence on the optimal activation temperature. Nevertheless, a higher amount of inert materials and as a consequence a lower amount of reactive clays, results in a lower portlandite consumption. As a result the quantity of inert impurities in clays can be negatively linearly correlated to the portlandite consumption. A quick estimation of the portlandite consumption of calcined kaolinite rich clays is based on the percentage of kaolinite present in the original sample and can be expressed accordingly:

$$\% \text{ Portl. Consumption} = 0.44 * \% \text{ kaolinite} + 20.97$$

Illite is not completely inert, nevertheless its actual contribution to the pozzolanic reactivity is limited and rather insignificant. The presence of smectite provides additional portlandite consumption, especially at longer curing times of 56 and 90 days, since smectite is marked by a low reaction rate. Up to 30% of calcite can be beneficial to improve the pozzolanic potential of the samples, especially since at early stages the reaction is significantly faster than for normal kaolinite clay. The benefit of calcining calcite that present in the original sample compared to adding calcite afterwards is that when the calcined samples are exposed to air, new less crystalline calcite is formed which is less reactive than regular calcite. In general the pozzolanic reactivity of mineral impurities can be summarized as follows: Muscovite < Quartz = Feldspar < Illite << Calcite < Smectite. Furthermore it can be concluded that a kaolinite content of only 40%, or smectite content of 50% is still sufficient to provide a medium reactive pozzolanic material. When reactive minerals like smectite or calcite are present this percentage can even be further reduced.

6. Grain size

The grain size of the calcined clay is influenced by the chosen calcination temperature and the mineralogical composition of the sample. Higher calcination temperatures or the presence of 2:1 Al clays will enhance agglomeration of the particles resulting in a coarse grain size. When the samples are used unground, the coarser grain size distribution will lead to less reaction surface and less nucleation sites. As a consequence the reaction rate drops significantly and even up to 28 days their reactivity is considerably lower compared to the same sample that was ground after calcination. Because the grain size is an important controlling parameter of the portlandite consumption, also the size of the reactive kaolinite particles can play a major role. Kaolinite rich clays that have less kaolinite present in the clay fraction <2 µm and consist of rather coarse kaolinite particles, possess an inferior pozzolanic reactivity in comparison to their kaolinite content. This demonstrates detailed clay mineralogy of the original sample provides insight in the reaction mechanism of the calcined clay. Furthermore, the presence of impurities can have an effect on the grain size, since some type of impurities like smectites, feldspar or muscovite enhance the sintering processes, which results in a coarser grain size and consequently a drop in reactivity when these samples are used unground in lime or cement pastes. When quartz is present, the clay particles are shielded from each other which prevents total sintering of the clay particles resulting in finer grains than in a pure clay sample.

OBJECTIVE 3: REACTION PRODUCTS

The effect of the addition of calcined clays on the reaction product assemblage depends strongly on the mineralogical composition of the clay sample. Kaolinite rich samples tend to favor the formation of the Al-rich strätlingite. Additionally other AFm phases like C_4AH_{13}, mono- and hemicarboaluminate are formed. The available silica is mainly built in C-S-H phases. 2:1 Al clays, like smectite and illite are marked by lower alumina concentrations and as a consequence only C-S-H, mono- and hemicarboaluminate are formed. When inert minerals are present, the assemblage of the reaction products is unaltered. Nevertheless the quantity of impurities that were presented in a clay sample had an effect on the amount of the formed hydration products. Especially strätlingite and C-S-H were affected while the amount of mono and hemicarboaluminate remained fairly similar.

In the presence of calcite, monocarboaluminate was formed as the main hydration phase at the expense of strätlingite. This phenomenon is triggered by the reaction of calcium carbonate with alumina. Only for kaolinite-rich samples that contain ≤15% of calcite, strätlingite could still be detected. The timing of the formation of strätlingite in kaolinite-rich samples depends on two variables, namely the kaolinite content and the Si/Al ratio of the amorphous material. Lower amount of kaolinite or an increase of the Si/Al ratio, caused by the presence of smectite or illite in the clay, will result in a delay of the strätlingite formation.

OBJECTIVE 4: MINERALOGICAL MODEL

The portlandite consumption at different ages of a natural clay can be predicted by a linear combination of the kaolinite content (K) of the clay, the bulk smectite content (S) and the specific surface area (SSA) of the calcined clay. The mathematical regression model can be summarized in the following equation:

$$P_t = a_0 + a_1*K + a_2*S + a_3*SSA$$

At 28 days the pozzolanic reactivity can be entirely estimated based on the mineralogical composition of the starting material. This indicates that a detailed mineralogical characterization of the starting material is of key importance in understanding the reactivity of calcined clays.

Furthermore this model can be extended to other kaolinite- or smectitic-rich clay deposits. The only drawback is that this model can only be applied to ground calcined clay samples, otherwise the particle size distribution should be included.

10.2 PERSPECTIVES

Several research question regarding the suitability of calcined clays as SCM and the influence of impurities are answered in this study. However there are still some issues that need to be resolved. First of all the predictive model should be further extended, so that parameters like the grain size and the calcite content can be fully implemented in the model. Furthermore additional validation samples of non-kaolinitic clays would improve the application possibilities of the proposed model. The main focus should be on low grade clays and waste materials. The portlandite consumption of calcined clay does not entirely reflect the whole pozzolanic reactivity of the material. The strength development of both mortar and cement is also influenced by the reaction kinetics and the pore volume and should therefore be investigated in more detail. A similar model can be set up whereby the strength is used instead of only the portlandite consumption.

This pozzolanic reactivity model can be supplemented by thermodynamic modeling to calculate and predict the assemblage of the hydration products and the composition of the pore solution. This would help to further understand the calcined clay cement reaction evolution over time. Additionally the variability of the dissolution rates of different clay minerals and mixed clays would give also more insight in the initial phase of the reaction processes. These steps in the early hydration of the blended cements can be interesting, since often the achieved early strength of calcined clay blended cements is insufficient due to the combination of dilution and later start of the pozzolanic reaction. Both types of modeling would help to gain insight in the reaction process and kinetics of the calcined clay cement system and allow to properly select potential candidate clays.

Regarding pure clays there are still some uncertainties regarding the influence of the characteristics of smectitic clays on the pozzolanic reactivity and their thermal behavior. It was already indicated that the octahedral occupancy can have a significant influence on the amorphisation of the smectitic clay. This should be confirmed by a larger data set containing both cis and trans vacant clays. The changes in the structure upon calcination should be further closely monitored by means of NMR. Additionally the influence of the dominant exchangeable cation should be investigated to a greater extend. These insight could help to be able to enhance certain less favorable clays.

Additionally calcite-rich clays can be a promising pozzolanic material and the reaction between calcined calcite-rich clay and cement should be studied in more detail for different types of clay minerals. The benefits of adding calcite (uncalcined) in the form of limestone to the blended cements are already demonstrated in the past. However more difficulties arise when the calcite is simultaneously calcined with the clay. Special attention should be given to the positive effects of calcite on the early stage of the reaction since general calcined clay blended cements show rather limit strength in the first day due to the combination of the dilution effect and the late start of the pozzolanic reaction.

An important research question that should be tackled is the quantification of the amorphous content of calcined clays and later on of the calcined clay blended cement pastes. For kaolinitic clays that are calcined at optimal temperatures (700-900°C) there is no direct problem since all the kaolinite becomes amorphous and the amorphous content of the calcined clay can still be quantified by both Rietveld based software or with software that rely on whole-pattern fitting for pure mineral standards like Quanta. However for smectitic, illitic or kaolinitic clays that contain a considerable amount of 2:1 clays the quantification of the amorphous content is no longer straightforward. The

main problem is that only part of the clay minerals become amorphous while the other part is partially altered and becomes semi crystalline. The peak position of the semi-crystalline phases can no longer be correlated directly to the peak reflections of the original material. Furthermore the applied temperature and the structure of the initial clay influence the actual positions, shape and intensity of the remaining peak reflections. Therefore the pattern of one smectitic clay calcined at 800°C might not necessary correspond to a smectite with a slightly different structure. A highly promising new quantification technique is the PONCKS method (Partial Or No Know Crystal Structure), whereby the traditional Rietveld refinement is combined with implementing standard of to the whole pattern fitting method. Results derived from the thesis of Bruneel (2016) indicate that XRD patterns of the calcined smectitic clays could indeed be modeled based by the PONCKS method. These patterns can directly be used as standard to quantify the amount of calcined clay prensent in calcined clay cement pastes and additionally also the newly formed reaction phases can be quantified. However to quantity the amorphous content of the calcined sample itself at different calcination temperatures multiple validation samples are necessary to create a reliable quantification.

REFERENCES

Adriaens, R. (2015) Neogene and Quaternary Clay Minerals in the Southern Nort Sea. Doctoral dissertation, KU Leuven, 271 p.

Alonso, S., and Palomo, A. (2001) Calorimetric study of alkaline activation of calcium hydroxide-metakaolin solid mixtures. Cement and Concrete Research, 31, 25–30.

Al-Rawas, A.A., and Hago, A.W. (2006) Evaluation of field and laboratory produced burnt clay pozzolans. Applied Clay Science, 31, 29–35.

Alther, G.R. (1983) The Methylene Blue Test for Bentonite Liner Quality Control. Geotechnical Testing Journal, 6, (3) 128-132.

Alujas, A., Fernández, R., Quintana, R., Scrivener, K.L., and Martirena, F. (2015) Pozzolanic reactivity of low grade kaolinitic clays: influence of calcination temperature and impact of calcination products on OPC hydration. Applied Clay Science, 108, 94–101.

Ambroise, J. (1984) Elaboration de liants pouzzolaniques a moyenne température et étude de leurs propriétés physico-chimiques et mécaniques, in "Laboratoire matériaux Minéraux.

Ambroise, J., Murat, M., and Péra, J. (1985) Hydration reaction and hardening of calcined clays and related minerals. V. Extension of the reasearch and general conclusions. Cement and Concrete Composites, 15, 261–268.

Ambroise, J., Maximilien, S., Pera, J., and National, I. (1994) Properties of Metakaolin Blended Cements. Advanced Cement based materials, 1, 161–168.

Amin, N.-, Alam, S., and Gul, S. (2015) Assessment of pozzolanic activity of thermally activated clay and its impact on strength development in cement mortar. RSC Adv., 5, 6079–6084.

Andrejkovičová, S., Velosa, A.L., Ferraz, E., and Rocha, F. (2014) Influence of clay minerals addition on mechanical properties of air lime-metakaolin mortars. Construction and Building Materials, 65, 132–139.

Antoni, M. (2013) Investigation of cement substitution by blends of calcined clays and limestone. Doctoral dissertation, École Polytechnique de Lausanne, 224p.

Antoni, M., Rossen, J., Martirena, F., and Scrivener, K. (2012a) Cement substitution by a combination of metakaolin and limestone. Cement and Concrete Research, 42, 1579–1589.

Antoni, M., Rossen, J., Martirena, F., and Scrivener, K. (2012b) Cement substitution by a combination of metakaolin and limestone. Cement and Concrete Research, 42, 1579–1589.

Aubert, J.E., Segui, P., Husson, B., and Measson, M. (2012) A method developed to quantify lime and gypsum consumed by mineral additions. Cement and Concrete Composites, 34, 874–880.

Ayub, M., Yusuf, M., Beg, M.A., and Faruqi, F.A. (1988) Pozzolanic propertiesof burned clays. Pakistan Journal of Scientific Industrial Research, 31, 1–10.

Badogiannis, E., and Tsivilis, S. (2009) Exploitation of poor Greek kaolins: Durability of metakaolin concrete. Cement and Concrete Composites, 31, 128–133.

Badogiannis, E., Kakali, G., and Tsivilis, S. (2005) Metkaolin as supplementary cementitious material Optimization of kaolin to metakaolin conversion. Journal of Thermal Analysis and Calorimetry, 81, 457–462.

Bailey, S.W. (1963) Polymorphism of the kaolin minerals. The American Mineralogist, 48, 1196-1209

Barcelo, L., Kline, J., Walenta, G., and Gartner, E. (2013) Cement and carbon emissions. Materials and Structures, 47, 1055–1065.

Baudet, G., Perrotel, V., Seron, A., and Stellatelli, M. (1999) Two dimensions comminution of kaolinite clay particles. Powder Technology, 105, 125–134.

Benea, M., and Gorea, M. (2004) Mineralogy and technological properties of some kaolin types used in the ceramic industry. Studia UBB, Geologia, 33–39.

Benezet, J.C., and Benhassaine, A. (1999) Grinding and pozzolanic reactivity of quartz powders. Powder Technology, 105, 167–171.

Benezet, J.C., and Benhassaine, A. (1999) Influence de la taille des particules sur la réactivité pouzzolanique de poudres de quartz. Bulletin de Laboratoires des Pont et Chaussées, 219, 17–28.

Bich, C., Ambroise, J., and Péra, J. (2009) Influence of degree of dehydroxylation on the pozzolanic activity of metakaolin. Applied Clay Science, 44, 194–200.

Bonavetti, V.L., Rahhal, V.F., and Irassar, E.F. (2001) Studies on the carboaluminate formation in limestone filler-blended cements. Cement and Concrete Research, 31, 853–859.

Bortnikov, N.S., Novikov, V.M., Dubinina, E.O., Savko, a. D., Berketa, a. G., and Krainov, a. V. (2011) Oxygen Isotope Composition of Kaolinite Rocks as an Indicator of Different Stages of Their Lithogenesis. Doklady Earth Sciences, 438, 697–700.

Bortnikov, N.S., Novikov, V.M., Soboleva, S. V., Savko, a. D., Boeva, N.M., Zhegallo, E. a., and Bushueva, E.B. (2012) The role of organic matter in the formation of fireproof clay of the Latnenskoe deposit. Doklady Earth Sciences, 444, 634–638.

Bortnikov, N.S., Novikov, V.M., Savko, A.D., Boeva, N.M., Zhegallo, E.A., Bushueva, E.B., Krainov, A. V, and Dmitriev, D.A. (2013) Structural-Morphological Features of Kaolinite from Clayey Rocks Subjected to Different Stages of Lithogenesis : Evidence from the Voronezh Anteclise. Lithology and Mineral Resources, 48, 384–397.

Boxill, L. (2011) Potential for use of methylene bleu index testing to enhance geotechnical characterization of oil sands ores and tailings. In: Proceedings Tailings and Mine Waste, Vancouver, 15 p.

Brindley, G.W., and Brown, G. (1980) Crystal structures of clay minerals and their X-ray indentification, Mineralogical Society of Great Britain and Ireland, London, 495 p.

Britt, J. (2007) The Complete Guide to High-Fire Glazes, Sterling Publishing Company, New York, 184 p.

Brunauer, S., Emmett, P.H., and Teller, E. (1938) Adsorption of Gases in Multimolecular Layers. Journal of American Chemical Society, 60, 309–319.

Bruneel, Y. (2016) Quantification of complex mineral phases using PONCKS-assisted Rietveld refinement. master thesis, KU Leuven, 283 p.

Bushnell-Watson, S.M., and Sharp, J.H. (1985) The detection of the carboalimnate phase in hydrated high aluminacements by differential thermal analysis. Thermochimica Acta, 93, 613–616.

Cara, S., Carcangiu, G., Massidda, L., Meloni, P., Sanna, U., and Tamanini, M. (2006) Assessment of pozzolanic potential in lime–water systems of raw and calcined kaolinic clays from the Donnigazza Mine (Sardinia–Italy). Applied Clay Science, 33, 66–72.

Cases, J.M., Lièтard, O., Yvon, J., and Delon, J.F. (1982) Étude des propiértés cristallochimiques, morphologiques, superficielles de kaolinites désordonnées. Bull Mineral, 105, 439–455.

Castillo, R., Fernández, R., Antoni, M., Scrivener, K., Alujas, A., and Martirena, J.F. (2010) Activation of low grade clays at high temperatures. Revista Ingeniería de Construcción, 25, 329–352.

Chakchouk, A., Samet, B., and Mnif, T. (2006) Study on the potential use of Tunisian clays as pozzolanic material. Applied Clay Science, 33, 79–88.

Chakchouk, A., Trifi, L., Samet, B., and Bouaziz, S. (2009) Formulation of blended cement: Effect of process variables on clay pozzolanic activity. Construction and Building Materials, 23, 1365–1373.

Chiappone, A., Marello, S., Scavia, C., and Massimo, S. (2004) Clay mineral characterization through the methylene blue test: comparison with other experimental techniques and applications of the method. Canadian Geotechnical Journal, 41, 1168-1178.

Chipera, S.J., and Bish, D.L. (2001) B aseline studies of the clay minerals society source clays: powder X-ray diffraction analyses. Clay and Clay Minerals, 49, 398–409.

Cizer, Ö. (2009) Competition between Carbonation and Hydration on the Hardening of Calcium Hydroxide and Calcium Silicate Binders. Doctoral dissertation, KU Leuven, 271 p.

Damidot, D., Lothenbach, B., Herfort, D., and Glasser, F.P. (2011) Thermodynamics and cement science. Cement and Concrete Research, 41, 679–695.

Damtoft, J.S., Lukasik, J., Herfort, D., Sorrentino, D., and Gartner, E.M. (2008) Sustainable development and climate change initiatives. Cement and Concrete Research, 38, 115–127.

Danner, T. (2013) Reactivity of Calcinated Clays. Doctoral dissertation, Norwegian University of Science and Technology, 229 p.

Danner, T., Justnes, H., Norden, G., and Ostnor, T. (2015) Feasibility of calcined marlas an alternative pozzolanic material. In: Scrivener, K, and Favier, A. (editors), Calcined Clays for Sustainable Concrete Proceedings of the 1st International Conference on Calcined Clays for Sustainable Concrete Vol. 10, 67–74.

De Jonghe, L.C. and Rahaman, M.N. (2013) Sintering of Ceramics. In: Somiya, S. (editor) Handbook of Advanced Ceramics, Materials, Applications and Properties, Academic Press, Tokyo, 187-264.

De Silva, P.S., and Glasser, F.P. (1992) pozzolanic activation of metakaolin. Advanced Cement Research, 4, 167–178.

de Silva, P.S., and Glasser, F.P. (1993) Phase relations in the system CaO-Al_2O_3-SiO_2-H_2O relevant to metakaolin - calcium hydroxide hydration. Cement and Concrete Research, 23, 627–639.

Ding, J., Fu, Y., and Beaudoin, J.J. (1995) Strätlingite formation in high alumina cement - silica fume systems: Significance of sodium ions. Cement and Concrete Research, 25, 1311–1319.

Drits, V.A., Besson, G., and Muller, F. (1995) An improved model for structural transformations of heat-treated aluminous dioctahedral 2:1 layer silicates. Clay and Clay Minerals, 43, 718–731.

Duminuco, P., Messiga, B., and Riccardi, M.P. (1998) Firing process of natural clays. Some microtextures and related phase compositions. Thermochimica Acta, 321, 185–190.

Earnest, C.M. (1988) Thermogravimetry of selected clays and clay products. In: Earnest, C.M. (editor), Compositional Analysis by Thermogravimetry, American Society for Testing and Materials, Baltimore, 272–289.

Elert, K., Sebastián, E., Valverde, I., and Rodriguez-Navarro, C. (2008) Alkaline treatment of clay minerals from the Alhambra Formation: Implications for the conservation of earthen architecture. Applied Clay Science, 39, 122–132.

Emmerich, K. (2011) Thermal analysis in the characterization and processing of industrial minerals. In: Christidis, G. (editor), Advances in the Characterization of Industrial Minerals, The Mineralogical Society of Great Britain and Ireland, Twickenham, 129–170.

Emmerich, K., Madsen, F.T., and Kahr, G. (1999) Dehydroxylation behavior of heat-treated and steam-treated homoionic cis-vacant montmorillonites. Clays and Clay Minerals, 47, 591–604.

Eshel, G., Levy, G.J., Mingelgrin, U., and Singer, M.J. (2004) Critical evaluation of the use of laser diffraction for particle-size distribution analysis. Soil Science Society of America Journal, 68, 736–743.

EU (2015) Eurostat Statistical Books: Energy, Transport and Environment indicators, Publications Office of the European Union, 222 p.

European Commision (2011) A roadmap for moving to a competitive low carbon economy in 2050.

European Committe for Standardization (2000) EN197-1: Composition, Specifications and Conformity Criteria dor Comman Cements, 29 p.

Farmer, V.C. (1973) The infrared spectra of minerals. Mineralogical Society, London, 539 p.

Fernandez, R. (2009) Calcined Clayey Soils as a Potential Replacement for Cement in Developing Countries. Doctoral dissertation, École Polytechnique de Lausanne, 178 p.

Fernandez, R., Martirena, F., and Scrivener, K.L. (2011) The origin of the pozzolanic activity of calcined clay minerals: a comparison between kaolinite, illite and montmorillonite. Cement and Concrete Research, 41, 113–122.

Ferraz, E., Andrejkovičová, S., Hajjaji, W., Velosa, A.L., Silva, A.S., and Rocha, F. (2015) Pozzolanic activity of metakaolins by the French standard of the modified Chapelle test: A direct methodology. Acta Geodynamica et Geomaterialia, 12, 289–298.

Forrester, J.A. (1974) Burnt clay pozzolans. In: Proceedings of the meeting on small-scale manufacture of cement materials, Intermed Technological Publications, London, 53–59.

Frías, M., and Cabrera, J. (2001) Influence of MK on the reaction kinetics in MK/lime and MK-blended cement systems at 20°C. Cement and Concrete Research, 31, 519–527.

Frost, R.A.Y.L., and Vassallo, A.M. (1996) The Dehysdroxylation of the Kaolinite Clay Minerals Using Infrared Emission Spectroscopy, 44, 635–651.

Gabrovšek, R., Vuk, T., and Kaučič, V. (2008) The preparation and thermal behavior of calium monocarboaluminate. acta chimica slovenica, 55, 942–950.

Galan, E., Aparicio, P., Gonzalez, I., and Miras, A. (1998) Contribution of multivariate analysis to the correlation of some properties of kaolin with its mineralogical and chemical composition. Clay Minerals, 33, 65–75.

Gallé, C. (2001) Effect of drying on cement-based materials pore structure as identified by mercury intrusion porosimetry - A comparative study between oven-, vacuum-, and freeze-drying. Cement and Concrete Research, 31, 1467–1477.

Galos, K. (2011) Influence of mineralogical composition of applied ball clays on properties of porcelain tiles. Ceramics International, 37, 851–861.

Gameiro, A.L., Silva, A.S., Veiga, M. do R., and Velosa, A.L. (2012) Lime-metakaolin hydration products: A microscopy analysis produkti hidracije Apno-metakaolin: Mikroskopska analiza. Materiali in Tehnologije, 46, 145–148.

Gamelas, J.A.F., Ferraz, E., and Rocha, F. (2014) An insight into the surface properties of calcined kaolinitic clays: The grinding effect. Colloids and Surfaces A: Physicochemical and Engineering Aspects, 455, 49–57.

Garg, N., and Skibsted, J. (2014) Thermal activation of a pure montmorillonite clay and its reactivity in cementitious systems. Journal of Physical Chemistry C, 118, 11464–11477.

Garg, N., and Skibsted, J. (2015) Heated montmorillonite: structure, reactivity and dissolution. In Calcined Clays for Sustainable Concrete Proceedings of the 1st International Conferenve on Calcined Clays for Sustainable Concrete, 10, 117–124.

Garrels, R.M., and Mackenzie, F.T. (1971) Evolution of Sedimentary Rocks. Norton, New York, 397 p.

Gartner, E. (2004) Industrially interesting approaches to "low-CO_2" cements. Cement and Concrete Research, 34, 1489–1498.

Gautier, J.M., Oelkers, E.H., Schott, J. (2001) Are quartz dissolution rates proportional to B.E.T. surface areas? Geochimica et Cosmochimica Acta , 65 (7), 1059-1070.

Ghrici, M., Kenai, S., and Said-Mansour, M. (2007) Mechanical properties and durability of mortar and concrete containing natural pozzolana and limestone blended cements. Cement and Concrete Composites, 29, 542–549.

Gilson, J.P. (1987) Penta-co-ordinated aluminium inzeolites and aluminosilicates. Journal of the Chemical Society, 2, 91–92.

Grim, R.E. (1968) Clay mineralogy, 2nd edition. McGraw-Hill Book Company, New York, 582 p.

Guggenheim, S., and van Groos, K.A.F. (2001) B asline studiesof the clay minerals society source clays: thermal analysis. Clays, 49, 433–443.

Guggenheim, S., Vhang, Y.-H., and Koster Van Groos, A., F. (1987) Muscovite dehydroxylation: High Temprature Studies. American Mineralogist, 72, 537–550.

Guggenheim, S., Martin, R.T., Alietti, A., Drits, V.A., Formoso, M.L.L., Galán, E., Köster, H.M., Morgan, D.J., Paquet, H., Watanabe, T., and others (1995) Definition of clay and clay mineral: Joint report of the AIPEA nomenclature and CMS nomenclature committees. Clays and Clay Minerals, 43, 255–256.

Güven, N. (1988) Smectites. In: Bailey, S.W. (editor), Volume 19: Hydrous phyllosilicates (exclusive of micas), Mineralogical Society of America, Madison, 497–560.

Habert, G., Billard, C., Rossi, P., Chen, C., and Roussel, N. (2010) Cement production technology improvement compared to factor 4 objectives. Cement and Concrete Research, 40, 820–826.

Haha, M. Ben, Lothenbach, B., Le Saout, G., and Winnefeld, F. (2012) Influence of slag chemistry on the hydration of alkali-activated blast-furnace slag - Part II: Effect of Al2O3. Cement and Concrete Research, 42, 74–83.

He, C., Makovicky, E., and Osbaeck, B. (1994) Thermal stability and pozzolanic activity of calcined kaolin. Applied Clay Science, 9, 165–187.

He, C., Osbaeck, B., and Makovicky, E. (1995a) Pozzolanic reactions of six principal clay minerals: activation, reactivity assesments and technological effects. Cement and Concrete Research, 25, 1691–1702.

He, C., Makovicky, E., and ??sb??ck, B. (1995b) Thermal stability and pozzolanic activity of calcined illite. Applied Clay Science, 9, 337–354.

He, C., Makovicky, E., and Osbaeck, B. (1996) Thermal treatment and pozzolanic activity of Na- and Ca-montmorillonite. Applied Clay Science, 10, 351–368.

He, C., Makovicky, E., and Osb??ck, B. (2000) Thermal stability and pozzolanic activity of raw and calcined mixed-layer mica/smectite. Applied Clay Science, 17, 141–161.

Heikal, M., Radwan, M.M., and Morsy, M.S. (2004) Influence of curing temperature on the physicomechanical, characteristics of calcium aluminate cement with air-cooled slag or water-cooled slag. Ceramics - Silikaty, 48, 185–196.

Hinckley, D.N. (1962) Variability an “crystallinity” values among the koalin deposits of the coastal plain of Georgia and South Carolina. Clay and Clay Minerals, 11, 229–235.

Hubert, F., Caner, L., Meunier, A., and Lanson, B. (2009) Advances in characterization of soil clay mineralogy using X-ray diffraction: From decomposition to profile fitting. European Journal of Soil Science, 60, 1093–1105.

Ilic, B., Mitrovic, A., and Milicic, L. (2010) Thermal treatment of kaolin clay to obtain metakaolin. Hemijska industrija, 64, 351–356.

Ipavec, A., Gabrovšek, R., Vuk, T., Kaučič, V., MačEk, J., and Meden, A. (2011) Carboaluminate phases formation during the hydration of calcite-containing Portland cement. Journal of the American Ceramic Society, 94, 1238–1242.

Jackson, M.L. (1975) Soil chemical analysis – Advanced course, 2nd edition. Published by the author, Madison, Wisconsin, 895 p.

Jiang, T., Li, G., Qiu, G., Fan, X., and Huang, Z. (2008) Thermal activation and alkali dissolution of silicon from illite. Applied Clay Science, 40, 81–89.

Juenger, M.C.G., and Siddique, R. (2015) Recent advances in understanding the role of supplementary cementitious materials in concrete. Cement and Concrete Research, 78, 71–80.

Justnes, H., Weerdt, K. De, Vikan, H., Norwegian, T., and Directorate, R. (2011) Calcined Marl and Clay As Mineral Addition for More Sustainable Concrete Structures. In: Proceedings of the 36th Conference on our world in Concrete & Structures, CI-Premier, Singapore, 10 p.

Kakali, G., Perraki, T., Tsivilis, S., and Badogiannis, E. (2001) Thermal treatment of kaolin: the effect of mineralogy on the pozzolanic activity. Applied Clay Science, 20, 73–80.

Karathanasis, A.D. (2008) Thermal analysis of soil minerals. In Methods of Soil Analysis Part 5-Mineralogical Methods pp. 117–160. Soill Science Society of America, Madison.

Kittel, C., and McEuen, P. (1976) Introduction to Solid State Physics, 8th edision. Wiley and Sons, New York, 703 p.

Kleeberg, R. (2005) Results of the second Reynolds Cup contest in quantitative mineral analysis. Internation Unio of Crystallography. Commision on powder Diffraction Newsletter, 30, 22–24.

Klein, C., Dutrow, B., and Dana, J.D. (2002) Manual of Minerals, Wiley and Sons, New York, 641 p.

Kloprogge, T.J., and Frost, R.L. (1999) Infrared emission spectroscopy study of the dehydroxylation of 10Å halloysite from a Neogene cryptokarst of South Belgium. Geologica Belgica, 2, 213–220.

Knapen, E., Cizer, O., Van Balen, K., and Van Gemert, D. (2009) Effect of free water removal from early-age hydrated cement pastes on thermal analysis. Construction and Building Materials, 23, 3431–3438.

Kogel, J.E., Trivedi, N.C., Barker, J.M., and Stanley, T.K. (2006) Industrial Minerals & Rocks, 7th edision. Society for Mining, Metallurgy, and Exploration, Inc., Littleton - Colerado, 1548 p.

Konert, M., and Vandenberghe, J. (1997) Comparison of laser grain size analysis with pipette and sieve analysis: A solution for the underestimation of the clay fraction. Sedimentology, 44, 523–535.

Kuzel, H.J., and Pöllmann, H. (1991) Hydration of C3A in the presence of $Ca(OH)_2$, $CaSO_4.2H_2O$ and CaCO3. Cement and Concrete Research, 21, 885–895.

Lang, E. (2002) Blast furnace cements. In: Bensted, J. and Barnes, P. (editors), Structure and Performance of Cements, Spon Press, London and New York, 310-325.

Lee, V.G., and Yeh, T.H. (2008) Sintering effects on the development of mechanical properties of fired clay ceramics. Materials Science and Engineering A, 485, 5–13.

Levitskaya, Y.F., Omel(chenko, Y.A., and Énglund, A. é. (2002) Raw materials: Deposits of clay in Russia. Glass and Ceramics, 59, 63–68.

Liebig, E., and Althaus, E. (1997) Kaolinite and montmorillonite as pozzolan in components in lime mortars - untreated and after thermal activation. ZKG International, 50, 282–290.

Lièтard, O. (1977) Contribution à l'étude des propiétés phisicochimiques, cristallographique et morphologiques des kaolins. Doctoral dissertation, L'Institut National Polytechnique de Lorraine, 345 p.

Lippmaa, E., Mägi, M., and Tarmak, M. (1982) A high resolution ^{29}Si NMR study of the hydration of tricalciumsilicate. Cement and Concrete research, 12, 597–602.

Lothenbach, B., Le Saout, G., Gallucci, E., and Scrivener, K. (2008) Influence of limestone on the hydration of Portland cements. Cement and Concrete Composites, 38, 848–860.

Lothenbach, B., Scrivener, K., and Hooton, R.D. (2011) Supplementary cementitious materials. Cement and Concrete Research, 41, 1244–1256.

Mackenzie, R.C., and Bishui, B.M. (1958) No Title. Clay Mineral Bulletin, 20, 276–286.

Madejov, J., Komadel, P., Madejova, J., and Madejová, J. (2001) base line studies of the clay minerals society source clays: infrared methods. Clay and Clay Minerals, 49, 410–432.

Madejova, J. (2003) FTIR techniques in clay mineral studies. Vibrational Spectroscopy, 31, 1–10.

Martin-Calle (1989) Pouzzolanicité d'argiles thermiquement activées: Influence de la minéralogie et des conditions de calcination. Doctoral dissertation, INSA de Toulouse, 220 p.

Massaza, F. (2009) Properties and applications of natural pozzolanas. In: Benstedt J. and Barnes P. (Editors), Structure and Performance of Cements, Spon Press, London and New York, 326-352.

Matschei, T., Lothenbach, B., and Glasser, F.P. (2007a) The AFm phase in Portland cement. Cement and Concrete Research, 37, 118–130.

Matschei, T., Lothenbach, B., and Glasser, F.P. (2007b) The role of calcium carbonate in cement hydration. Cement and Concrete Research, 37, 551–558.

Mazzucato, E., Artioli, G., and Gualtieri, A. (1999) High temperature dehydroxylation of muscovite-2M: a kinetic study by in situ XRPD. Physics and Chemistry of Minerals, 26, 375–381.

Mertens, G. (2009) Characterization of historical mortars and mineralogical study of the physico-chemical reactions on the pozzolan-lime binder interface. Doctoral dissertation, KU Leuven, 266 p.

Mertens, G., Snellings, R., Van Balen, K., Bicer-Simsir, B., Verlooy, P., and Elsen, J. (2009) Pozzolanic reactions of common natural zeolites with lime and parameters affecting their reactivity. Cement and Concrete Research, 39, 233–240.

Metha, P.K. (1987) Natural pozzolans: Supplementary cementing materials for concrete. CANMET Special Publication, 86, 1–33.

Metha, P.K. (1989) Pozzolanic and cementitious by-products in concrete. Another look. ACI Special Publication, 114, 1–44.

Meunier, A. (2005) Clays. Springer-Verlag, Berlin,472 p.

Meunier, A., and Velde, B. (2004) Illite: origins, evolution and metamorphism. Springer Berlin Heidelberg, 286 p.

Michot, L.J., and Villiéras, F. (2006) Surface Area and Porosity. In: Bergaya, F., Theng, K.G. and Lagaly, G. (editors), Handbook of Clay Science, Elsevier, Amsterdam, 965–978.

Mielenz, R.C., White, L.P., and Glantz, O.J. (1950) Effect of calcination on natural pozzolanz. Symp on Use of Pozzolanic Materials in Mortars and Concrete. ASTM Special Technical publication, 99, 43–92.

Mielenz, R.C., Green, K.T., and Schieltz, N.C. (1951) Natural pozzolans for concrete. Economic Geology, 46, 311–328.

Mitrović, A., and Zdujić, M. (2014) Preparation of pozzolanic addition by mechanical treatment of kaolin clay. International Journal of Mineral Processing, 132, 59–66.

Moore, D.M., and Reynolds, R.C. (1997) X-Ray Diffraction and the Identification and Analysis of Clay Minerals, Oxford University Press, New York, 387 p.

Müller, C.J. (2005) Pozzolanic activity of natural clay minerals with respect to environmental geotechnics, 125 p.

Murat, M. (1983) Hydration reaction and hardening of calcined clays and related minerals. Cement and Concrete Research, 13, 511–518.

Murray, H.H. (2007) Applied Clay Mineralogy Occurences, processing ans application of Kaolins, bentonites, Palygorskite-Sepiolite, and Common Clays, 1ste edition, Elsevier, Amsterdam, 180 p.

Muzylev, N.A., Mikhin, V.P., and Goryushkin, V. V. (2001) Areas of application of clays of the Latneskoe deposit. Refractories and Inustrial Ceramics, 42, 157–159.

Muzylev, N.A., Mikhin, V.P., and Goryushkin, V. V. (2006) Ceramic clays from Voronezh oblast. Glass and Ceramics (English translation of Steklo i Keramika), 63, 307–310.

NF P 18-513 (2013) Métakaolin, addition pouzzolanique pour bétons: définitions, spécification, citères de conformité.

Ohunakin, O.S., Leramo, O.R., Abidakun, O.A., Odunfa, M.K., and Bafuwa, O.B. (2013) Energy and cost analysis of cement production using the wet and dry processes in Nigeria. Energy and Power Engineering, 5, 537–550.

Okoronkwo, M.U., and Glasser, F.P. (2016) Stability of strätlingite in the CASH system. Materials and Structures, 4305–4318.

Omotoso, O., McCarty, D.K., Hillier, S., and Kleeberg, R. (2006) Some successful approaches to quantitative mineral analysis as revealed by the 3rd reynolds cup contest. Clays and Clay Minerals, 54, 748–760.

Østnor, T., Justnes, H., and Danner, T. (2015) Reactivity and microstructure of clacined marl as supplementary cementitious material. In: Scrivener, K, and Favier, A. (editors) Calcined Clays for Sustainable Concrete Proceedings of the 1st International Conference on Calcined Clays for Sustainable Concrete Vol. 10, 237–244.

Panna, W. (2014) Analysis of smectite content in some raw clay minerals based on sorption-spectrophotometric studies. Chemik, 68, 7, 612-619.

Plançon, A. (1988) The Hinckley Index for Kaolinites. Clay Minerals, 23, 249–260.

Ramachandran, V.S. (1996) Concrete Admixtures handbook, 2nd edition: Properties, Science and Technology. Noyes publication, New Jersey, 1153 p.

Richardson, I.G. (2008) The calcium silicate hydrates. Cement and Concrete Research, 38, 137–158.

Richardson, I.G., and Groves, G.W. (1993) The incorporation of minor and trace elements into calcium silicate hydrate (CSH) gel in hardened cement pastes. Cement and Concrete Research, 23, 131–138.

Rocha, J., and Klinowski, J. (1990) ^{29}Si and ^{27}Al magic-angle-spinning NMR studies of the thermal transformation of kaolinite. Physics and Chemistry of Minerals, 17, 179–186.

Rojas, M.F., and Cabrera, J. (2002) The effect of temperature on the hydration rate and stability of the hydration phases of metakaolin-lime-water systems. Cement and Concrete Research, 32, 133–138.

Roszczynialski, W. (2002) Determination of pozzolanic activity of materials by thermal analysis. Journal of Thermal Analysis and Calorimetry, 70, 387–392.

Saad, M.N., De Andrade, W.P., and Paulon, V.A. (1982) Properties of mass concrete containing an active pozzolan made from clay. Concrete International, 4, 59–65.

Sabir, B.., Wild, S., and Bai, J. (2001) Metakaolin and calcined clays as pozzolans for concrete: a review. Cement and Concrete Composites, 23, 441–454.

Sánchez Berriel, S., Favier, A., Rosa Domínguez, E., Sánchez Machado, I.R., Heierli, U., Scrivener, K., Martirena Hernández, F., and Habert, G. (2016) Assessing the environmental and economic potential of Limestone Calcined Clay Cement in Cuba. Journal of Cleaner Production, 124, 361–369.

Sanz, J. (2006) Nuclear Magnetic Resonance Spectroscopy. In: Bergaya, F., Theng, K.G. and Lagaly, G. (editors), Handbook of Clay Science. Elsevier, Amsterdam, 919–938.

Schneider, M., Romer, M., Tschudin, M., and Bolio, H. (2011) Sustainable cement production—present and future. Cement and Concrete Research, 41, 642–650.

Serry, M. a., Taha, a. S., El-Hemaly, S. a. S., and El-Didamony, H. (1984) Metakaolin—lime hydration products. Thermochimica Acta, 79, 103–110.

Shvarzman, A., Kovler, K., Grader, G.S., and Shter, G.E. (2003) The effect of dehydroxylation/amorphization degree on pozzolanic activity of kaolinite. Cement and Concrete Research, 33, 405–416.

Si-Ahmed, M., Belakrouf, A., and Kenai, S. (2012) Influence of metakaolin on the performance of mortars and concretes. International Journal of Civil, Environmental, Structural,Construction and Architectural Engineering, 6, 1354–1357.

Silva, A.S., Gameiro, A., Grilo, J., Veiga, R., and Velosa, A. (2014) Long-term behavior of lime-metakaolin pastes at ambient temperature and humid curing condition. Applied Clay Science, 88-89, 49–55.

Singh, M., and Garg, M. (2006) Reactive pozzolana from Indian clays-their use in cement mortars. Cement and Concrete Research, 36, 1903–1907.

Sirotin, V.I., Shatrov, V.A., Koval, S.A., Bugel'skii, Y.Y., Voitsekhovskii, G.V., and Nikul'shin, A.S. (2005) Lithology and geochemistry of Albian-Cenomanian sandy sequences of the Voronezh anteclise and their paleogeographic implication. Lithology and Mineral Resources, 40, 138–149.

Snellings, R. (2016) X-ray powder diffraction applied to cement. In: Scrivener, K., Snelling, R. and Lothenbach, B. (editors) A Practical Guide to Microstructural Analysis of Cementitious Materials, CRD Press, London, 107-176.

Snellings, R., Mertens, G., and Elsen, J. (2012) Supplementary Cementitious Materials. Reviews in Mineralogy and Geochemistry, 74, 211–278.

Snellings, R., Cizer, Ö., Horckmans, L., Durdzinski, P.T., Dierckx, P., Nielsen, P., Van Balen, K., and Vandewalle, L. (2016) Properties and pozzolanic reactivity of flash calcined dredging sediments. Applied Clay Science, 129, 35–39.

Spence, R.J.S., and Cook, D.J. (1983) Building Materials in Developing Countries. Wiley and Sons, London, 338 p.

Środoń, J. (1984) X-ray powder diffraction identification of illitic materials. Clay and Clay Minerals, 32, 337–349.

Środoń, J., Drits, V.A., Mccarty, D.K., Hsieh, J.C.C., and Eberl, D.D. (2001) Quantitative X-Ray Diffraction Analysis of Clay-Bearing Rocks from Random Preparations, 49, 514–528.

Środoń, J., Zeelmaekers, E., and Derkowski, A. (2009) The charge of component layers of illite-smectite in bentonites and the nature of end-member illite. Clays and Clay Minerals, 57, 649–671.

Stucki, J.W., BAsh, D.L., and Mumpton, F.A. (1990) Thermal analysis in clay science. In: CMS workshop lectures, volume 3, 584–585.

Suhr, N.H., and Ingamells, C.O. (1966) Solution technique for analysis of silicates. Analytical Chemistry, 38, 730–734.

Szegvari, A., and Yang, M. (1999) Attritor grinding and dispersing. In: Szegevari, A. Seminar on Dispersion of Pigments and Resins in Fluid Media. Kent State University, Union Process Inc., Ohio, p 7.

Taylor, H.F.W. (1997) Cement Chemistry, Thomas Telford, London, 437 p.

Taylor-Lange, S.C., Lamon, E.L., Riding, K.A., and Juenger, M.C.G. (2015) Calcined kaolinite-bentonite clay blends as supplementary cementitious materials. Applied Clay Science, 108, 84–93.

Tironi, A., Trezza, M. a., Scian, A.N., and Irassar, E.F. (2012) Kaolinitic calcined clays: Factors affecting its performance as pozzolans. Construction and Building Materials, 28, 276–281.

Tironi, A., Trezza, M.A., Scian, A.N., and Irassar, E.F. (2013) Assessment of pozzolanic activity of different calcined clays. Cement and Concrete Composites, 37, 319–327.

Tironi, A., Trezza, M.A., Scian, A.N., and Irassar, E.F. (2014a) Potential use of Argentine kaolinitic clays as pozzolanic material. Applied Clay Science, 101, 468–476.

Tironi, A., Trezza, M.A., Scian, A.N., and Irassar, E.F. (2014b) Thermal analysis to assess pozzolanic activity of calcined kaolinitic clays. Journal of Thermal Analysis and Calorimetry, 117, 547–556.

Todor, N. (1976) Thermal Analysis of Minerals, Abacus Press, Tunbridge Wells, 256 p.

Trindade, M.J., Dias, M.I., Coroado, J., and Rocha, F. (2009) Mineralogical transformations of calcareous rich clays with firing: A comparative study between calcite and dolomite rich clays from Algarve, Portugal. Applied Clay Science, 42, 345–355.

Tschegg, C., Ntaflos, T., and Hein, I. (2009) Thermally triggered two-stage reaction of carbonates and clay during ceramic firing - A case study on Bronze Age Cypriot ceramics. Applied Clay Science, 43, 69–78.

Van Den Heuvel, C. (2015) Mineralogical study of the potential of kaolinite rich calcined clays as supplementary cementitious materials. Master thesis, KU Leuven 146 p.

Van Olphen, H., and Fripiat, J.J. (1979) Data handbook for clay materials and other non-metallic minerals, Pergamon Press, Oxford, 346 p.

Vance, K., Aguayo, M., Oey, T., Sant, G., and Neithalath, N. (2013) Hydration and strength development in ternary portland cement blends containing limestone and fly ash or metakaolin. Cement and Concrete Composites, 39, 93–103.

Vdovic, N., Jurina, I., Škapin, S.D., and Sondi, I. (2010) The surface properties of clay minerals modified by intensive dry milling - revisited. Applied Clay Science, 48, 575–580.

Waples, D.W., and Waples, J.S. (2004) A review and evaluation of specific heat capacities of rocks, minerals, and subsurface fluids. Part 1: Minerals and Nonporous Rocks. Natural Resources Research, 13, 97–122.

Wilson, M.J. (1994) Clay Mineralogy: Spectroscopic and Chemical Determinative Methods, 1st edition, Chapman & Hall, London, 367 p.

Wolters, F., and Emmerich, K. (2007) Thermal reactions of smectites-relation of dehydroxylation temperature to octahedral structure. Thermochimica Acta, 462, 80–88.

Worrell, E., Price, L., Martin, N., Hendriks, C., and Meida, L.O. (2001) Carbon dioxide emissions from the global cement industry. Annual Revision Energy Environment, 26, 303–329.

Zeelmaekers, E. (2011) Computerized qualitative and quantitative clay mineralogy: introduction and application to known geological cases. Doctoral dissertation, KU Leuven, 397 p.

Zhang, J., Liu, G., Chen, B., Song, D., Qi, J., and Liu, X. (2014) Analysis of CO_2 Emission for the cement manufacturing with alternative raw materials: A LCA-based framework. Energy Procedia, 61, 2541–2545.

Zhang, M.H., and Malhotra, V.M. (1995) Characteristics of a thermally activated alumino-silicate pozzolanic material and its use in concrete. Cement and Concrete Research, 25, 1713–1725.

Zhang, X., Dean, K., and Burgar, I.M. (2010) A high-resolution solid-state NMR study on starch–clay nanocomposites and the effect of aging on clay dispersion. Polymer Journal, 42, 689–695.

APPENDICES

I. SAMPLE LIST

	Sample	Nr.	Description	Calcined
CHAPTER 4	K1	RAS09	Pure high ordered white kaolinite	CAS19 (500°C), CAS29 (700°C), CAS39 (900°C), CAS49 (800°C)
	K2	RAS01	Pure high ordered white kaolinite (KGA-1)	CAS11 (500°C), CAS21 (700°C), CAS31 (900°C), CAS41 (800°C)
	K3	RAS02	Pure medium ordered white kaolinite (KGA-2)	CAS12 (500°C), CAS22 (700°C), CAS32 (900°C), CAS42 (800°C)
	H1	RAS03	Pure white halloysite	CAS13 (500°C), CAS23 (700°C), CAS33 (900°C), CAS43 (800°C)
	S1	RAS06	Pure Na-montmorillonite (SWy-1)	CAS16 (700°C), CAS26 (800°C), CAS36 (900°C)
	S2	RAS07	Pure Ca-montmorillonite (SAz-1)	CAS17 (700°C), CAS27 (800°C), CAS37 (900°C)
	S3	RAS08	Pure hectorite (SHCa-1)	CAS18 (700°C), CAS28 (800°C), CAS38 (900°C)
	I1	RAS05	Pure illitic clay (IMt-1)	CAS15 (700°C), CAS25 (800°C), CAS35 (900°C)
CHAPTER 5	60%Q	MIS05BR	Mixture with 60% quartz and 40% kaolinite (K1)	MIS05B (800°C), MIS01 (700°C), MIS09 (900°C)
	45%Q	MIS06R	Mixture with 45% quartz and 65% kaolinite (K1)	MIS06 (800°C), MIS02 (700°C), MIS10 (900°C)
	30%Q	MIS07R	Mixture with 30% quartz and 70% kaolinite (K1)	MIS07 (800°C), MIS03 (700°C), MIS11 (900°C)
	15%Q	MIS08R	Mixture with 15% quartz and 85% kaolinite (K1)	MIS08 (800°C), MIS04 (700°C), MIS12 (900°C)
	40%F	MIS17R	Mixture with 40% feldspar and 60% kaolinite (K1)	MIS17 (800°C), MIS13 (700°C), MIS21 (900°C)
	30%F	MIS18R	Mixture with 30% feldspar and 70% kaolinite (K1)	MIS18 (800°C), MIS14 (700°C), MIS22 (900°C)
	20%F	MIS19R	Mixture with 20% feldspar and 80% kaolinite (K1)	MIS19 (800°C), MIS15 (700°C), MIS23 (900°C)
	10%F	MIS20R	Mixture with 10% feldspar and 90% kaolinite (K1)	MIS20 (800°C), MIS16 (700°C), MIS24 (900°C)
	40%Mu	MIS37R	Mixture with 40% muscovite and 60% kaolinite (K1)	MIS37 (800°C)
	30%Mu	MIS38R	Mixture with 30% muscovite and 70% kaolinite (K1)	MIS38 (800°C), MIS38700 (700°C), MIS38900 (900°C)
	20%Mu	MIS39R	Mixture with 20% muscovite and 80% kaolinite (K1)	MIS39 (800°C)

	Sample	Nr.	Description	Calcined
CHAPTER 5	10%Mu	MIS40R	Mixture with 10% muscovite and 90% kaolinite (K1)	MIS40 (800°C)
	60%Ca	MIS25R	Mixture with 60% calcite and 40% kaolinite (K1)	MIS25 (800°C)
	45%Ca	MIS26R	Mixture with 45% calcite and 65% kaolinite (K1)	MIS26 (800°C)
	30%Ca	MIS27R	Mixture with 30% calcite and 70% kaolinite (K1)	MIS27 (800°C), MIS27700 (700°C), MIS27900 (900°C)
	15%Ca	MIS28R	Mixture with 15% calcite and 85% kaolinite (K1)	MIS28 (800°C)
	60%S	MIS29R	Mixture with 60% smectite and 40% kaolinite (K1)	MIS29 (800°C)
	45%S	MIS30R	Mixture with 45% smectite and 65% kaolinite (K1)	MIS30 (800°C)
	30%S	MIS31R	Mixture with 30% smectite and 70% kaolinite (K1)	MIS31 (800°C), MIS31700 (700°C), MIS31900 (900°C)
	15%S	MIS32R	Mixture with 15% smectite and 85% kaolinite (K1)	MIS32 (800°C)
	60%I	MIS33R	Mixture with 60% illite and 40% kaolinite (K1)	MIS33 (800°C)
	45%I	MIS34R	Mixture with 45% illite and 65% kaolinite (K1)	MIS 34 (800°C)
	30%I	MIS35R	Mixture with 30% illite and 70% kaolinite (K1)	MIS 35 (800°C), MIS35700 (700°C), MIS35900 (900°C)
	15%I	MIS36R	Mixture with 15% illite and 85% kaolinite (K1)	MIS36 (800°C)
CHAPTER 6	R-KF	SIS12	Kaolinitic white clay	FIS12 (750°C) (VAS06)
	Archi.	SIS09	Kaolinitic grey clay with gravel	FIS09 (750°C) (VAS11)
	KA Hostun	SIS04	Kaolinitic white clay	FIS04 (750°C) (VAS04)
	R-ALK R	SIS11	Kaolinitic white clay	FIS11 (750°C) (VAS07)
	WS 35/38	SIS40	Kaolinitic grey clay	FIS40 (800°C) (VAS09)
	Argilla bianca	SIS05	Kaolinitic orange/yellow clay	FIS05 (750°C) (VAS05)
	CS S	SIS39	Kaolinitic brown/grey clay	FIS39 (800°C) (VAS08)
CHAPTER 7	SM1	VAS02R	Smectitic dark grey clay (EZT54)	VAS02 (800°C)
	SM2	VAS13R	Smectitic grey clay	VAS13 (800°C)
	SM3	SIS07	Smectitic Brown to grey clay	VAS10 (800°C)
	SM4	VAS03R	Smectitic grey clay (EZT60)	VAS03 (800°C)
	SM5	VAS01R	Smectitic grey clay (EZT4)	VAS01 (800°C)

	Sample	Nr.	Description	Calcined
CHAPTER 8	CV15	VO14CV15	Kaolinitic grey clay	VO14CV15CAL800(800°C)
	CV18	VO14CV18	Kaolinitic black clay	VO14CV18CAL800 (800°C)
	CV19	VO14CV19	Kaolinitic brown clay iron rich	VO14CV19CAL800 (800°C)
	CV22	VO14CV22	Kaolinitic light grey clay	VO14CV22CAL800 (800°C), VO14CV22CAL650 (650°C)
	CV24	VO14CV24	Kaolinitic grey clay	VO14CV24CAL800 (800°C)
	CV25	VO14CV25	Kaolinitic grey clay	VO14CV25CAL800 (800°C), VO14CV25CAL650 (650°C)
	CV27	VO14CV27	Kaolinitic dark grey clay	VO14CV27CAL800 (800°C)
	CV29	VO14CV29	Kaolinitic dark grey to black clay with sand layers	VO14CV29CAL800 (800°C)
	CV30	VO14CV30	Kaolinitic grey clay with sand layers and pyrite	VO14CV30CAL800 (800°C)
	CV33	VO14CV33	Kaolinitic organic rich dark grey clay with pyrite	VO14CV33CAL800 (800°C)
	CV35	VO14CV35	Kaolinitic lignite clay	VO14CV35CAL800 (800°C)
	CV37	VO14CV37	Kaolinitic grey clay with pyrite	VO14CV37CAL800 (800°C)
	CV41	VO14CV41	Kaolinitic light grey sandy clay	VO14CV41CAL800 (800°C)
	CV48	VO14CV48	Green to red glauconite clay	VO14CV48CAL800 (800°C)
	CV52	VO14CV52	Kaolinitic light grey clay	VO14CV52CAL800 (800°C)
	CV71	VO14CV71	Kaolinitic brown to yellow clay	VO14CV71CAL800 (800°C)
	CV78	VO14CV78	Soil red clay	VO14CV78CAL800 (800°C)

II. BULK CHEMISTRY

	SAMPLE	SiO_2	Al_2O_3	Fe_2O_3	CaO	MgO	K_2O	Na_2O	TiO_2	LOI
CHAPTER 4	K1	45.82	38.79	0.56	0.01	0.05	0.03	0.20	0.42	14.12
	K2	46.24	40.03	0.27	0.03	0.04	0.03	0.02	1.59	11.76
	K3	44.77	38.45	1.12	0.02	0.06	0.05	0.01	2.23	13.29
	H1	44.85	38.62	0.17	0.04	0.04	n.d.	n.d.	0.01	16.27
	S1	58.03	19.60	4.08	0.02	2.36	0.04	3.04	0.09	12.74
	S2	57.72	16.92	1.49	3.31	5.82	0.03	0.06	0.22	14.41
	S3	52.62	0.46	0.34	2.28	23.67	0.09	0.15	0.02	20.48
	I1	52.62	22.63	6.64	0.12	2.32	7.72	0.48	0.78	6.68
CHAPTER 6	R-KF	51.27	34.62	0.52	0.11	0.18	0.48	0.03	0.21	12.48
	Archi.	51.04	34.07	0.79	0.05	0.16	1.56	0.04	0.96	11.09
	KA Hostun	64.40	23.35	0.91	0.22	0.13	0.45	0.03	0.26	8.71
	R-ALK R	63.44	24.23	0.71	0.10	0.21	4.00	0.14	0.19	6.96
	WS 35/38	57.57	35.76	1.75	0.51	0.66	1.82	0.14	1.79	13.18
	Argilla bianca	57.89	25.11	3.54	0.41	0.63	1.97	1.50	0.25	8.4
	CS S	52.20	33.31	9.24	0.59	0.66	2.61	0.21	1.19	13.37
CHAPTER 7	SM1	58.66	15.19	6.57	2.45	1.81	0.63	0.01	3.40	11.23
	SM2	60.94	16.39	3.64	3.61	1.72	1.89	0.39	0.90	10.05
	SM3	47.31	14.07	6.45	11.14	4.01	2.66	1.05	0.62	12.61
	SM4	63.23	13.01	4.07	1.43	2.48	2.66	0.04	1.20	8.89
	SM5	73.75	9.76	2.02	2.15	0.97	2.35	0.20	0.58	6.83
CHAPTER 8	VO14CV15	67.61	19.82	1.71	0.26	0.24	0.33	0.04	1.20	8.73
	VO14CV18	52.36	29.86	1.05	0.57	0.36	0.42	0.06	2.03	13.23
	VO14CV19	47.03	34.26	1.11	0.51	0.37	0.31	0.06	1.56	14.72
	VO14CV22	45.71	35.41	0.56	0.57	0.33	0.18	0.05	1.48	15.66
	VO14CV24	47.32	32.74	0.90	0.60	0.37	0.25	0.05	2.04	15.67
	VO14CV25	50.27	32.38	0.92	0.44	0.34	0.41	0.07	1.63	13.47
	VO14CV27	57.32	25.70	1.57	0.50	0.31	0.42	0.05	1.50	12.55
	VO14CV29	47.92	28.81	1.05	0.80	0.35	0.41	0.06	1.60	18.96
	VO14CV30	59.83	24.55	0.89	0.34	0.26	0.52	0.04	1.27	12.25
	VO14CV33	58.62	19.66	1.34	0.56	0.26	0.41	0.03	1.17	17.90

	SAMPLE	SiO_2	Al_2O_3	Fe_2O_3	CaO	MgO	K_2O	Na_2O	TiO_2	LOI
CHAPTER 8	**VO14CV35**	41.84	25.16	3.10	2.16	0.60	0.13	0.05	2.90	23.98
	VO14CV37	49.95	31.83	0.57	0.58	0.55	0.15	0.04	2.14	14.15
	VO14CV41	61.45	24.68	0.72	0.42	0.36	0.19	0.04	1.62	10.48
	VO14CV48	69.14	103.9	5.48	27.24	1.91	2.7	0.25	0.69	8.09
	VO14CV52	45.21	29.03	1.07	1.11	0.36	0.28	0.07	1.83	20.98
	VO14CV71	58.83	24.54	4.06	0.30	0.27	0.51	0.04	1.02	10.25
	VO14CV78	64.72	12.25	4.92	3.54	1.39	1.73	0.43	0.75	9.85

III. BULK MINERALOGICAL COMPOSITION

	Sample	Qz	Kspar	Plag	Ca + Dol	Pyr	Al-oxide	Fe-oxide	Gyp	Anat	Mus	Amor.	Kaol	2:1 Al	2:1 Fe
CHAPTER 4	K1	0	0	0	0	0	0	0	0	0.5	0	0	99.5	0	0
	K2	0	0	0	0	0	0	0	0	1.5	0	0	98.5	0	0
	K3	0	0	0	0	0	0	0	0	2	0	0	98	0	0
	H1	0	0	0	0	0	0	0	0	0	0	0	100	0	0
	S1	2	0	0	0	0	0	0	0	0	0	0	0	98	0
	S2	0.5	0	0	0	0	0	0	0	0	0	0	0	99.5	0
	S3	2	0	0	0	0	0	0	0	0	0	0	0	98	0
	I1	5	0	0	0	0	0	0	0	1	0	0	2	92	0
CHAPTER 6	R-KF	8	0	0	0	0	0	0	0	0	5	0	87	0	0
	Archi.	8	0	0	0	0	0	1	0	1	3	0	68	19	0
	KA Hostun	37.5	0	0	0	0	0	0	0	0.5	3	0	57	2	0
	R-ALK R	21	19	0	0	0	0	0	0	0	3	0	55	2	0
	WS 35/38	9	2	0	0	0	0	1	0	2	6	4	46	30	0
	Argilla bianca	16.5	21	0	0	0	0	1	0	0.5	10	0	43	8	0
	CS S	9	3	0	0	0	0	3	0	2	18	5	42	18	0

	Sample	Qz	Kspar	Plag	Ca + Dol	Pyr	Al-oxide	Fe-oxide	Gyp	Anat	5Mus	Amor	Kaol	Chlo	2:1 Al	2:1 Fe
CHAPTER 7	SM1	12	2	0	0	0	0	0	0	1	0	0	2	0	83	0
	SM2	20	6	6	3	0.5	0.5	0	0	0	5	0	0.5	1	58	0
	SM3	14	5.5	1.5	18	0	0	0	0	0.5	4	0	2	7	47	0
	SM4	31	11	2	0	0.5	0.5	0	2	1	0	0	6	6	41	0
	SM5	52.5	8	3	0	0	0	0	4	0.5	0	0	3	0	29	0
CHAPTER 8	CV15	46.5	0.5	0	0	0	0	0	0	1	**1**	7	38	0	6	0
	CV18	15	2	0	0	0	0.5	0	0	2	5	6	59.5	0	10	0
	CV19	4	3	0	0	0	0	0	0	2	0	0	76	0	15	0
	CV22	1	1	0	0	0	0	0	0	2	0	6	78	0	12	0
	CV24	7	1	0	0	0	1	0	0	2	0	5	69	0	15	0
	CV25	9	1	0	0	0	0	0	0	2	0	8	63	0	17	0
	CV27	28	0.5	0	0	0	0.5	0	0	1	3	8	49	0	10	0
	CV29	13	1	0	0	0	1	0	0	2	3	10	57	0	13	0
	CV30	33	0	0	0	0	0.5	0	0	1	2	4	49.5	0	10	0
	CV33	30	1	0	0	0	0.5	0	0	1	2	11	43.5	0	11	0
	CV37	8	2	0	0	0	0	0	0	2	0	0	72	0	16	0

Sample	Qz	Kspar	Plag	Ca + Dol	Pyr	Al-oxide	Fe-oxide	Gyp	Anat	Mus	Amor	Kaol	Chlo	2:1 Al	2:1 Fe
CV41	37	0.5	0	0	0	0	0	0	1	1	5	47.5	0	8	0
CV48	41	6	2	0	0	0	0	0	0	10	6	3	0	16	16
CV52	12	1	0	0	0	1	0.5	0	2	0	17	50.5	0	16	0
CV71	29	0	0	0	0	0	3	0	1	4	5	47	0	11	0
CV78	47.5	3	2	3	0	0	1	0	0.5	7	4	4	0	20	8

CHAPTER 8

IV. CLAY MINERALOGY

	Sample	Kaol	Hal.	Chlor	Illite	Smect	I/S	Ratio I/S	K/S	Ratio K/S	Qtz	Smect bulk	Illite bulk	I/S bulk
CHAPTER 4	K1	100	0	0	0	0	0	-	0	-	0	-	-	-
	K2	100	0	0	0	0	0	-	0	-	0	-	-	-
	K3	100	0	0	0	0	0	-	0	-	0	-	-	-
	H1	0	100	0	0	0	0	-	0	-	0	-	-	-
	S1	0	0	0	0	0	0	-	0	-	2	-	-	-
	S2	0	0	0	0	0	0	-	0	-	0.5	-	-	-
	S3	0	0	0	0	0	0	-	0	-	2	-	-	-
	I1	2	0	0	92	5	0	-	0	-	1	-	-	-
CHAPTER 6	R-KF	99	0	0	1	0	0	-	0	-	0	0	0	0
	Archi.	27.6	0	0	72.4	0	0	-	0	-	0	0	19	0
	KA Hostun	98	0	0	2	0	0	-	0	-	0	0	2	0
	R-ALK R	84.3	0	0	8.5	0	7.2	80:20	0	-	0	0	1	1
	WS 35/38	65.3	0	0	14.9	12.7	7.1	70:30	0	-	0	11	13	6
	Argilla bianca	35.3	0	0	15.2	0	12.4	70:30	37.1	78:22	0	0	4.5	3.5
	CS S	59.4	0	0	27.2	7.1	6.3	70:30	0	-	0	3	12	3

	Sample	Kaol	Hal.	Chlor	Illite	Smect	I/S	Ratio I/S	K/S	Ratio K/S	Qtz	Smect bulk	Illite bulk	I/S bulk
CHAPTER 7	SM1	1	0	0	0	93	6	66:34	0	-	0	78	0	5.0
	SM2	1	0	0	9	85	5	70:30	0	-	0	49.8	5.3	2.9
	SM3	3	0	2.5	12	68.5	14	70:30	0	-	0	34.1	6	7.0
	SM4	7.5	0	0.5	15.5	53.5	22	66:34	1	85:15	0	24.1	7	9.9
	SM5	1	0	0	9	54	36	66:34	0	-	0	15.3	2.5	10.2
CHAPTER 8	CV15	75	0	0	1	12	4	30:70	8	73:27	0	4.2	0.4	1.4
	CV18	63	0	0	0	22	8	30:70	7	73:27	0	7.3	0	2.7
	CV19	64	0	0	0	23	5	30:70	8	73:27	0	12.3	0	2.7
	CV22	74	0	0	1	13	4	30:70	8	73:27	0	8.7	0.7	2.7
	CV24	64	0	0	0	26	5	30:70	5	73:27	0	12.6	0	2.4
	CV25	67	0	0	0	8	8	30:70	17	73:27	0	8.5	0	8.5
	CV27	60	0	0	1	28	6	30:70	5	73:27	0	8	0.3	1.7
	CV29	63	0	0	1	27	4	30:70	5	73:27	0	11	0.4	1.6
	CV30	62	0	0	5	27	6	30:70	7	73:27	0	7.1	1.3	1.6
	CV33	74	0	0	5	8	5	30:70	6	73:27	0	4.9	3.1	3.1
	CV37	60	0	0	0	24	6	30:70	10	73:27	0	12.8	3.2	3.2

Sample	Kaol	Hal.	Chlor	Illite	Smect	I/S	Ratio I/S	K/S	Ratio K/S	Qtz	Smect bulk	Illite bulk	I/S bulk
CV41	67	0	0	0	20	5	30:70	8	73:27	0	6.4	0	1.6
CV48	1	0	0	3	79	17	65:35	0	-	0	12.8	0.5	2.7
CV52	61	0	0	1	27	6	30:70	5	73:27	0	12.7	0.5	2.8
CV71	89	0	0	2	6	3	30:70	0	-	0	6.0	2	3
CV78	8	0	0	11	52	29	65:35	0	-	0	11.3	2.4	6.3

CHAPTER 8

V. POZZOLANIC REACTIVITY

	Sample	Calc. T	3d	7d	14d	28d	56d	90d
CHAPTER 4	K1	500°C	-	28.5	-	51.8	54.6	-
	K1	700°C	25.0	38.7	52.6	65.8	68.6	68.6
	K1	800°C	26.3	38.6	54.8	66.8	69.1	69.6
	K1	900°C	-	37.2	-	64.5	68.1	-
	K2	500°C	24.1	35.8	-	59.1	-	-
	K2	700°C	24.9	37.0	53.0	64.1	68.1	69.0
	K2	800°C	24.9	37.7	51.2	62.8	67.7	67.9
	K2	900°C	23.9	37.5	51.0	63.3	67.9	68.3
	K3	500°C	29.6	45.2	-	64.8	-	-
	K3	700°C	30.2	46.1	60.8	63.8	64.6	64.8
	K3	800°C	30.7	46.3	63.2	66.8	67.4	67.5
	K3	900°C	25.6	42.0	60.1	66.3	67.7	68.5
	H1	500°C	33.7	48.2	-	61.7	65.9	-
	H1	700°C	34.4	49.5	-	64.8	67.0	-
	H1	800°C	34.9	52.9	63.8	67.5	67.6	67.7
	H1	900°C	34.8	48.7	61.9	65.6	66.9	67.4
	S1	700°C	17.1	20.0	-	28.4	32.5	-
	S1	800°C	14.3	19.2	24.3	30.1	37.1	42.9
	S1	900°C	13.2	13.8	-	22.6	29.1	-
	S1 Ca	800°C	17.9	23.6	29.5	33.5	40.6	46.4
	S2	700°C	15.3	18.8	-	29.2	38.1	-
	S2	800°C	16.3	22.5	29.8	36.7	47.7	52.1
	S2	900°C	12.4	14.6	-	19.5	26.4	-
	S3	700°C	-	17.0	-	18.1	21.5	-
	S3	800°C	16.5	17.5	18.5	18.4	21.9	23.0
	S3	900°C	-	14.6	-	16.8	19.5	-
	I1	700°C	14.7	13.7	-	15.7	-	-
	I1	800°C	13.2	14.8	-	17.6	21.6	-
	I1	900°C	14.5	17.0	21.0	25.7	30.0	33.2

	Sample	Calc. T	3d	7d	14d	28d	56d	90d
CHAPTER 5	60%Q	800°C	26.3	28.0	36.4	40.4	40.6	40.3
	45%Q	800°C	20.2	36.1	40.5	43.4	47.5	47.8
	30%Q	800°C	23.5	36.3	44.5	52.4	53.5	54.8
	15%Q	800°C	24.3	37.5	48.5	58.4	60.6	61.5
	30%Q	700°C	23.9	-	46.2	52.9	-	-
	30%Q	900°C	23.2	-	45.3	52.5	-	-
	40%F	800°C	23.1	-	41.2	48.5	49.0	49.5
	30%F	800°C	24.2	36.0	44.6	53.3	54.0	54.4
	20%F	800°C	25.8	-	47.1	58.3	58.9	59.2
	10%F	800°C	25.5	-	50.4	60.8	63.5	63.6
	30%F	700°C	-	-	-	55.0	-	-
	30%F	900°C	-	-	-	53.2	-	-
	40%Mu	800°C	-	25.3	36.4	45.3	48.8	48.3
	30%Mu	800°C	-	28.0	39.9	50.5	54.2	54.4
	20%Mu	800°C	-	28.5	42.7	55.2	58.7	58.9
	10%Mu	800°C	-	29.4	45.5	58.3	63.0	63.1
	30%Mu	700°C	-	-	-	49.9	-	-
	30%Mu	900°C	-	-	-	50.2	-	-
	60%Ca	800°C	8.8	24.7	32.3	34.3	34.6	34.0
	45%Ca	800°C	15.7	-	42.7	45.8	47.8	49.0
	30%Ca	800°C	23.8	46.9	54.8	60.5	60.9	61.3
	15%Ca	800°C	26.2	36.6	58.2	65.3	68.8	68.5
	30%Ca	700°C	-	-	-	59.8	-	-
	30%Ca	900°C	-	-	-	55.6	-	-
	60%S	800°C	-	26.1	36.6	47.9	56.2	60.2
	45%S	800°C	22.5	31.8	44.0	55.6	62.8	65.4
	30%S	800°C	23.2	33.5	46.4	61.5	65.1	67.3
	15%S	800°C	23.7	34.7	50.0	64.0	67.1	67.8
	30%S	700°C	-	56.1	-	-	-	-
	30%S	900°C	-	55.8	-	-	-	-
	60%I	800°C	20.5	27.5	36.1	41.1	41.9	44.5
	45%I	800°C	21.9	33.7	41.9	48.3	50.7	51.9
	30%I	800°C	21.9	35.6	44.6	55.0	56.2	56.4
	15%I	800°C	22.6	36.8	47.7	59.7	62.6	62.8
	30%I	700°C	-	52.1	-	-	-	-
	30%I	900°C	-	53.4	-	-	-	-

	Sample	Calc. T	3d	7d	14d	28d	56d	90d
CHAPTER 6	R-KF	750°C	21.6	34.0	50.9	57.5	59.8	59.9
	Archi.	750°C	19.8	26.2	34.1	43.3	48.7	50.0
	KA Hostun	750°C	20.2	28.1	44.6	46.5	47.7	49.5
	R-ALK R	750°C	23.7	29.1	37.0	41.3	43.4	43.6
	WS 35/38	800°C	24.2	37.2	42.1	44.7	46.8	47.7
	Argilla bianca	750°C	21.8	29.5	35.6	38.2	40.8	42.2
	CS S	800°C	23.8	31.6	38.8	40.1	41.5	42.6
	Coarse R-KF	750°C	-	29.7	45.1	55.9	-	-
	Coarse KA Hostun	750°C	-	23.7	36.4	45.6	-	-
	Coarse R-ALK R	750°C	-	20.9	28.9	35.4	-	-
	Coarse WS 35/38	800°C	-	24.7	32.2	35.3	-	-
	Coarse Argilla bianca	750°C	-	24.1	29.9	34.6	-	-
	Coarse CS S	800°C	-	24.6	31.4	34.3	-	-
CHAPTER 7	SM1	800°C	-	17.0	22.0	26.3	31.5	37.7
	SM2	800°C	16.3	20.5	25.9	32.2	37.5	40.3
	SM3	800°C	15.9	18.8	22.6	27.2	31.6	35.6
	SM4	800°C	-	17.4	22.0	25.5	29.1	32.2
	SM5	800°C	-	17.0	20.3	24.0	26.2	26.9

	Sample	Calc. T	3d	4d	7d	14d	28d	56d	90d
CHAPTER 8	CV15	800°C	21.1	-	31.0	39.0	44.5	43.8	43.8
	CV18	800°C	24.6	-	34.9	46.7	53.6	53.7	54.3
	CV22	800°C	25.9	-	39.0	53.1	57.7	60.6	62.5
	CV22	650°C	-	26.1	49.2	54.5	56.4	57.5	-
	CV24	800°C	-	29.3	39.2	51.3	55.7	55.8	56.5
	CV25	800°C	24.3	-	37.4	50.2	55.1	56.8	58.3
	CV25	650°C	-	27.3	47.3	52.7	56.8	55.3	-
	CV25 (C)	800°C	20.1	-	-	38.1	43.8	46.7	48.7
	CV27	800°C	24.5	-	34.8	44.7	46.2	46.6	46.9
	CV29	800°C	-	-	33.3	46.1	47.7	49.5	49.0
	CV30	800°C	-	26.8	33.5	46.2	47.2	48.6	49.6
	CV33	800°C	23.7	-	36.6	42.2	45.6	45.8	47.1
	CV35	800°C	-	27.7	34.5	44.0	47.6	50.5	50.4
	CV37	800°C	24.9	-	36.5	48.6	53.4	58.5	57.6
	CV41	800°C	-	23.1	29.3	38.5	43.1	42.1	43.2
	CV48	800°C	-	26.5	28.3	31.4	37.8	40.3	43.4
	CV52	800°C	28.4	-	42.2	50.1	53.1	52.7	54.9
	CV71	800°C	-	22.8	-	42.0	46.4	49.4	47.4
	CV78	800°C	-	20.1	-	25.9	28.2	31.7	31.9

VI. MINERALOGICAL MODEL

7 days of curing:

Function Parameters	T-test p1	T-test p2	T-test p3	R^2	p-value
K	$1.04E^{-06}$			0.552	$1.04E^{-06}$
S	$1.90\ E^{-02}$			0.148	0.019
I	$8.10\ E^{-02}$			0.070	0.081
Al_2O_3	$2.21\ E^{-02}$			0.141	0.211
SiO_2	$2.79\ E^{-01}$			0.007	0.279
d50	$7.01\ E^{-03}$			0.197	0.007
SSA	$3.37E^{-07}$			0.584	$3.37E^{-07}$
K + S	$2.38E^{-05}$	$6.61\ E^{-01}$		0.539	$7.49E^{-06}$
K + I	$7.38E^{-06}$	0.93		0.536	$8.23E^{-06}$
K + Cal	$1.10\ E^{-06}$	0.394		0.548	$5.71\ E^{-06}$
K + SSA	**$4.79\ E^{-05}$**	**$1.59\ E^{-05}$**		**0.780**	**$6.38\ E^{-10}$**
K + d50	$4.54\ E^{-05}$	$4.39\ E^{-01}$		0.546	$6.09\ E^{-06}$
K + P0	$5.95\ E^{-08}$	$1.14\ E^{-02}$		0.632	$3.19\ E^{-07}$
K + 1/P0	$7.73\ E^{-06}$	$7.98\ E^{-01}$		0.537	$8.00\ E^{-06}$
K + HI	$6.30\ E^{-08}$	$1.25\ E^{-02}$		0.630	$3.464\ E^{-07}$
$Al_2O_3 + SiO_2$	$3.20\ E^{-02}$	$4.36\ E^{-01}$		0.130	$5.41\ E^{-02}$
AlO_3 + SSA	$2.56\ E^{-01}$	$3.99\ E^{-06}$		0.589	$1.48\ E^{-06}$
Al_2O_3 + K	$7.39\ E^{-02}$	$4.39\ E^{-06}$		0.587	$1.62\ E^{-06}$
K + SSA + S	$1.25\ E^{-03}$	$2.44\ E^{-05}$	$8.27\ E^{-01}$	0.756	$5.04\ E^{-09}$
K + SSA + P0	$1.69\ E^{-02}$	$4.49\ E^{-04}$	$4.62\ E^{-01}$	0.760	$3.93\ E^{-09}$
K + SSA + HI	$1.32\ E^{-02}$	$3.98\ E^{-04}$	$4.34\ E^{-01}$	0.761	$3.792\ E^{-09}$
K^2	$1.80\ E^{-06}$			0.535	$1.80\ E^{-06}$
K + K^2	$2.28\ E^{-01}$	$5.10\ E^{-01}$		0.543	$6.63\ E^{-06}$
K^2 + SSA	$8.20\ E^{-04}$	$1.55\ E^{-04}$		0.713	$9.61\ E^{-09}$
K + SSA^2	$1.71\ E^{-06}$	$2.43\ E^{-05}$		0.757	$9.60\ E^{-10}$
K + K^2 + SSA	$1.23\ E^{-02}$	$2.88\ E^{-01}$	$1.56\ E^{-05}$	0.765	$2.92\ E^{-09}$
K + SSA + SSA^2	$5.29\ E^{-04}$	$3.69\ E^{-01}$	$8.59\ E^{-01}$	0.755	$5.08\ E^{-09}$

14 days of curing

Function Parameters	T-test p1	T-test p2	T-test p3	R^2	p-value
K	2.79 E^{-11}			0.781	2.79 E^{-11}
S	1.74 E^{-02}			0.152	1.75 E^{-02}
I	2.67 E^{-02}			0.129	2.67 E^{-02}
Al_2O_3	4.43 E^{-04}			0.330	4.43 E^{-04}
SiO_2	1.51 E^{-01}			0.038	1.51 E^{-01}
d50	7.58 E^{-03}			0.194	7.58 E^{-03}
SSA	3.58 E^{-05}			0.432	3.58 E^{-05}
K + S	1.81 E^{-10}	6.70 E^{-02}		0.799	6.69 E^{-11}
K + I	6.38 E^{-10}	6.65 E^{-01}		0.775	3.35 E^{-10}
K + Cal	4.57 E^{-11}	4.32 E^{-01}		0.778	2.69 E^{-10}
K + SSA	**8.83 E^{-10}**	**7.77 E^{-04}**		**0.859**	**1.18 E^{-12}**
K + d50	2.10 E^{-09}	9.00 E^{-01}		0.773	3.66 E^{-10}
K + P0	2.97 E^{-12}	9.15 E^{-03}		0.822	1.16 E^{-11}
K + 1/P0	1.83 E^{-09}	3.78 E^{-01}		0.779	2.48 E^{-10}
K + HI	1.79 E^{-12}	6.68 E^{-03}		0.826	8.73 E^{-12}
Al_2O_3 + SiO_2	8.40 E^{-04}	2.67 E^{-01}		0.335	1.25 E^{-03}
AlO_3 + SSA	4.92 E^{-03}	4.11 E^{-04}		0.558	4.09 E^{-06}
Al_2O_3 + K	2.57 E^{-01}	1.46 E^{-08}		0.783	1.92 E^{-10}
K + SSA + S	5.36 E^{-09}	1.38 E^{-03}	0.11 E^{-01}	0.858	3.37 E^{-12}
K + SSA + P0	1.83 E^{-06}	3.50 E^{-02}	0.74 E^{-01}	0.844	1.18 E^{-11}
K + SSA + HI	7.24 E^{-07}	4.44 E^{-02}	6.20 E^{-01}	0.845	1.10 E^{-11}
K^2	4.49 E^{-11}			0.774	4.49 E^{-11}
K + K^2	8.07 E^{-02}	1.42 E^{-01}		0.790	1.23 E^{-11}
K^2 + SSA	2.37 E^{-08}	1.59 E^{-02}		0.810	3.03 E^{-11}
K + SSA^2	1.00 E^{-10}	3.89 E^{-03}		0.832	5.31 E^{-12}
K + K^2 + SSA	1.20 E^{-02}	6.87 E^{-01}	2.74 E^{-03}	0.845	1.15 E^{-11}
K + SSA + SSA^2	4.86E^{-07}	1.66 E^{-02}	8.93 E^{-02}	0.869	2.89 E^{--12}

56 days of curing

Function Parameters	T-test p1	T-test p2	T-test p3	R^2	p-value
K	1.30 E^{-08}			0.666	1.30 E^{-08}
S	3.85 E^{-01}			0.026	3.85 E^{-01}
I	1.39 E^{-02}			0.163	1.39 E^{-02}
Al_2O_3	8.02 E^{-05}			0.400	8.02 E^{-05}
SiO_2	3.52 E^{-01}			0.030	3.52 E^{-01}
d50	7.76 E^{-02}			0.072	7.76 E^{-02}
SSA	1.15 E^{-02}			0.173	1.15 E^{-02}
K + S	**8.82 E^{-14}**	**5.54 E^{-07}**		**0.861**	**3.82 E^{-13}**
K + I	2.77 E^{-07}	3.04 E^{-01}		0.668	7.61 E^{-08}
K + Cal	2.16 E^{-08}	1.88 E^{-01}		0.676	5.40 E^{-08}
K + SSA	5.15 E^{-07}	6.63 E^{-01}		0.657	1.18 E^{-07}
K + d50	5.53 E^{-08}	2.47 E^{-01}		0.671	6.60 E^{-08}
K + P0	1.58 E^{-08}	1.58 E^{-01}		0.679	4.73 E^{-08}
K + 1/P0	1.37 E^{-07}	3.92 E^{-01}		0.657	1.20 E^{-07}
K + HI	1.37 E^{-07}	6.92 E^{-01}		0.657	1.20 E^{-07}
$Al_2O_3 + SiO_2$	1.49 E^{-04}	6.44 E^{-01}		0.374	4.34 E^{-04}
AlO_3 + S	1.30 E^{-04}	5.46 E^{-01}		0.387	4.02 E^{-04}
Al_2O_3 + K	6.05 E^{-01}	5.04 E^{-05}		0.658	1.14 E^{-07}
K + S + SSA	3.74 E^{-12}	9.17 E^{-07}	7.28 E^{-01}	0.857	3.98 E^{-12}
K^2	2.48 E^{-09}			0.702	2.48 E^{-09}
K + K^2	5.23 E^{-01}	6.61 E^{-02}		0.696	2.19 E^{-08}
K^2 + S	5.15 E^{-11}	2.05 E^{-03}		0.7816	2.14 E^{-10}
K + S^2	1.74 E^{-11}	7.32 E^{-05}		0.805	4.38 E^{-11}
K + K^2 + S	5.01 E^{-04}	7.27 E^{-01}	4.87 E^{-06}	0.857	3.978 E^{-12}
K + S + S^2	2.96 E^{-13}	4.79 E^{-04}	7.32 E^{-02}	0.872	8.33 E^{-13}

90 days of curing

Function Parameters	T-test p1	T-test p2	T-test p3	R^2	p-value
K	1.83 E^{-06}			0.534	1.83 E^{-06}
S	8.39 E^{-01}			0.001	8.39 E^{-01}
I	2.30 E^{-02}			0.137	0.23 E^{-02}
Al_2O_3	2.28 E^{-04}			0.358	2.28 E^{-04}
SiO_2	4.15 E^{-01}			0.023	4.15 E^{-01}
d50	1.60 E^{-01}			0.035	1.60 E^{-01}
SSA	1.73 E^{-02}			0.152	1.73 E^{-02}
K + S	**2.32 E^{-12}**	**1.83 E^{-07}**		**0.820**	**1.40 E^{-11}**
K + I	2.48 E^{-05}	3.70 E^{-01}		0.531	9.39 E^{-06}
K + Cal	2.70 E^{-06}	1.43 E^{-01}		0.554	4.75 E^{-06}
K + SSA	4.24 E^{-05}	6.02 E^{-01}		0.522	1.23 E^{-05}
K + d50	3.68 E^{-06}	2.43 E^{-01}		0.541	7.05 E^{-06}
K + P0	1.02 E^{-06}	1.20 E^{-01}		0.558	4.11 E^{-06}
K + 1/P0	1.03 E^{-05}	6.91 E^{-01}		0.520	1.30 E^{-05}
K + HI	1.02 E^{-06}	1.35 E^{-01}		0.555	4.52 E^{-06}
$Al_2O_3 + SiO_2$	3.90 E^{-04}	7.36 E^{-01}		0.337	1.20 E^{-03}
AlO_3 + S	1.05 E^{-04}	1.60 E^{-01}		0.381	4.66 E^{-04}
Al_2O_3 + K	4.43 E^{-01}	2.13 E^{-03}		0.528	1.05 E^{-05}
K + S + SSA	8.47 E^{-11}	3.39 E^{-07}	8.05 E^{-01}	0.814	1.29 E^{-10}
K^2	1.94 E^{-07}			0.600	1.94 E^{-07}
K + K^2	9.13 E^{-01}	4.08 E^{-02}		0.586	1.68 E^{-06}
K^2 + S	1.88 E^{-10}	1.45 E^{-04}		0.755	1.10 E^{-09}
K + S^2	5.86 E^{-10}	4.04 E^{-05}		0.738	2.68 E^{-09}
K + K^2 + S	3.40 E^{-03}	5.72 E^{-01}	2.11 E^{-06}	0.816	1.14 E^{-10}
K + S + S^2	6.90 E^{-12}	2.30 E^{-04}	5.75 E^{-02}	0.837	2.15 E^{-11}